NAVAL POSTGRADUATE SCHOOL
Monterey, California

THESIS

DESIGN INVESTIGATION FOR A MICROSTRIP
PHASED ARRAY ANTENNA
FOR THE ORION SATELLITE

by

Mark B. Smith

June 1988

Thesis Advisor Michael A. Morgan

Approved for public release; distribution is unlimited.

Unclassified

security classification of this page

REPORT DOCUMENTATION PAGE

1a Report Security Classification: Unclassified		1b Restrictive Markings	
2a Security Classification Authority		3 Distribution Availability of Report: Approved for public release; distribution is unlimited.	
2b Declassification/Downgrading Schedule			
4 Performing Organization Report Number(s)		5 Monitoring Organization Report Number(s)	
6a Name of Performing Organization: Naval Postgraduate School	6b Office Symbol (*if applicable*): 39	7a Name of Monitoring Organization: Naval Postgraduate School	
6c Address (*city, state, and ZIP code*): Monterey, CA 93943-5000		7b Address (*city, state, and ZIP code*): Monterey, CA 93943-5000	
8a Name of Funding Sponsoring Organization	8b Office Symbol (*if applicable*)	9 Procurement Instrument Identification Number	
8c Address (*city, state, and ZIP code*)		10 Source of Funding Numbers	
		Program Element No	Project No / Task No / Work Unit Accession No

11 Title (*include security classification*): DESIGN INVESTIGATION FOR A MICROSTRIP PHASED ARRAY ANTENNA FOR THE ORION SATELLITE

12 Personal Author(s): Mark B. Smith

13a Type of Report	13b Time Covered	14 Date of Report (*year, month, day*)	15 Page Count
Master's Thesis	From To	June 1988	199

16 Supplementary Notation: The views expressed in this thesis are those of the author and do not reflect the official policy or position of the Department of Defense or the U.S. Government.

17 Cosati Codes			18 Subject Terms (*continue on reverse if necessary and identify by block number*)
Field	Group	Subgroup	ORION satellite, conformal phased array antenna

19 Abstract (*continue on reverse if necessary and identify by block number*)

Students at the Naval Postgraduate School are designing a general purpose mini-satellite that can be launched from a "Get-Away-Special" cannister located in the cargo bay of the Space Shuttle and will be compatible with expendable launch vehicles as well. This thesis defines preliminary antenna design parameters for the telemetry system of the ORION mini-satellite. These antenna design parameters may be used for investigations of various proposed antenna systems and the design parameters also allow for trade-off studies with the mission capabilities and subsystems of the satellite. An investigation is made into the feasibility of using conformal microstrip patch array antennas for the telemetry, tracking and command (TT&C) systems. It is necessary to have two separate microstrip patch array antennas for the telemetry system: one uplink and one downlink antenna. The microstrip patch array antenna can operate as either an omnidirectional antenna or a directional antenna by changing the phase of the individual patch feeds. This feature gives the microstrip patch array antenna more flexibility for meeting the needs of potential users.

20 Distribution/Availability of Abstract	21 Abstract Security Classification	
☒ unclassified unlimited ☐ same as report ☐ DTIC users	Unclassified	
22a Name of Responsible Individual: Michael A. Morgan	22b Telephone (*include Area code*): (408) 646-2677	22c Office Symbol: 62Mw

DD FORM 1473,84 MAR 83 APR edition may be used until exhausted
All other editions are obsolete

security classification of this page

Unclassified

Approved for public release; distribution is unlimited.

Design Investigation for a Microstrip Phased Array Antenna
for the ORION Satellite

by

Mark B. Smith
Lieutenant, United States Navy
B.S., University of Washington, 1980

Submitted in partial fulfillment of the
requirements for the degree of

MASTER OF SCIENCE IN ELECTRICAL ENGINEERING

from the

NAVAL POSTGRADUATE SCHOOL
June 1988

ABSTRACT

Students at the Naval Postgraduate School are designing a general purpose mini-satellite that can be launched from a "Get-Away-Special" cannister located in the cargo bay of the Space Shuttle and will be compatible with expendable launch vehicles as well. This thesis defines preliminary antenna design parameters for the telemetry system of the ORION mini-satellite. These antenna design parameters may be used for investigations of various proposed antenna systems and the design parameters also allow for trade-off studies with the mission capabilities and subsystems of the satellite. An investigation is made into the feasibility of using conformal microstrip patch array antennas for the telemetry, tracking and command (TT&C) systems. It is necessary to have two separate microstrip patch array antennas for the telemetry system: one uplink and one downlink antenna. The microstrip patch array antenna can operate as either an omnidirectional antenna or a directional antenna by changing the phase of the individual patch feeds. This feature gives the microstrip patch array antenna more flexibility for meeting the needs of potential users.

TABLE OF CONTENTS

I. INTRODUCTION 1
A. OBJECTIVES 1
B. SUMMARY OF FINDINGS 2
C. ORGANIZATION OF STUDY 3

II. THE ORION PROGRAM 5
A. THE ORION SATELLITE 6
B. THE TELEMETRY, TRACKING AND COMMAND SYSTEM 8
1. The U.S. Air Force Satellite Control Network 8
2. The U.S. Air Force Space-Ground Link System 10

III. ORION SATELLITE ANTENNA REQUIREMENTS 12
A. ORION ANTENNA SPECIFICATIONS 13
1. ORION Antenna Radiation Pattern 13
2. Continuity 13
3. Shape 13
4. Size 14
5. Frequency of Operation 14
6. Bandwidth 14
7. Impedance 14
8. Polarization Properties 14
9. Gain 14
10. Power Handling Capacity 15
11. Mass 15
12. Cost 16
B. SUMMARY OF ORION ANTENNA SPECIFICATIONS 16

IV. MICROSTRIP PATCH ARRAY ANTENNA FUNDAMENTALS 18
A. THE MICROSTRIP PATCH ANTENNA 21
B. CIRCULAR ARRAY FUNDAMENTALS 25
C. OMNIDIRECTIONAL RADIATION PATTERN 28

D. DIRECTIVE GAIN PATTERN 29
E. DIRECTIONAL ANTENNA RADIATION PATTERN 30

V. PRELIMINARY PHYSICAL DESIGN 31
A. ORION SATELLITE UPLINK ANTENNA DESIGN 31
1. Uplink Microstrip Patch Dimensions 31
2. Number of Patches Needed for the Uplink Array 33
3. Omnidirectional Uplink Radiation Patterns 34
4. Omnidirectional Uplink Directive Gain Patterns 38
B. ORION SATELLITE DOWNLINK ANTENNA DESIGN 46
1. Downlink Microstrip Patch Dimensions 46
2. Number of Patches Needed for the Downlink Array 47
3. Omnidirectional Downlink Radiation Patterns 47
4. Omnidirectional Downlink Directive Gain Patterns 52
C. DIRECTIONAL DOWNLINK ANTENNA DESIGN 69
1. Downlink Directional Radiation Patterns 69
2. Downlink Directional Directive Gain Patterns 73

VI. CONCLUSIONS AND RECOMMENDATIONS 86

APPENDIX A. ANTENNA GAIN SPECIFICATION DERIVATION 88
A. SGLS GROUND STATION TO ORION RF UPLINK 89
1. SGLS Ground Station Output Power 89
2. Uplink Free Space Losses 90
3. Atmospheric and Rain Attenuation 92
4. Polarization Loss 94
5. Modulation Losses 94
6. Motorola S-Band Transponder Receiving Characteristics 97
7. ORION Satellite Line Losses 98
8. Uplink Service Margins 98
9. ORION Satellite Uplink Antenna Gain Specifications 98
B. ORION TO SGLS GROUND STATION DOWNLINK 100
1. SGLS Carrier 1 Downlink Analysis 100
a. Motorola S-Band Transponder Output Power 100
b. Satellite Line Losses 100

c. Downlink Free Space Loss 100
d. Polarization Loss 102
e. Atmospheric and Rain Attenuation 102
f. SGLS Ground Station Antenna Gain 102
g. Modulation Losses 102
h. Ground Station Receiver Sensitivity 103
i. Downlink Service Margins 103
j. Carrier 1 ORION Satellite Antenna Gain Requirement 103
2. Carrier 2 Downlink Analysis 104
a. Gain Requirement based on 512 kbps Carrier 2 Data Rate 105
b. Gain Requirement based on 1.024 Mbps Carrier 2 Data Rate ... 105
C. ORION ANTENNA GAIN SPECIFICATIONS 107
D. MATHCAD PROGRAM FOR CALCULATING ANTENNA GAIN .. 107

APPENDIX B. OMNIDIRECTIONAL RADIATION PATTERN 120

APPENDIX C. OMNIDIRECTIONAL AVERAGE RADIATION INTENSITY 139

APPENDIX D. OMNIDIRECTIONAL DIRECTIVE GAIN PATTERN 143

APPENDIX E. DOWNLINK OMNI RADIATION PATTERN RESULTS ... 153

APPENDIX F. DIRECTIONAL DOWNLINK RADIATION PATTERN 168

APPENDIX G. DIRECTIONAL AVERAGE RADIATION INTENSITY ... 175

APPENDIX H. DIRECTIONAL DIRECTIVE GAIN PATTERN 178

LIST OF REFERENCES 185

INITIAL DISTRIBUTION LIST 187

LIST OF TABLES

Table 1. AFSCN REMOTE TRACKING STATIONS. 8
Table 2. GAIN REQUIREMENTS FOR THE ORION SATELLITE. 17
Table 3. UPLINK ROLL PLANE GAIN FOR COMBINATION 1. 40
Table 4. UPLINK ELEVATION PLANE GAIN FOR COMBINATION 1. . . . 41
Table 5. UPLINK ROLL PLANE GAIN FOR COMBINATION 2. 44
Table 6. UPLINK ELEVATION PLANE GAIN FOR COMBINATION 2. . . . 45
Table 7. DOWNLINK ROLL PLANE GAIN FOR COMBINATION 1. 54
Table 8. DOWNLINK ELEVATION PLANE GAIN FOR COMBINATION 1. 55
Table 9. DOWNLINK ROLL PLANE GAIN FOR COMBINATION 2. 58
Table 10. DOWNLINK ELEVATION PLANE GAIN FOR COMBINATION 2. 59
Table 11. DOWNLINK ROLL PLANE GAIN FOR COMBINATION 3. 62
Table 12. DOWNLINK ELEVATION PLANE GAIN FOR COMBINATION 3. 63
Table 13. DOWNLINK ROLL PLANE GAIN FOR COMBINATION 4. 66
Table 14. DOWNLINK ELEVATION PLANE GAIN FOR COMBINATION 4. 67
Table 15. N = 12 DIRECTIONAL DOWNLINK ROLL PLANE GAIN. 75
Table 16. N = 12 DIRECTIONAL DOWNLINK ELEVATION PLANE GAIN. . 76
Table 17. N = 15 DIRECTIONAL DOWNLINK ROLL PLANE GAIN. 79
Table 18. N = 15 DIRECTIONAL DOWNLINK ELEVATION PLANE GAIN. . 80
Table 19. N = 16 DIRECTIONAL DOWNLINK ROLL PLANE GAIN. 83
Table 20. N = 16 DIRECTIONAL DOWNLINK ELEVATION PLANE GAIN. . 84
Table 21. ORBIT GEOMETRIES AND UPLINK FREE SPACE LOSSES. 92
Table 22. ORION UPLINK GAIN REQUIREMENTS. 99
Table 23. ORION DOWNLINK FREE SPACE LOSSES. 101
Table 24. CARRIER 1 DOWNLINK ANTENNA GAIN REQUIREMENTS. . 104
Table 25. CARRIER 2 DOWNLINK ANTENNA GAIN REQUIREMENTS. . 106
Table 26. ORION ANTENNA GAIN SPECIFICATIONS-SUMMARY. 107

LIST OF FIGURES

Figure 1. The ORION Satellite. 7
Figure 2. Cut-Away of the ORION Satellite. 7
Figure 3. AFSCN Remote Tracking Station Locations. 9
Figure 4. Typical Uplink Carrier Spectrum. 10
Figure 5. Single Antenna Spherical Coordinate System. 18
Figure 6. Antenna Shift from Reference Point. 20
Figure 7. Microstrip Patch Antenna. 21
Figure 8. Rectangular Microstrip Patch Antenna. 22
Figure 9. Microstrip Patch Antenna Radiating Slot. 23
Figure 10. Circular Array. 25
Figure 11. Leading and Trailing Edge Slot Geometry. 26
Figure 12. Variation of Bandwidth with Operating Frequency. 32
Figure 13. Uplink Roll Plane Radiation Pattern for Combination 1. 36
Figure 14. Uplink Elevation Plane Radiation Pattern for Combination 1. 36
Figure 15. Uplink Roll Plane Radiation Pattern for Combination 2. 37
Figure 16. Uplink Elevation Plane Radiation Pattern for Combination 2. 37
Figure 17. Uplink Roll Plane Gain Pattern for Combination 1. 39
Figure 18. Uplink Elevation Plane Gain Pattern for Combination 1. 39
Figure 19. Uplink Roll Plane Gain Pattern for Combination 2. 43
Figure 20. Uplink Elevation Plane Gain Pattern for Combination 2. 43
Figure 21. Downlink Roll Plane Radiation Pattern for Combination 1. 48
Figure 22. Downlink Elevation Plane Radiation Pattern for Combination 1. 48
Figure 23. Downlink Roll Plane Radiation Pattern for Combination 2. 49
Figure 24. Downlink Elevation Plane Radiation Pattern for Combination 2. 49
Figure 25. Downlink Roll Plane Radiation Pattern for Combination 3. 50
Figure 26. Downlink Elevation Plane Radiation Pattern for Combination 3. 50
Figure 27. Downlink Roll Plane Radiation Pattern for Combination 4. 51
Figure 28. Downlink Elevation Plane Radiation Pattern for Combination 4. 51
Figure 29. Downlink Roll Plane Gain Pattern for Combination 1. 53
Figure 30. Downlink Elevation Plane Gain Pattern for Combination 1. 53
Figure 31. Downlink Roll Plane Gain Pattern for Combination 2. 57

Figure 32. Downlink Elevation Plane Gain Pattern for Combination 2. 57
Figure 33. Downlink Roll Plane Gain Pattern for Combination 3. 61
Figure 34. Downlink Elevation Plane Gain Pattern for Combination 3. 61
Figure 35. Downlink Roll Plane Gain Pattern for Combination 4. 65
Figure 36. Downlink Elevation Plane Gain Pattern for Combination 4. 65
Figure 37. Directional Roll Plane Radiation Pattern - 12 Patch Array. 70
Figure 38. Directional Elevation Plane Radiation Pattern - 12 Patch Array. 70
Figure 39. Directional Roll Plane Radiation Pattern - 15 Patch Array. 71
Figure 40. Directional Elevation Plane Radiation Pattern - 15 Patch Array. 71
Figure 41. Directional Roll Plane Radiation Pattern - 16 Patch Array. 72
Figure 42. Directional Elevation Plane Radiation Pattern - 16 Patch Array. 72
Figure 43. Directional Roll Plane Gain Pattern - 12 Patch Array. 74
Figure 44. Directional Elevation Plane Gain Pattern - 12 Patch Array. 74
Figure 45. Directional Roll Plane Gain Pattern - 15 Patch Array. 78
Figure 46. Directional Elevation Plane Gain Pattern - 15 Patch Array. 78
Figure 47. Directional Roll Plane Plane Gain Pattern - 16 Patch Array. 82
Figure 48. Directional Elevation Plane Gain Pattern - 16 Patch Array. 82
Figure 49. Basic Satellite Link. 88
Figure 50. Satellite to Ground Station Slant Range. 90
Figure 51. Atmospheric Attenuation. 93
Figure 52. Rain Attenuation. 93

I. INTRODUCTION

Students at the Naval Postgraduate School are in the process of designing a small multi-purpose satellite, named ORION, that can be easily adapted to perform a variety of specific missions. One of the purposes of this program is to provide students with experience in the design process of a complex engineering problem. The program has been divided into different areas of responsibility, one of which is a telemetry system [Ref. 1: pp. 2-4]. Part of the telemetry system is the satellite antenna. Captain D.L. Peters, U.S. Army, a former Naval Postgraduate student, investigated several antennas for the ORION satellite and recommended the use of a conical log spiral antenna [Ref. 2: p. 64]. It was recommended that a conformal microstrip patch antenna be more thoroughly investigated for use with the ORION satellite. This thesis investigates the conformal microstrip patch antenna. The antenna will play an important part in the overall design of the satellite, affecting the satellite configuration, weight, and power requirements.

A. OBJECTIVES

The primary objectives of this thesis are:

- Define the design parameters of the antenna system so that different designs may be evaluated for feasibility;
- Investigate the feasibility of a conformal phased array antenna design for both omnidirectional and directional coverage.

In any design process, various alternative designs are considered and there must be some evaluation parameters by which the designs may be judged as to their ability to perform the desired function. An investigation was conducted to determine the suitability of a conformal microstrip patch phased array antenna for the ORION satellite once those design parameters were established.

Microstrip antennas have several advantages over conventional antennas and can be used over a range of frequencies from 100 Megahertz to 50 Gigahertz. The major advantages are:

- Lightweight and low volume
- Low fabrication cost
- Low profile conformal configurations

- Low scattering cross section (the ratio of the power that the antenna scatters to the incident power density)
- Linear, circular polarizations possible
- Feed systems can be integrated into the antenna itself.

There are some disadvantages to microstrip antennas including:

- Narrow bandwidth
- Half-plane radiation patterns
- Limitations on maximum gain
- Lower power handling capabilities. [Ref. 3: pp. 2-3]

The advantages of using a microstrip patch antenna in this application outweigh the disadvantages. Since the antenna can be made conformal, the antenna can be integrated into the structure of the satellite. This can reduce the mass of the structure and eliminate the need for an antenna deployment system. This conformal antenna has no moving parts which results in a more reliable system. The disadvantages are not too confining for the ORION satellite except for the narrow bandwidth constraint. One of the attributes of a microstrip patch array antenna is the ability to change the radiation pattern by changing the phase of the feeds to the individual elements. This makes it possible to go from an omnidirectional radiation pattern to a directional one. With a directional radiation pattern, the gain can be increased dramatically over the omnidirectional pattern. A directional transmission also limits interference with other satellites and ground stations. Also, being a directional antenna, it can be used with any satellite stabilization technique such as spin stabilization, 3-axis stabilization and gravity gradient stabilization.

B. SUMMARY OF FINDINGS

The antenna subsystem of the telemetry, tracking and command system must operate in an omnidirectional mode during satellite orbit insertion. The gain requirements for the antenna are basically altitude dependent once the transmitters for both the ground stations and satellite have been selected.

Microstrip patch array antennas can meet the specifications for the ORION satellite. Because of narrow bandwidth limitations, separate uplink and downlink antennas are required. The uplink array antenna requires 12 rectangular microstrip patches that are 5.36 by 6.46 centimeters in size mounted on a dielectric substrate that is 0.61 centi-

meters thick. The dielectric substrate should have a dielectric constant (ε_r) of approximately 2.32. This array has a minimum gain in the roll plane of 1.7 dB and a 60° beamwidth in the elevation plane that meets the uplink gain specification of -1.8 dB. The downlink array antenna, when operating in an omnidirectional mode, will perform adequately up to an altitude of approximately 650 nm. The downlink patches are rectangular, measuring 4.29 centimeters in length and 5.17 centimeters in width. The downlink array consists of 16 patches mounted on a dielectric substrate ($\varepsilon_r = 2.32$) that is 0.39 centimeters thick. By changing the phase of the feed to the individual patches, the radiation pattern of the antenna can be made directional. The 16 patch downlink array will operate at altitudes up to 2200 nm with a roll plane beamwidth of 10° and an elevation plane beamwidth of 46°. The minimum gain of the directional downlink gain pattern is 7.1 dB which is the gain specification for an ORION satellite operating at an altitude of 2200 nm.

C. ORGANIZATION OF STUDY

This thesis has been organized to cover the antenna design in a straight forward manner. Chapter II discusses the ORION program and gives the historical perspective of the project. Up to this point in the design, there have been several decisions concerning the TT&C system that affect the antenna design and those decisions are also discussed. Chapter III is a compilation of the antenna system specifications that will enable the TT&C system to operate properly in orbit. The most important parameter, the gain specification, are developed in Appendix A and summarized in Chapter III. Chapter IV contains the basic fundamentals concerning how a microstrip patch antenna works and how an array of microstrip patches can produce an omnidirectional radiation pattern and, with an appropriate feed system, can also produce a directional radiation pattern. Chapter V applies the fundamentals of Chapter IV to the ORION satellite and shows that microstrip patch array antennas are feasible for use on the ORION satellite. Chapter VI summarizes the findings and offers recommendations for further study of the microstrip patch array antenna for this application.

As mentioned above, Appendix A is a study of the gain requirements for the antenna system. Appendix B is a computer program that produces graphs of the roll and elevation radiation patterns for an array with a specified number of elements and phasing. The results of the program are also included for the uplink antennas. Appendix C is a computer program that calculates the normalized radiation intensity which is used for developing the directive gain pattern for array antennas. Appendix D is a computer

program that calculates and produces the directive gain pattern. Appendix E contains graphs of possible radiation patterns for the downlink using the program in Appendix B. Appendix F is a computer program that generates a directional radiation pattern that may be used on the downlink. Appendix G is a program to calculate the normalized average radiation intensity for the directional antenna. Appendix H is a program for generating the directive gain pattern for a directional antenna.

All of the computer programs in the appendices were written and computed using MathCAD 2.0. MathCAD is a mathematical formula formatter and solver that allows the user to input equations exactly as they would be written on paper. [Ref. 4]

II. THE ORION PROGRAM

The ORION program was conceived by Dr. Allen E. Fuhs, formerly of the Naval Postgraduate School, in the fall of 1984 [Ref. 5: p. 39]. U.S. space philosophy has been dominated by large and expensive satellite designs which have severely restricted access to space of smaller payloads. In the early days of space exploration, all satellites were small out of necessity and many significant discoveries were made such as the Van Allen Belt detected by Explorer 1 [Ref. 6]. Today, there is renewed interest in satellites that can provide access to space for payloads that are incompatible with large satellite designs.

The design philosophy behind the ORION program incorporates five broad areas of concern:

- Affordability
- Cost Effectiveness
- General Purpose
- Reliability
- Safety [Ref. 5: p. 73].

The ORION program has been organized to investigate ten areas of satellite design:

- Attitude Control
- Computer Hardware Software and Data Storage
- Electrical Power
- Propulsion
- Structural Dynamics
- Structural Design
- Thermal Control
- Telemetry
- Reliability
- Space Environment [Ref. 1: p. 4]

As with most engineering design, it is impossible to design a system that will be truly generic, i.e., a design that will do all things for all people. The driving force behind any engineering design is the perceived need for a system to solve a specific problem. At this

stage in the design of the ORION satellite, there are several proposed missions for the satellite. Without a specific mission, the design is proceeding based on the original concept of a small multi-use satellite with the above listed concerns as a guide.

Engineering design usually involves many tradeoffs and compromises while trying to meet the overall specifications. Such is the case with ORION. There have been studies of several satellite design areas. Boyd, in Reference 3, discusses the history of small satellites, the origination of the ORION program and preliminary designs for the structure, propulsion and attitude control systems for the ORION satellite. Every decision concerning the mission or capabilities places restrictions and limits on the design of the satellite. The following sections describe the satellite based on decisions made up to this point and the baseline parameters for the telemetry system.

A. THE ORION SATELLITE

The ORION satellite is to be designed to provide fully autonomous operations of a 50 to 130 lbs. payload by providing:

- Propulsion for orbital insertion and station keeping
- Attitude control
- Telemetry
- Data processing
- Data storage
- Electrical power
- Thermal control

It will be capable of being launched from an extended "Get-Away-Special" cannister located in the cargo bay of the Space Shuttle, or from expendable launch vehicles. When launched from the Space Shuttle at an altitude of 135 nm, ORION will be capable of achieving orbits up to an 800 nm circular orbit or an elliptical orbit with an apogee of 2200 nm. [Ref. 1: pp. 2-3]

The ORION satellite is cylindrical with a diameter of 19 inches and height of 35 inches. The weight of the satellite will be approximately 250 to 275 lbs. Four stabilizing booms extend from the body of the satellite to provide spin stabilization about the longitudinal axis of the satellite with rotation rates anticipated to be between 30 and 100 revolutions per minute. Current configurations of the ORION satellite are shown in Figure 1 and Figure 2 on page 7. [Ref. 7]

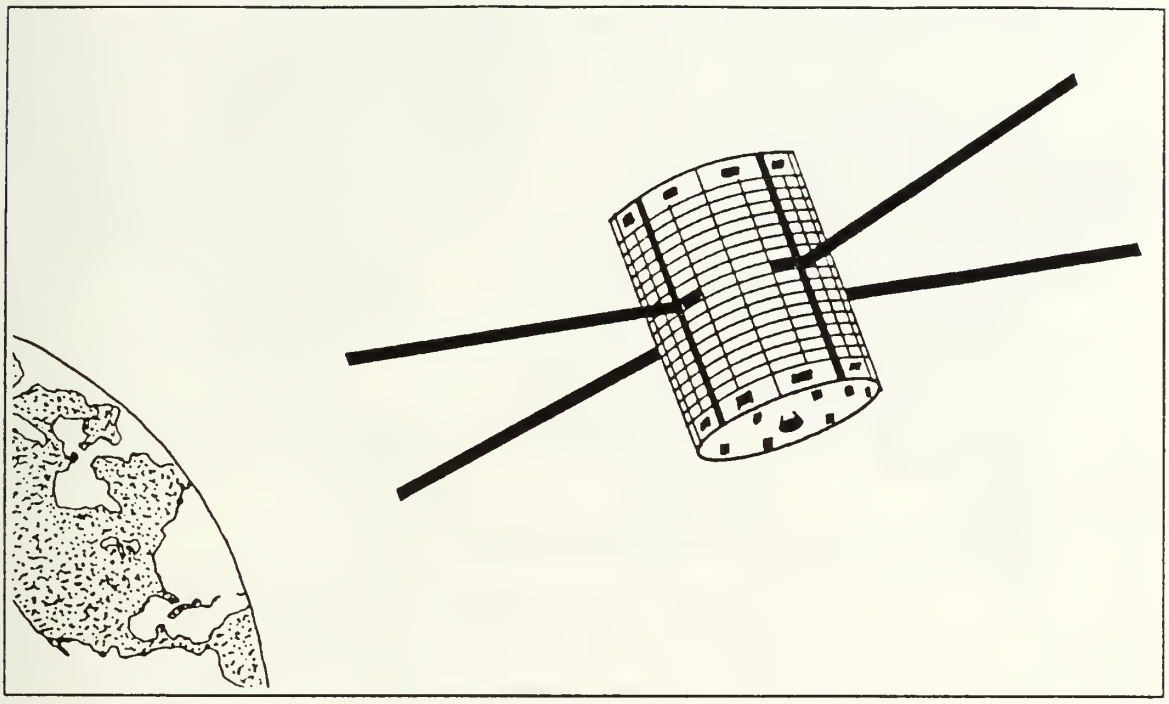

Figure 1. The ORION Satellite.

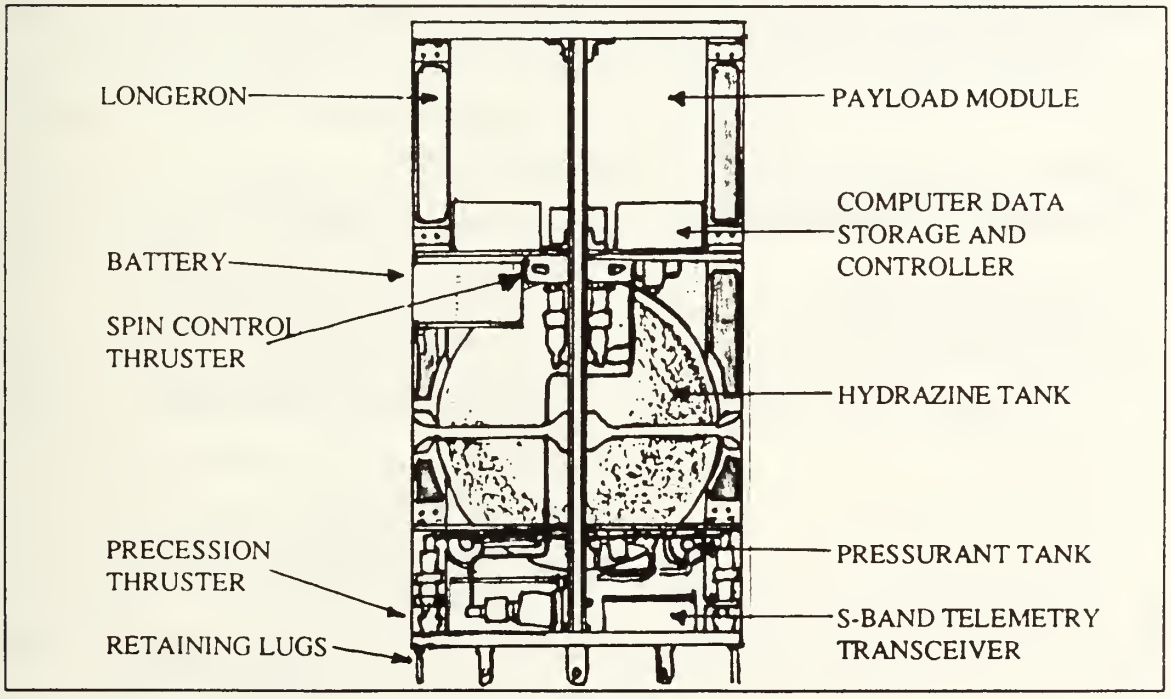

Figure 2. Cut-Away of the ORION Satellite.

B. THE TELEMETRY, TRACKING AND COMMAND SYSTEM

One of the design areas is the telemetry, tracking and command (TT&C) system. The TT&C system provides a means of controlling the satellite and communicating data between the satellite and the ground stations. The TT&C system will be composed of the following elements:

- A transmitter/receiver
- An RF combiner splitter assembly
- Antennas
- Encryption equipment(possibly) [Ref. 1: p. 9]

The following sections describe the ground station network and the space-ground link system.

1. The U.S. Air Force Satellite Control Network

The U.S. Air Force Satellite Control Network (AFSCN) has been selected to provide the control of the ORION satellite. It is tasked with providing tracking, telemetry and control functions for national space programs. The AFSCN is controlled by the Satellite Operations Center in Colorado Springs, Colorado and the Satellite Test Center in Sunnyvale, California. It operates twelve remote tracking stations, listed in Table 1, located at seven sites dispersed around the world as shown in Figure 3 on page 9. [Ref. 8 : pp. 1.2-1 to 1.2-2]

Table 1. AFSCN REMOTE TRACKING STATIONS.

Remote Tracking Station	Location
NHS-New Hampshire	Manchester, New Hampshire
VTS-Vandenberg AFB	Lompoc, California
HTS-Hawaii	Kaeha Point, Oahu, Hawaii
GTS-Guam	Guam
IOS-Indian Ocean	Mahe, Seychelles
TTS-Thule	Thule, Greenland
TCS-Oakhanger	Oakhanger, England

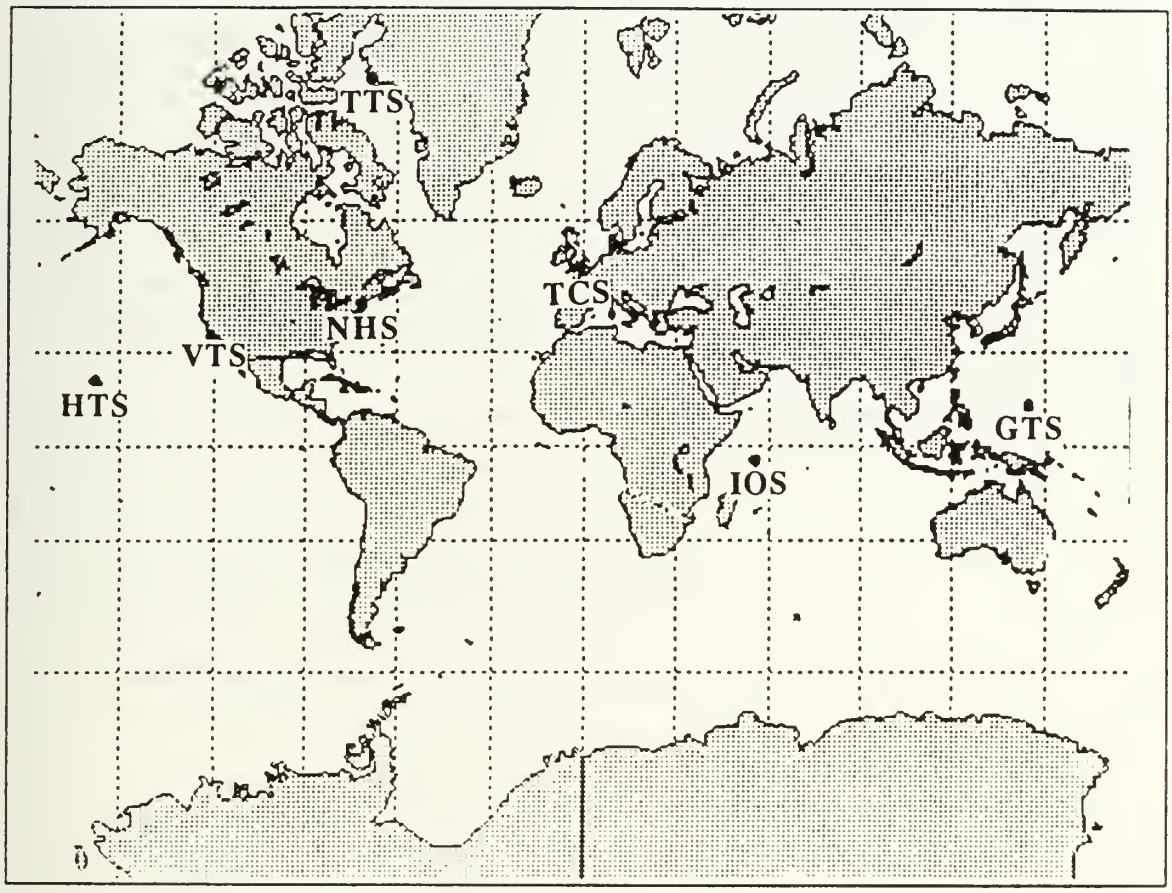

Figure 3. AFSCN Remote Tracking Station Locations.

The RTS are capable of tracking, receiving data, determining satellite position and commanding satellites as they pass within range.

The characteristics of signals which may be received from spacecraft by the RTSs are limited by the capabilities of the antenna systems in the AFSCN system. The list below indicates the minimum capabilities of the antennas in the AFSCN.

- Uplink Frequency - 1.75 to 1.85 Gigahertz
- Downlink Frequency - 2.2 to 2.3 Gigahertz
- Beamwidth - 0.55 degree +/- 0.25 degree
- Gain -
  - Uplink - 42.7 dB
  - Downlink - 47.0 dB (see Appendix A)
- Polarization - Right-Hand Circular (linearly polarized signals can be received at 3 dB below the RHCP level) [Ref. 8: pp. 2.2-2 to 2.2-10]

2. The U.S. Air Force Space-Ground Link System

The part of the AFSCN that communicates with satellites is called the Space-Ground Link System (SGLS). SGLS provides 20 uplink channels from 1.75 to 1.85 Gigahertz and 20 downlink frequency channels from 2.2 to 2.3 Gigahertz. The exact frequencies are given by Klements in Reference 6. The uplink channels are used for commanding satellites and the downlink channels are used for tracking and telemetry. The command information and psuedo-random noise (PRN) ranging information are frequency modulated (FM) onto the uplink channel. The uplink carrier spectrum is shown in Figure 4 [Ref. 8: p. 2.3-30].

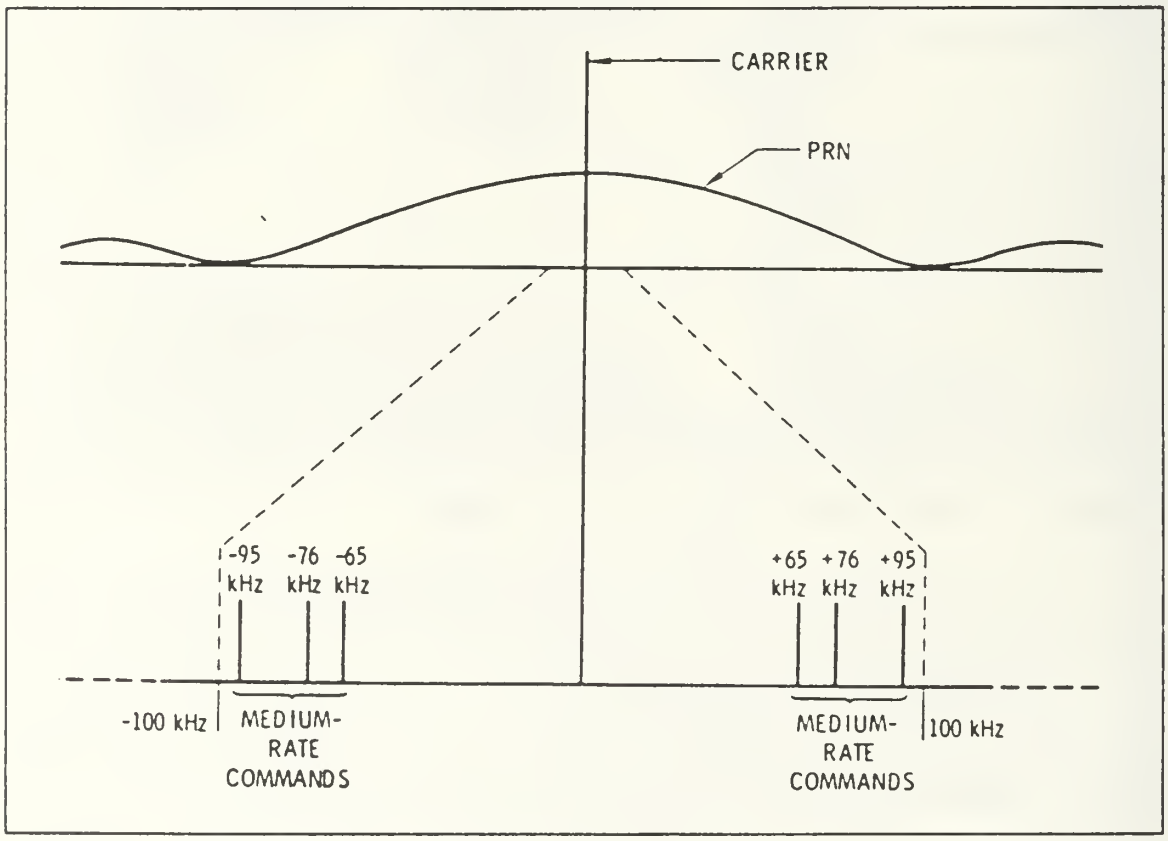

Figure 4. Typical Uplink Carrier Spectrum.

The downlink channels provide two downlink carriers which are received simultaneously at a ground station. The two downlink carriers are called Carrier 1 and Carrier 2, where Carrier 1 is a pilot signal for antenna autotracking, range rate tracking and low speed Pulse Code Modulation (PCM) or analog telemetry. The Carrier 1 services may include one or two subcarriers, downlink PRN ranging and command data or a single Pulse

Code Modulation Pulse Shift Keying (PCM/PSK) direct modulation service. The multi-tone modulation scheme is known as "Frequency Modulation of a Carrier by a Frequency-Modulated Subcarrier" (FM FM). Carrier 2 is fixed 5 Megahertz below the frequency of Carrier 1. Carrier 2 is frequency modulated by a single intermediate frequency that has telemetry data encoded. Any number of PCM schemes may be used to encode telemetry data with data rates from 128 kbps to 1.024 Mbps. [Ref. 8: p. 2.3-1 to 2.3-35]

It has been proposed to use an S-band transponder manufactured by Motorola for the telemetry system on the ORION satellite. This transponder is currently being used in a number of satellites. It is capable of providing 2.0 Watts of RF power into a 50 Ohm load with a VSWR of less than 2:1. The receiver sensitivity is -104 dBm [Refs. 2: p. 13, 9: p. 4]. Carrier 2, being used for telemetry, requires more power to be able to pass high bit rates. In most satellites, a separate power amplifier is used to increase the power of the Carrier 2 signal up to 10 or 20 Watts.

III. ORION SATELLITE ANTENNA REQUIREMENTS

Antenna synthesis is a process where the desired radiation pattern is initially specified, followed by the development of a method or combination of methods to arrive at an antenna configuration which produces a radiation pattern that approximates the desired pattern. The antenna variables that an engineer has to work with are listed below.

- Radiation Pattern
  - Omnidirectional
  - Directional
- Continuity
  - Continuous
  - Discrete-Array
- Shape
  - Linear
  - Planar
  - Conformal
  - Three-Dimensional
- Size
- Frequency of Operation
- Bandwidth
- Impedance
- Polarization Properties
- Gain
- Power Handling Capacity
- Mass
- Cost

There are other considerations that affect the design of the antenna. The integration of the antenna into the satellite structure will determine the required structural loading and placement of components of the TT&C system. [Ref. 10: pp. 520-521]

Antenna synthesis methods are categorized by antenna type. Antenna types usually fall into one of the following categories:

- Monopoles and Dipoles
- Loop Antennas
- Microstrip Antennas
- Slot Antennas
- Leaky-Wave Antennas
- Long-Wire Antennas
- Helical Antennas
- Horn Antennas
- Lens Antennas
- Reflector Antennas
- Aperture Antennas

Antenna synthesis methods are different for the different antenna types [Ref. 11: pp. v-vi]. A general solution to the antenna problem would provide the antenna type and excitation that gives a good approximation to the desired radiation pattern while meeting all of the other specifications. Unfortunately, no general solution exists. There is no single method that will give the best radiation pattern approximation while satisfying all of the other requirements. [Ref. 10: pp. 520-521]

A. ORION ANTENNA SPECIFICATIONS

1. ORION Antenna Radiation Pattern

The ORION satellite will need an omnidirectional radiation pattern during deployment of the satellite into its final orbit. An omnidirectional radiation pattern may also be used for the TT&C system as its primary mode, although a directional radiation pattern would be more desirable.

2. Continuity

There is no specified requirement for the ORION antenna as far as continuity is concerned. It can be either continuous or discrete.

3. Shape

The shape of the antenna has not been specified but the antenna will need to be compatible with the satellite physical configuration. The ORION satellite fills the extended GAS cannister, so the antenna will either have to be a deployable antenna that

fits inside the satellite for launch and deployment or must be a conformal antenna that is integrated into the structure of the satellite.

4. **Size**

The size of the antenna is relatively unimportant other than it must fit in the satellite or is conformal. If the antenna is to be a deployable antenna, it will have to compete for volume with the payload or another subsystem of the satellite. Conversely, a conformal antenna size is constrained by the dimensions of the satellite. The cylindrical body of the ORION satellite is covered by solar cells. If a conformal array that fits around the body of the satellite is to be used, a study will be needed to determine if the amount of power generated by the available solar cells will be adequate. The preliminary size constraint is .15 cubic feet [Ref. 5: p. 128].

5. **Frequency of Operation**

Since the ORION satellite will operate with SGLS, the frequencies are:

- Uplink - 1750 to 1850 Megahertz
- Downlink - 2200 to 2300 Megahertz

6. **Bandwidth**

For a single antenna to cover the entire SGLS frequency range, it must have a bandwidth of 550 Megahertz. For many antenna types, a 550 Megahertz bandwidth is difficult to achieve. It is possible to have 2 antennas, an uplink antenna and a downlink antenna. For the SGLS frequencies, this translates into a 100 Megahertz bandwidth for each antenna.

7. **Impedance**

The Motorola S-band transponder is designed to deliver RF energy to a 50 Ohm load. Therefore the impedance of the antenna should be 50 Ohms.

8. **Polarization Properties**

The antennas in the AFSCN are designed to receive right-hand circularly polarized signals. Linearly polarized signals can be received by the remote tracking station antennas at 3 dB below signals that are right-hand circularly polarized.

9. **Gain**

The satellite antenna gain is dependent upon many factors. The frequency, bandwidths, slant range (satellite to ground station distance), and data rates are a few of these factors. All of these factors are used in a satellite link equation to determine the required satellite antenna gain necessary for the satellite to communicate with the

ground stations. As stated earlier, the ORION satellite is to be capable of 800 nm circular orbits and elliptical orbits with apogee altitudes up to 2200 nm. During orbit insertion, the orientation of the satellite will vary. For the ground stations to maintain control over the satellite, the satellite must be capable of receiving command signals from almost any direction relative to the satellite. Therefore, the radiation pattern of the uplink antenna needs to be as close to omnidirectional as possible. The gain from a truly omnidirectional antenna is 0 dB in all directions. Realizable antennas approximating omnidirectional coverage usually have ripples and/or holes in their radiation patterns where the gain is much less than 0 dB in some directions while being greater than 0 dB in other directions. Once the satellite is stabilized in its final orbit, it is possible to have directional antennas that point toward ground stations. The gain in the desired direction is significantly higher than an omnidirectional antenna.

Boyd, in Reference 5, has a table that shows that most small satellites have been used in circular orbits with altitudes between 200 to 500 nm, with inclinations between 60° to 120° . For the purposes of this design, a spin-stablized satellite with its spin axis perpendicular to the plane of the satellite orbit will be assumed. This orientation is the one that is most used for spin-stabilized satellites. Appendix A examines the gain requirements for the ORION satellite antenna system and the assumptions on which the gain requirements are based. The gain requirements are dependent upon the altitude of the satellite and different information signals contained in the uplink and downlink carriers. Table 2 in section B shows the gain requirements for the altitude capabilities for the ORION satellite, as computed in Appendix A.

10. Power Handling Capacity

The Motorola transponders are capable of delivering 2 Watts to the antenna, but the Carrier 2 signal is boosted to 10 Watts so the antenna must be capable of handing 10 Watts.

11. Mass

The mass of the antenna has not been broken out separately from the entire TT&C system. The entire TT&C system has a preliminary mass allocation of 10 lb [Ref. 5: p. 127]. This figure will have to be revised as the mass of the Motorola transponder has a mass of 7.7 lbs. That leaves only 2.3 lbs for the Carrier 2 power amplifier, feed systems and antenna. As an estimate for the mass of the antenna, a mass of 4 lbs will be used.

12. Cost

Mosier, in Reference 1, has estimated the cost of antennas for a single satellite to be $60,000. Ball Aerospace Corporation has designed, tested and flown several microstrip patch antennas on satellites. A discussion with their antenna design engineers revealed that to fully design, build, test and space qualify an antenna, the cost is approximately $250,000. Once an antenna has been developed, the cost of follow on antennas of this type is approximately $20,000 each. The engineers also hinted that some of their designs may be adequate for use on a satellite such as ORION.

B. SUMMARY OF ORION ANTENNA SPECIFICATIONS

- Radiation Pattern -
  - Omnidirectional - for orbit insertion
  - Directional - for normal operation
- Continuity - no firm specification
- Shape - no firm specification
- Size - less than or equal to .15 cubic feet
- Frequency of Operation -
  - Uplink - 1750 to 1850 Megahertz
  - Downlink - 2200 to 2300 Megahertz
- Bandwidth -
  - Single Antenna - 550 Megahertz
  - Dual Antenna -
    - Uplink - 100 Megahertz
    - Downlink - 100 Megahertz
- Impedance - 50 Ohms
- Polarization -
  - First Choice - Right-Hand Circular
  - Second Choice - Linear

- Gain -

Table 2. GAIN REQUIREMENTS FOR THE ORION SATELLITE.

Altitude in nm	Slant Range in nm	Uplink Gain in dB	Downlink Gain in dB
100	835.93	-16.4	-7.5
200	1190.62	-13.3	-4.4
300	1468.45	-11.5	-2.6
400	1707.38	-10.2	-1.3
500	1921.96	-9.2	-0.3
600	2119.60	-8.3	0.6
700	2304.67	-7.6	1.3
800	2479.98	-6.9	1.9
900	2647.46	-6.4	2.5
1000	2808.53	-5.9	3.0
1100	2964.23	-5.4	3.5
1200	3115.35	-5.0	3.9
1300	3262.55	-4.6	4.3
1400	3406.32	-4.2	4.7
1500	3547.08	-3.9	5.0
1600	3685.18	-3.5	5.4
1700	3820.91	-3.2	5.7
1800	3954.51	-2.9	6.0
1900	4086.19	-2.6	6.3
2000	4216.13	-2.3	6.5
2100	4344.48	-2.1	6.8
2200	4471.39	-1.8	7.1

  - Uplink Gain Specification - -1.8 dB (2200 nm altitude)
  - Downlink Gain Specification - 7.1 dB (2200 nm altitude)
- Power Handling Capacity -
  - Minimum - 2 Watts
  - Maximum - 10 Watts
- Mass -less than or equal to 4 lbs
- Cost - less than or equal to $60,000

IV. MICROSTRIP PATCH ARRAY ANTENNA FUNDAMENTALS

An array antenna is composed of individual radiating elements arranged in a spatial distribution. The purpose of an array antenna is to achieve specific values of directivity or beamwidth which are not possible with a single antenna. By choosing appropriate excitation of amplitude and phase and the spatial orientation of the individual elements of the array, the antenna radiation pattern can be shaped as necessary.

Consider a single antenna located at the origin of the spherical coordinate system as shown in Figure 5.

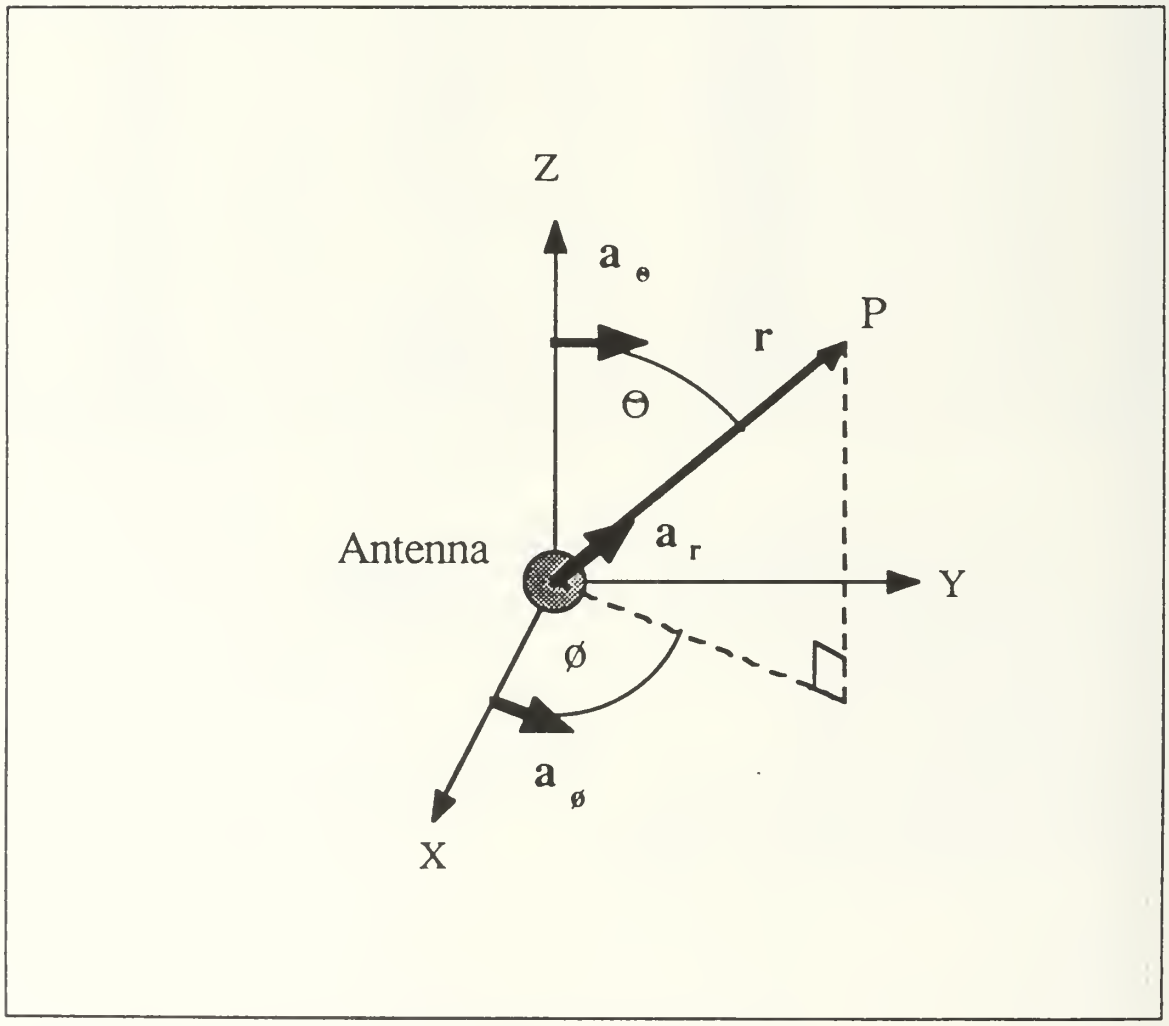

Figure 5. Single Antenna Spherical Coordinate System.

The electric field generated by the antenna at the far-field point, P, can be expressed as:

$$\mathbf{E}(\mathbf{r}) = E_\theta(r, \theta, \phi)\mathbf{a}_\theta + E_\phi(r, \theta, \phi)\mathbf{a}_\phi \tag{4.1}$$

where,

$$E_\theta(r, \theta, \phi) = \mathrm{f}_\theta(\theta, \phi)\frac{e^{-jkr}}{r} \tag{4.2}$$

$$E_\phi(r, \theta, \phi) = \mathrm{f}_\phi(\theta, \phi)\frac{e^{-jkr}}{r} \tag{4.3}$$

$$k = \frac{2\pi}{\lambda} \tag{4.4}$$

The terms f_θ and f_ϕ are components of the complex radiation vector which embody all angular dependence and polarization characteristics of the antenna.

$$\mathbf{f} = \mathrm{f}_\theta(\theta, \phi)\mathbf{a}_\theta + \mathrm{f}_\phi(\theta, \phi)\mathbf{a}_\phi \tag{4.5}$$

Equation (4.1) applies only when the point P is in the far field. The far field conditions are:

$$r > \frac{2D^2}{\lambda}$$

$$r \gg D$$

$$r \gg \lambda$$

where,

D is the maximum dimension of the antenna,

r is the distance to the field point,

λ is the operating frequency free space wavelength.

If the antenna is moved from the reference point as shown in Figure 6 on page 20, the phase component changes. The change can be expressed as $e^{jk\mathbf{a}_r \cdot \mathbf{r}'}$.

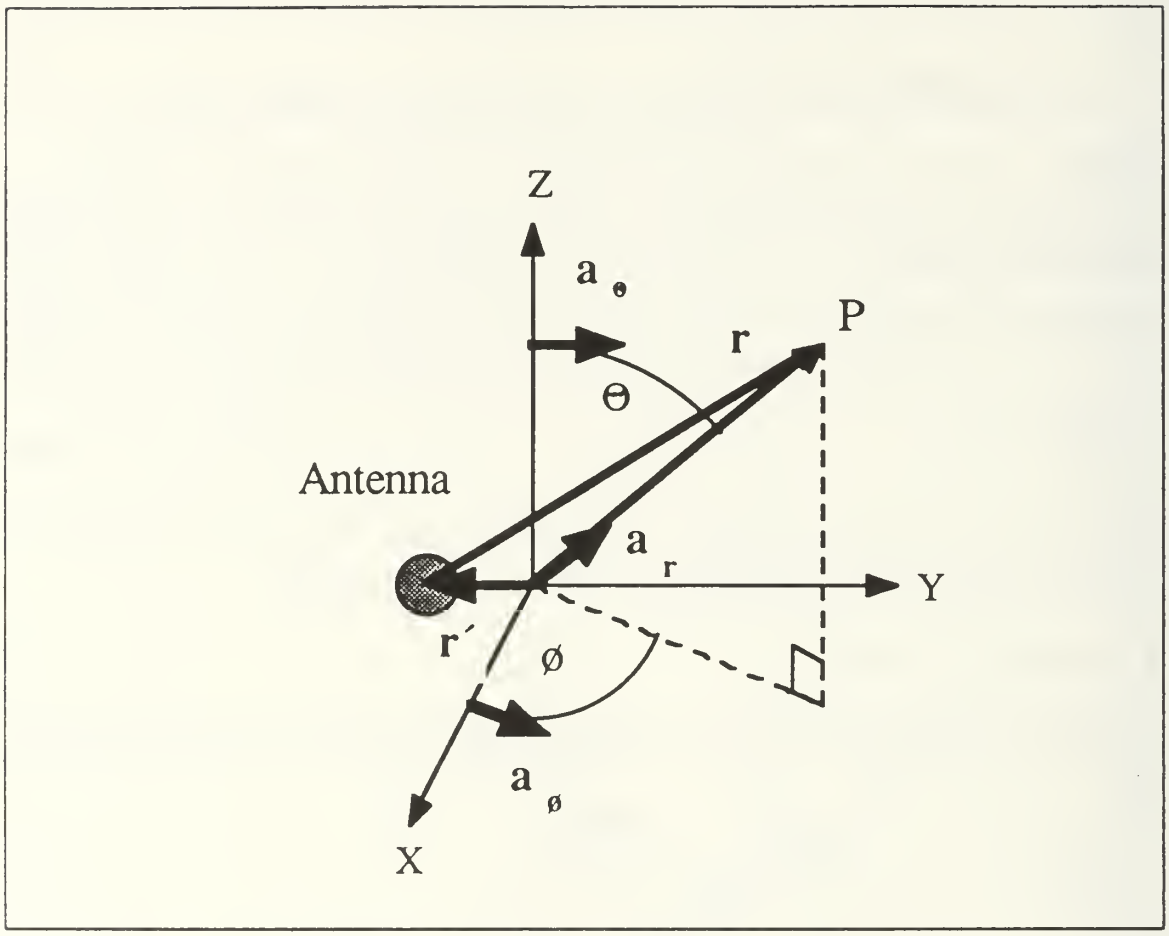

Figure 6. Antenna Shift from Reference Point.

The electric field components in the far-field become:

$$E_\theta(r, \theta, \phi) \approx f_\theta(\theta, \phi) \frac{e^{-jkr}}{r} e^{jk\mathbf{a}_r \cdot \mathbf{r}'} \tag{4.6}$$

$$E_\phi(r, \theta, \phi) \approx f_\phi(\theta, \phi) \frac{e^{-jkr}}{r} e^{jk\mathbf{a}_r \cdot \mathbf{r}'} \tag{4.7}$$

The electric field radiated from an array of individual antennas located at points $\mathbf{r}'_1$, $\mathbf{r}'_2$, etc., is obtained by summing the electric fields generated by each antenna.

$$\mathrm{E}(\mathrm{r}) \approx \frac{e^{-jkr}}{r} \sum_{n=1}^{N} \mathbf{f}_n(\theta, \phi) e^{jk\mathbf{a}_r \cdot \mathbf{r}'_n} \tag{4.8}$$

To develop the radiation pattern for a microstrip patch circular array antenna, it is necessary to first describe the attributes of a single microstrip patch antenna and then describe the circular spatial relationship of the individual microstrip patches. [Ref. 12: pp. 48-49]

A. THE MICROSTRIP PATCH ANTENNA

A microstrip patch antenna consists of a radiating patch on one side of a dielectric substrate and a ground plane on the other side as shown in Figure 7 [Ref. 3: pp. 2-3].

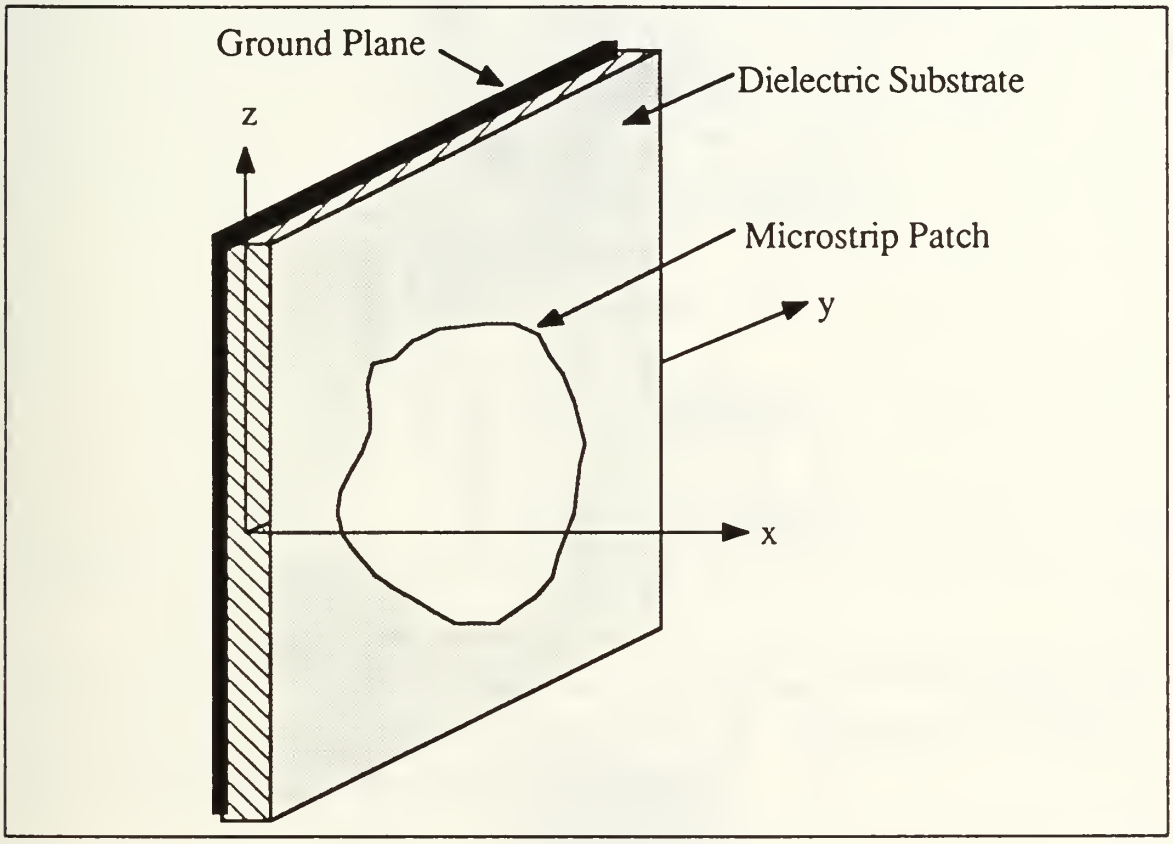

Figure 7. Microstrip Patch Antenna.

The radiating patch is normally made of copper and/or gold plating and can be any shape. The dielectric substrate can be made from many materials. The choice of substrate material is heavily influenced by a number of factors such as the dielectric constant (ε_r), frequency, thermal coefficients, and physical properties. Bahl and Bhartia discuss substrate selection in more detail in Reference 3. To simplify the analysis of microstrip patches, simple shapes such as rectangles and circles are used for the radiating patch.

To understand the radiation mechanism of a microstrip patch antenna, consider a rectangular patch where the thickness is small compared to the wavelength as shown in Figure 8. The feed of the microstrip patch determines the polarization properties. The patch shown is for a linearly polarized patch.

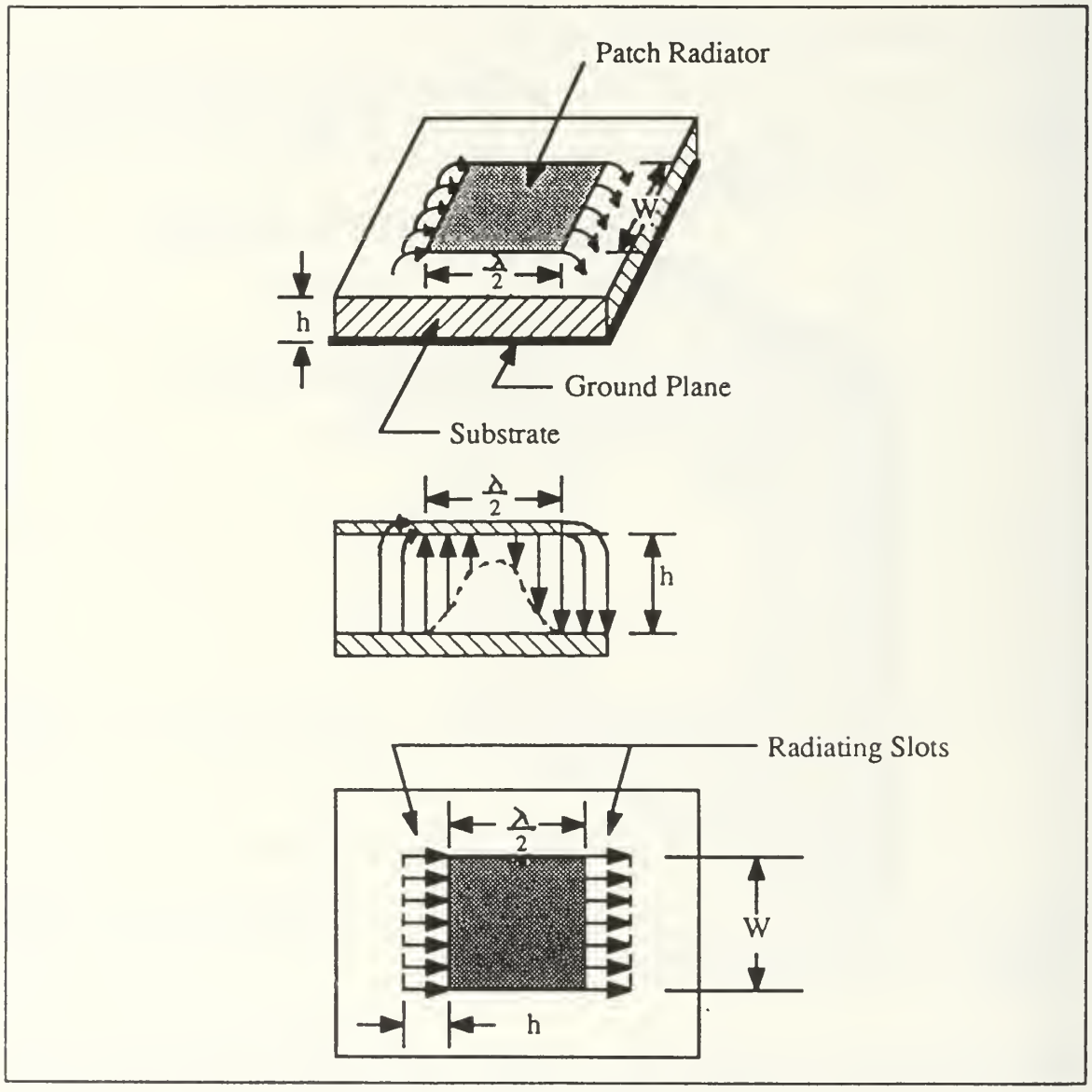

Figure 8. Rectangular Microstrip Patch Antenna.

Assuming the electric field is constant along the width, *W*, and the thickness, *h*, the electric field can be represented by the arrows in the figure. The electric field varies

along the length of the patch in an approximately sinusoidal manner. Radiation comes from the fringing fields at the open circuited edges of the patch.

Consider a radiating slot of a microstrip patch antenna with a coordinate system as shown in Figure 9.

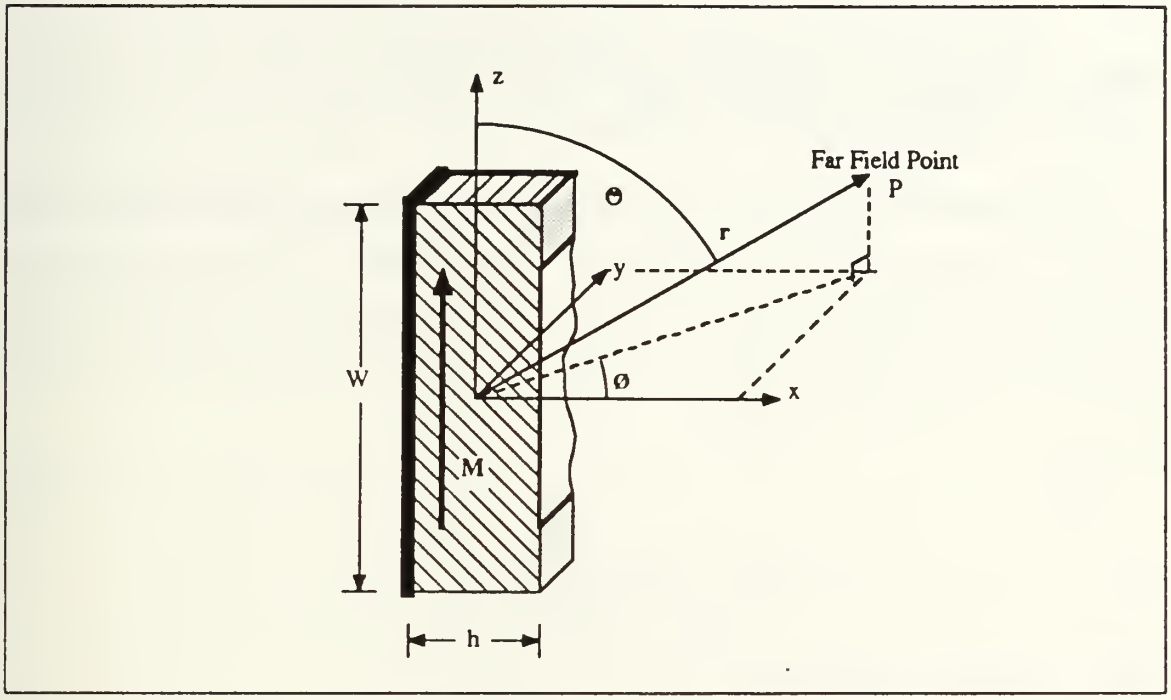

Figure 9. Microstrip Patch Antenna Radiating Slot.

Assuming the $h \ll \lambda$, the electric field in the patch width, W, may be replaced by an equivalent magnetic current, M. The field radiated by a single slot is the same as a magnetic dipole that has a magnetic current of:

$$\mathbf{M} = 2\frac{V}{h}\mathbf{a}_z \tag{4.9}$$

where

V is the voltage across the slot.

The factor of 2 arises from the positive image of M near the ground plane. In the far field, the electric field components are:

$$E_\theta(r, \theta, \phi) = 0 \tag{4.10}$$

$$E_{\phi}(r, \theta, \phi) = -j2VWk \frac{e^{-jkr}}{4\pi r} F(\theta, \phi) \tag{4.11}$$

where,

$$F(\theta, \phi) = \frac{\sin\left(\frac{kh}{2} \sin\theta \cos\phi\right)}{\frac{kh}{2} \sin\theta \cos\phi} \frac{\sin\left(\frac{kW}{2} \cos\theta\right)}{\frac{kW}{2} \cos\theta} \sin\theta \tag{4.12}$$

The dimensions and physical characteristics of the microstrip patch antenna determine the operating frequency and bandwidth of the antenna. The following equations are engineering approximations for the dimensions of the patch and the theory behind the equations is beyond the scope of this presentation. The thickness of the antenna can be found by the following equation:

$$h = \frac{BW}{128f^2} \tag{4.13}$$

where

h is the thickness of the antenna in inches.

BW is the bandwidth in Megahertz

f is the operating frequency in Gigahertz [Ref. 11: pp. 7-2 to 7-8].

The length, L, determines the operating frequency of the antenna and is usually a little less that half a wavelength in the dielectric substrate.

$$L = 0.49 \frac{\lambda_0}{\sqrt{\varepsilon_r}} \tag{4.14}$$

where

λ_0 is the free space wavelength.

The width, W, of the patch can be found from:

$$W = \frac{\lambda}{2} \sqrt{\frac{2}{\varepsilon_r + 1}} \tag{4.15}$$

For a circularly polarized patch, the feed produces variations of the fields along the width of the patch. The modeling of the circularly polarized patch is much more involved and beyond the scope of this thesis. The rest of this chapter covers a linearly polarized patch. [Ref 3: p. 57]

B. CIRCULAR ARRAY FUNDAMENTALS

The circular array describes the spatial relationships of the radiating elements with respect to a reference point. Consider a circular array of N radiating elements (shown as dots) in Figure 10.

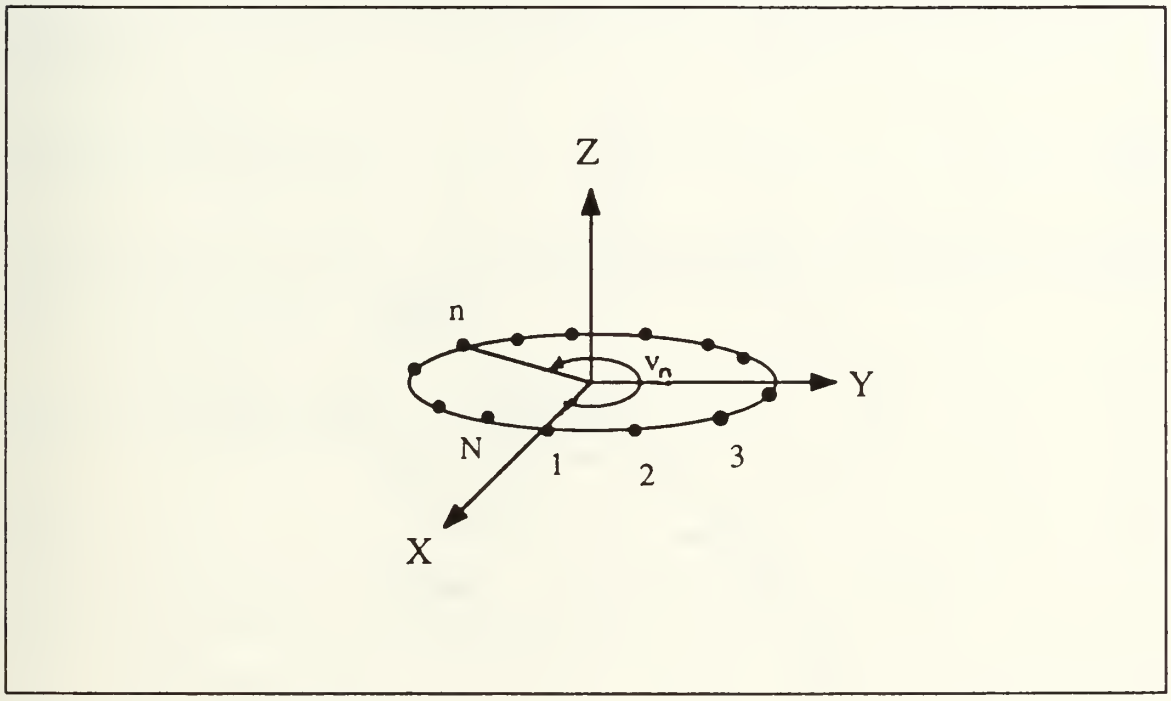

Figure 10. Circular Array.

If the reference point of the antenna is the origin of the coordinate system shown, the location of the nth element is:

$$r'_n = a\cos v_n \mathbf{a}_x + a\sin v_n \mathbf{a}_y \tag{4.16}$$

where,

$$v_n = \frac{2\pi}{N}(n-1) \tag{4.17}$$

This equation for the locations of the radiating elements assumes that the elements are equally spaced around the ring. That is not the case with the microstrip patches, since each patch has 2 radiating slots, one located on each side of the patch, and the spacing between the patches may not be the same as the length of each patch. The slots on the leading edge of each patch are equally spaced, as are the slots on the trailing edge. The leading edge slots can be considered as one array and the trailing edge slots may be considered another array. Figure 11 shows the relationship between the leading edge slot and the trailing edge slot of a patch.

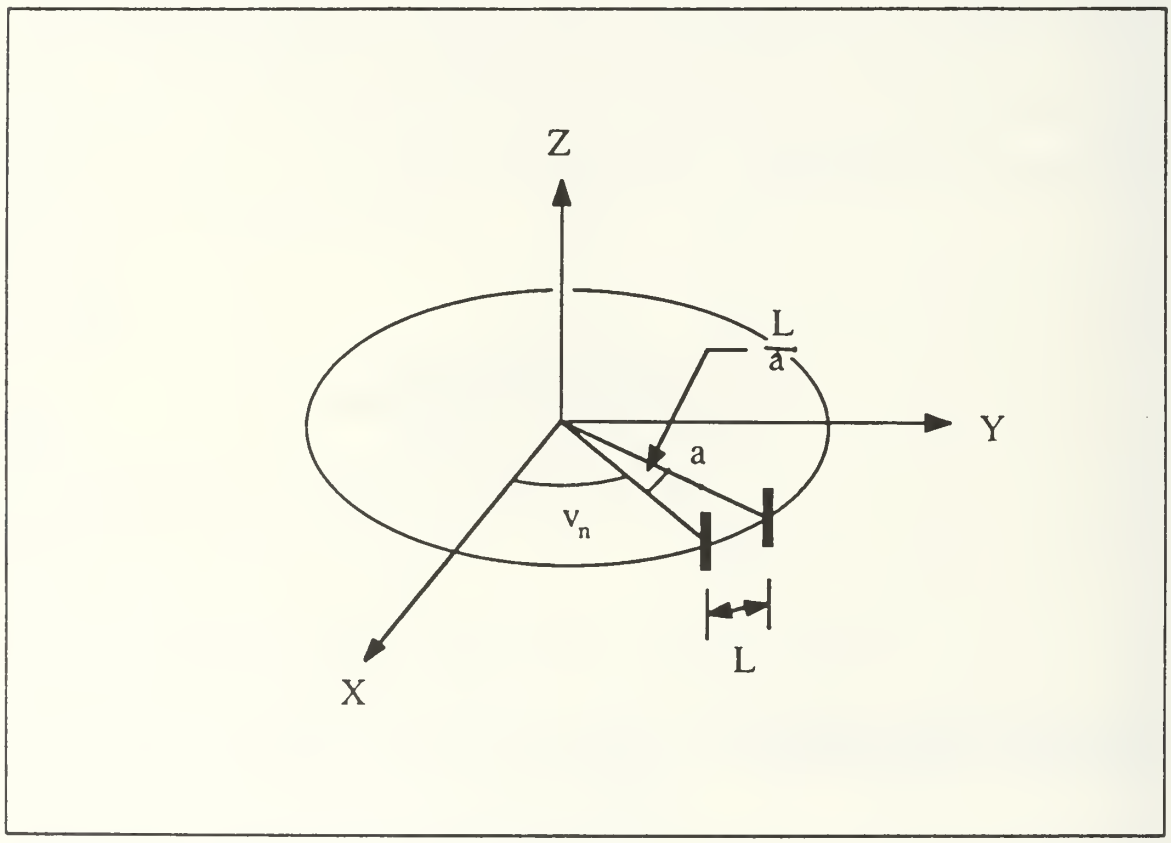

Figure 11. Leading and Trailing Edge Slot Geometry.

The location of the trailing edge slot of the *n*th patch is:

$$r'_n = a\cos\left(v_n + \frac{L}{a}\right)a_x + a\sin\left(v_n + \frac{L}{a}\right)a_y \qquad (4.18)$$

The microstrip patch antenna can now be considered as the combination of the leading edge slot array and the trailing edge slot array. Equate equations (4.2) and (4.10):

$$E_\theta(r, \theta, \phi) = \mathrm{f}_\theta(\theta, \phi)\frac{e^{-jkr}}{r} = 0$$

Therefore,

$$\mathrm{f}_\theta(\theta, \phi) = 0 \tag{4.19}$$

Equating equations (4.3) and (4.11):

$$E_\phi(r, \theta, \phi) = \mathrm{f}_\phi(\theta, \phi)\frac{e^{-jkr}}{r} = -j2VWk\frac{e^{-jkr}}{4\pi r}F(\theta, \phi)$$

Therefore,

$$\mathrm{f}_\phi(\theta, \phi) = -\frac{jVWk}{2\pi}F(\theta, \phi) \tag{4.20}$$

Substituting equations (4.18), (4.19) and (4.20) into equation (4.8) produces the electric field for the leading edge slot array.

$$\mathbf{E}_{\mathrm{LE}}(\mathbf{r}) = \frac{e^{-jkr}}{r}\sum_{n=1}^{N}\mathrm{f}_{\phi n}(\theta, \phi)\mathbf{a}_\phi e^{jk\mathbf{a}_r \cdot \mathbf{r}'_n}$$

Now,

$$\begin{aligned}\mathbf{a}_r \cdot \mathbf{r}'_n &= (\cos\theta\sin\phi\mathbf{a}_x + \sin\theta\sin\phi\mathbf{a}_y + \cos\theta\mathbf{a}_z)\cdot(a\cos v_n\mathbf{a}_x + a\sin v_n\mathbf{a}_y)\\ &= a\cos\theta\sin\phi\cos v_n + a\sin\theta\sin\phi\sin v_n\\ &= a\sin\theta\cos(\phi - v_n)\end{aligned}$$

The magnitude of the electric field is:

$$E_{\mathrm{LE}}(r, \theta, \phi) = \frac{e^{-jkr}}{r}\sum_{n=1}^{N}\left(\frac{-jV_nWk}{2\pi}\right)F(\theta, \phi)e^{jka\sin\theta\cos(\phi - v_n)} \tag{4.21}$$

Let the patch excitation coefficient, a_n, be:

$$a_n = -\frac{jV_nWk}{2\pi}$$

Finally, the equation for the leading edge slot array is:

$$E_{LE}(r, \theta, \phi) = \frac{e^{-jkr}}{r} \sum_{n=1}^{N} F(\theta, \phi) a_n e^{jka \sin\theta \cos(\phi - v_n)} \tag{4.22}$$

Following the same derivation for the trailing edge slot array, the electric field is:

$$E_{TE}(r, \theta, \phi) = \frac{e^{-jkr}}{r} \sum_{n=1}^{N} F(\theta, \phi) a_n e^{jka \sin\theta \cos\left(\phi - v_n - \frac{L}{a}\right)} \tag{4.23}$$

The total electric field is:

$$\begin{aligned} E(r, \theta, \phi) &= E_{LE} + E_{TE} \\ &= \frac{e^{-jkr}}{r} \sum_{n=1}^{N} F(\theta, \phi) a_n \left[e^{jka \sin\theta \cos(\phi - v_n)} + e^{jka \sin\theta \cos\left(\phi - v_n - \frac{L}{a}\right)} \right] \\ &= f_n(\theta, \phi) \frac{e^{-jkr}}{r} \end{aligned} \tag{4.24}$$

The radiation pattern for the antenna is defined as :

$$f(\theta, \phi) = \sum_{n=1}^{N} F(\theta, \phi) a_n \left[e^{jka \sin\theta \cos(\phi - v_n)} + e^{jka \sin\theta \cos\left(\phi - v_n - \frac{L}{a}\right)} \right] \tag{4.25}$$

[Ref. 10: p. 27]

C. OMNIDIRECTIONAL RADIATION PATTERN

This circular array antenna can produce an approximation to an omnidirectional radiation pattern in the roll plane ($\theta = \frac{\pi}{2}$) of the satellite, when the phasing of the input signal is fed to the patches correctly. For an omnidirectional radiation pattern, the excitation coefficient must be:

$$a_n = e^{-j\left(2\pi \frac{v}{N}\right)n} \tag{4.26}$$

where the phases of excitation decrease uniformly around the circular array so that the total decrease in phase is an integral multiple υ of 2π [Ref. 13: p. 164]. The final form for an omnidirectional array antenna radiation pattern is:

$$f(\theta, \phi) = \sum_{n=1}^{N} F(\theta, \phi) e^{\left(-j\frac{2\pi\upsilon}{N}\right)n} \left[e^{jka\sin\theta\cos(\phi - v_n)} + e^{jka\sin\theta\cos\left(\phi - v_n - \frac{L}{a}\right)} \right] \tag{4.27}$$

D. DIRECTIVE GAIN PATTERN

The directive gain of an antenna is defined as:

$$D(\theta, \phi) = \frac{U(\theta, \phi)}{U_{ave}} \tag{4.28}$$

where,

$$U(\theta, \phi) = \frac{|f(\theta, \phi)|^2}{2\eta_0} \tag{4.29}$$

and η_0 is the free space impedance.

$$\eta_0 = 120\pi \text{ Ohms} \tag{4.30}$$

$U(\theta, \phi)$ is called the radiation intensity, which is the power radiated in a given direction per unit solid angle. Radiation intensity is in units of Watts per steradian [Ref. 10: p. 33]. The average radiation intensity can be expressed as:

$$U_{ave} = \frac{1}{4\pi}\int_0^{2\pi}\int_0^{\pi} U(\theta, \phi) d\Omega = \frac{1}{4\pi}\int_0^{2\pi}\int_0^{\pi} \frac{|f(\theta, \phi)|^2}{2\eta_0} \sin\theta d\theta d\phi \tag{4.31}$$

The final form of the directive gain equation is:

$$D(\theta, \phi) = \frac{|f(\theta, \phi)|^2}{\frac{1}{4\pi}\int_0^{2\pi}\int_0^{\pi} |f(\theta, \phi)|^2 \sin\theta d\theta d\phi} \tag{4.32}$$

This equation is valid for both the omnidirectional and directional radiation patterns and will produce the gain figures that will be compared to the antenna specifications in Chapter III.

E. DIRECTIONAL ANTENNA RADIATION PATTERN

To produce an array antenna that can point in a specified direction, start with equation (4.26). To produce a directional radiation pattern the excitation coefficient, a_n, is:

$$a_n = e^{-jka \sin\theta_0 \cos(\phi_0 - \nu_n)} \quad \text{for the leading edge slots} \tag{4.33}$$

and

$$a_n = e^{-jka \sin\theta \cos\left(\phi_0 - \nu_n - \frac{L}{a}\right)} \quad \text{for the trailing edge slots.} \tag{4.34}$$

The desired radation direction is θ_0, ϕ_0. [Ref. 13: p. 165]

Substituting equation (4.33) into equation (4.25), the radiation pattern for a directional antenna is:

$$f(\theta, \phi) = \sum_{n=1}^{N} F(\theta, \phi) \left\{ e^{jka[\sin\theta \cos(\phi - \nu_n) - \sin\theta_0 \cos(\phi_0 - \nu_n)]} + e^{jka\left[\sin\theta \cos\left(\phi - \nu_n - \frac{L}{a}\right) - \sin\theta_0 \cos\left(\phi_0 - \nu_n - \frac{L}{a}\right)\right]} \right\} \tag{4.35}$$

V. PRELIMINARY PHYSICAL DESIGN

This chapter applies the fundamentals in Chapter IV to the ORION satellite to determine the feasibility of a microstrip patch array antenna system. The main drawback to microstrip patch antennas, in this kind of application, is the narrow bandwidth of the antenna. The bandwidth is usually less than 4% of the operating frequency. The bandwidth requirement determines the thickness of the patch according to equation (4.13). For a bandwidth of 550 Megahertz, which covers both the uplink and downlink frequency bands, the thickness would have to be:

$$h = \frac{BW}{128f^2} = \frac{550}{128(2.025)^2} = 1.05 \text{ inches} = 2.66 \text{ centimeters}$$

Discussions with antenna design engineers at Ball Aerospace Corporation revealed that the thickness of realizable microstrip patches are less than ½ inch. Therefore, it is necessary to consider an uplink antenna and a downlink antenna for the ORION satellite.

A. ORION SATELLITE UPLINK ANTENNA DESIGN

The design of the uplink antenna is accomplished by first determining the physical dimensions of the individual microstrip patches. Once those dimensions have been determined, it is necessary to specify how many patches are needed for the uplink array. The number of patches that meet the physical constraints of the dimensions of the satellite and patch spacing requirements may vary between a minimum and maximum number of patches. Radiation patterns are then developed for various combinations of the number of patches and the phasing of each patch. The combinations that produce fair approximations of an omnidirectional radiation pattern are then selected for further investigation by developing the directive gain radiation patterns.

1. Uplink Microstrip Patch Dimensions

The first dimension to find is the thickness, h, of the microstrip patch. The thickness is found from equation (4.13).

$$h = \frac{BW}{128f^2}$$

The bandwidth for the uplink is 100 Megahertz. For design purposes, the frequency is the middle frequency of the uplink band.

f = 1800 Megahertz = 1.8 Gigahertz

$$h = \frac{100}{128(1.8)^2} = 0.24 \text{ inch} = 0.61 \text{ centimeters}$$

The length, L, of a microstrip patch is calculated using equation (4.14).

$$L = 0.49 \frac{\lambda_0}{\sqrt{\varepsilon_r}}$$

The free space wavelength, λ_0, of the center frequency (1800 Megahertz) of the uplink band is:

$$\lambda_0 = \frac{c}{f} = \frac{2.997925 \times 10^8}{1800 \times 10^6} = 0.1666 \text{ meters} = 16.66 \text{ centimeters.}$$

The dielectric constant, ε_r, is dependent upon the dielectric substrate material. There is a relationship between the dielectric constant and the bandwidth of the microstrip patch as shown in Figure 12. The bandwidth, as a percentage of the operating frequency, is greater for substrates with low dielectric constants. [Ref. 3: p. 63]

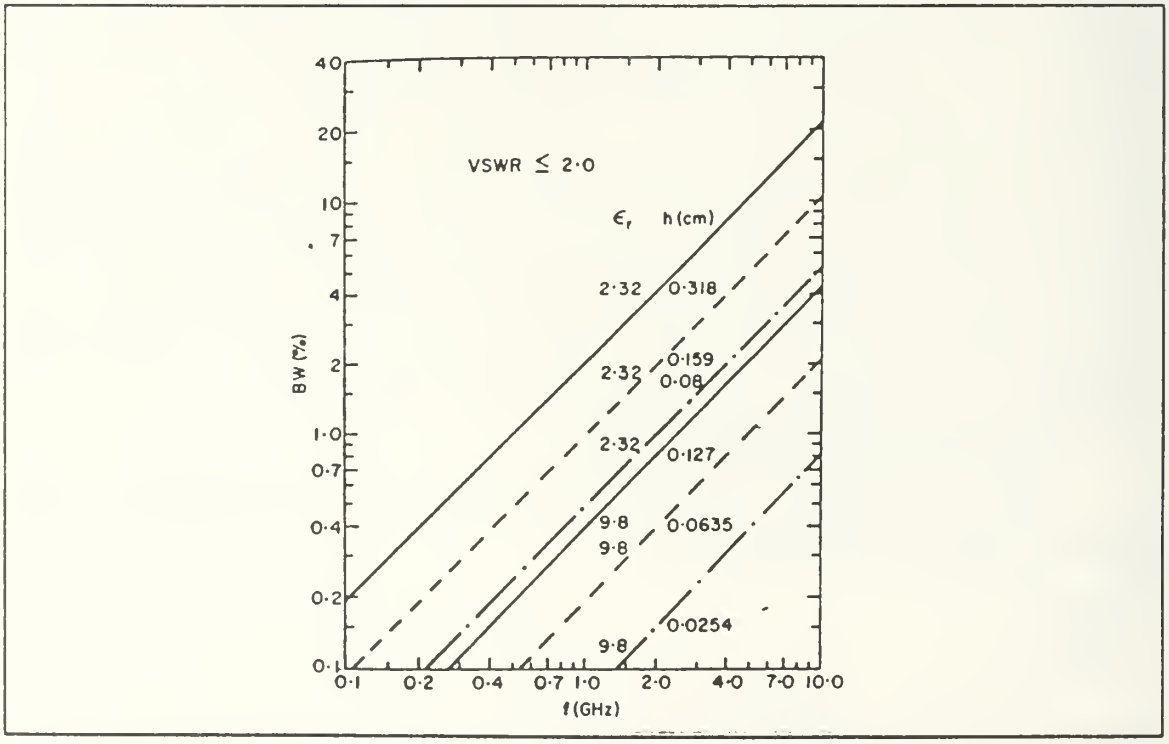

Figure 12. Variation of Bandwidth with Operating Frequency.

Many materials used as substrates have dielectric constants between 2 and 2.5. A commonly used value for the dielectric constant is 2.32. One of the materials that has this dielectric constant is PTFE Glass Microfiber (RT Duroid) 5870, which is used in many applications because the dielectric constant does not vary over a wide range of frequencies. Therefore, for purposes of this design:

$\varepsilon_r = 2.32$

Now, the length is:

$$L = 0.49 \frac{\lambda_0}{\sqrt{\varepsilon_r}} = 0.49 \frac{16.66}{\sqrt{2.32}} = 5.36 \text{ centimeters}$$

The width, W, of the patch is calculated from equation (4.15).

$$W = \frac{\lambda_0}{2} \sqrt{\frac{2}{\varepsilon_r + 1}} = \frac{16.66}{2} \sqrt{\frac{2}{2.32 + 1}} = 6.46 \text{ centimeters.}$$

2. Number of Patches Needed for the Uplink Array

Now it is necessary to determine how many patches are required to form the uplink array. To approximate a uniform roll plane (ϕ-plane) pattern, the center-to-center spacing of the patches should not exceed 0.7 λ_0 and the spacing should not be less than 0.35 λ_0, because mutual coupling between the patches becomes excessive. [Ref. 11: p. 7-21]

An equation to determine the minimum number of patches, N_{min}, that will fit around the circumference, C, of the ORION satellite is:

$$C = N_{min} \times L + N_{min}(0.7\lambda_0)$$

Solving for N_{min}:

$$N_{min} = \frac{C}{L + 0.7\lambda_0} \tag{5.1}$$

$C = \pi \times$ diameter $= \pi \times 19$ inches $= 59.69$ inches $= 151.61$ centimeters

$$N_{min} = \frac{151.61}{5.36 + 0.7(16.66)} = 8.91 \approx 9 \text{ patches}$$

A similar equation to find the maximum number of patches, N_{max}, is:

$$N_{max} = \frac{C}{L + 0.35\lambda_0} = \frac{151.61}{5.36 + 0.35(16.66)} = 13.55 \approx 13 \text{ patches} \tag{5.2}$$

$9 \leq N \leq 13$

N_{min} was rounded up because eight patches would exceed the maximum center-to-center spacing and N_{max} was rounded down so as not to go below the minimum spacing of $0.35\lambda_0$.

3. Omnidirectional Uplink Radiation Patterns

For the uplink, the number of patches may range from 9 to 13. The factor υ, in equation (4.26), was chosen to range from 1 to 6. The radiation pattern for the various combinations of N and υ can be computed by equation (4.27).

$$f(\theta, \phi) = \sum_{n=1}^{N} F(\theta, \phi) e^{\left(-j\frac{2\pi\upsilon}{N}\right)n} \left[e^{jka\sin\theta\cos(\phi - \nu_n)} + e^{jka\sin\theta\cos\left(\phi - \nu_n - \frac{L}{a}\right)} \right]$$

where,

$$F(\theta, \phi) = \frac{\sin\left(\frac{kh}{2}\sin\theta\cos\phi\right)}{\frac{kh}{2}\sin\theta\cos\phi} \frac{\sin\left(\frac{kW}{2}\cos\theta\right)}{\frac{kW}{2}\cos\theta} \sin\theta$$

$F(\theta, \phi)$ is composed of two sinc functions times $\sin\theta$. Looking at the first sinc function, if $\frac{kh}{2}$ is small, the sinc function is approximately equal to one.

$$\text{sinc} = \frac{\sin\left(\frac{kh}{2}\sin\theta\cos\phi\right)}{\frac{kh}{2}\sin\theta\cos\phi} \approx 1 \quad \text{for all } \theta \text{ and } \phi$$

For this design,

$$\frac{kh}{2} = \frac{2\pi}{\lambda_0}\frac{h}{2} = \frac{\pi h}{\lambda_0} = \frac{0.61\pi}{16.66} = 0.11$$

With 0.11 as the argument, the sinc function varies between 0.997 and 1.000 for both planes. Therefore, the first sinc function will be approximated as one and dropped from $F(\theta, \phi)$, yielding:

$$F(\theta) = \frac{\sin\left(\frac{kW}{2}\cos\theta\right)}{\frac{kW}{2}\cos\theta}\sin\theta \tag{5.3}$$

The omnidirectional radiation pattern becomes:

$$f(\theta, \phi) = \sum_{n=1}^{N} F(\theta) e^{\left(-j\frac{2\pi\upsilon}{N}\right)n}\left[e^{jka\sin\theta\cos(\phi - v_n)} + e^{jka\sin\theta\cos\left(\phi - v_n - \frac{L}{a}\right)}\right] \tag{5.4}$$

Appendix B is a MathCAD program that calculates and graphs equation (5.4). Also, Appendix B shows representative radiation patterns for several combinations of N and υ . A visual inspection of the radiation patterns was used to choose those patterns which best approximated an omnidirectional radiation pattern. The criteria for choosing what combinations of N and υ to best approximate an omnidirectional radiation pattern was based on how close the patterns in the roll plane resembled an omnidirectional pattern. Most of the combinations were discounted because of the number of lobes in the roll and elevation planes. As the phasing factor, υ, increases, the ripple in the roll plane pattern became more pronounced. The ripples turned into lobes. For those combinations with reasonably uniform roll plane patterns, the ripple decreased as the number of patches increased.

The combinations of N and υ that best approximate an omnidirectional radiation pattern are:

$N = 12 \quad \upsilon = 1$

and

$N = 13 \quad \upsilon = 1$

The roll and elevation plane radiation patterns for these combinations are shown in Figures 13 and 14 on page 36 and Figures 15 and 16 on page 37.

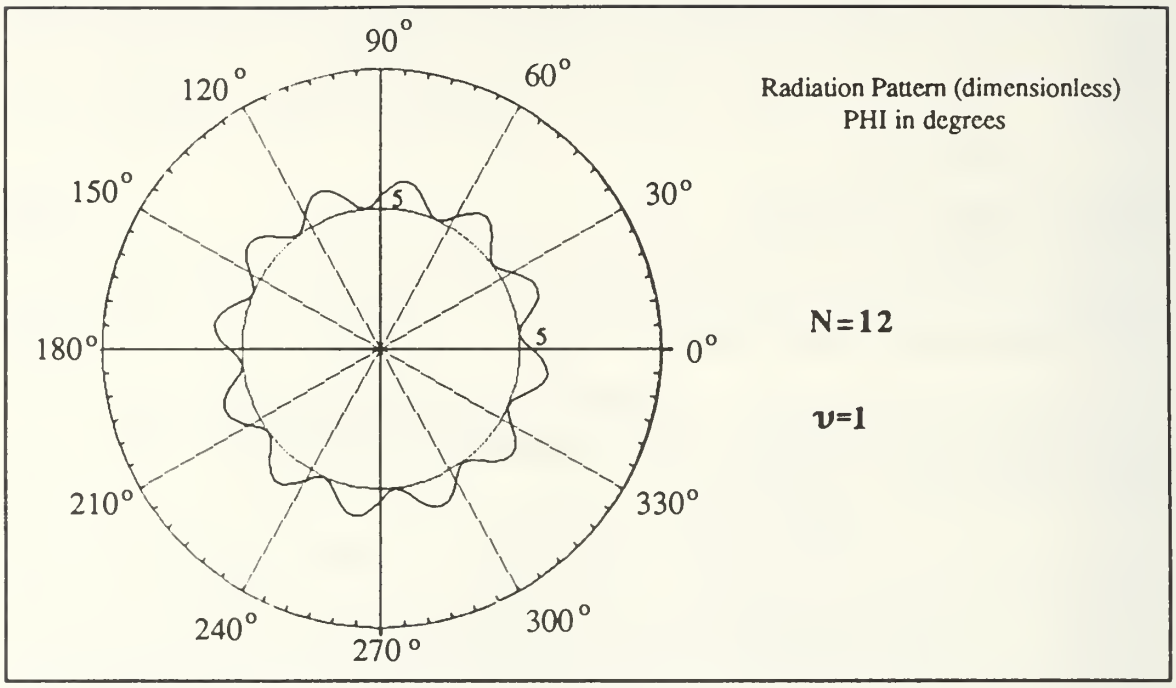

Figure 13. Uplink Roll Plane Radiation Pattern for Combination 1.

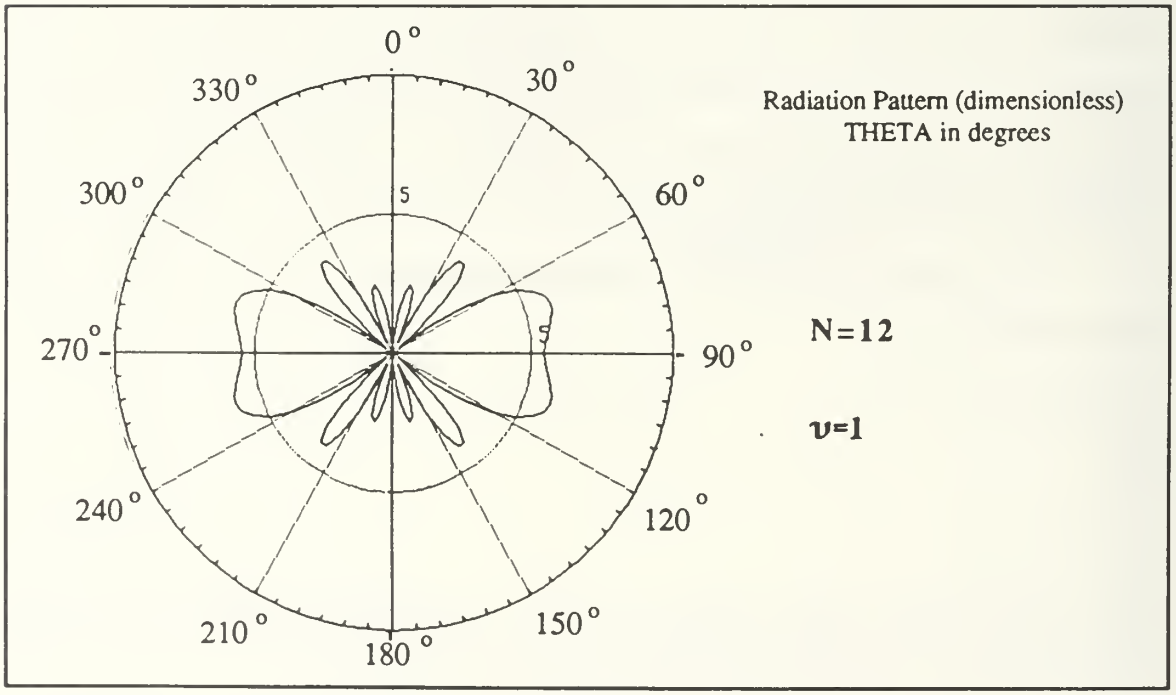

Figure 14. Uplink Elevation Plane Radiation Pattern for Combination 1.

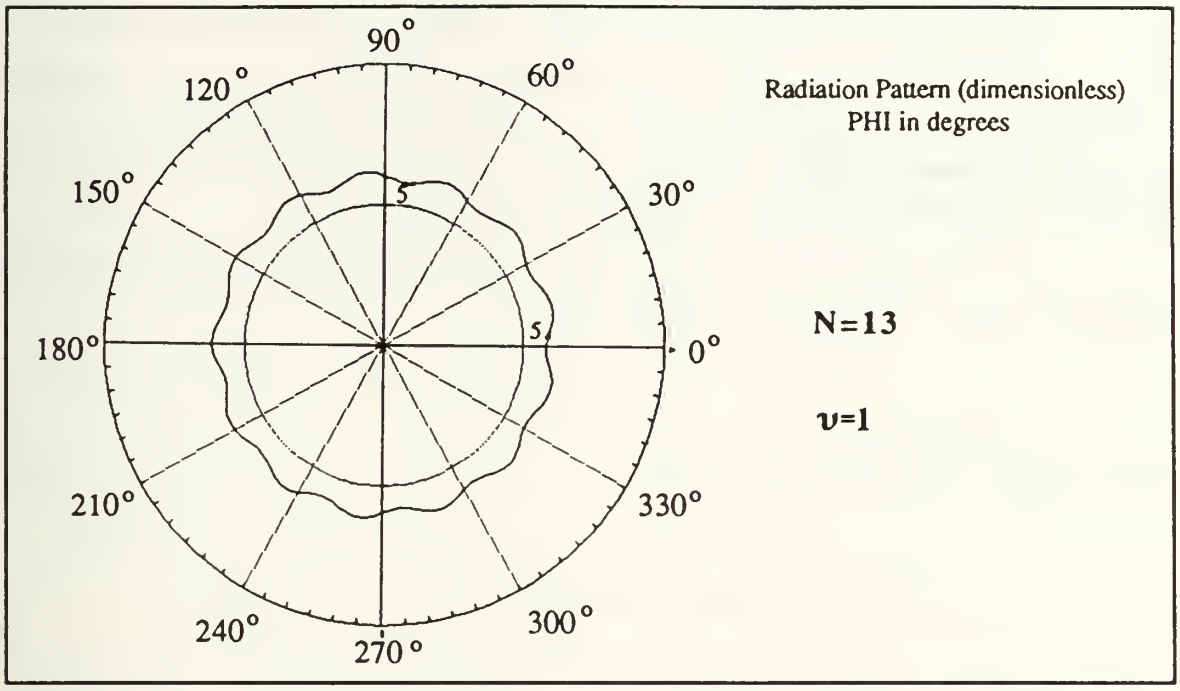

Figure 15. Uplink Roll Plane Radiation Pattern for Combination 2.

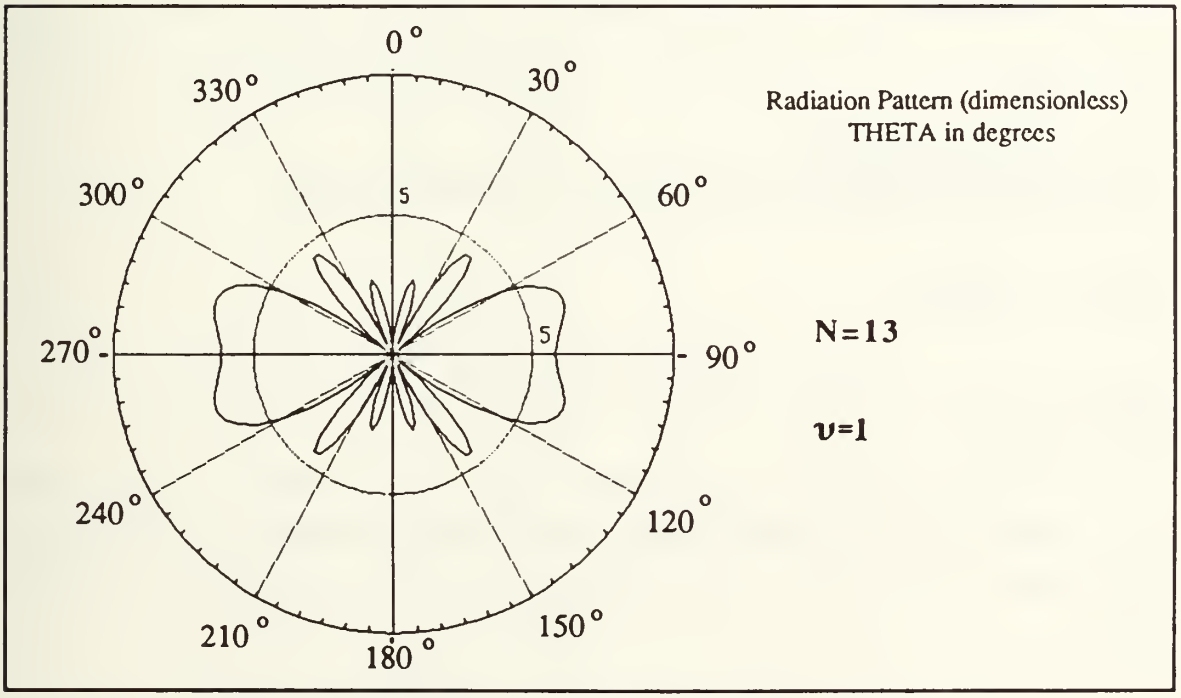

Figure 16. Uplink Elevation Plane Radiation Pattern for Combination 2.

4. Omnidirectional Uplink Directive Gain Patterns

The directive gain pattern provides more insight into the power distribution of the antenna. The directive gain determines the angles θ and ϕ to provide the necessary power in the transmitted signal required for reception by the ground station. By comparing the minimum gain in the directive gain pattern to the gain specification in Chapter III, the altitude at which the array will work can be found.

To determine the gain for the uplink array antenna, equation (4.31), the average radiation intensity, U_{ave}, must first be calculated.

$$U_{\text{ave}} = \frac{1}{4\pi} \int_0^{2\pi} \int_0^{\pi} \frac{|f(\theta, \phi)|^2}{2\eta_0} \sin\theta d\theta d\phi \tag{5.5}$$

Appendix C is a MathCAD program that evaluates:

$$\frac{1}{4\pi} \int_0^{2\pi} \int_0^{\pi} |f(\theta, \phi)|^2 \sin\theta d\theta d\phi$$

For the combination of $N = 12$ and $v = 1$:

$$U_{\text{ave}} = \frac{19.64}{2\eta_0}$$

The directive gain pattern, equation (4.32) may now be written as:

$$D(\theta, \phi) = \frac{|f(\theta, \phi)|^2}{2\eta_0 U_{\text{ave}}} \tag{5.6}$$

Equation (5.6) for the directive gain, is programmed in Appendix D and the results are linearly plotted.

The directive gain patterns, for $N = 12$ and $v = 1$, are shown in Figures 17 and 18 on page 39 for the roll and elevation planes. The slight asymmetry of the elevation plane pattern is due to the way the patches (i.e., slots) are oriented in the reference frame.

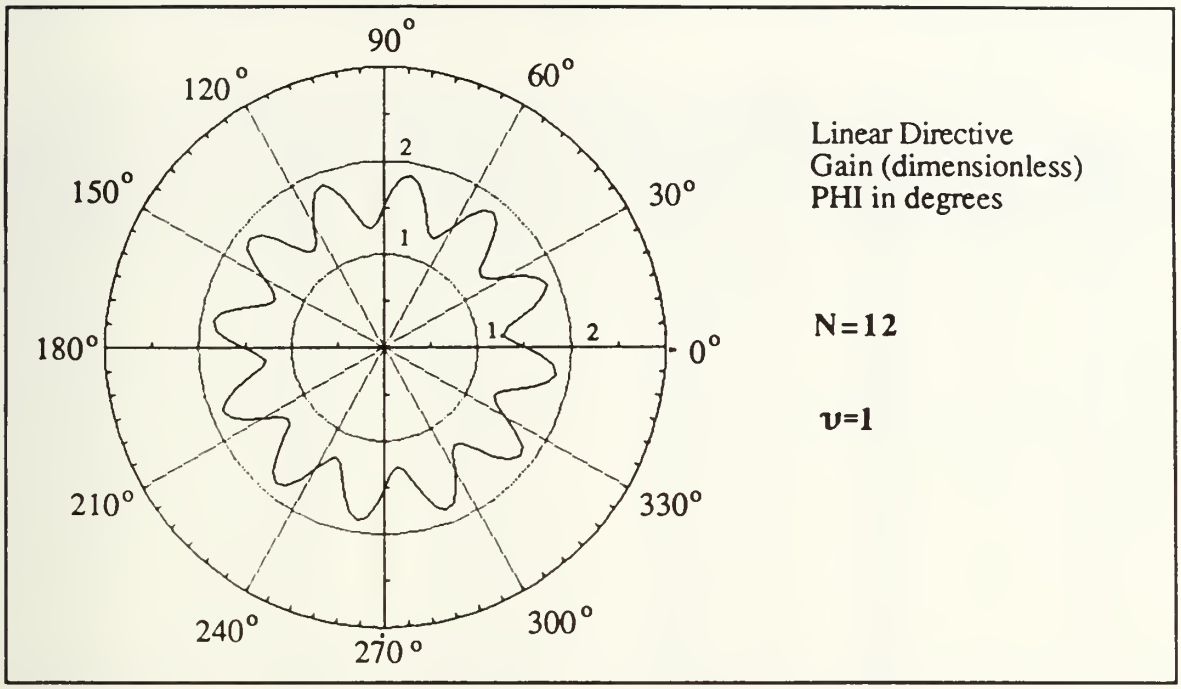

Figure 17. Uplink Roll Plane Gain Pattern for Combination 1.

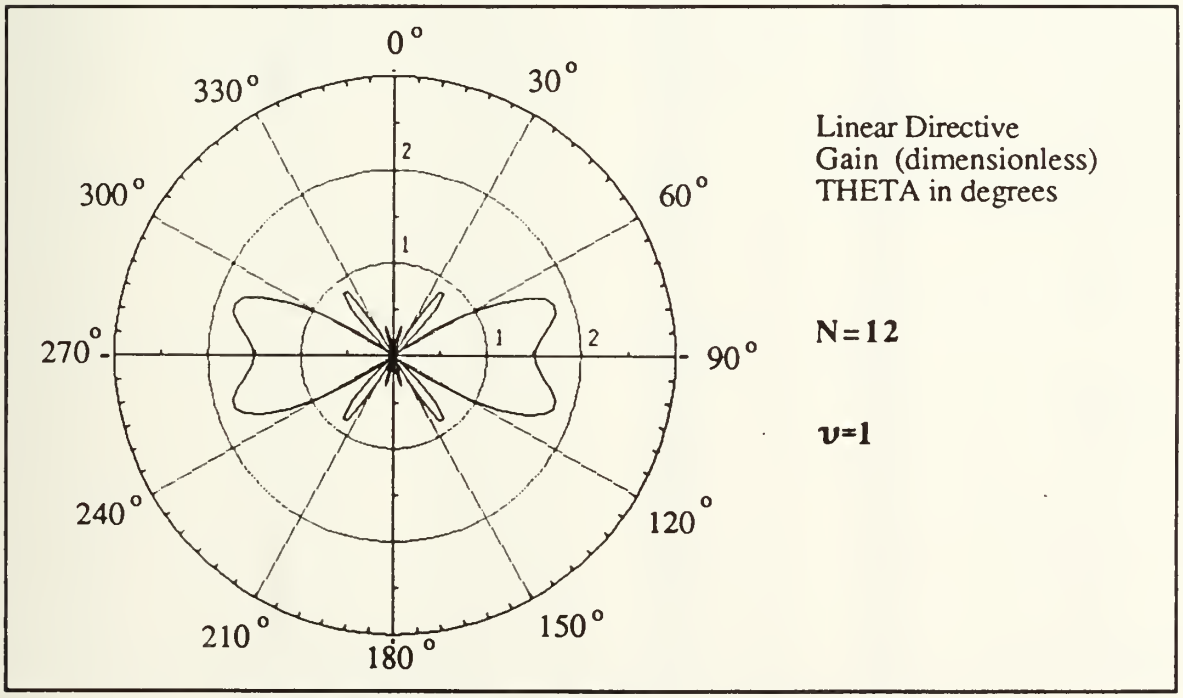

Figure 18. Uplink Elevation Plane Gain Pattern for Combination 1.

The gain for the roll and elevation planes are listed in Tables 3 and 4 for $N = 12$ and $v = 1$.

Table 3. UPLINK ROLL PLANE GAIN FOR COMBINATION 1.

ϕ degrees	Gain dB	ϕ degrees	Gain dB	ϕ degrees	Gain dB
0	1.8	120	1.8	240	1.8
3	1.3	123	1.3	243	1.3
6	1.1	126	1.1	246	1.1
9	1.2	129	1.2	249	1.2
12	1.7	132	1.7	252	1.7
15	2.2	135	2.2	255	2.2
18	2.5	138	2.5	258	2.5
21	2.7	141	2.7	261	2.7
24	2.6	144	2.6	264	2.6
27	2.3	147	2.3	267	2.3
30	1.8	150	1.8	270	1.8
33	1.3	153	1.3	273	1.3
36	1.1	156	1.1	276	1.1
39	1.2	159	1.2	279	1.2
42	1.7	162	1.7	282	1.7
45	2.2	165	2.2	285	2.2
48	2.5	168	2.5	288	2.5
51	2.7	171	2.7	291	2.7
54	2.6	174	2.6	294	2.6
57	2.3	177	2.3	297	2.3
60	1.8	180	1.8	300	1.8
63	1.3	183	1.3	303	1.3
66	1.1	186	1.1	306	1.1
69	1.2	189	1.2	309	1.2
72	1.7	192	1.7	312	1.7
75	2.2	195	2.2	315	2.2
78	2.5	198	2.5	318	2.5
81	2.7	201	2.7	321	2.7
84	2.6	204	2.6	324	2.6
87	2.3	207	2.3	327	2.3
90	1.8	210	1.8	330	1.8
93	1.3	213	1.3	333	1.3
96	1.1	216	1.1	336	1.1
99	1.2	219	1.2	339	1.2
102	1.7	222	1.7	342	1.7
105	2.2	225	2.2	345	2.2
108	2.5	228	2.5	348	2.5
111	2.7	231	2.7	351	2.7
114	2.6	234	2.6	354	2.6
117	2.3	237	2.3	357	2.3

Table 4. UPLINK ELEVATION PLANE GAIN FOR COMBINATION 1.

θ degrees	Gain dB	θ degrees	Gain dB	θ degrees	Gain dB
0	$-\infty$	120	-0.5	240	-0.5
3	-26.0	123	-3.2	243	1.0
6	-14.7	126	-8.0	246	1.9
9	-9.0	129	-23.8	249	2.4
12	-5.9	132	-11.3	252	2.5
15	-4.8	135	-4.8	255	2.5
18	-5.5	138	-1.9	258	2.4
21	-8.8	141	-0.6	261	2.2
24	-20.6	144	-0.7	264	2.0
27	-12.8	147	-2.1	267	1.8
30	-5.3	150	-5.3	270	1.8
33	-2.1	153	-12.8	273	1.8
36	-0.7	156	-20.6	276	2.0
39	-0.6	159	-8.8	279	2.2
42	-1.9	162	-5.5	282	2.4
45	-4.8	165	-4.8	285	2.5
48	-11.4	168	-5.9	288	2.5
51	-24.8	171	-9.0	291	2.4
54	-8.0	174	-14.7	294	2.0
57	-3.2	177	-26.0	297	1.0
60	-0.5	180	$-\infty$	300	-0.5
63	1.0	183	-26.0	303	-3.2
66	1.9	186	-14.7	306	-8.0
69	2.4	189	-9.0	309	-24.8
72	2.5	192	-5.9	312	-11.3
75	2.5	195	-4.8	315	-4.8
78	2.4	198	-5.5	318	-1.9
81	2.2	201	-8.8	321	-0.6
84	2.0	204	-20.6	324	-0.7
87	1.8	207	-12.8	327	-2.1
90	1.8	210	-5.3	330	-5.3
93	1.8	213	-2.1	333	-12.8
96	2.0	216	-0.7	336	-20.6
99	2.2	219	-0.6	339	-8.8
102	2.4	222	-1.9	342	-5.5
105	2.5	225	-4.8	345	-4.8
108	2.5	228	-11.3	348	-5.9
111	2.4	231	-24.8	351	-9.0
114	1.9	234	-8.0	354	-14.7
117	1.0	237	-3.2	357	-26.0

For this array, $N = 12$ and $v = 1$, the minimum and maximum gain in the roll plane are:

$G_{min} = 1.1$ dB at $\phi = 6°$

$G_{max} = 2.7$ dB at $\phi = 21°$

The maximum ripple in the roll plane is 1.6 dB. In the elevation plane, the gain pattern is not uniform like the roll plane. It is necessary to define the width of the main beam. Beamwidth is normally measured by the half-power points (3 dB down from the maximum of the main lobe). From Figure 18 on page 39 and Table 4, the maximum gain shown is 2.5 dB and occurs at $\theta = 74°$. The half-power gain is -0.5 dB and occurs at $\theta = 60°$ and $\theta = 120°$. Therefore, the half-power beamwidth is:

$HP_\theta = 60°$ $\quad 60° \leq \theta \leq 120°$

For use on the ORION satellite, the beamwidth necessary to maintain communications can be defined as the beamwidth that is above the gain specification. The gain specification for the uplink is:

$G_{spec} = -1.8$ dB

The beamwidth of the elevation pattern that meets the specification is within a degree of the half-power beamwidth.

$HP_\theta = 60°$

For a 12 patch array with $v = 1$, the realizable gain meets the specification in the roll plane and in the elevation plane with a beamwidth of 60°.

The next combination to examine is $N = 13$ and $v = 1$. The average radiation intensity for an array with $N = 13$ and $v = 1$ is:

$$U_{ave} = \frac{22.98}{2\eta_0}$$

Figures 19 and 20 on page 43 show the directive gain patterns generated from equation (5.6) for $N = 13$ and $v = 1$.

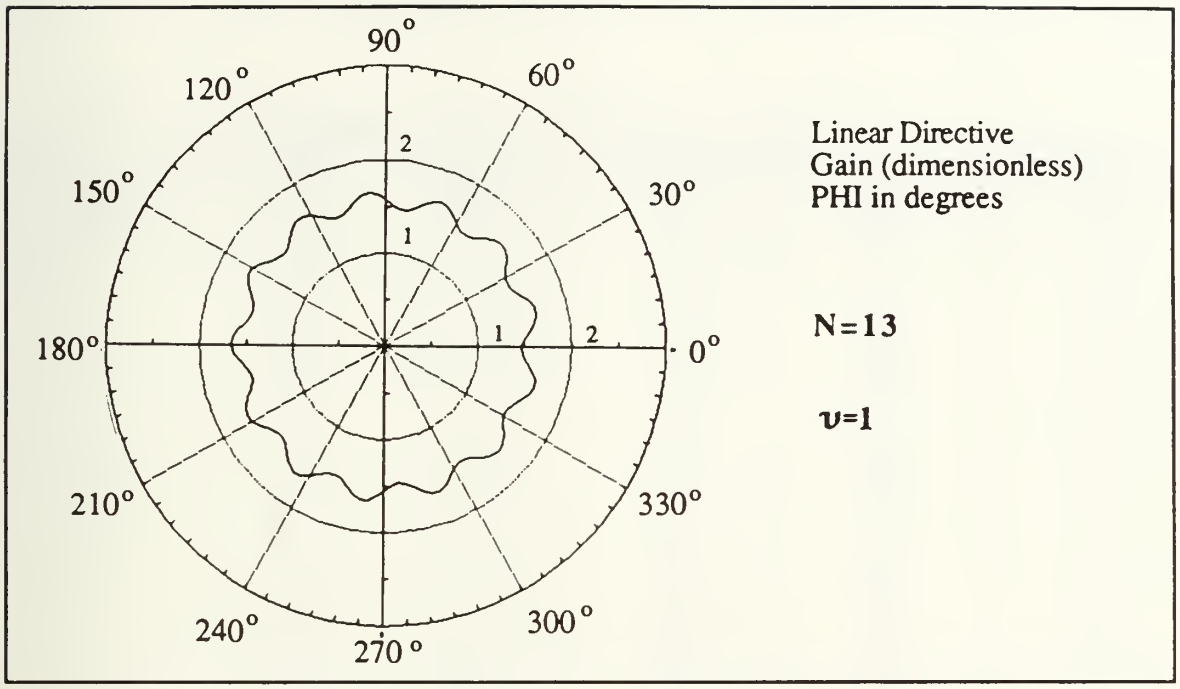

Figure 19. Uplink Roll Plane Gain Pattern for Combination 2.

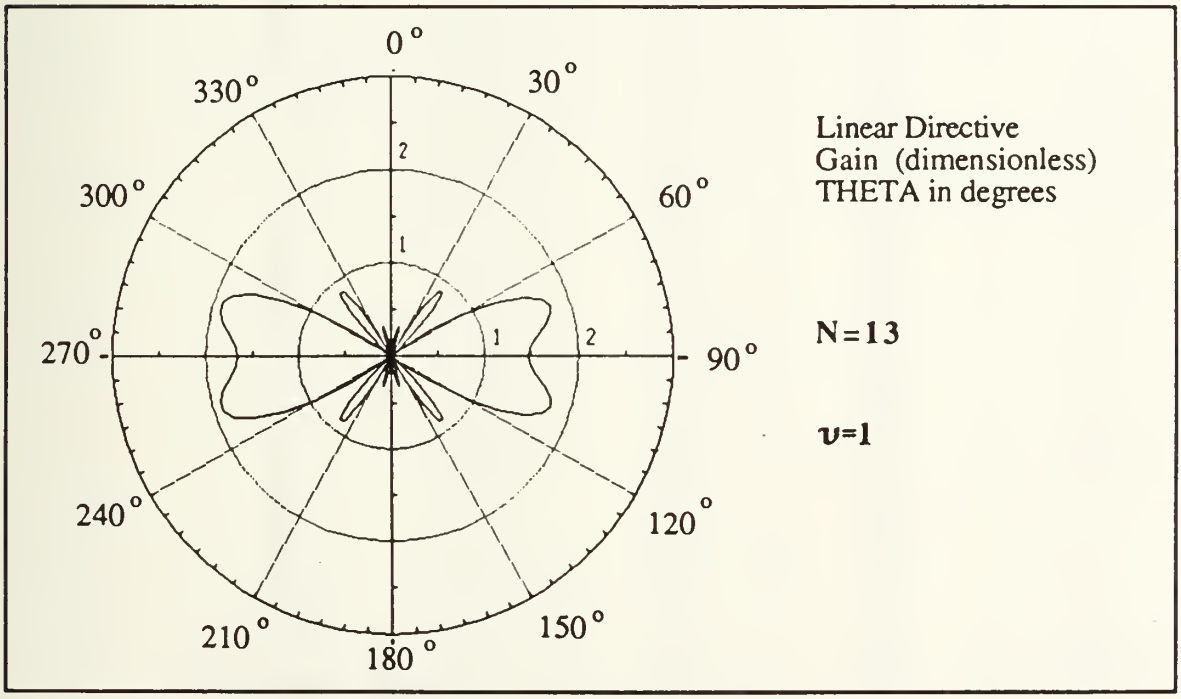

Figure 20. Uplink Elevation Plane Gain Pattern for Combination 2.

The gain for the roll and elevation planes are listed in Tables 5 and 6 for $N = 13$ and $v = 1$.

Table 5. UPLINK ROLL PLANE GAIN FOR COMBINATION 2.

ϕ degrees	Gain dB	ϕ degrees	Gain dB	ϕ degrees	Gain dB
0	1.7	120	2.1	240	2.0
3	1.8	123	2.2	243	1.9
6	1.9	126	2.2	246	1.7
9	2.1	129	2.1	249	1.7
12	2.2	132	1.9	252	1.7
15	2.2	135	1.7	255	1.9
18	2.1	138	1.7	258	2.1
21	1.9	141	1.7	261	2.2
24	1.7	144	1.9	264	2.2
27	1.7	147	2.1	267	2.1
30	1.7	150	2.2	270	2.0
33	1.9	153	2.2	273	1.7
36	2.1	156	2.1	276	1.7
39	2.2	159	1.9	279	1.7
42	2.2	162	1.8	282	1.9
45	2.1	165	1.7	285	2.0
48	1.9	168	1.7	288	2.2
51	1.8	171	1.9	291	2.2
54	1.7	174	2.0	294	2.1
57	1.7	177	2.2	297	2.0
60	1.8	180	2.2	300	1.8
63	2.0	183	2.1	303	1.7
66	2.2	186	2.0	306	1.7
69	2.2	189	1.8	309	1.8
72	2.1	192	1.7	312	2.0
75	2.0	195	1.7	315	2.2
78	1.8	198	1.8	318	2.2
81	1.7	201	2.0	321	2.1
84	1.7	204	2.1	324	2.0
87	1.8	207	2.2	327	1.8
90	2.0	210	2.2	330	1.7
93	2.1	213	2.0	333	1.7
96	2.2	216	1.8	336	1.8
99	2.2	219	1.7	339	2.0
102	2.0	222	1.7	342	2.1
105	1.8	225	1.8	345	2.2
108	1.7	228	2.0	348	2.2
111	1.7	231	2.1	351	2.0
114	1.8	234	2.2	354	1.9
117	1.9	237	2.2	357	1.7

Table 6. UPLINK ELEVATION PLANE GAIN FOR COMBINATION 2.

θ degrees	Gain dB	θ degrees	Gain dB	θ degrees	Gain dB
0	$-\infty$	120	-0.5	240	-0.4
3	-26.0	123	-3.2	243	1.2
6	-14.7	126	-8.0	246	2.1
9	-8.9	129	-23.9	249	2.6
12	-5.9	132	-11.3	252	2.8
15	-4.7	135	-4.8	255	2.8
18	-5.5	138	-1.8	258	2.7
21	-8.8	141	-0.6	261	2.5
24	-20.6	144	-0.7	264	2.4
27	-12.8	147	-2.0	267	2.2
30	-5.3	150	-5.3	270	2.2
33	-2.0	153	-12.8	273	2.2
36	-0.7	156	-20.6	276	2.4
39	-1.6	159	-8.8	279	2.5
42	-1.8	162	-5.5	282	2.7
45	-4.8	165	-4.7	285	2.8
48	-11.3	168	-5.9	288	2.8
51	-23.9	171	-8.9	291	2.6
54	-8.0	174	-14.7	294	2.1
57	-3.2	177	-26.0	297	1.2
60	-0.5	180	$-\infty$	300	-0.4
63	1.0	183	-26.0	303	-3.0
66	1.9	186	-14.7	306	-7.9
69	2.4	189	-8.9	309	-23.2
72	2.5	192	-5.9	312	-11.4
75	2.5	195	-4.7	315	-4.8
78	2.3	198	-5.5	318	-1.9
81	2.1	201	-8.8	321	-0.6
84	1.9	204	-20.6	324	-0.7
87	1.7	207	-12.8	327	-2.0
90	1.7	210	-5.3	330	-5.3
93	1.7	213	-2.0	333	-12.8
96	1.9	216	-0.7	336	-20.6
99	2.1	219	-0.6	339	-8.8
102	2.3	222	-1.9	342	-5.5
105	2.5	225	-4.8	345	-4.7
108	2.5	228	-11.4	348	-5.9
111	2.4	231	-23.2	351	-8.9
114	1.9	234	-7.9	354	-14.7
117	1.0	237	-3.0	357	-26.0

For the 13 patch array, the minimum and maximum gain in the roll plane are:

$G_{min} = 1.7$ dB at $\theta = 0°$

$G_{max} = 2.2$ dB at $\theta = 13°$

The maximum ripple is 0.5 dB. The gain in the roll plane is always greater than the uplink specification. From Figure 20 on page 43 and Table 6, the half-power beamwidth is:

$HP_\theta = 60°$ $60° \leq \theta \leq 120°$

The beamwidth is approximately the same for the gain specification.

Comparing the gains of the two arrays shows that the 12 patch array has more gain than the 13 patch array. Since both of the arrays meet the specification for the satellite, the 12 patch array is the primary candidate for use with the ORION satellite because of cost, weight and simplicity considerations.

B. ORION SATELLITE DOWNLINK ANTENNA DESIGN

The design of the downlink antenna is accomplished by following the same steps as the uplink. First, determine the dimensions of the microstrip patch, find the minimum and maximum number of patches that will fit around the circumference of the satellite that meet the minimum and maximum patch spacing requirements, generate radiation patterns for different combinations of N and v, select the most promising patterns for further analysis and generate the directive gain patterns.

1. Downlink Microstrip Patch Dimensions

The thickness of the microstrip patch is found from equation (4.13) with the center frequency (2250 Megahertz) of the downlink frequency band.

$$h = \frac{BW}{128f^2} = \frac{100}{128(2.25)^2} = 0.15 \text{ inch} = 0.39 \text{ centimeters}$$

The length, L, of the patch is found from equation (4.14).

$$\lambda_0 = \frac{c}{f} = \frac{2.997925 \times 10^8}{2250 \times 10^6} = 0.1332 \text{ meters} = 13.32 \text{ centimeters}$$

$$L = 0.49 \frac{\lambda_0}{\sqrt{\varepsilon_r}} = \frac{0.49 \times 13.32}{\sqrt{2.32}} = 4.29 \text{ centimeters}$$

The width, W, of the patch is calculated from equation (4.15).

$$W = \frac{\lambda_0}{2}\sqrt{\frac{2}{\varepsilon_r + 1}} = \frac{13.32}{2}\sqrt{\frac{2}{2.32 + 1}} = 5.17 \text{ centimeters}$$

2. Number of Patches Needed for the Downlink Array

Using equations (5.1) and (5.2), the minimum and maximum number of patches are determined.

$$N_{\min} = \frac{C}{L + 0.7\lambda_0} = \frac{151.61}{4.29 + 0.7(13.32)} = 11.14 \approx 12$$

$$N_{\max} = \frac{C}{L + 0.35\lambda_0} = \frac{151.61}{4.29 + 0.35(13.32)} = 16.94 \approx 16$$

$$12 \leq N \leq 16$$

3. Omnidirectional Downlink Radiation Patterns

Using equation (5.4) with $12 \leq N \leq 16$ and $1 \leq \upsilon \leq 6$, plots of the downlink omnidirectional radiation patterns were produced. The radiation pattern plots for $12 \leq N \leq 16$ with $1 \leq \upsilon \leq 3$ are in Appendix E. From those plots, it is apparent that as the number of patches increases, the ripple in the roll plane gets smaller and the beamwidth in the elevation plane also decreases. While the decrease in the ripple is desirable, the decrease in the elevation beamwidth is undesirable when trying to approximate an omnidirectional antenna. The most promising combinations for producing an omnidirectional radiation pattern in the roll plane are:

$N = 12 \quad \upsilon = 2$

$N = 15 \quad \upsilon = 1$

$N = 16 \quad \upsilon = 1$

$N = 16 \quad \upsilon = 3$

The roll and elevation plane radiation patterns for the four combinations are shown in the figures on the pages that follow.

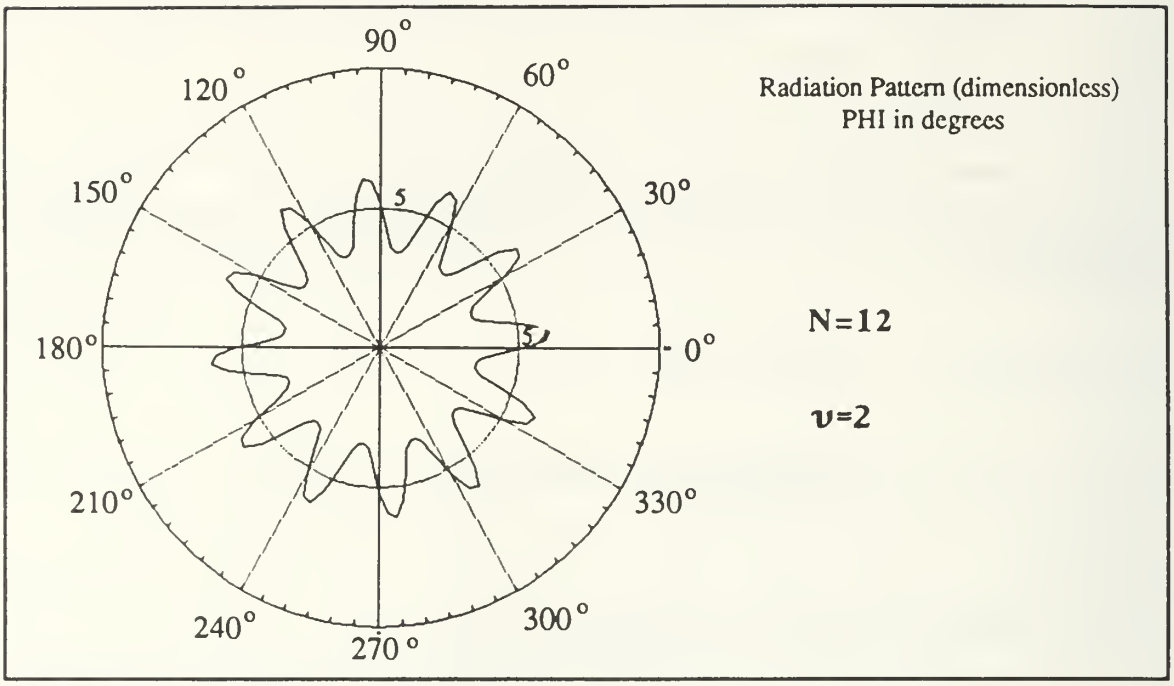

Figure 21. Downlink Roll Plane Radiation Pattern for Combination 1.

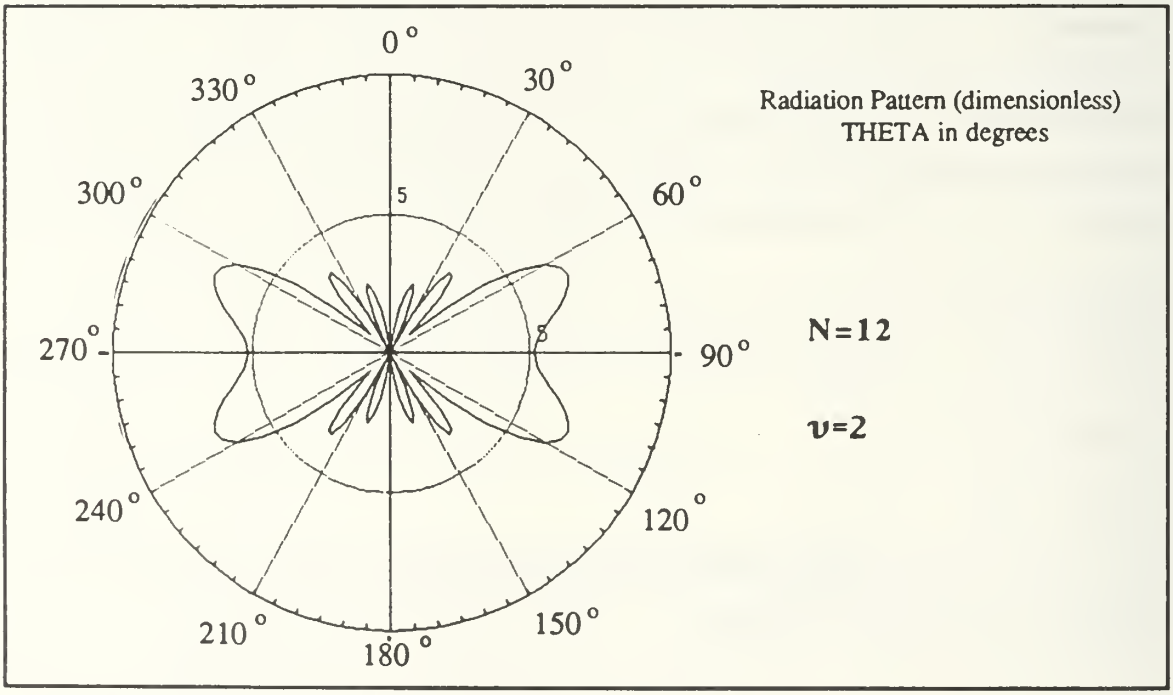

Figure 22. Downlink Elevation Plane Radiation Pattern for Combination 1.

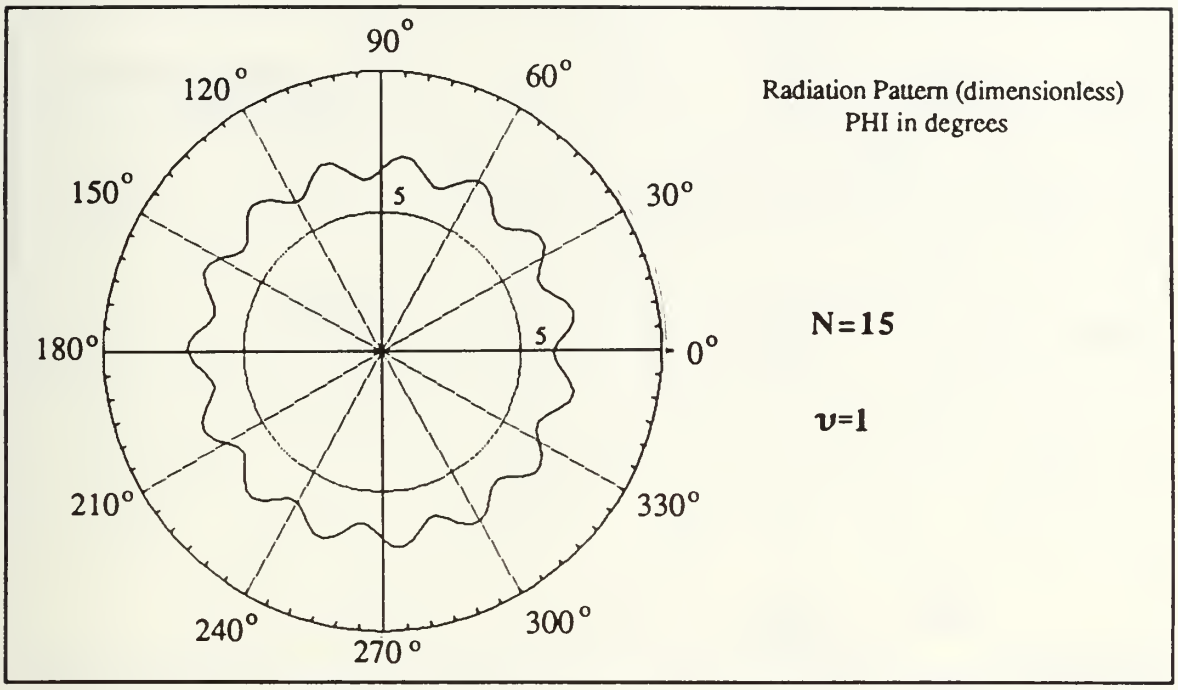

Figure 23. Downlink Roll Plane Radiation Pattern for Combination 2.

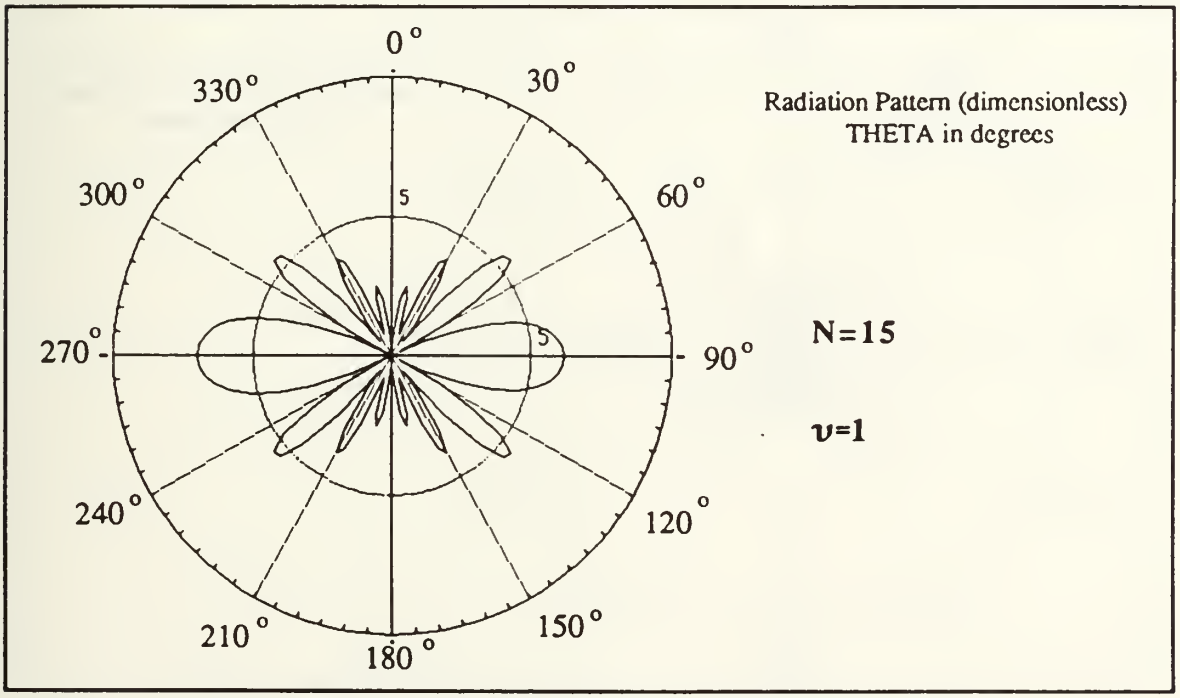

Figure 24. Downlink Elevation Plane Radiation Pattern for Combination 2.

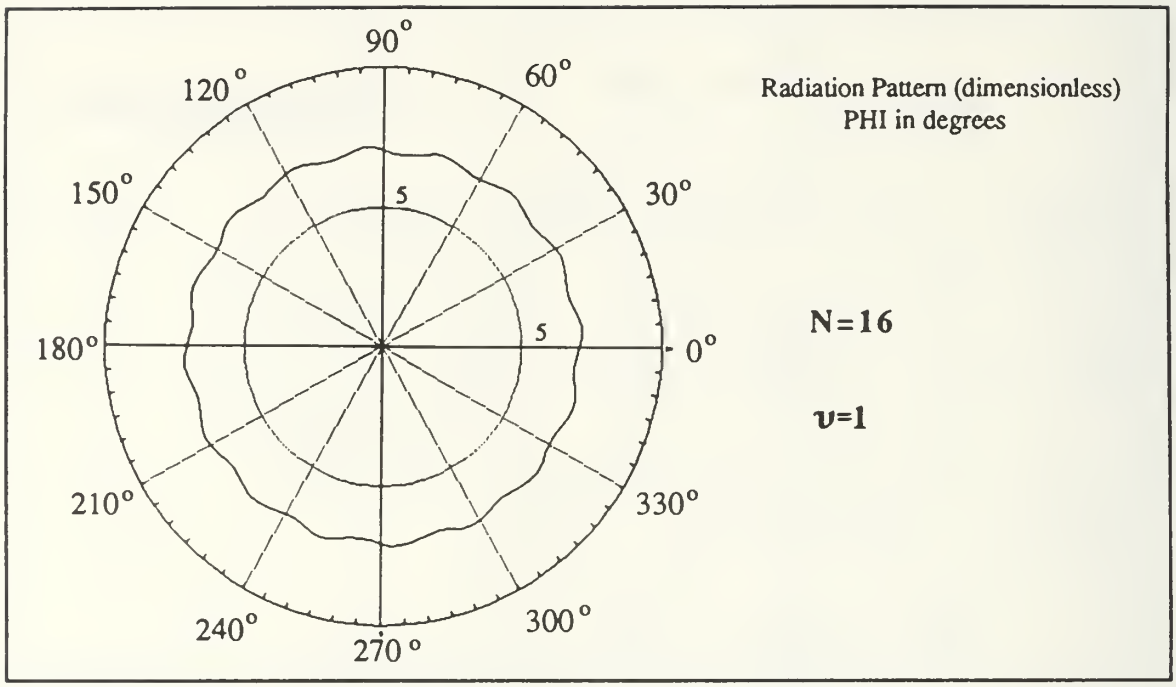

Figure 25. Downlink Roll Plane Radiation Pattern for Combination 3.

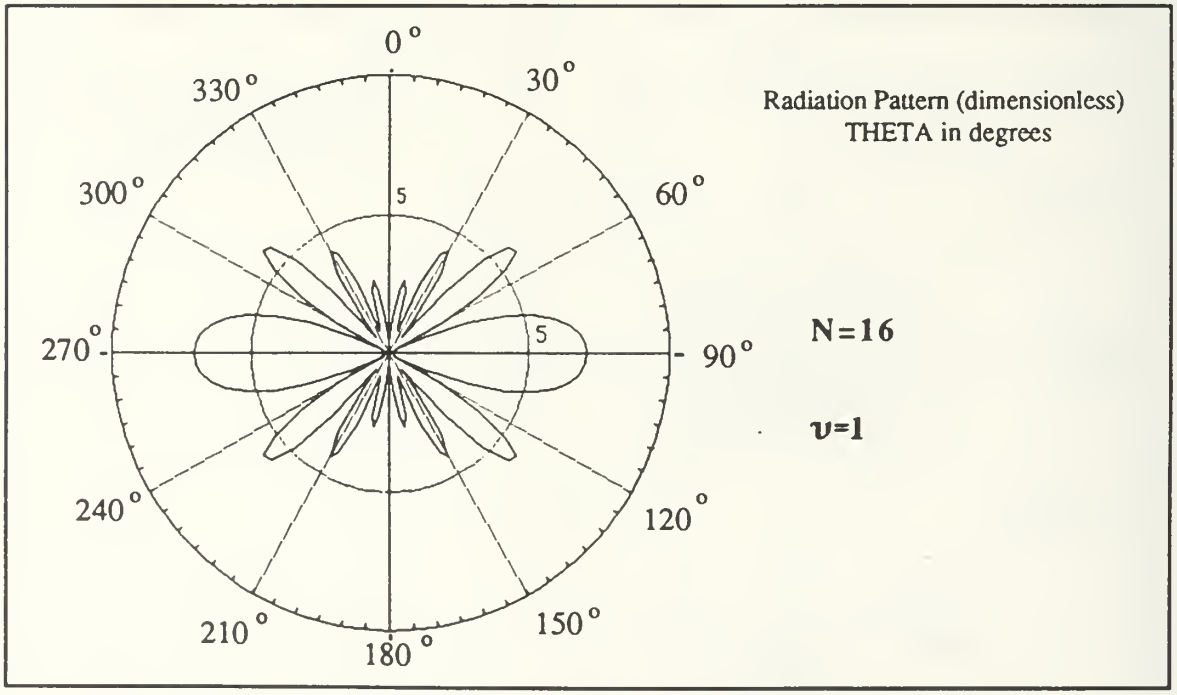

Figure 26. Downlink Elevation Plane Radiation Pattern for Combination 3.

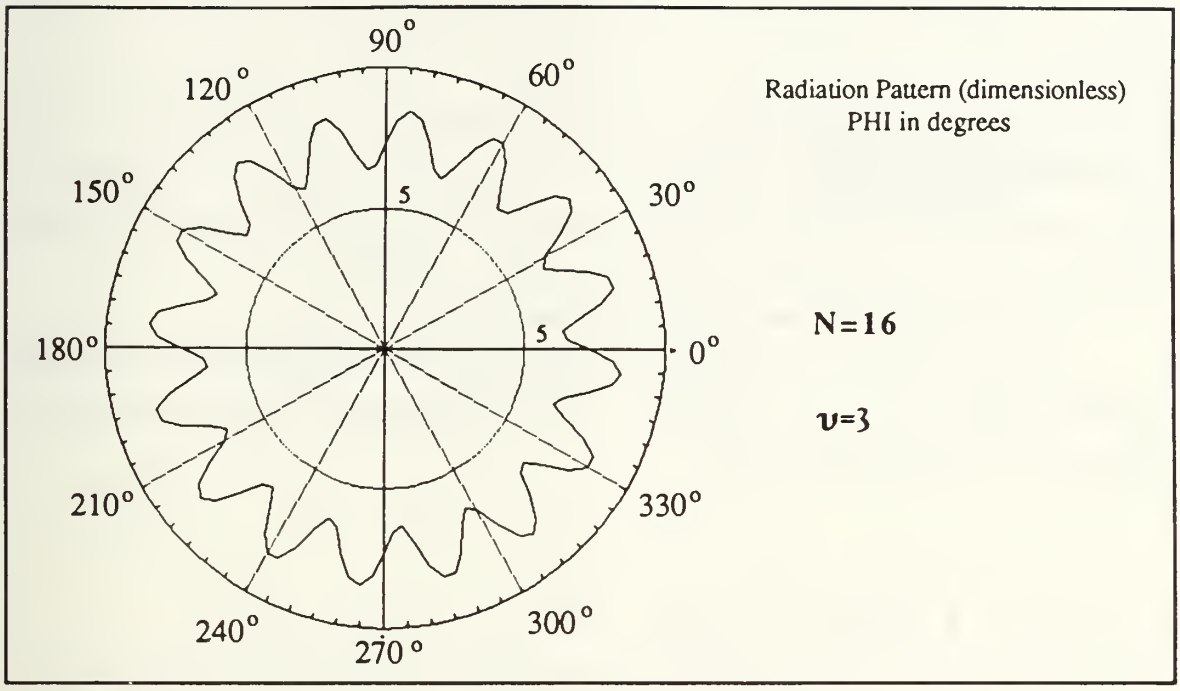

Figure 27. Downlink Roll Plane Radiation Pattern for Combination 4.

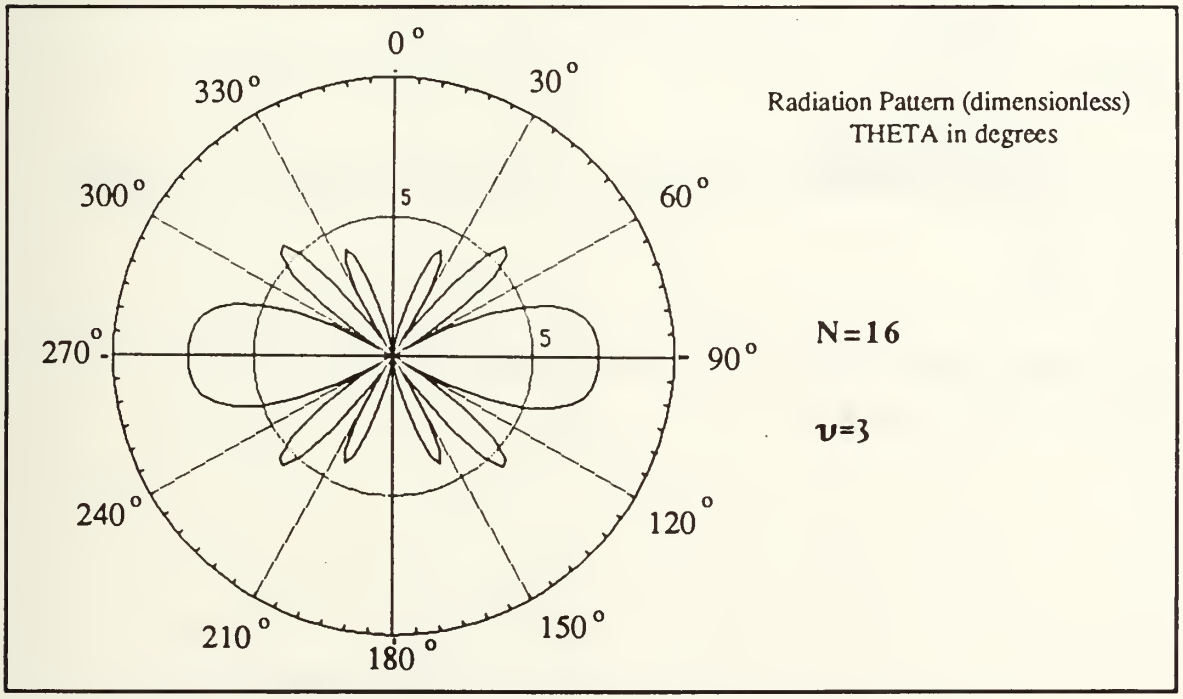

Figure 28. Downlink Elevation Plane Radiation Pattern for Combination 4.

The combination of $N = 12$, $\upsilon = 2$, and $N = 16$, $\upsilon = 3$ were selected for further analysis because the beamwidth in the elevation plane is wider than for the other combinations, even though the ripple in the roll plane is more pronounced. From Figure 50 and Table 21 in Appendix A, the angle α corresponds to the view angle that equates to how much of the earth the satellite can "see" for a range of altitudes. The closer the beamwidth is to 2α, the larger the antenna's earth footprint and the longer the satellite will be able to communicate with a ground station.

4. Omnidirectional Downlink Directive Gain Patterns

Following the same steps as in the uplink, the directive gain patterns for the possible downlink arrays are generated. First, it is necessary to find the average radiation intensity using equation (5.5):

$$U_{\text{ave}} = \frac{1}{4\pi} \int_0^{2\pi} \int_0^{\pi} \frac{|f(\theta, \phi)|^2}{2\eta_0} \sin\theta d\theta d\phi$$

Next determine the directive gain using equation (5.6):

$$D(\theta, \phi) = \frac{\dfrac{|f(\theta, \phi)|^2}{2\eta_0}}{U_{\text{ave}}}$$

For the combination of $N = 12$ and $\upsilon = 2$, the average radiation intensity is:

$$U_{\text{ave}} = \frac{17.86}{2\eta_0}$$

The roll and elevation planes directive gain patterns for $N = 12$ and $\upsilon = 2$ are shown in Figure 29 and 30 on page 53.

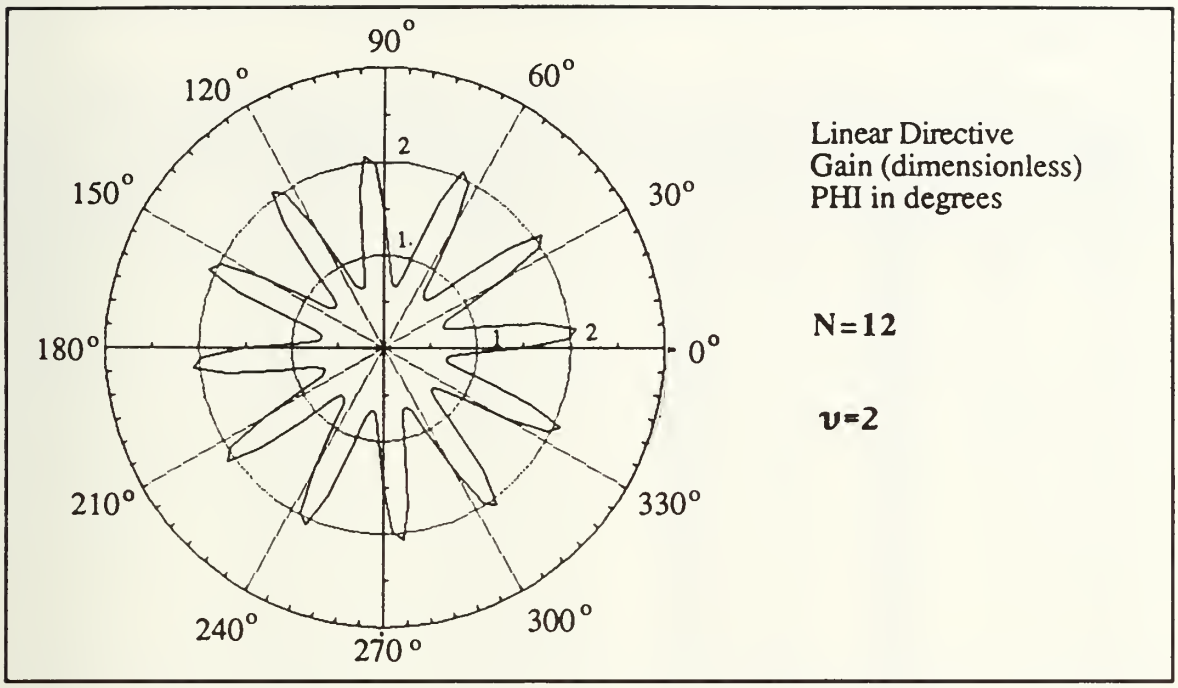

Figure 29. Downlink Roll Plane Gain Pattern for Combination 1.

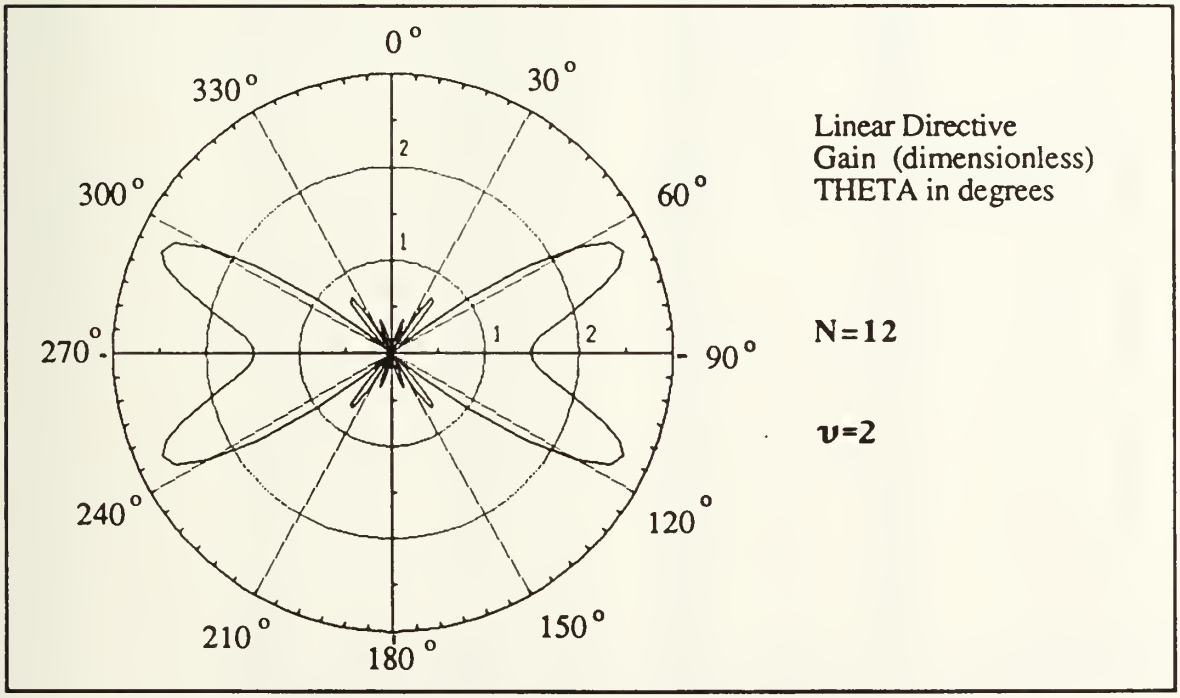

Figure 30. Downlink Elevation Plane Gain Pattern for Combination 1.

The gain for the roll and elevation planes are listed in the following tables for $N = 12$ and $v = 2$.

Table 7. DOWNLINK ROLL PLANE GAIN FOR COMBINATION 1.

ϕ degrees	Gain dB	ϕ degrees	Gain dB	ϕ degrees	Gain dB
0	1.8	120	1.7	240	1.7
3	3.0	123	3.0	243	3.0
6	3.2	126	3.2	246	3.2
9	2.3	129	2.3	249	2.3
12	0.7	132	0.7	252	0.7
15	-0.9	135	-0.9	255	-0.9
18	-1.6	138	-1.6	258	-1.6
21	-1.7	141	-1.7	261	-1.7
24	-1.3	144	-1.3	264	-1.3
27	0.0	147	0.0	267	0.0
30	1.7	150	1.7	270	1.7
33	3.0	153	3.0	273	3.0
36	3.2	156	3.2	276	3.2
39	2.3	159	2.3	279	2.3
42	0.7	162	0.7	282	0.7
45	-0.9	165	-0.9	285	-0.9
48	-1.6	168	-1.6	288	-1.6
51	-1.7	171	-1.7	291	-1.7
54	-1.3	174	-1.3	294	-1.3
57	0.0	177	0.0	297	0.0
60	1.7	180	1.7	300	1.7
63	3.0	183	3.0	303	3.0
66	3.2	186	3.2	306	3.2
69	2.3	189	2.3	309	2.3
72	0.7	192	0.7	312	0.7
75	-0.9	195	-0.9	315	-0.9
78	-1.6	198	-1.6	318	-1.6
81	-1.7	201	-1.7	321	-1.7
84	-1.3	204	-1.3	324	-1.3
87	0.0	207	0.0	327	0.0
90	1.7	210	1.7	330	1.7
93	3.0	213	3.0	333	3.0
96	3.2	216	3.2	336	3.2
99	2.3	219	2.3	339	2.3
102	0.7	222	0.7	342	0.7
105	-0.9	225	-0.9	345	-0.9
108	-1.6	228	-1.6	348	-1.6
111	-1.7	231	-1.7	351	-1.7
114	-1.3	234	-1.3	354	-1.3
117	0.0	237	0.0	357	0.0

Table 8. DOWNLINK ELEVATION PLANE GAIN FOR COMBINATION 1.

θ degrees	Gain dB	θ degrees	Gain dB	θ degrees	Gain dB
0	$-\infty$	120	3.6	240	3.6
3	-40.0	123	2.3	243	4.2
6	-23.0	126	0.0	246	4.3
9	-13.8	129	-4.1	249	4.2
12	-8.3	132	-12.9	252	3.8
15	-5.2	135	-10.2	255	3.3
18	-4.1	138	-4.0	258	2.8
21	-5.2	141	-1.6	261	2.4
24	-9.8	144	-1.3	264	2.0
27	-33.9	147	-3.1	267	1.8
30	-8.2	150	-8.1	270	1.7
33	-3.1	153	-33.9	273	1.8
36	-1.3	156	-9.8	276	2.0
39	-1.6	159	-5.2	279	2.4
42	-4.0	162	-4.1	282	2.8
45	-10.2	165	-5.2	285	3.3
48	-12.9	168	-8.3	288	3.8
51	-4.1	171	-13.8	291	4.2
54	0.0	174	-23.0	294	4.3
57	2.3	177	-40.2	297	4.2
60	3.6	180	$-\infty$	300	3.6
63	4.2	183	-40.2	303	2.3
66	4.3	186	-23.0	306	0.0
69	4.2	189	-13.8	309	-4.1
72	3.8	192	-8.3	312	-12.9
75	3.3	195	-5.2	315	-10.2
78	2.8	198	-4.1	318	-4.0
81	2.4	201	-5.2	321	-1.6
84	2.0	204	-9.8	324	-1.3
87	1.8	207	-33.9	327	-3.1
90	1.7	210	-8.1	330	-8.1
93	1.8	213	-3.1	333	-33.9
96	2.0	216	-1.3	336	-9.8
99	2.4	219	-1.6	339	-5.2
102	2.8	222	-4.0	342	-4.1
105	3.3	225	-10.2	345	-5.2
108	3.8	228	-12.9	348	-8.3
111	4.2	231	-4.1	351	-13.8
114	4.3	234	0.0	354	-23.0
117	4.2	237	2.3	357	-40.2

In the roll plane, the minimum and maximum gains for $N = 12$ and $\upsilon = 2$ are:

$G_{min} = -1.7$ dB at $\phi = 21°$

$G_{max} = 3.2$ dB at $\phi = 36°$

The ripple in the roll plane is 4.9 dB as shown in Figure 29 on page 53. The receiver must be able to receive the input signal even though the power of the signal fluctuates by 4.9 dB. If the satellite is spin-stabilized at a rate of 100 RPM, the power fluctuations in the received signal should not affect the quality of the signal as long as the data rate is much higher than the rate of the power fluctuations. This is the case here, so there should be no problem with the ripple as long as the minimum power is above the gain specification. The elevation plane radiation pattern for $N = 12$ and $\upsilon = 2$ (Figure 22 on page 48) is very deceptive because it looks like it has a fairly wide main beam. The elevation plane directive gain pattern (Figure 30 on page 53) shows that it almost has two large beams. At $\theta = 90°$, the beam is almost 3 dB down for the maximum of 4.3 dB. By strict definition, the half-power beamwidth is:

$HP_\theta = 68°$ $56° \leq \theta \leq 124°$

The minimum gain of this array will not meet the gain specification of:

$G_{spec} = 7.1$ dB

for the downlink. Considering this gain pattern in three-dimensions, the minimum gain is the lesser of the minimum gain of the roll pattern or the half-power point of the elevation pattern. In this case, the minimum gain is -1.7 dB. By comparing this gain to the downlink gain specifications in Table 2 on page 17, this antenna will work up to an altitude of approximately 350 nm.

For the combination of $N = 15$ and $\upsilon = 1$, the average radiation intensity is:

$$U_{ave} = \frac{18.00}{2\eta_0}$$

The roll and elevation planes directive gain patterns are shown in Figure 31 and 32 on page 57 for $N = 15$ and $\upsilon = 1$.

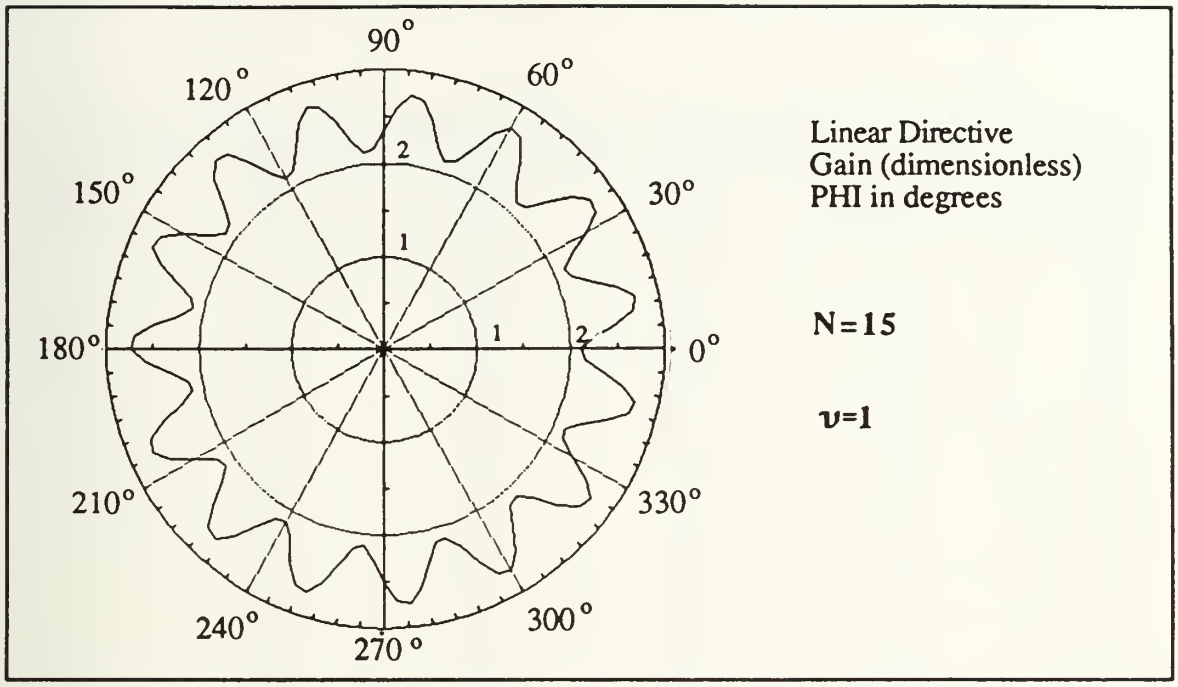

Figure 31. Downlink Roll Plane Gain Pattern for Combination 2.

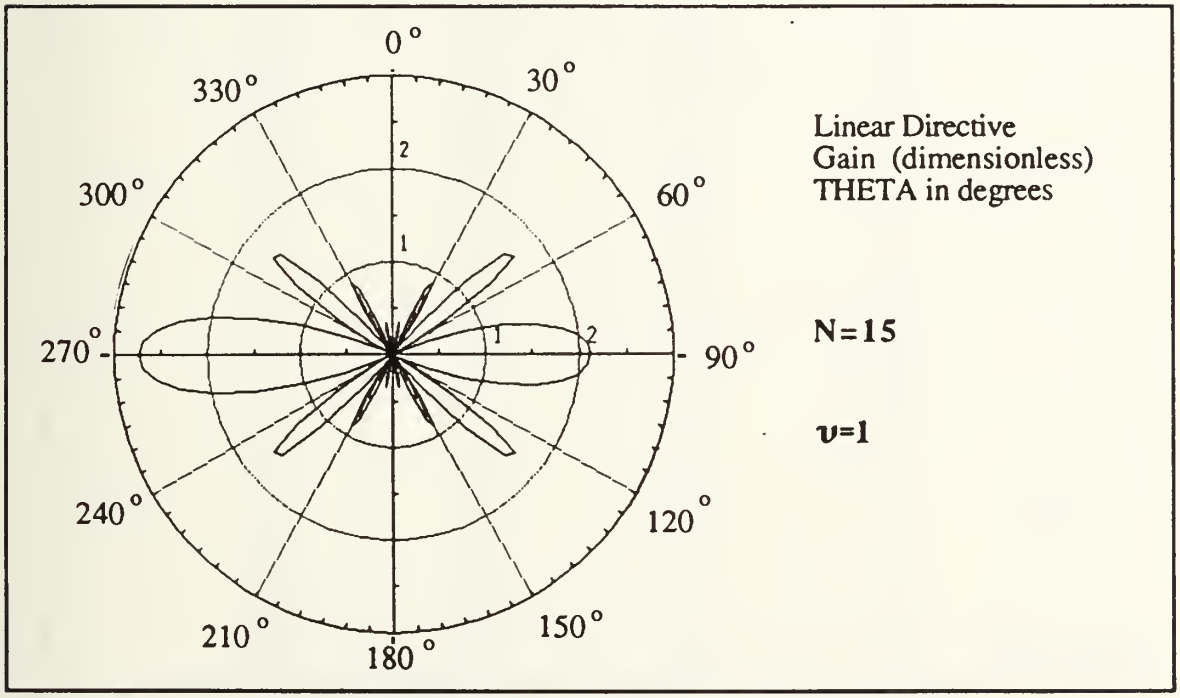

Figure 32. Downlink Elevation Plane Gain Pattern for Combination 2.

The gain for the roll and elevation planes are listed in Tables 9 and 10 for $N = 15$ and $v = 1$.

Table 9. DOWNLINK ROLL PLANE GAIN FOR COMBINATION 2.

ϕ degrees	Gain dB	ϕ degrees	Gain dB	ϕ degrees	Gain dB
0	3.2	120	3.2	240	3.2
3	3.5	123	3.5	243	3.5
6	3.9	126	3.9	246	3.9
9	4.3	129	4.3	249	4.3
12	4.3	132	4.3	252	4.3
15	4.1	135	4.1	255	4.1
18	3.7	138	3.7	258	3.7
21	3.3	141	3.3	261	3.3
24	3.2	144	3.2	264	3.2
27	3.5	147	3.5	267	3.5
30	3.9	150	3.9	270	3.9
33	4.3	153	4.3	273	4.3
36	4.3	156	4.3	276	4.3
39	4.1	159	4.1	279	4.1
42	3.7	162	3.7	282	3.7
45	3.3	165	3.3	285	3.3
48	3.2	168	3.2	288	3.2
51	3.5	171	3.5	291	3.5
54	3.9	174	3.9	294	3.9
57	4.3	177	4.3	297	4.3
60	4.3	180	4.3	300	4.3
63	4.1	183	4.1	303	4.1
66	3.7	186	3.7	306	3.7
69	3.3	189	3.3	309	3.3
72	3.2	192	3.2	312	3.2
75	3.5	195	3.5	315	3.5
78	3.9	198	3.9	318	3.9
81	4.7	201	4.3	321	4.3
84	4.3	204	4.3	324	4.3
87	4.1	207	4.1	327	4.1
90	3.7	210	3.7	330	3.7
93	3.3	213	3.3	333	3.3
96	3.2	216	3.2	336	3.2
99	3.5	219	3.5	339	3.5
102	3.9	222	3.9	342	3.9
105	4.3	225	4.3	345	4.3
108	4.3	228	4.3	348	4.3
111	4.1	231	4.1	351	4.1
114	3.7	234	3.7	354	3.7
117	3.3	237	3.3	357	3.3

Table 10. DOWNLINK ELEVATION PLANE GAIN FOR COMBINATION 2.

θ degrees	Gain dB	θ degrees	Gain dB	θ degrees	Gain dB
0	$-\infty$	120	-6.6	240	-7.3
3	-21.9	123	-1.5	243	-33.7
6	-11.1	126	1.1	246	-8.5
9	-6.1	129	2.2	249	-2.8
12	-4.5	132	2.1	252	0.1
15	-5.9	135	0.4	255	1.8
18	-13.1	138	-3.6	258	2.9
21	-14.4	141	-15.6	261	3.6
24	-4.4	144	-9.3	264	4.0
27	-1.1	147	-2.6	267	4.3
30	-0.6	150	-0.6	270	4.3
33	-2.6	153	-1.1	273	4.3
36	-9.3	156	-4.4	276	4.0
39	-15.6	159	-14.4	279	3.6
42	-3.6	162	-13.1	282	2.9
45	0.4	165	-5.9	285	1.8
48	2.1	168	-4.5	288	0.1
51	2.2	171	-6.1	291	-2.8
54	1.1	174	-11.1	294	-8.5
57	-1.5	177	-21.9	297	-33.7
60	-6.6	180	$-\infty$	300	-7.3
63	-22.6	183	-21.9	303	-1.8
66	-10.4	186	-11.1	306	0.9
69	-4.0	189	-6.1	309	2.1
72	-0.0	192	-4.5	312	2.0
75	0.8	195	-5.9	315	0.4
78	1.9	198	-13.1	318	-3.6
81	2.6	201	-14.4	321	-15.7
84	3.0	204	-4.4	324	-9.3
87	3.2	207	-1.1	327	-2.6
90	3.2	210	-0.6	330	-0.6
93	3.2	213	-2.6	333	-1.1
96	3.0	216	-9.3	336	-4.4
99	2.6	219	-15.7	339	-14.4
102	1.9	222	-3.6	342	-13.1
105	0.8	225	0.4	345	-5.9
108	-0.9	228	2.0	348	-4.5
111	-4.0	231	2.1	351	-6.1
114	-10.4	234	0.9	354	-11.1
117	-22.6	237	-1.8	357	-21.9

The minimum and maximum gain for this array in the roll plane for $N = 15$ and $v = 1$ are:

$G_{min} = 3.2$ dB at $\phi = 0°$

$G_{max} = 4.3$ dB at $\phi = 11°$

By the addition of more patches, the roll plane ripple has been reduced to 1.1 dB. The graph of the elevation plane gain pattern shows the significant narrowing of the mainlobe. The maximum gain in the elevation plane is 4.3 dB at $\theta = 270°$. The half-power beamwidth is:

$HP_\theta = 32°$ $254° \leq \theta \leq 286°$

At $\theta = 90°$, the gain is 3.2 dB. The half-power beamwidth is still the same.

$HP_\theta = 32°$ $74° \leq \theta \leq 106°$

Considering the three-dimensional pattern, the minimum gain is:

$G_{min} = 0.8$ dB

located at:

$\theta = 74°$

$\phi = 0°$

This antenna does not meet the downlink gain specification but will work up to an altitude of approximately 550 nm.

From equation (5.5), the average radiation intensity for an array with $N = 16$ and $v = 1$ is:

$$U_{ave} = \frac{19.46}{2\eta_0}$$

The directive gain patterns are shown in Figures 33 and 34 on page 61 for $N = 16$ and $v = 1$.

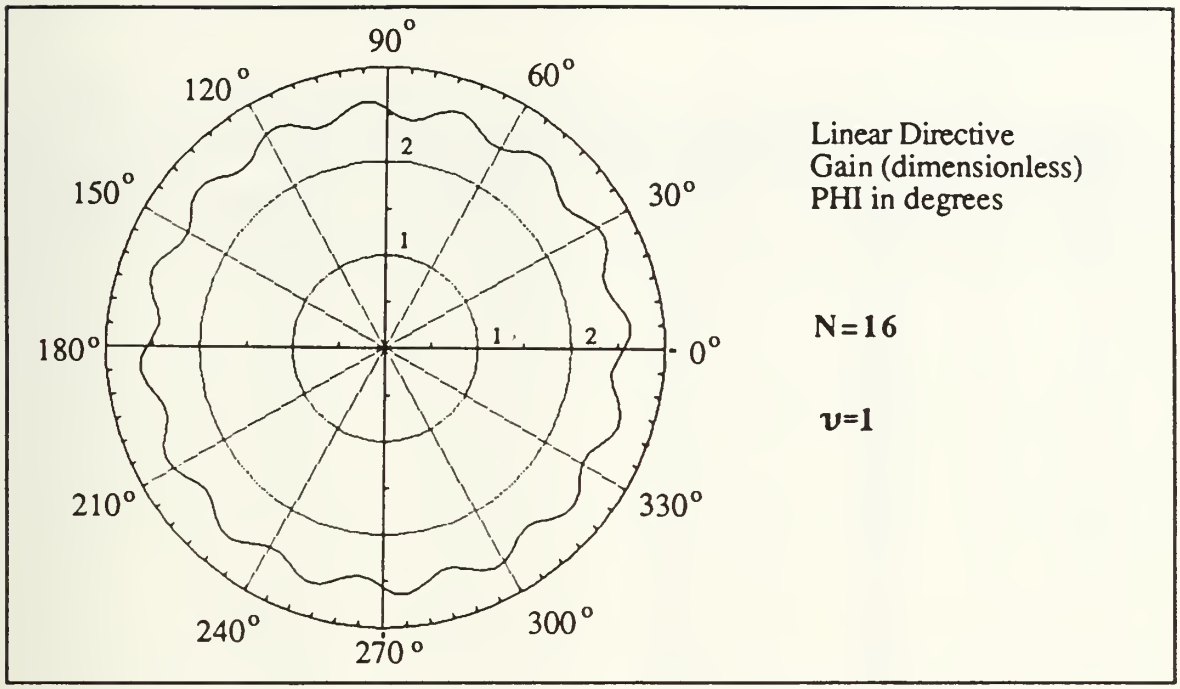

Figure 33. Downlink Roll Plane Gain Pattern for Combination 3.

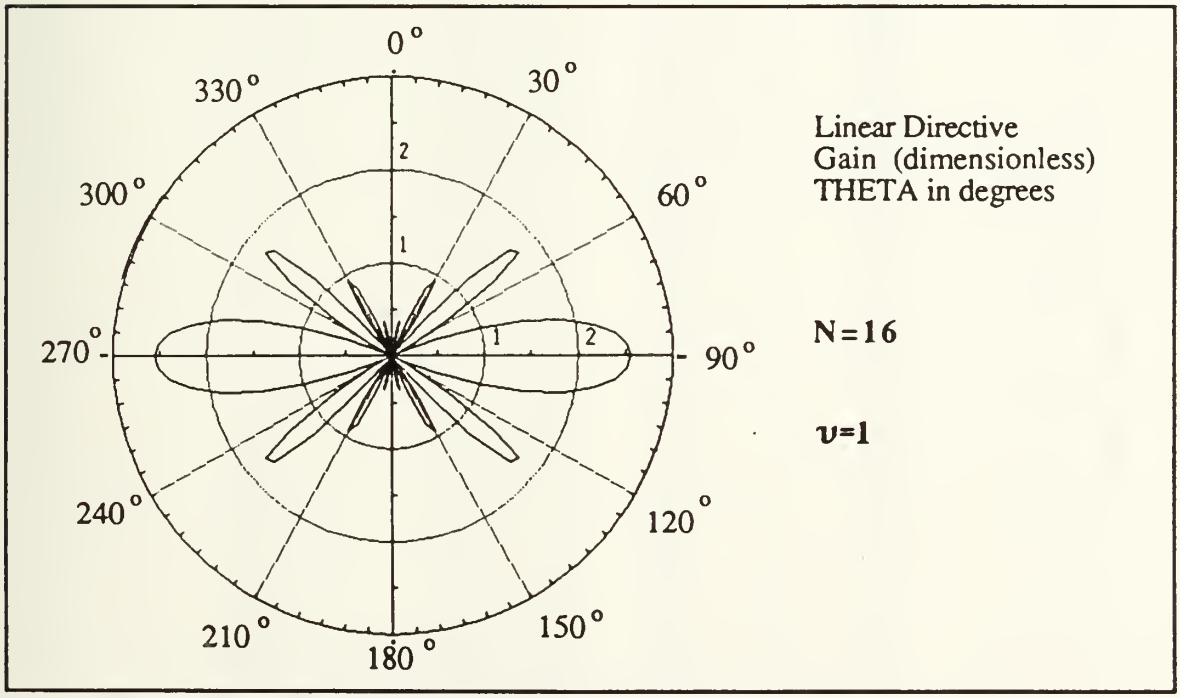

Figure 34. Downlink Elevation Plane Gain Pattern for Combination 3.

The gain for the roll and elevation planes are listed in the following tables for $N = 16$ and $v = 1$.

Table 11. DOWNLINK ROLL PLANE GAIN FOR COMBINATION 3.

ϕ degrees	Gain dB	ϕ degrees	Gain dB	ϕ degrees	Gain dB
0	4.0	120	4.1	240	3.8
3	4.1	123	4.0	243	3.8
6	4.1	126	3.9	246	3.9
9	4.1	129	3.8	249	4.1
12	4.1	132	3.9	252	4.1
15	3.8	135	4.0	255	4.1
18	3.8	138	4.1	258	4.0
21	3.9	141	4.1	261	3.9
24	4.1	144	4.1	264	3.8
27	4.1	147	3.9	267	3.9
30	4.1	150	3.8	270	4.0
33	4.0	153	3.8	273	4.1
36	3.9	156	3.9	276	4.1
39	3.8	159	4.1	279	4.1
42	3.9	162	4.1	282	3.9
45	4.0	165	4.1	285	3.8
48	4.1	168	4.0	288	3.8
51	4.1	171	3.9	291	3.9
54	4.1	174	3.8	294	4.1
57	3.9	177	3.9	297	4.1
60	3.8	180	4.0	300	4.1
63	3.8	183	4.1	303	4.0
66	3.9	186	4.1	306	3.9
69	4.1	189	4.1	309	3.8
72	4.1	192	3.9	312	3.9
75	4.1	195	3.8	315	4.0
78	4.0	198	3.8	318	4.1
81	3.9	201	3.9	321	4.1
84	3.8	204	4.1	324	4.1
87	3.9	207	4.1	327	3.9
90	4.0	210	4.1	330	3.8
93	4.1	213	4.0	333	3.8
96	4.1	216	3.9	336	3.9
99	4.1	219	3.8	339	4.1
102	4.0	222	3.9	342	4.1
105	3.8	225	4.0	345	4.1
108	3.8	228	4.1	348	4.0
111	3.9	231	4.1	351	3.9
114	4.1	234	4.1	354	3.8
117	4.1	237	3.9	357	3.9

Table 12. DOWNLINK ELEVATION PLANE GAIN FOR COMBINATION 3.

θ degrees	Gain dB	θ degrees	Gain dB	θ degrees	Gain dB
0	$-\infty$	120	-6.8	240	-6.8
3	-21.7	123	-1.5	243	-26.5
6	-10.9	126	1.2	246	-9.2
9	-6.0	129	2.3	249	-3.2
12	-4.3	132	2.2	252	-0.2
15	-5.7	135	0.6	255	1.6
18	-12.9	138	-3.4	258	2.7
21	-14.2	141	-15.5	261	3.3
24	-4.2	144	-9.1	264	3.7
27	-0.9	147	-2.4	267	3.9
30	-0.4	150	-0.4	270	4.0
33	-2.4	153	-0.9	273	3.9
36	-9.1	156	-4.2	276	3.7
39	-15.5	159	-14.2	279	3.3
42	-3.4	162	-12.9	282	2.7
45	0.6	165	-5.7	285	1.6
48	2.2	168	-4.3	288	-0.2
51	2.3	171	-6.0	291	-3.2
54	1.3	174	-10.9	294	-9.2
57	-1.5	177	-21.7	297	-26.5
60	-6.8	180	$-\infty$	300	-6.8
63	-26.5	183	-21.7	303	-1.5
66	-9.2	186	-10.9	306	1.2
69	-3.2	189	-6.0	309	2.3
72	-0.2	192	-4.3	312	2.2
75	1.6	195	-5.7	315	0.6
78	2.7	198	-12.9	318	-3.4
81	3.3	201	-14.2	321	-15.5
84	3.7	204	-4.2	324	-9.1
87	3.9	207	-0.9	327	-2.4
90	4.0	210	-0.4	330	-0.4
93	3.9	213	-2.4	333	-0.9
96	3.7	216	-9.1	336	-4.2
99	3.3	219	-15.5	339	-14.2
102	2.7	222	-3.4	342	-12.9
105	1.6	225	0.6	345	-5.7
108	-0.2	228	2.2	348	-4.3
111	-3.2	231	2.3	351	-6.0
114	-9.2	234	1.2	354	-10.9
117	-26.5	237	-1.5	357	-21.7

The minumum and maximum gain in the roll pattern for $N = 16$ and $v = 1$ are:

$G_{min} = 3.8$ dB at $\phi = 16°$

$G_{max} = 4.1$ dB at $\phi = 27°$

The ripple is now down to 0.3 dB. This shows that the ripple does decrease as the number of patches increases. The half-power beamwidth did not change from the previous combination. The maximum gain shown in the elevation plane is 4.0 dB at $\theta = 90°$. The half-power beamwidth is:

$HP_\theta = 32°$ $74° \leq \theta \leq 106°$

Considering the three-dimensional directive gain pattern, the minimum gain occurs at a half-power point in the elevation plane.

$G_{min} = 1.0$ dB

at

$\theta = 74°$

$\phi = 15°$

Comparing this minimum gain with the downlink specification, this array will work up to an altitude of approximately 650 nm. At 650 nm, the look angle (2α) is approximately 114°. The footprint of this array would cover less than one third of what the satellite can "see".

For the combination of $N = 16$ and $v = 3$, the average radiation intensity is:

$$U_{ave} = \frac{26.62}{2\eta_0}$$

The directive gain patterns for $N = 16$ and $v = 3$ are shown in Figures 35 and 36 on page 65.

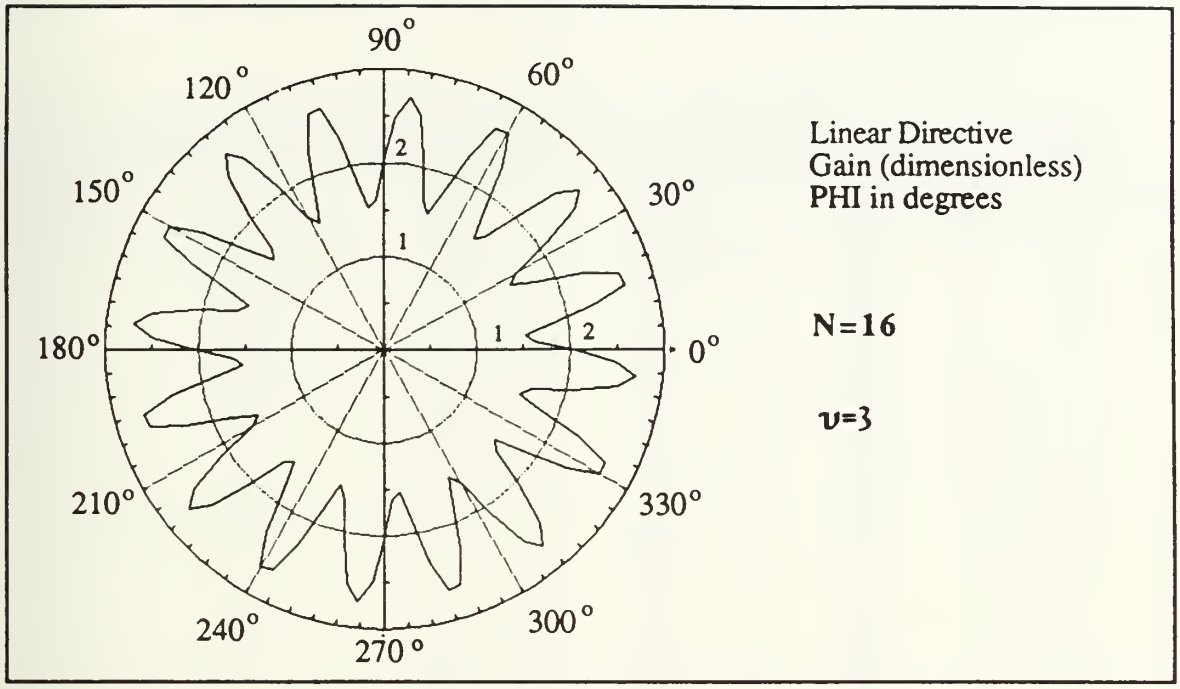

Figure 35. Downlink Roll Plane Gain Pattern for Combination 4.

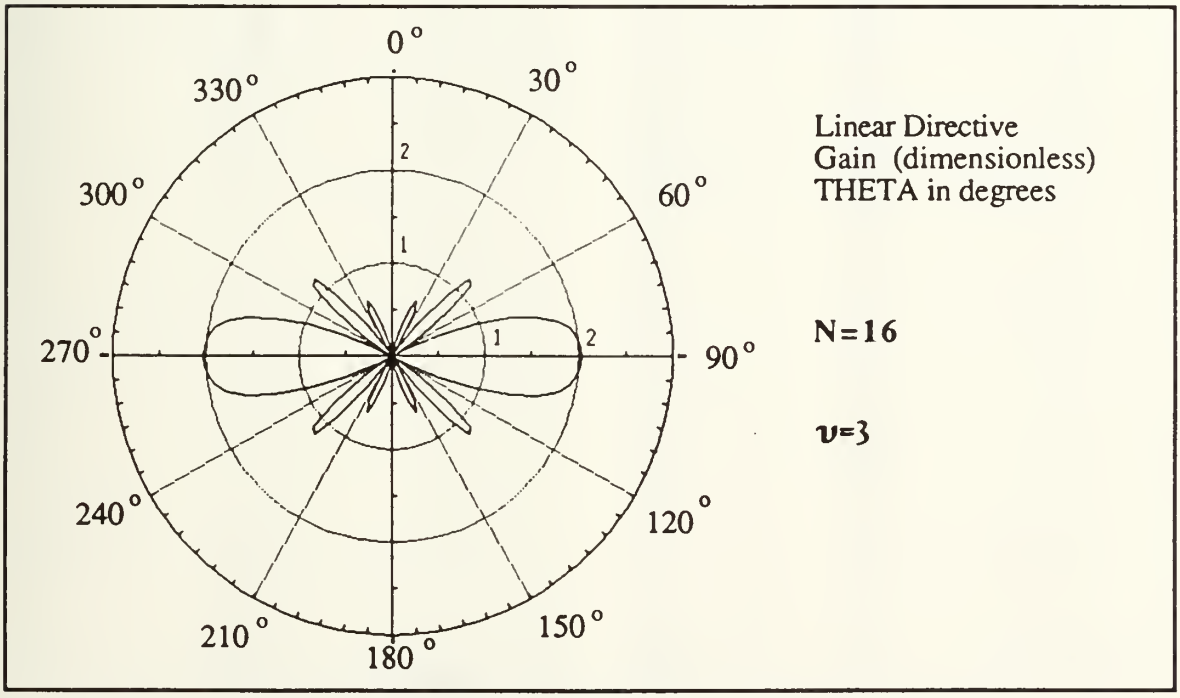

Figure 36. Downlink Elevation Plane Gain Pattern for Combination 4.

The gain for the roll and elevation planes are listed Tables 13 and 14 for $N = 16$ and $v = 3$.

Table 13. DOWNLINK ROLL PLANE GAIN FOR COMBINATION 4.

ϕ degrees	Gain dB	ϕ degrees	Gain dB	ϕ degrees	Gain dB
0	3.4	120	2.5	240	4.6
3	2.5	123	3.5	243	4.6
6	2.2	126	4.4	246	3.9
9	3.0	129	4.7	249	2.9
12	4.0	132	4.3	252	2.2
15	4.6	135	3.4	255	2.5
18	4.6	138	2.5	258	3.5
21	3.9	141	2.2	261	4.4
24	2.9	144	3.0	264	4.7
27	2.2	147	4.0	267	4.3
30	2.5	150	4.6	270	3.4
33	3.5	153	4.6	273	2.5
36	4.4	156	3.9	276	2.2
39	4.7	159	2.9	279	3.0
42	4.3	162	2.2	282	4.0
45	3.4	165	2.5	285	4.6
48	2.5	168	3.5	288	4.6
51	2.2	171	4.4	291	3.9
54	3.0	174	4.7	294	2.9
57	4.0	177	4.3	297	2.2
60	4.6	180	3.4	300	2.5
63	4.6	183	2.5	303	3.5
66	3.9	186	2.2	306	4.4
69	2.9	189	3.0	309	4.7
72	2.2	192	4.0	312	4.3
75	2.5	195	4.6	315	3.4
78	3.5	198	4.6	318	2.5
81	4.4	201	3.9	321	2.2
84	4.7	204	2.9	324	3.0
87	4.3	207	2.2	327	4.0
90	3.4	210	2.5	330	4.6
93	2.5	213	3.5	333	4.6
96	2.2	216	4.4	336	3.9
99	3.0	219	4.7	339	2.9
102	4.0	222	4.3	342	2.2
105	4.6	225	3.4	345	2.5
108	4.6	228	2.5	348	3.5
111	3.9	231	2.2	351	4.4
114	2.9	234	3.0	354	4.7
117	2.2	237	4.0	357	4.3

Table 14. DOWNLINK ELEVATION PLANE GAIN FOR COMBINATION 4.

θ degrees	Gain dB	θ degrees	Gain dB	θ degrees	Gain dB
0	$-\infty$	120	-18.3	240	-18.3
3	-59.3	123	-11.3	243	-6.5
6	-35.8	126	-4.0	246	-2.2
9	-22.8	129	-0.6	249	0.2
12	-14.2	132	0.9	252	1.6
15	-8.4	135	1.1	255	2.5
18	-4.5	138	-0.1	258	3.0
21	-2.2	141	-3.3	261	3.2
24	-1.4	144	-11.2	264	3.4
27	-2.3	147	-16.1	267	3.4
30	-5.5	150	-5.5	270	3.4
33	-16.1	153	-2.3	273	3.4
36	-11.2	156	-1.4	276	3.4
39	-3.3	159	-2.2	279	3.2
42	-0.1	162	-4.5	282	3.0
45	1.1	165	-8.4	285	2.5
48	0.9	168	-14.2	288	1.6
51	-0.6	171	-22.8	291	0.2
54	-4.0	174	-35.8	294	-2.2
57	-11.3	177	-59.3	297	-6.5
60	-18.3	180	$-\infty$	300	-18.3
63	-6.5	183	-59.3	303	-11.3
66	-2.2	186	-35.8	306	-4.0
69	0.2	189	-22.8	309	-0.6
72	1.6	192	-14.2	312	0.9
75	2.5	195	-8.4	315	1.1
78	3.0	198	-4.5	318	-0.1
81	3.2	201	-2.2	321	-3.3
84	3.4	204	-1.4	324	-11.2
87	3.4	207	-2.3	327	-16.1
90	3.4	210	-5.5	330	-5.5
93	3.4	213	-16.1	333	-2.3
96	3.4	216	-11.2	336	-1.4
99	3.2	219	-3.3	339	-2.2
102	3.0	222	-0.1	342	-4.5
105	2.5	225	1.1	345	-8.4
108	1.6	228	0.9	348	-14.2
111	0.2	231	-0.6	351	-22.8
114	-2.2	234	-4.0	354	-35.8
117	-6.5	237	-11.3	357	-59.3

The minimum and maximum gain in the roll plane for $N = 16$ and $\upsilon = 3$ are:

$G_{min} = 2.2$ dB at $\phi = 6°$

$G_{max} = 4.7$ dB at $\phi = 39°$

The ripple in the roll plane is 2.5 dB. By changing υ, the ripple has increased. The maximum gain shown in the elevation plane is 3.4 dB at $\theta = 90°$. The half-power beamwidth is:

$HP_\theta = 40°$ $70° \leq \theta \leq 110°$

The beamwidth has increased but not by a significant amount. The minimum gain throughout the three-dimenional directive gain pattern occurs at a half-power point on a lobe centered on $\phi = 6°$ and $\theta = 70°$. It is:

$G_{min} = -0.8$ dB

at

$\phi = 6°$

$\theta = 70°$

The minimum ripple in the roll plane limits the gain in the three-dimensional pattern at a half-power point in the elevation beam. The effective altitude of this antenna is approximately 450 nm.

After going through the analysis, it is evident that none of the downlink omnidirectional arrays can meet the downlink specification. Another problem is the lack of beamwidth in the elevation plane. The next step is to examine the directional property of the downlink array to see if a directional array can meet the downlink specification.

C. DIRECTIONAL DOWNLINK ANTENNA DESIGN

As discussed in Chapter IV, it is possible to produce a directional radiation pattern with a microstrip patch array. To use a directional antenna on the ORION satellite, the satellite will have to be 3-axis stabilized or the antenna will have to be electronically despun. Only the phase of the transmitted signal must be changed to go from the omnidirectional pattern to a directional pattern. Only the three cases of $N = 12$, 15 and 16 will be evaluated as directional antennas.

1. Downlink Directional Radiation Patterns

To produce a directional radiation pattern, the excitation coefficient, a_n, for the leading and trailing edge slots must be expressed according to equations (4.33) and (4.34):

$a_n = e^{-jka \sin\theta_0 \cos(\phi_0 - \nu_n)}$ for the leading edge slots

and

$a_n = e^{-jka \sin\theta_0 \cos(\phi_0 - \nu_n - \frac{L}{a})}$ for the trailing edge slots.

where θ_0 and ϕ_0 are the desired radiation direction. The radiation pattern for the directional array antenna is expressed by equation (4.35):

$$f(\theta, \phi) = \sum_{n=1}^{N} F(\theta, \phi) \left\{ e^{jka[\sin\theta \cos(\phi - \nu_n) - \sin\theta_0 \cos(\phi_0 - \nu_n)]} + e^{jka\left[\sin\theta \cos\left(\phi - \nu_n - \frac{L}{a}\right) - \sin\theta_0 \cos\left(\phi_0 - \nu_n - \frac{L}{a}\right)\right]} \right\} \tag{4.35}$$

The radiation patterns for the three cases under consideration are shown of the following pages (Figures 37 - 42) with:

$\theta_0 = 90°$

$\phi_0 = 0°$

for the desired radiation direction.

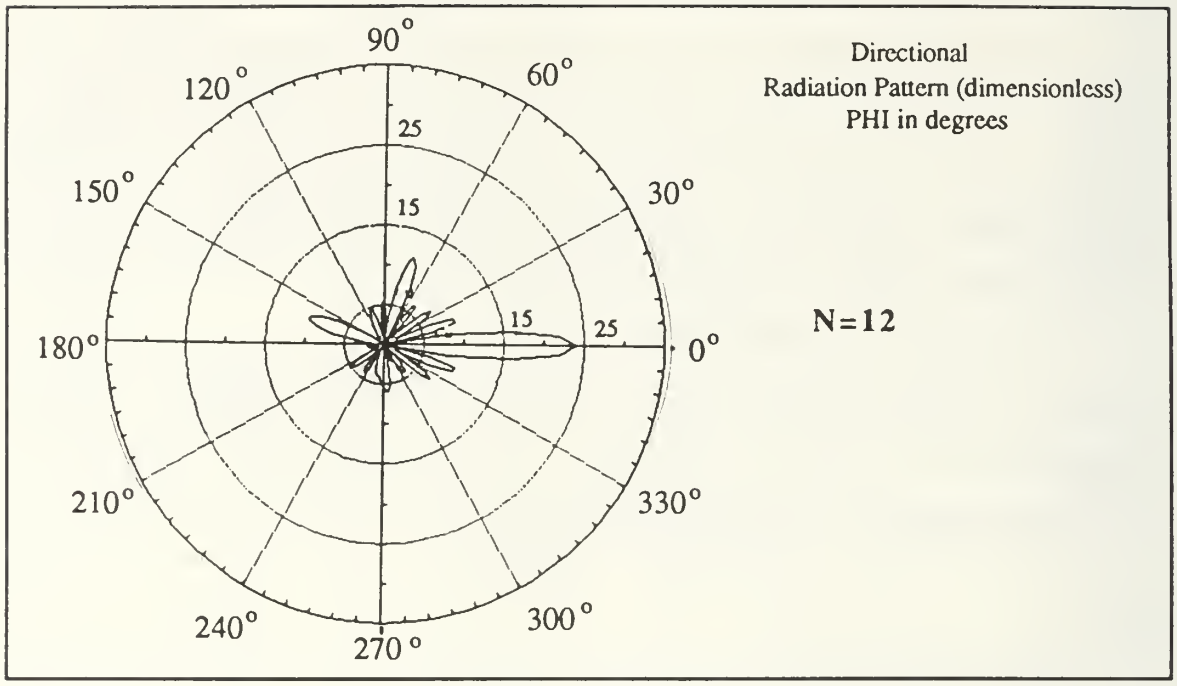

Figure 37. Directional Roll Plane Radiation Pattern - 12 Patch Array.

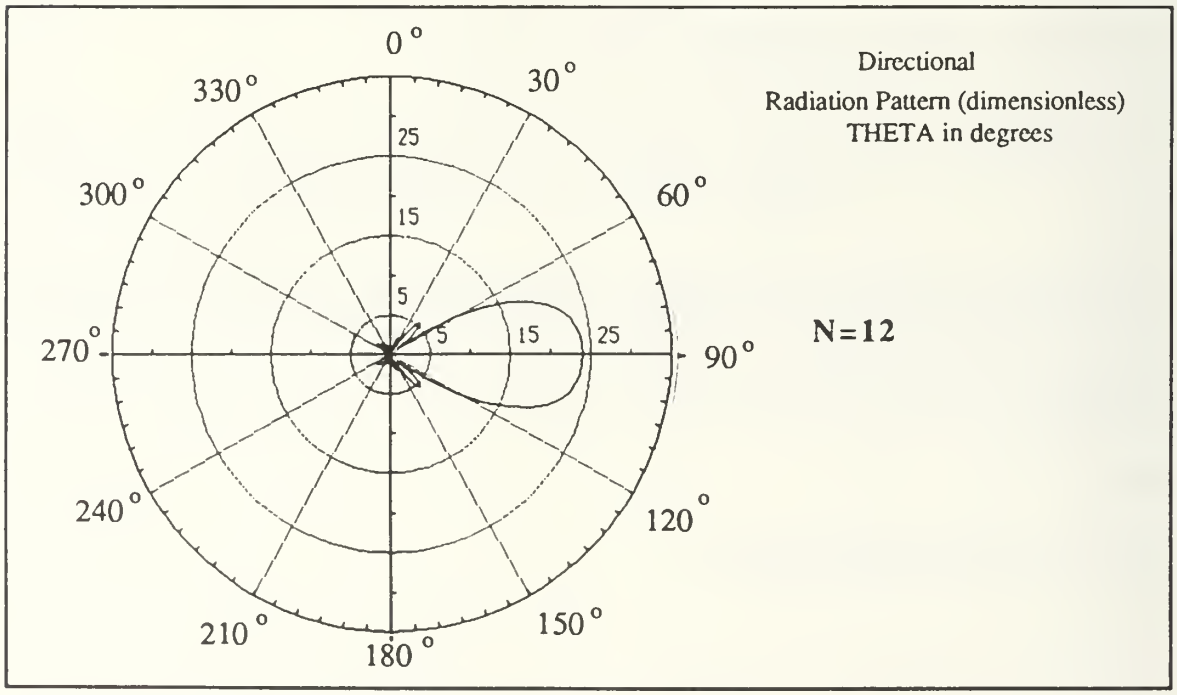

Figure 38. Directional Elevation Plane Radiation Pattern - 12 Patch Array.

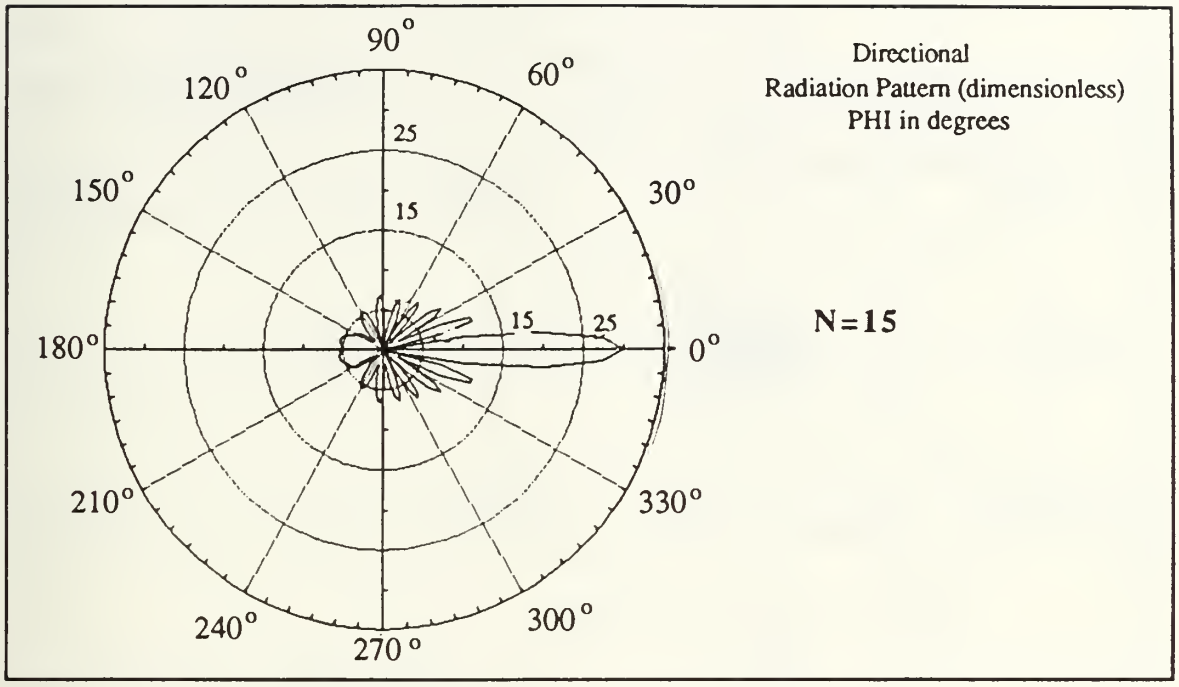

Figure 39. Directional Roll Plane Radiation Pattern - 15 Patch Array.

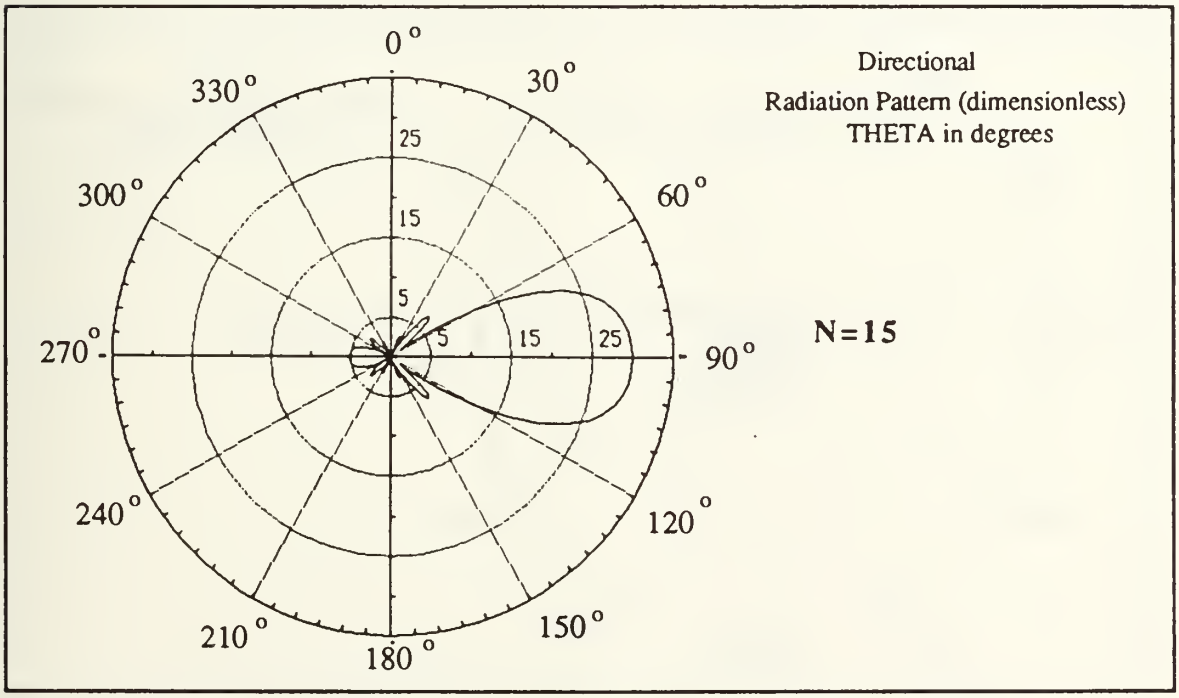

Figure 40. Directional Elevation Plane Radiation Pattern - 15 Patch Array.

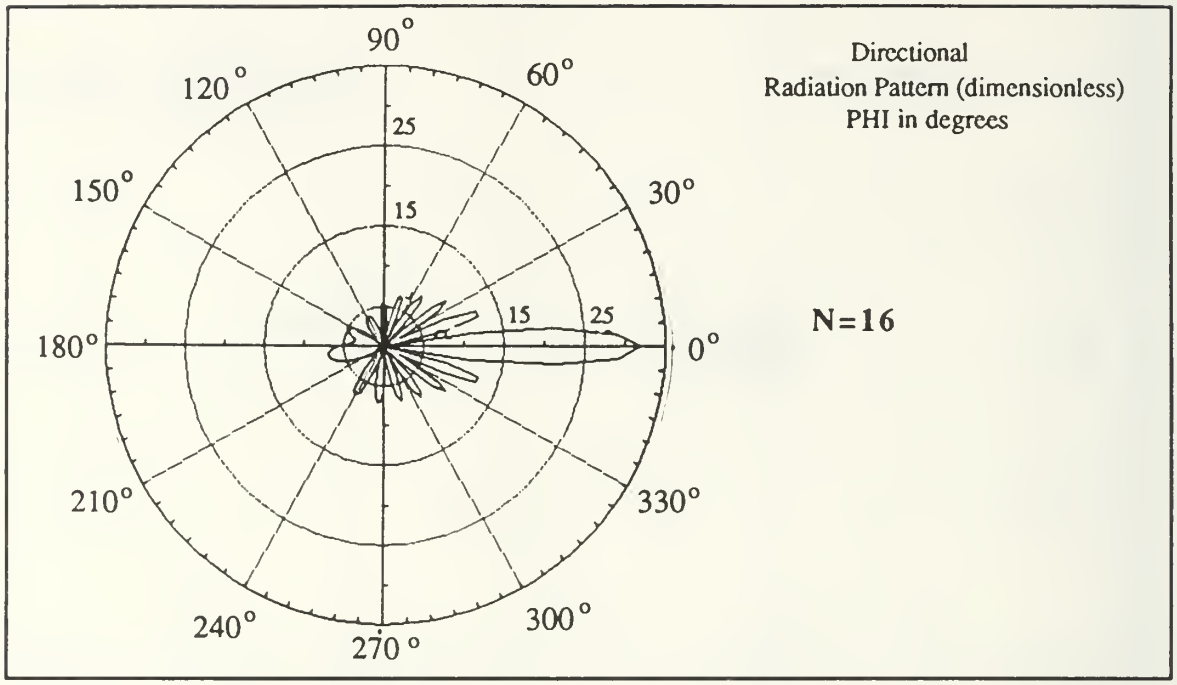

Figure 41. Directional Roll Plane Radiation Pattern - 16 Patch Array.

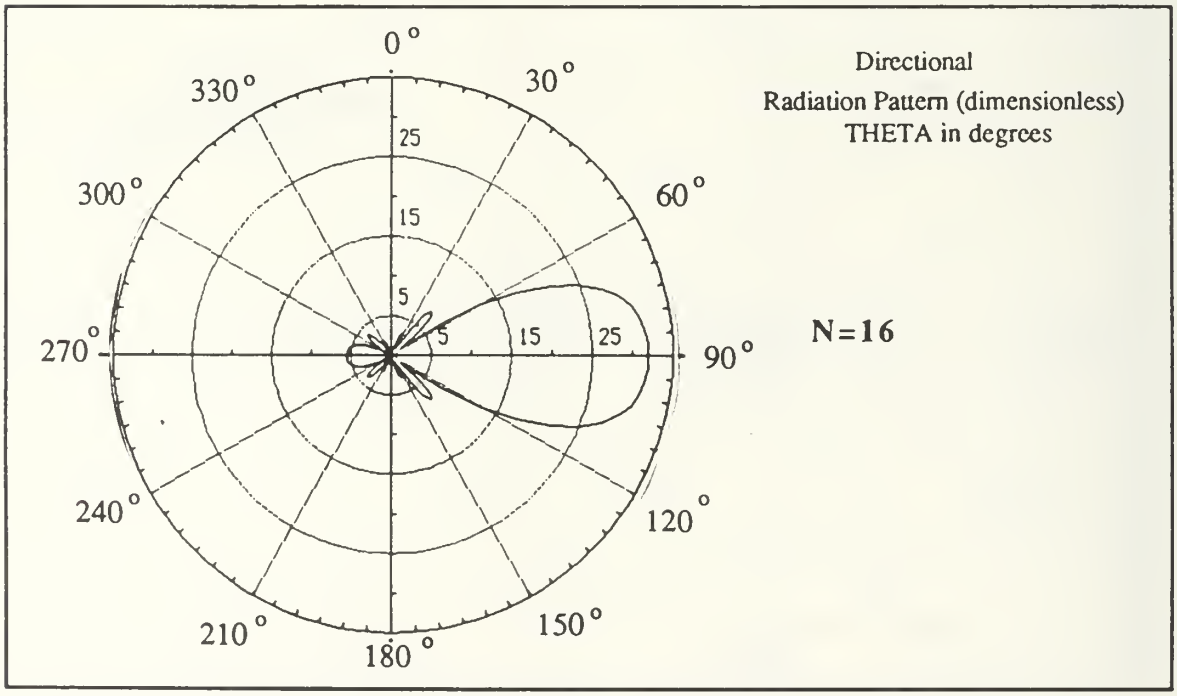

Figure 42. Directional Elevation Plane Radiation Pattern - 16 Patch Array.

From the previous figures, all three cases produce narrow directional beams in the roll plane and wide beams in the elevation plane.

2. Downlink Directional Directive Gain Patterns

The directive gain patterns will determine if the directional antennas will produce the required gain to meet the specification. The average radiation intensity can still be calculated from equation (4.31):

$$U_{ave} = \frac{1}{4\pi} \int_0^{2\pi} \int_0^{\pi} \frac{|f(\theta, \phi)|^2}{2\eta_0} \sin\theta d\theta d\phi$$

Appendix G is a MathCAD program that computes the average radiation intensity for a directional array. The directive gain, equation (4.32) also holds true for the directional array:

$$D(\theta, \phi) = \frac{|f(\theta, \phi)|^2}{\frac{1}{4\pi} \int_0^{2\pi} \int_0^{\pi} |f(\theta, \phi)|^2 \sin\theta d\theta d\phi}$$

Appendix H is a MathCAD program that computes and graphs the directional directive gain.

For an array with $N = 12$, the average radiation intensity is:

$$U_{ave} = \frac{30.53}{2\eta_0}$$

The directional directive gain patterns for $N = 12$ are shown in Figures 43 and 42 on page 74.

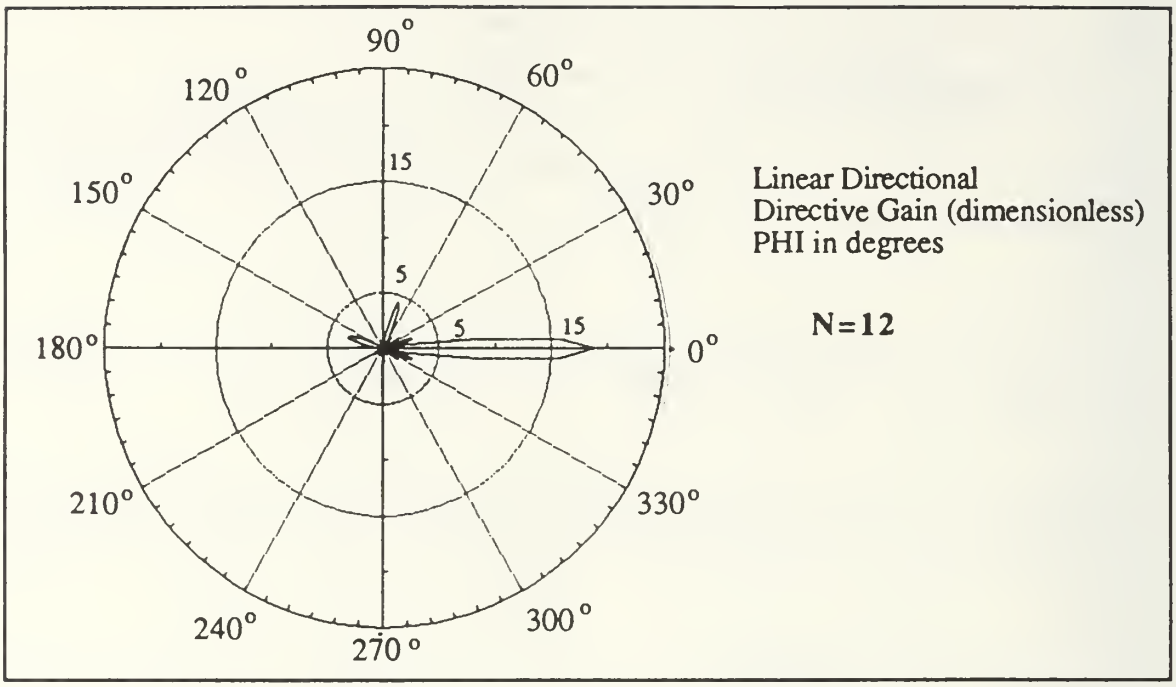

Figure 43. Directional Roll Plane Gain Pattern - 12 Patch Array.

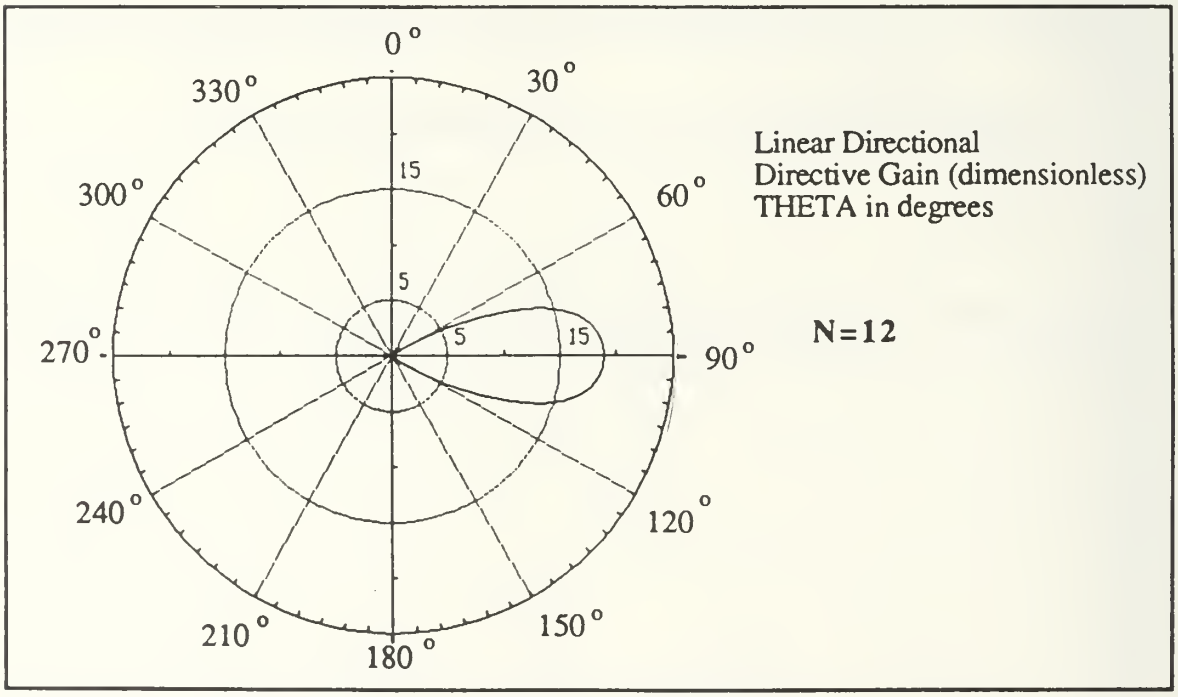

Figure 44. Directional Elevation Plane Gain Pattern - 12 Patch Array.

The directional directive gain for the roll and elevation planes for $N = 12$ are listed in Tables 15 and 16.

Table 15. N = 12 DIRECTIONAL DOWNLINK ROLL PLANE GAIN.

ϕ degrees	Gain dB	ϕ degrees	Gain dB	ϕ degrees	Gain dB
0	12.8	120	-5.9	240	-5.9
3	12.0	123	-9.0	243	-14.0
6	9.4	126	-12.3	246	-18.0
9	3.6	129	-14.8	249	-7.9
12	-24.6	132	-15.6	252	-4.6
15	0.7	135	-14.9	255	-3.2
18	4.5	138	-14.5	258	-2.8
21	4.4	141	-16.7	261	-2.6
24	1.1	144	-53.9	264	-2.1
27	-10.2	147	-11.3	267	-1.2
30	-5.7	150	-3.5	270	-0.1
33	0.8	153	1.0	273	0.7
36	2.2	156	3.7	276	0.6
39	0.6	159	5.0	279	-0.7
42	-5.5	162	5.1	282	-4.1
45	-17.0	165	4.1	285	-12.7
48	-2 6	168	1.7	288	-16.4
51	0.9	171	-2.3	291	-7.9
54	0.9	174	-8.2	294	-7.1
57	-2.4	177	-15.6	297	-12.1
60	-19.2	180	-18.5	300	-19.2
63	-3.4	183	-13.9	303	-6.0
66	3.0	186	-9.9	306	-2.3
69	5.7	189	-8.2	309	-2.1
72	6.4	192	-8.8	312	-6.0
75	5.4	195	-11.6	315	-39.1
78	2.4	198	-16.3	318	-4.2
81	-4.6	201	-18.8	321	0.9
84	-16.6	204	-13.9	324	2.3
87	-2.9	207	-7.8	327	0.9
90	-0.1	210	-3.5	330	-5.7
93	-0.5	213	-1.2	333	-10.2
96	-3.8	216	-0.5	336	1.1
99	-14.3	219	-1.8	339	4.4
102	-11.3	222	-5.9	342	4.5
105	-3.9	225	-20.7	345	0.7
108	-1.4	228	-9.9	348	-24.6
111	-0.9	231	-4.0	351	3.6
114	-1.7	234	-2.3	354	9.4
117	-3.4	237	-2.9	357	12.0

Table 16. N = 12 DIRECTIONAL DOWNLINK ELEVATION PLANE GAIN.

θ degrees	Gain dB	θ degrees	Gain dB	θ degrees	Gain dB
0	$-\infty$	120	4.9	240	-14.5
3	-31.3	123	0.7	243	-19.9
6	-22.4	126	-7.9	246	-32.1
9	-20.1	129	-13.9	249	-28.9
12	-24.9	132	-3.5	252	-22.1
15	-24.5	135	-0.4	255	-19.6
18	-13.2	138	0.1	258	-18.6
21	-8.9	141	-1.1	261	-18.3
24	-7.7	144	-4.6	264	-18.4
27	-9.6	147	-12.8	267	-18.5
30	-19.9	150	-19.9	270	-18.4
33	-12.8	153	-9.6	273	-18.3
36	-4.6	156	-7.7	276	-18.3
39	-1.1	159	-8.9	279	-18.6
42	0.1	162	-13.2	282	-19.6
45	-0.4	165	-24.5	285	-22.1
48	-3.5	168	-24.9	288	-28.9
51	-13.9	171	-20.1	291	-32.1
54	-7.9	174	-22.4	294	-19.9
57	0.7	177	-31.3	297	-14.5
60	4.9	180	$-\infty$	300	-11.3
63	7.6	183	-32.7	303	-9.4
66	9.4	186	-20.5	306	-8.7
69	10.6	189	-14.9	309	-9.2
72	11.4	192	-12.6	312	-11.4
75	12.0	195	-13.1	315	-17.2
78	12.3	198	-17.7	318	-33.0
81	12.4	201	-35.4	321	-14.9
84	12.7	204	-15.1	324	-10.6
87	12.7	207	-10.6	327	-9.4
90	12.8	210	-9.4	330	-10.6
93	12.7	213	-10.6	333	-15.1
96	12.7	216	-14.9	336	-35.4
99	12.6	219	-33.0	339	-17.7
102	12.3	222	-17.2	342	-13.1
105	12.0	225	-11.4	345	-12.6
108	11.4	228	-9.2	348	-14.9
111	10.6	231	-8.7	351	-20.5
114	9.4	234	-9.4	354	-32.7
117	7.6	237	-11.3	357	

The maximum directional gain in the roll plane for $N = 12$ is:

$G_{max} = 12.8$ dB at $\theta = 90°$ and $\phi = 0°$ as expected.

The roll plane has a narrow beamwidth with half-power points at:

$\phi = 355°$ and $\phi = 5°$.

This results in a roll plane half-power beamwidth of:

$HP_{\phi} = 10°$

The elevation plane half-power points occur at:

$\theta = 67°$ and $\theta = 113°$

The resulting elevation plane half-power beamwidth is:

$HP_{\theta} = 46°$

The beamwidth that will meet the downlink gain specification is the angular distance between the two points on the main beam where the gain is the same as the specification of 7.1 dB. In the roll plane the beamwidth is:

Roll Plane Beamwidth $= 14°$ $353° \leq \phi \leq 7°$

In the elevation plane, the beamwidth that meets the specification is:

Elevation Plane Beamwidth $= 54°$ $62° \leq \theta \leq 116°$

For a 15 patch array, the average radiation intensity is:

$$U_{ave} = \frac{39.44}{2\eta_0}$$

The directive gain patterns for $N = 15$ are shown in Figures 45 and 46 on page 78.

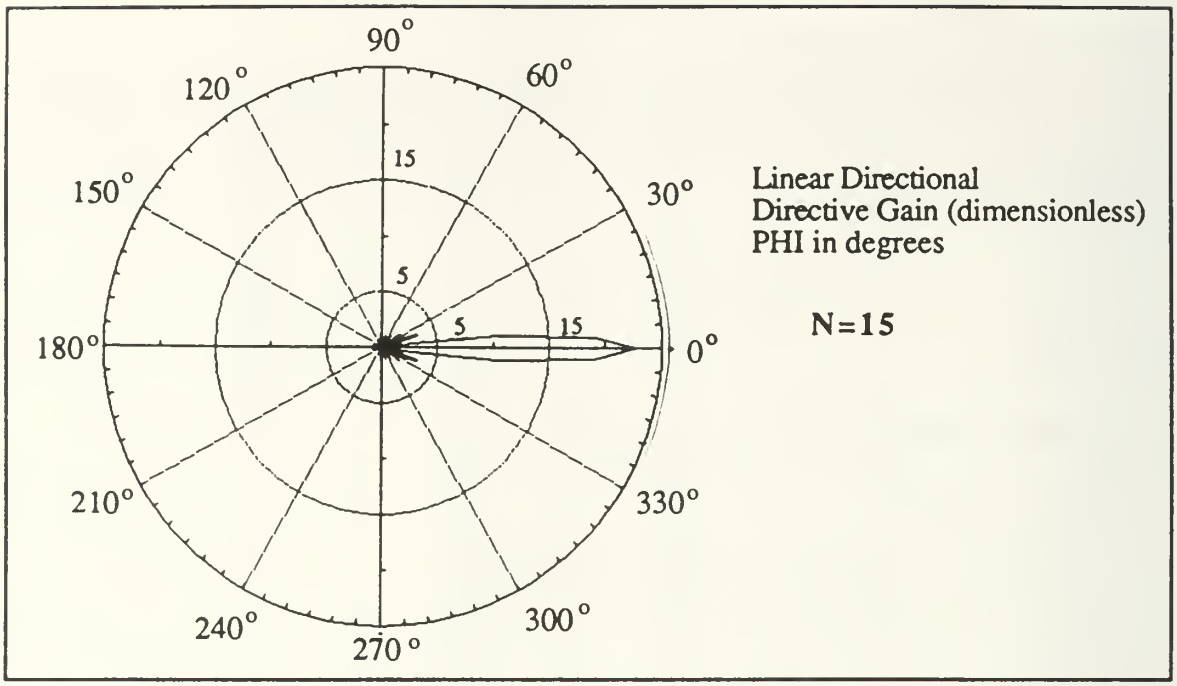

Figure 45. Directional Roll Plane Gain Pattern - 15 Patch Array.

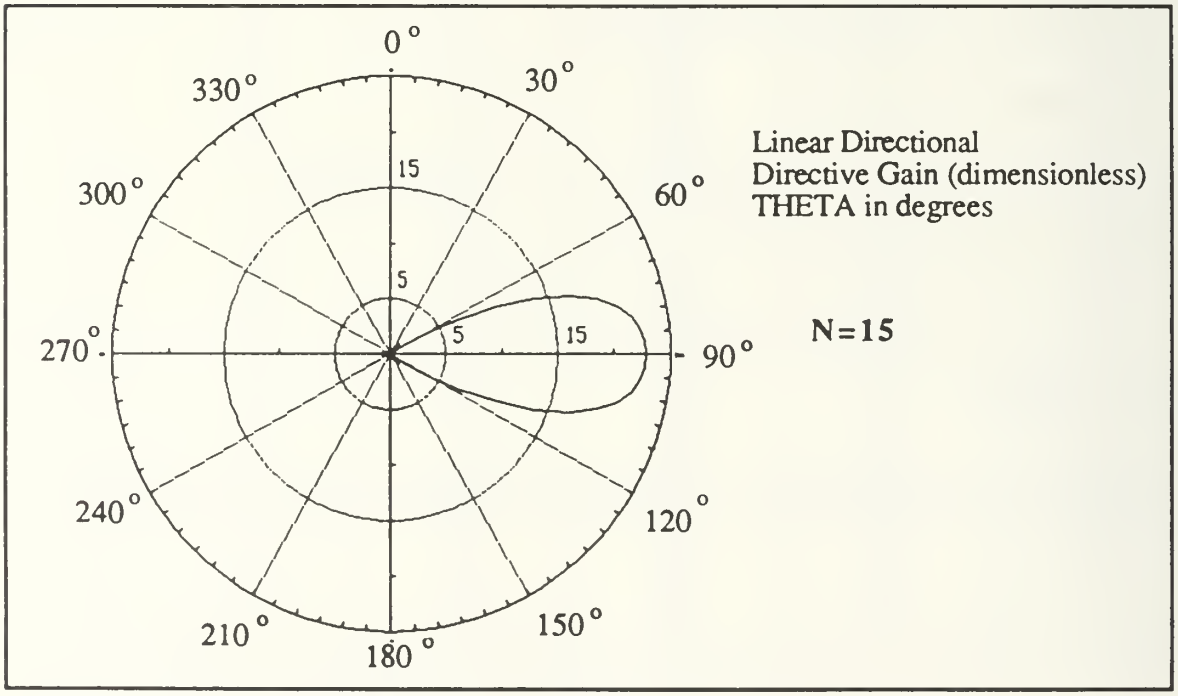

Figure 46. Directional Elevation Plane Gain Pattern - 15 Patch Array.

The directional directive gain in the roll and elevation planes for $N = 15$ are listed in Tables 17 and 18.

Table 17. N = 15 DIRECTIONAL DOWNLINK ROLL PLANE GAIN.

ϕ degrees	Gain dB	ϕ degrees	Gain dB	ϕ degrees	Gain dB
0	13.6	120	-1.3	240	-1.3
3	12.8	123	-2.0	243	-1.4
6	10.2	126	-3.3	246	-2.4
9	4.4	129	-5.7	249	-5.0
12	-23.8	132	-9.3	252	-10.0
15	1.5	135	-12.5	255	-10.2
18	5.4	138	-10.4	258	-4.5
21	5.3	141	-7.3	261	-1.2
24	1.9	144	-5.6	264	0.3
27	-9.3	147	-4.7	267	0.4
30	-4.9	150	-4.2	270	-0.7
33	1.7	153	-3.7	273	-3.7
36	3.1	156	-2.9	276	-10.3
39	1.6	159	-2.1	279	-11.4
42	-3.9	162	-1.5	282	-4.0
45	-22.9	165	-1.2	285	-0.6
48	-3.0	168	-1.1	288	0.5
51	0.9	171	-1.3	291	-0.4
54	1.4	174	-1.6	294	-4.2
57	-0.6	177	-1.8	297	-19.2
60	-6.9	180	-1.7	300	-6.9
63	-18.7	183	-1.5	303	-0.6
66	-4.2	186	-1.3	306	1.4
69	-0.4	189	-1.1	309	0.9
72	0.5	192	-1.1	312	-3.0
75	-0.7	195	-1.4	315	-22.9
78	-4.5	198	-1.9	318	-3.9
81	-15.9	201	-2.4	321	1.6
84	-10.3	204	-2.9	324	3.1
87	-3.0	207	-3.1	327	1.7
90	-0.1	210	-3.4	330	-4.9
93	0.8	213	-4.0	333	-9.3
96	0.3	216	-5.6	336	1.9
99	-2.0	219	-8.6	339	5.3
102	-6.9	222	-14.6	342	5.4
105	-21.8	225	-16.0	345	1.5
108	-10.0	228	-9.3	348	-23.8
111	-4.4	231	-5.5	351	4.4
114	-2.1	234	-3.3	354	10.2
117	-1.3	237	-1.9	357	12.8

Table 18. N = 15 DIRECTIONAL DOWNLINK ELEVATION PLANE GAIN.

θ degrees	Gain dB	θ degrees	Gain dB	θ degrees	Gain dB
0	$-\infty$	120	5.7	240	-23.2
3	-28.0	123	1.5	243	-12.8
6	-20.3	126	-7.1	246	-8.0
9	-18.3	129	-13.1	249	-5.4
12	-22.8	132	-2.6	252	-3.8
15	-24.7	135	0.4	255	-2.9
18	-12.5	138	1.0	258	-2.3
21	-8.1	141	-0.3	261	-2.0
24	-6.9	144	-3.8	264	-1.8
27	-8.8	147	-11.9	267	-1.8
30	-19.1	150	-19.1	270	-1.7
33	-11.9	153	-8.8	273	-1.8
36	-3.8	156	-6.9	276	-1.8
39	-0.3	159	-8.1	279	-2.0
42	1.0	162	-12.5	282	-2.3
45	0.4	165	-24.7	285	-2.9
48	-2.6	168	-22.8	288	-3.8
51	-13.1	171	-18.3	291	-5.4
54	-7.1	174	-20.3	294	-8.0
57	1.5	177	-28.0	297	-12.8
60	5.7	180	$-\infty$	300	-23.2
63	8.4	183	-41.8	303	-14.4
66	10.2	186	-24.3	306	-8.7
69	11.4	189	-18.1	309	-6.1
72	12.3	192	-16.2	312	-5.1
75	12.8	195	-18.6	315	-5.6
78	13.2	198	-32.3	318	-7.8
81	13.4	201	-16.9	321	-13.1
84	13.5	204	-11.1	324	-24.3
87	13.6	207	-9.1	327	-13.7
90	13.6	210	-9.7	330	-9.7
93	13.6	213	-13.7	333	-9.1
96	13.6	216	-24.3	336	-11.1
99	13.4	219	-13.1	339	-16.9
102	13.2	222	-7.8	342	-32.3
105	12.8	225	-5.6	345	-18.6
108	12.3	228	-5.1	348	-16.2
111	11.4	231	-6.1	351	-18.1
114	10.2	234	-8.7	354	-24.3
117	8.4	237	-14.4	357	-41.8

The maximum directional directive gain in the roll plane for $N = 15$ is:

$G_{max} = 13.6$ dB at $\theta = 90°$ and $\phi = 0°$

The half-power points in the roll plane occur at:

$\phi = 355°$

and

$\phi = 5°$

The resulting roll plane half-power beamwidth is:

$HP_{\varphi} = 10°$

The half-power points in the elevation plane occur at:

$\theta = 68°$

and

$\theta = 112°$

The resulting elevation plane half-power beamwidth is:

$HP_{\theta} = 44°$

The roll plane beamwidth meeting the gain specification is:

Roll Plane Beamwidth $= 14°$ $353° \leq \phi \leq 7°$

The elevation plane beamwidth meeting the gain specification is:

Elevation Plane Beamdwith $= 56°$ $62° \leq \theta \leq 118°$

For an array with $N = 16$, the average radiation intensity is:

$$U_{ave} = \frac{45.75}{2\eta_0}$$

The directive gain patterns are shown in Figures 47 and 48 on page 82.

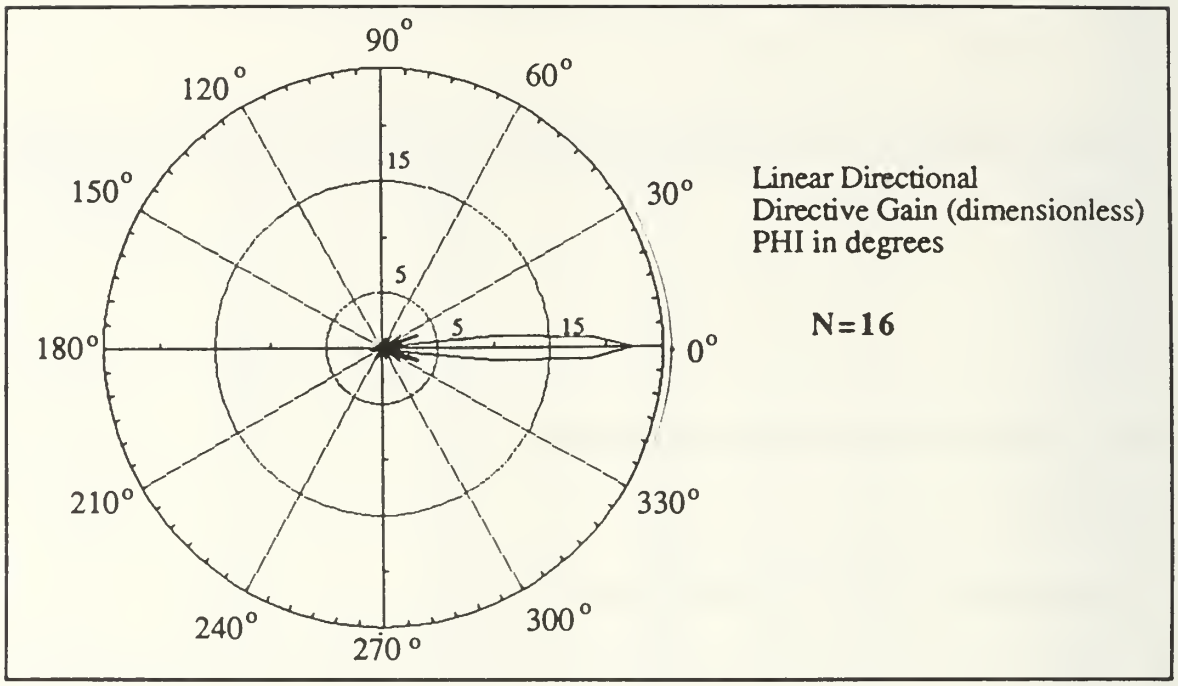

Figure 47. Directional Roll Plane Gain Pattern - 16 Patch Array.

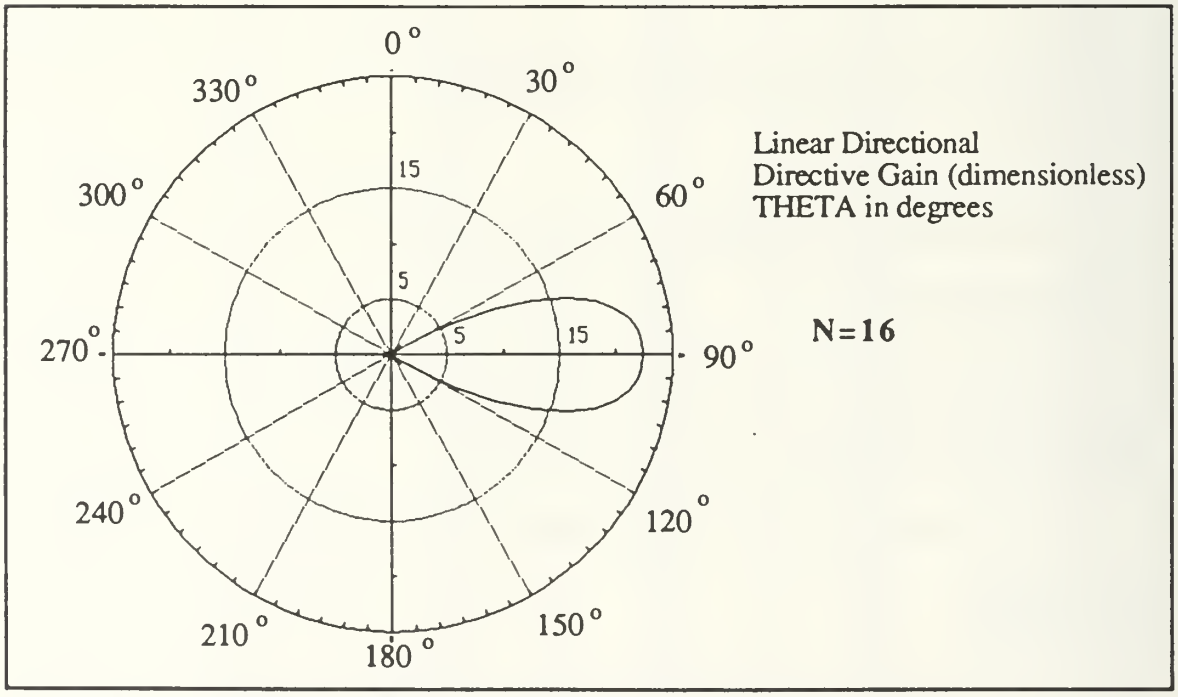

Figure 48. Directional Elevation Plane Gain Pattern - 16 Patch Array.

The directional directive gain for the roll and elevation planes for $N = 16$ are listed in Tables 19 and 20.

Table 19. N = 16 DIRECTIONAL DOWNLINK ROLL PLANE GAIN.

ϕ degrees	Gain dB	ϕ degrees	Gain dB	ϕ degrees	Gain dB
0	13.5	120	-4.2	240	0.4
3	12.7	123	-4.7	243	-0.3
6	10.1	126	-5.5	246	-2.5
9	4.3	129	-6.9	249	-7.4
12	-23.9	132	-9.8	252	-28.3
15	1.5	135	-16.2	255	-8.9
18	5.3	138	-26.9	258	-3.1
21	5.2	141	-11.9	261	-0.5
24	1.8	144	-7.0	264	0.4
27	-9.4	147	-4.5	267	0.1
30	-5.0	150	-3.2	270	-1.7
33	1.6	153	-2.8	273	-5.7
36	3.0	156	-3.1	276	-17.7
39	1.5	159	-3.7	279	-10.7
42	-4.0	162	-4.5	282	-3.3
45	-23.0	165	-5.1	285	-0.4
48	-3.1	168	-5.3	288	0.5
51	0.8	171	-4.9	291	-0.5
54	1.3	174	-4.0	294	-4.5
57	-0.8	177	-2.8	297	-20.3
60	-7.1	180	-1.7	300	-6.8
63	-18.6	183	-0.7	303	-0.7
66	-4.3	186	0.0	306	1.4
69	-0.7	189	0.3	309	0.8
72	-0.1	192	0.2	312	-3.0
75	-1.8	195	-0.3	315	-23.0
78	-6.8	198	-1.3	318	-4.0
81	-35.6	201	-2.6	321	1.5
84	-8.0	204	-4.1	324	3.0
87	-3.1	207	-5.9	327	1.6
90	-1.7	210	-7.8	330	-5.1
93	-2.3	213	-9.7	333	-9.4
96	-4.9	216	-12.2	336	1.8
99	-10.9	219	-16.6	339	5.2
102	-36.8	222	-34.3	342	5.3
105	-11.3	225	-16.2	345	1.5
108	-6.7	228	-8.6	348	-23.9
111	-4.9	231	-4.3	351	4.3
114	-4.1	234	-1.6	354	10.1
117	-4.0	237	-0.1	357	12.7

Table 20. N = 16 DIRECTIONAL DOWNLINK ELEVATION PLANE GAIN.

θ degrees	Gain dB	θ degrees	Gain dB	θ degrees	Gain dB
0	$-\infty$	120	5.7	240	-35.2
3	-28.1	123	1.4	243	-13.3
6	-20.4	126	-7.1	246	-8.1
9	-18.4	129	-13.2	249	-5.4
12	-22.9	132	-2.7	252	-3.8
15	-24.8	135	0.3	255	-2.8
18	-12.6	138	0.9	258	-2.2
21	-8.2	141	-0.4	261	-1.9
24	-7.0	144	-3.9	264	-1.8
27	-8.9	147	-12.0	267	-1.7
30	-19.2	150	-19.2	270	-1.7
33	-12.0	153	-8.9	273	-1.7
36	-3.9	156	-7.0	276	-1.8
39	-0.4	159	-8.2	279	-1.9
42	0.9	162	-12.6	282	-2.2
45	0.3	165	-24.8	285	-2.8
48	-2.7	168	-22.9	288	-3.8
51	-13.2	171	-18.4	291	-5.4
54	-7.1	174	-20.4	294	-8.1
57	1.4	177	-28.1	297	-13.3
60	5.7	180	$-\infty$	300	-35.2
63	8.3	183	-41.8	303	-14.5
66	10.1	186	-24.3	306	-8.6
69	11.3	189	-18.1	309	-5.8
72	12.2	192	-16.2	312	-4.8
75	12.7	195	-18.5	315	-5.2
78	13.1	198	-36.9	318	-7.3
81	13.3	201	-17.8	321	-12.3
84	13.4	204	-11.7	324	-31.8
87	13.5	207	-9.7	327	-15.4
90	13.5	210	-10.5	330	-10.5
93	13.5	213	-15.4	333	-9.7
96	13.4	216	-31.8	336	-11.7
99	13.3	219	-12.3	339	-17.8
102	13.1	222	-7.3	342	-36.9
105	12.7	225	-5.2	345	-18.5
108	12.2	228	-4.8	348	-16.2
111	11.3	231	-5.8	351	-18.1
114	10.1	234	-8.6	354	-24.3
117	8.3	237	-14.5	357	-41.8

The maximum directive gain in the roll plane for the 16 patch array is:

$G_{max} = 13.5$ dB at $\theta = 90°$ and $\phi = 0°$

The roll plane half-power points occur at:

$\phi = 355°$

and

$\phi = 5°$

The resulting roll plane half-power beamwidth is:

$HP_{\phi} = 10°$

The elevation plane half-power points occur at:

$\theta = 67°$

and

$\theta = 113°$

The resulting elevation plane half-power beamwidth is:

$HP_{\theta} = 46°$

The roll plane beamwidth meeting the specification is:

Roll Plane Beamwidth $= 14°$ $353° \leq \phi \leq 7°$

The elevation plane beamwidth meeting the specification is:

Elevation Plane Beamwidth $= 56°$ $62 \leq \theta \leq 118°$

The directive gain patterns are very similar for all three cases, with the maximum gain within 1 dB of each other and the beamwidths in both planes are within 2°. All three cases can meet the gain specification. The array which is best suited for ORION is the array which gives the best omnidirectional results. Therefore, the 16 patch array with $v = 1$ is chosen for the downlink antenna. This allows the downlink antenna to be operated in either the omnidirectional or the directional mode.

VI. CONCLUSIONS AND RECOMMENDATIONS

The ORION satellite is still in the early stages of design. As engineering is an iterative process, a baseline design for the satellite is being established with baseline designs for each of the subsystems. This thesis has defined the general design parameters for the telemetry, tracking and command system based on the general guidelines available at this time. The selection of the AFSCN as the ground station network sets the operating frequencies, data rates and the power requirements for signal reception. The orbital altitude and the available output power of the transponder set the gain requirements for the antenna. The design parameters in Chapter III are the baseline requirements for the ORION antenna.

The rest of this thesis has been devoted to studying the conformal microstrip patch array antenna as a candidate for use with the ORION satellite. The microstrip array has several advantages when used in this type of application. The antenna can be made very reliable because it has no moving parts. Since the array is conformal, it requires no deployment system thus adding to the reliability. It can also be made a structural member of the satellite body which can reduce the weight and volume requirements of the TT&C system. Another advantage of a conformal array is the ability to be used as an omnidirectional antenna or a directional antenna by electronically changing the phase of the signal fed to each patch. A disadvantage to the microstrip patch array is the inherently narrow bandwidth. This resulted in the requirement for separate uplink and downlink antennas. As shown in Chapter V, a 12 patch uplink array antenna will perform well at all of the design altitudes. The downlink presents a problem both because of the high gain requirements imposed by the limited power available from the transponder and the power required to be received by the ground station for information processing. In the omnidirectional mode, a 16 patch downlink array antenna cannot achieve the necessary gain to work at the extreme design altitude but will work in orbits up to 650 nm altitude. The downlink array can meet the gain specification in the directional mode at all design altitudes but would require the satellite to be 3-axis stablized or the antenna would have to be electronically despun. Even though the omnidirectional downlink array antenna cannot provide the specified gain, the microstrip array should still be considered a candidate for use on ORION. The necessity of communicating on the downlink is influenced by the specific mission and the ground station network. The

satellite in any of the proposed orbits will not be in continous communication with a ground station because the footprint of the satellite antenna pattern will not always cover two ground stations at the same time. The downlink will only be used to transmit payload data when in sight of a ground station. Since that is the case, some method of store and dump system for the payload data will have to be employed. The directional capability of the downlink antenna could allow burst transmissions of data at all proposed altitudes.

There are many areas of the microstrip patch array that still need to be investigated. Circular polarization is easily achieved with appropriate feeds to the patches. Modeling of a circularly polarized patch needs to be investigated since an additional 3 dB of link gain can be achieved through alleviating the polarization mismatch with the ground stations. The narrow beamwidth in the elevation plane could be widened by the addition of similar arrays conformally mounted on the satellite. A study needs to be conducted regarding the possible integration of the array antennas with the satellite structure, especially with concern for the amount of surface area required by the antennas that will no longer be available for solar cells. The power handling capabilities and impedance characteristics also need to be investigated. A prime area of investigation could be to find out if a control system could keep a directional antenna beam stable and pointing in the same direction while the satellite is spinning, thus allowing for operation of the downlink antenna in all the stabilization configurations.

APPENDIX A. ANTENNA GAIN SPECIFICATION DERIVATION

The ultimate goal of this analysis is the specification of the required antenna gain for the ORION satellite. The determination of the gain requirements for the ORION antenna involves many factors and is calculated based upon space-ground link equations. The primary factors in the link equations are:

- Satellite transmitter power, line losses, and antenna gain
- Free space loss, atmospheric attenuation and polarization losses
- Ground station transmitter power, line losses and antenna gain
- Information signal Modulation Indexes or phase deviations
- Receiving station sensitivities
- Required Signal to Noise Ratios (SNR) [Ref. 8: p. 5.1-1]

Figure 49 is a generic satellite link [Ref. 14: p. 130].

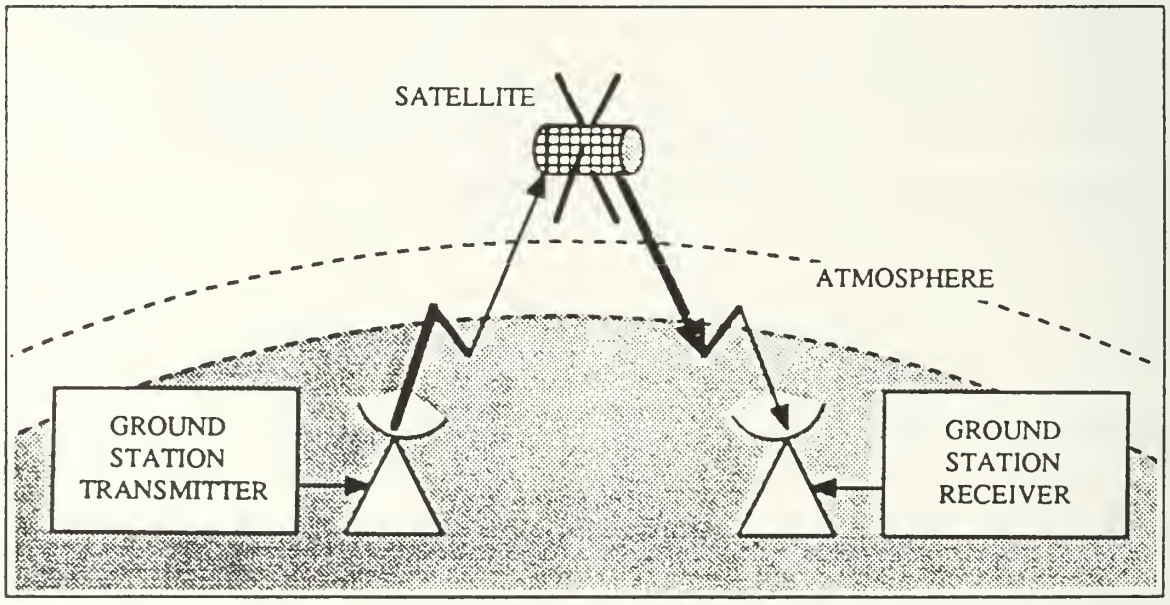

Figure 49. Basic Satellite Link.

Transmitter power, line losses and antenna gain contributions to the link calculations result in the effective radiative power (ERP) at the output of the ground station and satellite antennas. The free space losses, atmospheric attenuation and polarization losses are due to the propagation of radio frequency (RF) energy through space and the

atmosphere. The modulation indices are measures of the phase shift of the carrier signal caused by the amplitude of the information signals relative to the carrier's unmodulated condition. The modulation indices are also a measure of the power transferred from the unmodulated carrier to the various services; ranging and command signals on the uplink and ranging and telemetry signals on the downlink. The receiver sensitivity is a measure of the lowest signal the receiver can recover. The SNR depends on the type of signal transmitted, the type of modulation and the output signal to noise ratio required. The smallest TT&C antenna in the SGLS system is a 14 foot dish antenna co-located with a 46 foot dish antenna at Thule, Greenland. The 14 foot antenna has an uplink gain of 31.5 dB and a downlink gain of 33.5 dB. After performing link analysis with these antenna gains, it was not possible to communicate telemetry data on Carrier 2. There is only one 14 foot antenna in the SGLS system. Therefore, the ground station antenna gains are based on the 46 foot antennas.

The calculation of the link equation to determine the antenna gain is relatively straight forward. The transmitted power minus the losses arrives at the receiver. If the power received is above the receiver sensitivity, the information signals can be recovered.

A. SGLS GROUND STATION TO ORION RF UPLINK

1. SGLS Ground Station Output Power

From the information by Klements in Reference 6, SGLS can put out up to 10 kilowatts, but the normal operating output level of the transmitters is maintained at 1 kilowatt or less. Therefore, a transmitter output power of 1 kilowatt is used as a standard for link calculations. The SGLS antenna gain used for link calculation purposes is 45.0 dB for the uplink. This gain is referenced to the command transmitter output and includes feed and transmission line losses [Ref. 8: p. 5.1-14]. The SGLS ground station ERP can be calculated by the following equation.

$$ERP = P + G \text{ (dB)} \tag{A.1}$$

where

$P = 1$ kW $= 60.0$ dBm

$G = 42.7$ dB

Therefore,

$ERP = 102.7$ dBm

2. Uplink Free Space Losses

The uplink free space loss can be found from the following equation [Ref 14: p. 46].

$$L_u = 10 \log\left[\left(\frac{4\pi f_u d_u}{c}\right)^2\right] \qquad \text{(A.2)}$$

where

d_u = uplink slant range in meters

f_u = uplink carrier in Hertz

c = speed of light = 2.997925 x 10^8 meters/second

The slant range is the distance from the ground station to the satellite. Figure 50 shows the spatial relationship between the satellite and the ground station.

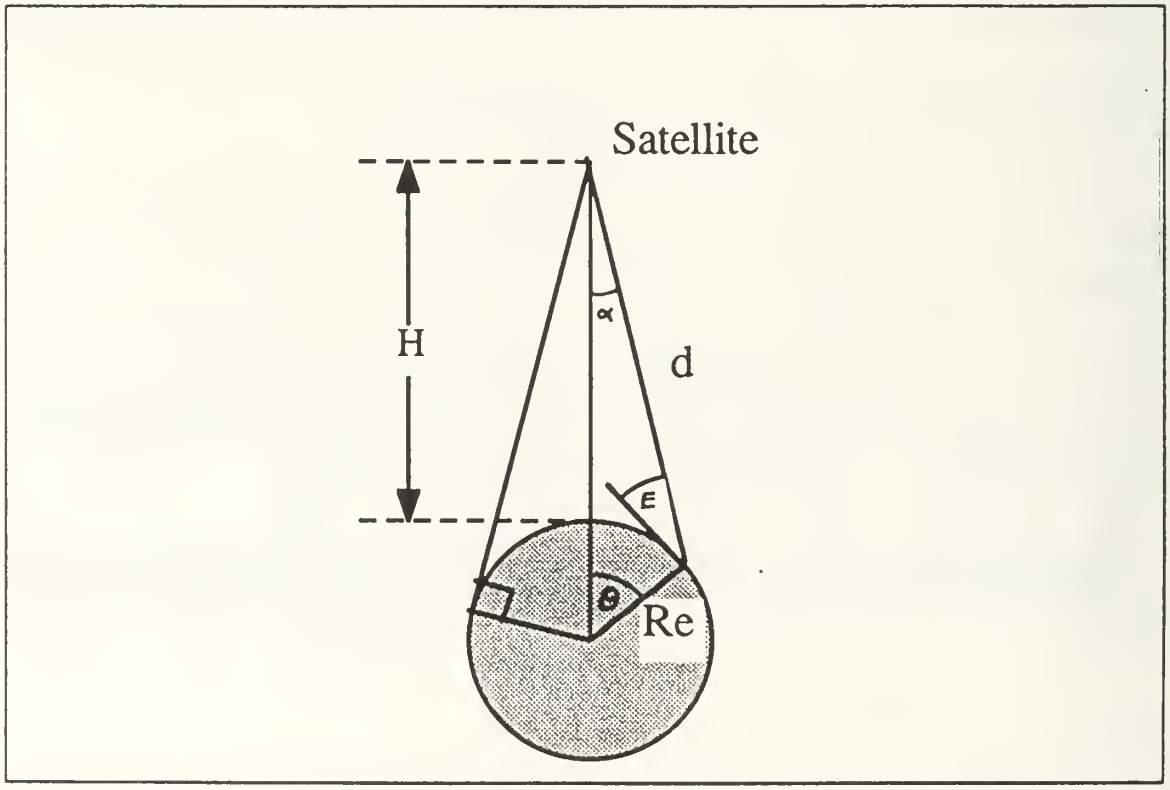

Figure 50. Satellite to Ground Station Slant Range.

The angles and distances in Figure 50 are related by the following equations [Ref. 14: p. 45].

$$d_u = \sqrt{(R_e + H)^2 + R_e^2 - 2R_e(R_e + H)\cos\theta} \tag{A.3}$$

$$\theta = \cos^{-1}\left\{ \sin\left[E + \sin^{-1}\left(\frac{R_e}{R_e + H} \cos E \right) \right] \right\} \tag{A.4}$$

$$\alpha = \sin^{-1}\left(\frac{R_e}{R_e + H} \cos E \right) \tag{A.5}$$

The slant range is the main variable in equation (A.2). The ORION satellite is to be capable of 800 nm circular orbits and elliptical orbits up to 2200 nm apogee altitudes. For the SGLS, an elevation angle of 5° is normally used in the link equation, but for the purposes of this design, the "worst case" will be assumed where the elevation angle will be 0° .

$E = 0° = 0.0$ radians

The mean equatorial radius of the earth is :

$R_e = 6{,}378{,}155$ meters

For the uplink design, the operating frequency is chosen in the middle of the uplink frequency band.

$f_u = 1800$ Megahertz $= 1800 \times 10^6$ Hertz

From this information, equations (A.2) through (A.5) can be used to find the angular relationships, the slant range and the free space losses for altitudes ranging from 100 nm to 2200 nm. The results are tabulated in Table 21.

Table 21. ORBIT GEOMETRIES AND UPLINK FREE SPACE LOSSES.

Altitude H in nm	α in degrees	θ in degrees	Slant Range in nm	Free Space Loss in dB
100	76.36	13.64	835.93	161.3
200	70.93	19.07	1190.62	164.4
300	66.91	23.09	1468.45	166.2
400	63.63	26.37	1707.38	167.6
500	60.84	29.16	1921.96	168.6
600	58.39	31.61	2119.60	169.4
700	56.21	33.79	2304.67	170.2
800	54.24	35.76	2479.98	170.8
900	52.45	37.55	2647.46	171.4
1000	50.80	39.20	2808.53	171.9
1100	49.28	40.72	2964.23	172.3
1200	47.87	42.13	3115.35	172.8
1300	46.55	43.45	3262.55	173.2
1400	45.31	44.69	3406.32	173.6
1500	44.15	45.85	3547.08	173.9
1600	43.06	46.94	3685.18	174.2
1700	42.03	47.97	3820.91	174.6
1800	41.05	48.95	3954.51	174.8
1900	40.12	49.88	4086.19	175.1
2000	39.24	50.76	4216.13	175.4
2100	38.40	51.60	4344.48	175.7
2200	37.60	52.40	4471.39	175.9

3. Atmospheric and Rain Attenuation

At the SGLS frequencies, atmospheric and rain attenuation is relatively small. A quick calculation can be made to give a reasonable estimate of these attenuations. Assuming the upper limit of the atmosphere is 70 km, the atmospheric and rain attenuations can be estimated from Figure 51 and Figure 52 on page 93. The "p" in Figure 52 is precipitation in mm/hr. The total atmospheric attenuation, L_{atm}, will be considered a combination of both atmospheric and rain attenuation. The attenuation at 2000 Megahertz is approximated at 0.01 dB/km from Figure 51 and 0.001 dB/km from Figure 52 on page 93. [Ref. 15: pp. 78-82]

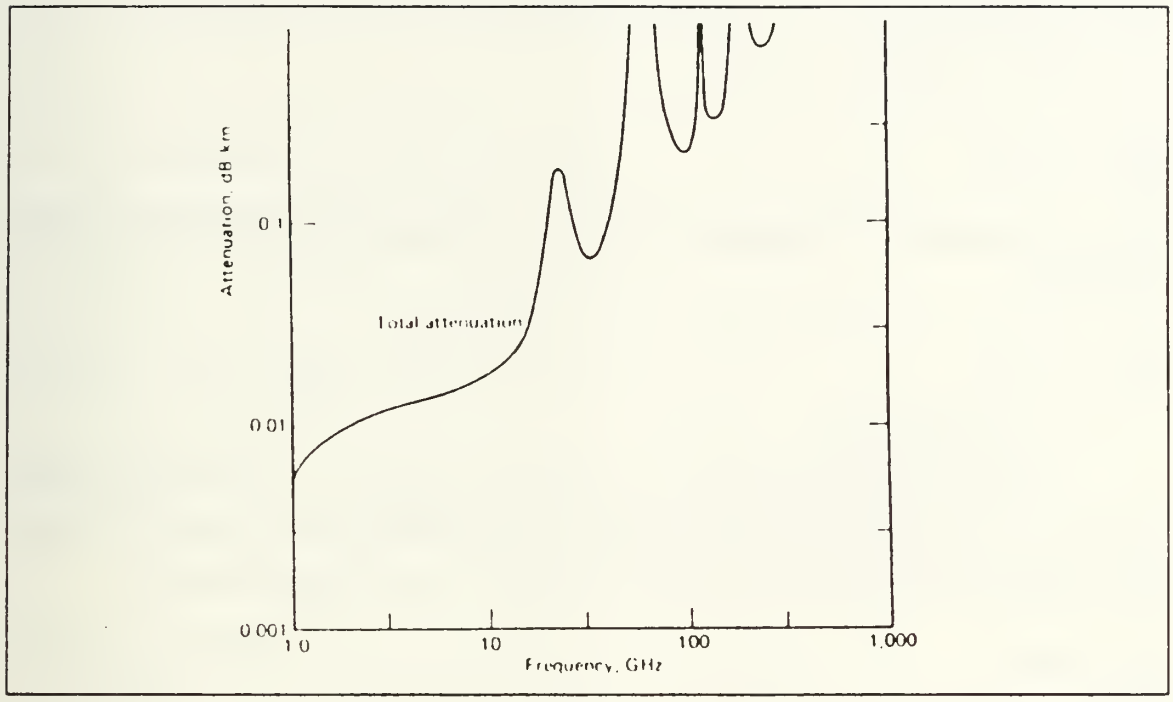

Figure 51. Atmospheric Attenuation.

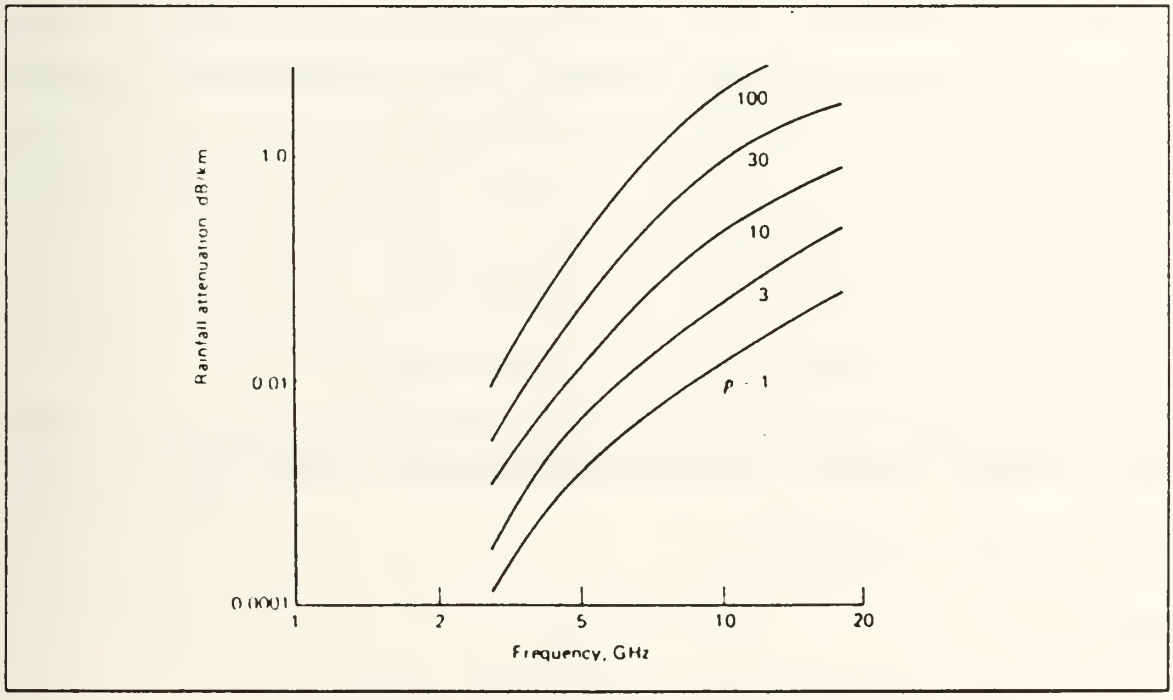

Figure 52. Rain Attenuation.

The total attenuation is:

$L_{atm} = (0.01 + 0.001)70$

$L_{atm} = 0.7$ dB

As a safety margin, the atmospheric attenuation will be rounded up to 1 dB for the link calculation.

$L_{atm} = 1.0$ dB

4. Polarization Loss

The transmitted signal is right-hand circularly polarized. If the satellite antenna is designed for right-hand polarization, there will be no Polarization Loss, L_{pol}. If a linearly polarized satellite antenna is used, there will be a 3 dB polarization loss.

$L_{pol} = 3.0$ dB

5. Modulation Losses

From the information presented so far, the total power present at the satellite antenna can be determined. It is necessary to determine how much of the total power is allocated to the carrier and both of the uplink services, ranging and command signals. As discussed in Chapter III, the command, ranging and telemetry signal are frequency modulated onto the carrier. The modulation index, β, represents the ratio of the maximum departure of the instantaneous frequency of the FM wave from the carrier frequency to the message bandwidth. Equations (A.6), (A.7) and (A.8) are engineering design equations that give reasonable values for the modulation losses due to the distribution of power between the carrier and the service signals.

To give some idea of how the equations were derived, a quick look at a single tone FM signal is beneficial. A single tone FM signal can be expressed as:

$s(t) = A_c \cos[2\pi f_c t + \beta \sin(2\pi f_m t)]$

where,

A_c is the maximum amplitude of the carrier signal

f_c is the carrier frequency

β is the modulation index for the information signal.

and

f_m is the frequency of the information signal.

The FM signal can be expressed as:

$$s(t) = \mathrm{Re}\left[e^{j2\pi f_c t} + e^{j\beta \sin(2\pi f_m t)}\right] = \mathrm{Re}\left[\tilde{s}(t)e^{j2\pi f_c t}\right]$$

where $\tilde{s}(t)$, is the complex envelope of $s(t)$.

$$\tilde{s}(t) = A_c e^{j\beta \sin(2\pi f_m t)}$$

Now, $\tilde{s}(t)$ can be expanded in the form of a complex Fourier Series:

$$\tilde{s}(t) = \sum_{n=-\infty}^{\infty} c_n e^{j2\pi n f_m t}$$

where,

$$c_n = f_m \int_{-\frac{1}{2}f_m}^{\frac{1}{2}f_m} \tilde{s}(t)e^{-j2\pi n f_m t}dt = f_m A_c \int_{-\frac{1}{2}f_m}^{\frac{1}{2}f_m} e^{j\beta \sin(2\pi f_m t) - j2\pi n f_m t}dt$$

Let $x = 2\pi f_m t$, then:

$$c_n = \frac{A_c}{2\pi} \int_{-\pi}^{\pi} e^{j(\beta \sin x - nx)}dx$$

This expression is very similar to the definition of an nth order Bessel Function of the first kind. In fact:

$$c_n = A_c \mathrm{J}_n(\beta)$$

So, now:

$$\tilde{s}(t) = A_c \sum_{n=-\infty}^{\infty} \mathrm{J}_n(\beta) e^{j2\pi n f_m t}$$

and

$$s(t) = A_c \mathrm{Re}\left[\sum_{n=-\infty}^{\infty} \mathrm{J}_n(\beta) e^{j2\pi (f_c + n f_m) t} \right] = A_c \sum_{n=-\infty}^{\infty} \mathrm{J}_n(\beta) \cos(\omega_c + \omega_m) t$$

The spectrum of $s(t)$ is found by taking the Fourier transform to get:

$$S(f) = \frac{A_c}{2} \sum_{n=-\infty}^{\infty} \mathrm{J}_n(\beta) [\delta(f - f_c - n f_m) + \delta(f + f_c + n f_m)]$$

The power in the signal is the sum of that contained in the individual spectral lines.

$$P = \frac{A_c^2}{2} \sum_{n=-\infty}^{\infty} \mathrm{J}_n^2(\beta)$$

The power of an FM signal is constant so that with several modulating signals, the power in any one signal is less than the power in the entire FM signal. This power reduction of a service signal is considered a loss and is related to the modulation index. The SGLS system involves multi-tone FM signals and a derivation similar to the single tone FM signal results in the modulation losses expressed by equations (A.6), (A.7) and (A.8). [Ref. 16: pp. 184-190]

For SGLS, the modulation index for the ranging signal, β_r, can be selected as either 0.125 or 0.3. The modulation index for the command signal, β_{cmd}, can be selected as either 0.3 or 1.0. Different combinations of these indexes result in different distributions of power of the uplink signal.

The loss of power (in dB) for the carrier due to both ranging and command tones being multiplexed on the carrier can be computed by the following equations [Ref. 8: p. 5.1-4].

$$ML_c = -10 \log\left[J_0^2(\beta_{cmd}) \cos^2(\beta_r)\right] \tag{A.6}$$

where,

ML_c = Modulation Loss of the Carrier

J_0 = Bessel Function of Zero Order

The modulation loss factor for the ranging signal, ML_r, can be calculated from equation (A.7).

$$ML_r = -10 \log\left[J_0^2(\beta_{cmd}) \sin^2(\beta_r)\right] \tag{A.7}$$

The modulation loss factor for the command signal, ML_{cmd}, can be calculated from equation (A.8).

$$ML_{cmd} = -10 \log\left[2J_1^2(\beta_{cmd}) \cos^2(\beta_r)\right] \tag{A.8}$$

where,

J_1 = Bessel Function of First Order

The most commonly used values for both β_r and β_{cmd} is 0.3. Using that value the modulation losses for the carrier, ranging signal and command signal can be calculated.

$$ML_c = 10 \log\left[J_0^2(0.3) \cos^2(0.3)\right] = 0.6 \text{ dB}$$

$$ML_r = 10 \log\left[J_0^2(0.3) \sin^2(0.3)\right] = 10.8 \text{ dB}$$

$$ML_{cmd} = 10 \log\left[2J_1^2(0.3) \cos^2(0.3)\right] = 14.0 \text{ dB}$$

6. Motorola S-Band Transponder Receiving Characteristics

The transponder is specified to have a receiver sensitivity, R_{sen}, of -104.0 dBm for a $\beta_{cmd} = 0.3$, with a 10^{-6} bit error rate (BER) [Ref. 9: p. 4].

$$R_{sen} = -104.0 \text{ dBm}$$

7. ORION Satellite Line Losses

At this point there are no firm guidelines for estimating the line losses of the satellite. In a satellite link calculation example by Klements in Reference 6, the satellite line losses, L_{satll}, are estimated to be 6.0 dB. Therefore, 6.0 dB will be used for the ORION satellite line losses.

$L_{satll} = 6.0$ dB

8. Uplink Service Margins

The signals in the uplink should have some safety margins built in so that adequate communications with the satellite can be maintained under conditions which are more severe than the design conditions. It will be assumed that a 5.0 dB service margin, SM, is adequate for the carrier, ranging and command signals.

$SM = 5.0$ dB

9. ORION Satellite Uplink Antenna Gain Specifications

The gain of the antenna can now be calculated by using the link equation. This equation basically sums up all of the parameters so far to solve for the antenna gain, G_{sant}. It is necessary to calculate the antenna gain based upon the power required for the carrier, ranging and command signals, and the gain is altitude dependent because of the free space loss term.

The link equation can be expressed as:

$$ERP - L_u - L_{atm} - L_{pol} - ML - L_{satll} + G_{sant} - R_{sen} = SM$$

Solving for G_{sant}:

$$G_{sant} = SM - ERP + L_u + L_{atm} + L_{pol} + ML + L_{satll} + R_{sen} \qquad \text{(A.9)}$$

The uplink gain specifications for the carrier, ranging and command signals are tabulated on the following page.

Table 22. ORION UPLINK GAIN REQUIREMENTS.

Altitude 11 in nm	Gain (carrier) in dB	Gain (ranging) in dB	Gain (command) in dB
100	-29.8	-19.6	-16.4
200	-26.7	-16.5	-13.3
300	-24.9	-14.7	-11.5
400	-23.6	-13.4	-10.2
500	-22.6	-12.3	-9.2
600	-21.7	-11.5	-8.3
700	-20.9	-10.7	-7.6
800	-20.3	-10.1	-6.9
900	-19.7	-9.6	-6.4
1000	-19.2	-9.0	-5.9
1100	-18.8	-8.6	-5.4
1200	-18.3	-8.1	-5.0
1300	-17.9	-7.7	-4.6
1400	-17.6	-7.4	-4.2
1500	-17.2	-7.0	-3.8
1600	-16.9	-6.7	-3.5
1700	-16.6	-6.4	-3.2
1800	-16.3	-6.1	-2.9
1900	-16.0	-5.8	-2.6
2000	-15.7	-5.5	-2.3
2100	-15.4	-5.2	-2.1
2200	-15.2	-5.0	-1.8

B. ORION TO SGLS GROUND STATION DOWNLINK

The derivation of the downlink antenna gain is similar to the uplink analysis. In Chapter II, it was mentioned that the downlink is actually composed of two carriers set 5 Megahertz apart. Carrier 1 is a pilot signal for ground station antenna autotracking, range rate tracking and low speed PCM or analog telemetry. Carrier 2 is used to carry digital bit streams at rates between 128 kbps to 1.024 Mbps. It is necessary to examine each of the downlink carriers separately.

1. SGLS Carrier 1 Downlink Analysis

The goal of the downlink analysis is to determine the required satellite antenna gain necessary to ensure a good link.

a. Motorola S-Band Transponder Output Power

The Motorola transponder is specified to have a minimum of 2 Watts output power.

$P = 2.00$ Watts $= 33.0$ dBm

b. Satellite Line Losses

As an estimation of the satellite line losses, a figure of -6 dB will be used, as in the uplink analysis. This is a rather severe approximation but it is better to err on the safe side. In an example link calculation by Klements in Reference 6, the satellite line losses are stated as -0.4 dB.

$L_{satll} = -6.0$ dB

c. Downlink Free Space Loss

The downlink free space loss is not quite the same as the uplink because the downlink frequency is higher than the uplink frequency. The design downlink frequency, f_d, will be the center of the downlink frequency band.

$f_d = 2250$ Megahertz $= 2250 \times 10^6$ Hertz

The slant ranges are the same as the uplink. Using equation (A.2), the free space losses can be calculated for the various altitudes as was done for the uplink analysis. The downlink free space losses for the various altitudes are in the table that follows.

Table 23. ORION DOWNLINK FREE SPACE LOSSES.

Altitude H in nm	Slant Range d_d in nm	Free Space Loss in dB
100	835.93	163.3
200	1190.62	166.4
300	1468.45	168.2
400	1707.38	169.5
500	1921.96	170.5
600	2119.60	171.4
700	2304.67	172.1
800	2479.98	172.7
900	2647.46	173.3
1000	2808.53	173.8
1100	2964.23	174.3
1200	3115.35	174.7
1300	3262.55	175.1
1400	3406.32	175.5
1500	3547.08	175.8
1600	3685.18	176.2
1700	3820.91	176.5
1800	3954.51	176.8
1900	4086.19	177.1
2000	4216.13	177.3
2100	4344.48	177.6
2200	4471.39	177.8

d. Polarization Loss

Even though the SGLS is designed to accept right-hand circularly polarized signals, a 3 dB loss will be used so that linearly polarized antenna designs can be considered.

$L_{pol} = 3.0$ dB

e. Atmospheric and Rain Attenuation

Quick reference to Figures 51 and 52 on page 93 shows the atmospheric and rain attenuation are approximately the same as the uplink.

$L_{atm} = 1.0$ dB

f. SGLS Ground Station Antenna Gain

The gain used in this link analysis is the gain of the 46 foot antennas that have a minimum gain of 47 dB.

$G_{ga} = 47.0$ dB

g. Modulation Losses

The Carrier 1 downlink is composed of the carrier, the ranging signal and the telemetry signal. Representative modulation indexes for the ranging and telemetry signals are:

$\beta_r = 0.3$

$\beta_t = 1.4$

The modulation losses, ML_c for the carrier, ML_r for the ranging signal and ML_t for the telemetry signal can be found using equations (A.10), (A.11) and (A.12) respectively [Ref. 8: p. 5.1-10].

$$ML_c = -10\log\left[2J_0^2(\beta_t)J_0^2(\beta_r)\right] \tag{A.10}$$

$$ML_r = -10\log\left[2J_1^2(\beta_r)J_0^2(\beta_t)\right] \tag{A.11}$$

$$ML_t = -10\log\left[2J_1^2(\beta_t)J_0^2(\beta_r)\right] \tag{A.12}$$

$$ML_c = -10\log\left[2J_0^2(1.4)J_0^2(0.3)\right] = 5.1 \text{ dB}$$

$$ML_r = -10\log\left[2J_1^2(0.3)J_0^2(1.4)\right] = 18.5 \text{ dB}$$

$$ML_t = -10\log\left[2J_1^2(1.4)J_0^2(0.3)\right] = 2.5 \text{ dB}$$

h. Ground Station Receiver Sensitivity

The receiver sensitivity for the carrier, ranging signal and the telemetry signal for the SGLS receivers has been determined by Klements in Reference 6 [Ref. 8: pp. 5.1-12, 5.1-13]. Factors that are important are:

- Boltzman's Constant
- Antenna Noise Temperature
- Noise Bandwidth
- Required Signal to Noise Ratio

The carrier sensitivity, R_c, ranging signal sensitivity, R_r , and the telemetry signal sensitivity, R_t are listed below.

$$R_c = -129.6 \text{ dBm}$$

$$R_r = -135.2 \text{ dBm}$$

$$R_t = -113.5 \text{ dBm}$$

i. Downlink Service Margins

The service margins for design purposes will be 5 dB as was the case for the uplink.

$$SM = 5.0 \text{ dB}$$

j. Carrier 1 ORION Satellite Antenna Gain Requirement

As with the uplink, the Carrier 1 downlink link calculation is a summing up of the factors and solving for the satellite antenna gain, G_{sant} . Three calculations must be made: one for the carrier, one for the ranging signal and one for the telemetry signal. The link equation is shown below.

$$P - L_{satll} + G_{sant} - L_d - L_{pol} - L_{atm} + G_{ga} - ML - R_c = SM$$

Solving for G_{sant}:

$$G_{sant} = SM - P + L_{satll} + L_d + L_{pol} + L_{atm} - G_{ga} + ML + R_c \quad \text{(A.13)}$$

Substituting in the values, the required satellite antenna gain for the Carrier 1 signals are listed in the following table.

Table 24. CARRIER 1 DOWNLINK ANTENNA GAIN REQUIREMENTS.

Altitude H in nm	Gain (carrier) in dB	Gain (ranging) in dB	Gain (telemetry) in dB
100	-26.2	-18.4	-12.7
200	-23.1	-15.3	-9.6
300	-21.3	-13.5	-7.8
400	-20.0	-12.2	-6.5
500	-19.0	-11.2	-5.5
600	-18.1	-10.3	-4.6
700	-17.4	-9.6	-3.9
800	-16.7	-9.0	-3.3
900	-16.2	-8.4	-2.7
1000	-15.7	-7.9	-2.2
1100	-15.2	-7.4	-1.7
1200	-14.8	-7.0	-1.3
1300	-14.4	-6.6	-0.9
1400	-14.0	-6.2	-0.5
1500	-13.6	-5.9	-0.2
1600	-13.3	-5.5	0.2
1700	-13.0	-5.2	0.5
1800	-12.7	-4.9	0.8
1900	-12.4	-4.6	1.1
2000	-12.1	-4.4	1.3
2100	-11.9	-4.1	1.6
2200	-11.6	-3.9	1.8

2. Carrier 2 Downlink Analysis

Carrier 2 is the main telemetry signal to carry the data produced by the satellite payload. The receiver sensitivity is dependent upon the bit rate of the data signal. The required power is affected by the Noise Bandwidth and the Signal to Noise Ratio. Both the Noise Bandwidth and the Signal to Noise Ratio are dependent on the bit rate of the data. For the purposes of this analysis, two different data bit rates, 512 kbps and 1.024 Mbps, will be examined. All of the factors discussed for Carrier 1 are the same except

the transmitter power, receiver sensitivity and there are neglible modulation losses. The transmitter power will be assumed to be 10.0 Watts (40.0 dBm).

a. Gain Requirement based on 512 kbps Carrier 2 Data Rate

The required power for a 512 kbps data rate has been calculated by Klements in Reference 6. The required power can be expressed as the receiver sensitivity.

$R = -102.6$ dBm

Using equation (A.13), dropping the modulation loss term and replacing R_c by R, the required satellite antenna gain can be calculated.

b. Gain Requirement based on 1.024 Mbps Carrier 2 Data Rate

The required power for a 1.024 Mbps data rate is -98.8 dBm [Ref. 8: p. 5.1-12].

$R = -98.8$ dBm

Using equation (A.13), the required satellite antenna gain can be calculated. The antenna gain specifications for Carrier 2 for the two different data rates are summarized in the following table.

Table 25. CARRIER 2 DOWNLINK ANTENNA GAIN REQUIREMENTS.

Altitude H in nm	Gain (512 kbps) in dB	Gain (1.024 Mbps) in dB
100	-11.3	-7.5
200	-8.2	-4.4
300	-6.4	-2.6
400	-5.1	-1.3
500	-4.1	-0.3
600	-3.2	0.6
700	-2.5	1.3
800	-1.9	1.9
900	-1.3	2.5
1000	-0.8	3.0
1100	-0.3	3.5
1200	0.1	3.9
1300	0.5	4.3
1400	0.9	4.7
1500	1.2	5.0
1600	1.6	5.4
1700	1.9	5.7
1800	2.2	6.0
1900	2.5	6.3
2000	2.7	6.5
2100	3.0	6.8
2200	3.2	7.0

C. ORION ANTENNA GAIN SPECIFICATIONS

The following table lists the most severe antenna gain specifications for both the uplink and downlink. These figures will be the specifications for the antennas.

Table 26. ORION ANTENNA GAIN SPECIFICATIONS-SUMMARY.

Altitude H in nm	Uplink Gain Specification in dB	Downlink Gain Specification in dB
100	-16.4	-7.5
200	-13.3	-4.4
300	-11.5	-2.6
400	-10.2	-1.3
500	-9.2	-0.3
600	-8.3	0.6
700	-7.6	1.3
800	-6.9	1.9
900	-6.4	2.5
1000	-5.9	3.0
1100	-5.4	3.5
1200	-5.0	3.9
1300	-4.6	4.3
1400	-4.2	4.7
1500	-3.8	5.0
1600	-3.5	5.4
1700	-3.2	5.7
1800	-2.9	6.0
1900	-2.6	6.3
2000	-2.3	6.5
2100	-2.1	6.8
2200	-1.8	7.0

D. MATHCAD PROGRAM FOR CALCULATING ANTENNA GAIN

The following pages of this appendix is a computer program that calculates the satellite geometries, slant ranges and gain requirements. The software that is used is called MathCAD 2.0 which is a product of the Mathsoft Corporation. MathCAD allows the user to type in mathmatical formulas just as written and then solves the equations. All of the mathematical in this thesis was computed by MathCAD.

ORION SATELLITE GAIN REQUIREMENT PROGRAM

This program is a "MathCAD" program. The values of the variables used in this program are from the data in in this appendix.

Uplink Analysis

P := 60 dBm — Ground station transmitter power

G := 42.7 dB — Ground station antenna gain

ERP := P + G — Ground station effective radiative power

ERP = dB

L_{atm} := 1 dB — Atmospheric and rain attenuation

L_{pol} := 3 dB — Polarization loss

There are 2 FM service signals on the uplink carrier. The next three parameters are the modulation loses for each service signal and the carrier.

ML_{c} := 0.59 dB — Modulation loss for the carrier

ML_{r} := 10.79 dB — Modulation loss for the ranging service signal

ML := 13.96 dB Modulation loss for the command
 cmd
service signal

R := -104 dB Satellite receiver sensitivity
 sen

L := 6 dB Satellite line losses
 satll

SM := 5 dB Service margin for the uplink analysis

The next part of this program generates the losses due to the RF energy propogating in free space. The free space loss is dependent on the distance between the satellite and the ground station and that distance is dependent on the satellite orbital altitude.

E := 0 radians Elevation angle of the ground
station antenna in radians

R := 6378155 meters Radius of the earth expressed in
 e
meters

$f_u := 1800 \cdot 10^6$ Hertz Middle frequency of the uplink band

$c := 2.997925 \cdot 10^8$ meters/second Speed of light

Now the geometry and slant range will be calculated for various satellite altitudes.

$i := 1 \,..22$

$H_i := 100 \cdot i \cdot 1852$ Satellite altitude converted from nautical miles into meters

$$\alpha_i := \operatorname{asin}\left[\frac{R_e}{R_e + H_i} \cdot \cos(E)\right]$$

Angle between the altitude of the satellite and the slant range from the satellite to the ground station

$$\theta_i := \operatorname{acos}\left[\sin\left[E + \operatorname{asin}\left[\frac{R_e}{R_e + H_i} \cdot \cos(E)\right]\right]\right]$$

Theta is the angle between the vector from the center of the earth and satellite and a vector from the center of the earth and the ground station.

$$d_{u_i} := \sqrt{\left[R_e + H_i\right]^2 + R_e^2 - 2 \cdot R_e \cdot \left[R_e + H_i\right] \cdot \cos\left[\theta_i\right]}$$

Slant range from the ground station to the satellite

$$L_{u_i} := 10 \cdot \log\left[\left[\frac{4 \cdot \pi \cdot f_{u_i} \cdot d_{u_i}}{c}\right]^2\right]$$

Free space loss for the uplink

Now the link equation can be presented and the antenna gain can be calculated for the carrier, ranging signal and command signal for various altitudes.

$$G_{santu1_i} := SM - ERP + L_{u_i} + L_{atm_i} + L_{pol} + ML_c + \ldots + L_{satll} + R_{sen}$$

Gain needed for the carrier in dB

$$G_{santu2_i} := SM - ERP + L_{u_i} + L_{atm_i} + L_{pol} + ML_r + \ldots + L_{satll} + R_{sen}$$

Gain needed for the ranging signal in dB

$$G_{santu3_i} := SM - ERP + L_{u_i} + L_{atm_i} + L_{pol} + ML_{cmd} + \ldots + L_{satll} + R_{sen}$$

Gain needed for the command signal in dB

The data generated by the above equations follows. The altitude and slant range of the satellite is coverted back into nautical miles and the angles are converted to degrees for presentation.

$H_i := i \cdot 100$ Altitude in nautical miles

$d_{u_i} := \frac{d_i}{1852}$ Slant range in nautical miles

$\alpha_i := \alpha_i \cdot \frac{180}{\pi}$ Angle alpha in degrees

$\theta_i := \theta_i \cdot \frac{180}{\pi}$ Angle theta in degrees

H_i	d_{u_i}	α_i	θ_i	L_{u_i}
100	835.93	76.36	13.64	161.35
200	1190.62	70.93	19.07	164.42
300	1468.45	66.91	23.09	166.24
400	1707.38	63.63	26.37	167.55
500	1921.96	60.84	29.16	168.58
600	2119.6	58.39	31.61	169.43
700	2304.67	56.21	33.79	170.16
800	2479.98	54.24	35.76	170.8
900	2647.46	52.45	37.55	171.36
1000	2808.53	50.8	39.2	171.88
1100	2964.23	49.28	40.72	172.34
1200	3115.35	47.87	42.13	172.78
1300	3262.55	46.55	43.45	173.18
1400	3406.32	45.31	44.69	173.55
1500	3547.08	44.15	45.85	173.9
1600	3685.18	43.06	46.94	174.24
1700	3820.91	42.03	47.97	174.55
1800	3954.51	41.05	48.95	174.85
1900	4086.19	40.12	49.88	175.13
2000	4216.13	39.24	50.76	175.4
2100	4344.48	38.4	51.6	175.66
2200	4471.39	37.6	52.4	175.91

H_i	d_{u_i}	G_{santu1_i}	G_{santu2_i}	G_{santu3_i}
100	835.93	-29.76	-19.56	-16.39
200	1190.62	-26.69	-16.49	-13.32
300	1468.45	-24.87	-14.67	-11.5
400	1707.38	-23.56	-13.36	-10.19
500	1921.96	-22.53	-12.33	-9.16
600	2119.6	-21.68	-11.48	-8.31
700	2304.67	-20.95	-10.75	-7.58
800	2479.98	-20.31	-10.11	-6.94
900	2647.46	-19.75	-9.55	-6.38
1000	2808.53	-19.23	-9.03	-5.86
1100	2964.23	-18.77	-8.57	-5.4
1200	3115.35	-18.33	-8.13	-4.96
1300	3262.55	-17.93	-7.73	-4.56
1400	3406.32	-17.56	-7.36	-4.19
1500	3547.08	-17.21	-7.01	-3.84
1600	3685.18	-16.87	-6.67	-3.5
1700	3820.91	-16.56	-6.36	-3.19
1800	3954.51	-16.26	-6.06	-2.89
1900	4086.19	-15.98	-5.78	-2.61
2000	4216.13	-15.71	-5.51	-2.34
2100	4344.48	-15.45	-5.25	-2.08
2200	4471.39	-15.2	-5	-1.83

$G_{santu1_i}, G_{santu2_i}, G_{santu3_i}$

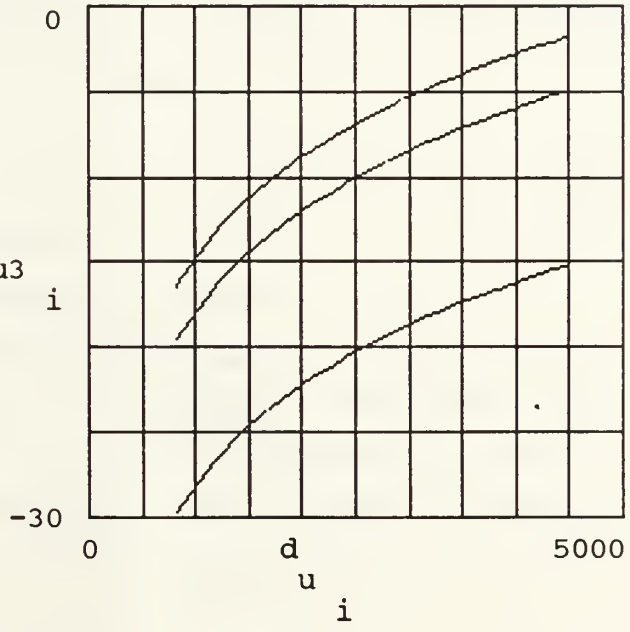

$G_{santu1_i}, G_{santu2_i}, G_{santu3_i}$

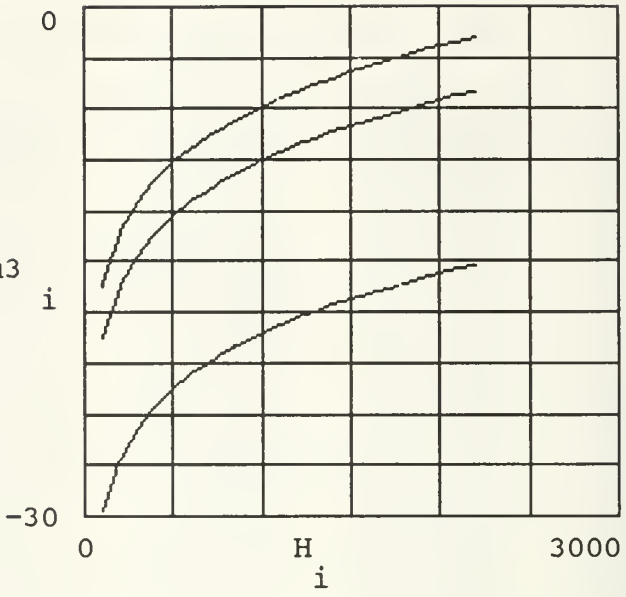

Downlink Analysis

This part of this program, calculates the the required gains for the downlink. Some of the parameters have changed as discussed in the Appendix. Since there are two separate downlink carriers, analysis will have to be done for each carrier.

Carrier 1

$P := 33.01$ dBm	Satellite transmitter power for the Carrier 1 signal
$G_{ga} := 47.00$ dB	Gain of the ground station receiving antenna
$f_d := 2250 \cdot 10^6$ Hertz	Middle frequency of the downlink band

$ML_c := 5.13\ dB$ Modulation loss of the carrier

$ML_r := 18.50\ dB$ Modulation loss for the ranging signal

$ML_t := 2.51\ dB$ Modulation loss for the telemetry signal

$R_c := -129.60\ dBm$ Ground station receiver sensitivity for the carrier

$R_r := -135.20\ dBm$ Ground station receiver sensitivity for the ranging signal

$R_t := -113.50\ dBm$ Ground station receiver sensitivity for the telemetry signal

All of the other parameters for the link equation remain the same as for the uplink except for the free space loss which is dependent on the downlink frequency.

$d_{d_i} := d_{u_i} \cdot 1852$ Converts the slant range back into meters

The free space loss is now calculated.

$$L_{d_i} := 10 \cdot \log\left[\left[\frac{4 \cdot \pi \cdot f_d \cdot d_{d_i}}{c}\right]^2\right]$$ Downlink free space loss for different altitudes

H i	L d i
100	163.29
200	166.36
300	168.18
400	169.49
500	170.52
600	171.37
700	172.1
800	172.73
900	173.3
1000	173.81
1100	174.28
1200	174.71
1300	175.12
1400	175.49
1500	175.84
1600	176.17
1700	176.49
1800	176.79
1900	177.07
2000	177.34
2100	177.6
2200	177.85

Now the required gains are calculated for Carrier 1 and the frequency modulated ranging and telemetry signals.

$$G_{santd1_i} := SM - P + L_{satll_i} + L_{d_i} + L_{pol} \ldots + L_{atm} - G_{ga} + ML_c + R_c$$

This is the gain requirement for the carrier in dB.

$$G_{santd2_i} := SM - P + L_{satll} + L_{d_i} + L_{pol} + \ldots$$

This

$$+ L_{atm} - G_{ga} + ML_{r} + R_{r}$$

This is the gain requirement for the ranging signal in dB.

$$G_{santd3_i} := SM - P + L_{satll} + L_{d_i} + L_{pol} + \ldots$$

$$+ L_{atm} - G_{ga} + ML_{t} + R_{t}$$

This is the gain requirement for the telemetry signal in dB.

Carrier 2

Now for the Carrier 2 Analysis. All of the parameters are the same except there are no modulation losses, the transmitter power is boosted to 10 Watts and the ground station receiver sensitivity is different for different data rates.

P := 40 dBm Boosted satellite transmitter power

R_1 := -102.6 dB Ground station receiver sensitivity for a 512 kbps data rate

$R_2 := -98.8\ dB$ Ground station receiver sensitivity for a 1.024 Mbps data rate

$$G_{santd4_i} := SM - P + L_{satll} + L_{d_i} + L_{pol} + \ldots + L_{atm} - G_{ga} + R_1$$

Gain requirement for Carrier 2 with a 512 kbps data rate in dB

$$G_{santd5_i} := SM - P + L_{satll} + L_{d_i} + L_{pol} + \ldots + L_{atm} - G_{ga} + R_2$$

Gain requirement for Carrier 2 with a 1.024 Mbps data rate in dB

H_i	G_{santd1_i}	G_{santd2_i}	G_{santd3_i}	G_{santd4_i}	G_{santd5_i}
100	-26.19	-18.42	-12.71	-11.31	-7.51
200	-23.12	-15.35	-9.64	-8.24	-4.44
300	-21.3	-13.53	-7.82	-6.42	-2.62
400	-19.99	-12.22	-6.51	-5.11	-1.31
500	-18.96	-11.19	-5.48	-4.08	-0.28
600	-18.11	-10.34	-4.63	-3.23	0.57
700	-17.38	-9.61	-3.9	-2.5	1.3
800	-16.75	-8.98	-3.27	-1.87	1.93
900	-16.18	-8.41	-2.7	-1.3	2.5
1000	-15.67	-7.9	-2.19	-0.79	3.01
1100	-15.2	-7.43	-1.72	-0.32	3.48
1200	-14.77	-7	-1.29	0.11	3.91
1300	-14.36	-6.59	-0.88	0.52	4.32
1400	-13.99	-6.22	-0.51	0.89	4.69
1500	-13.64	-5.87	-0.16	1.24	5.04
1600	-13.31	-5.54	0.17	1.57	5.37
1700	-12.99	-5.22	0.49	1.89	5.69
1800	-12.69	-4.92	0.79	2.19	5.99
1900	-12.41	-4.64	1.07	2.47	6.27
2000	-12.14	-4.37	1.34	2.74	6.54
2100	-11.88	-4.11	1.6	3	6.8
2200	-11.63	-3.86	1.85	3.25	7.05

$$d_{d_i} := \frac{d_{d_i}}{1852}$$

Converts the slant range into nautical miles

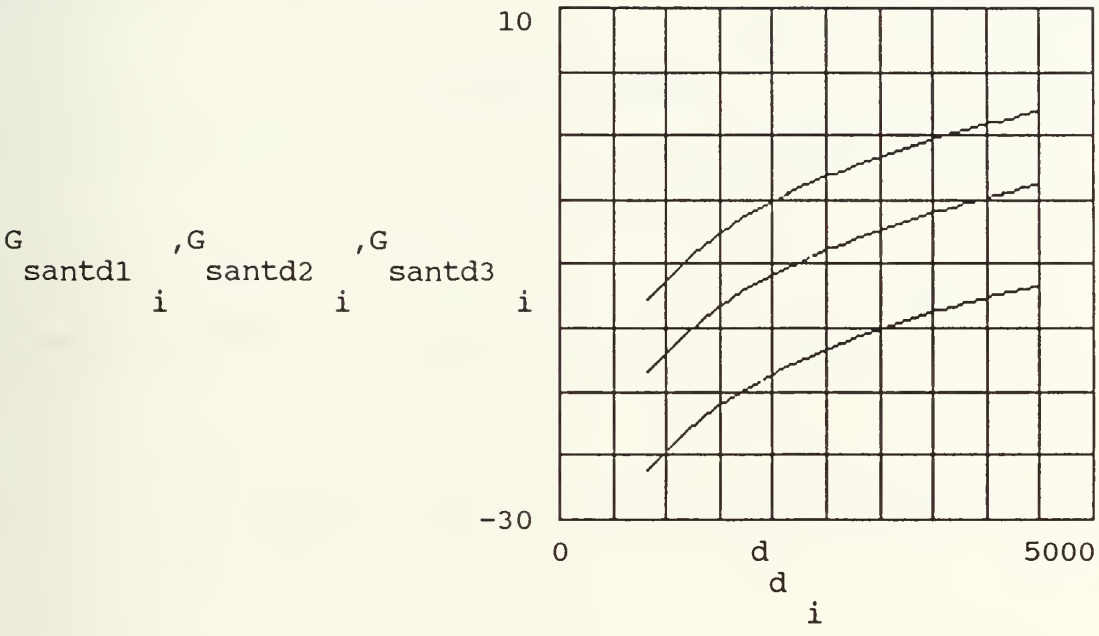

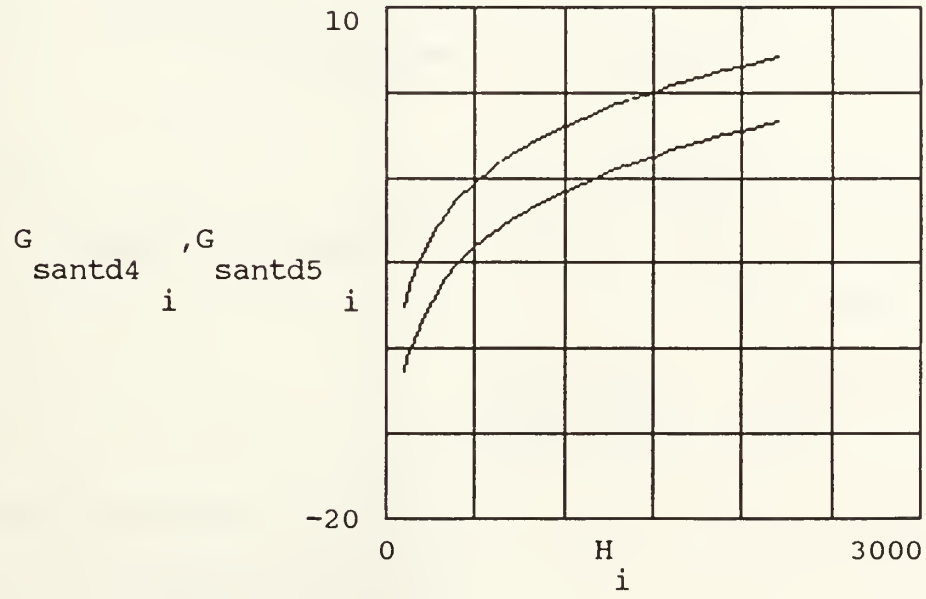

APPENDIX B. OMNIDIRECTIONAL RADIATION PATTERN

OMNIDIRECTIONAL RADIATION PATTERN

This program generates the radiation pattern for microstrip patch array antenna.

$N := 9$ Number of patches

$nu := 1$ Phasing variable

$f := 1800 \cdot 10^{6}$ Hertz Center frequency of the operating band

$c := 2.997925 \cdot 10^{8}$ meters/second Speed of light

$BW := 100 \cdot 10^{6}$ Hertz Bandwidth

$$h := \frac{BW}{128 \cdot 10^{6}} \cdot \left[\frac{10^{9}}{f}\right]^{2} \cdot 2.54$$ Thickness of the patch

$h = 0.612461$ centimeters

$\epsilon_r := 2.32$ Dielectric constant of the substrate material

$$W := \frac{c}{2 \cdot f} \cdot \left[\frac{\epsilon_r + 1}{2} \right]^{-\left[\frac{1}{2}\right]} \cdot 100$$ Width of the patch

$W = 6.463447$ centimeters

$\lambda_0 := \frac{c}{f} \cdot 100$ Free space wavelength of t

frequency

$\lambda_0 = 16.655139$ centimeters

$$l := 0.49 \cdot \left[\frac{\lambda_0}{\sqrt{\epsilon_r}} \right]$$ length of the patch

$l = 5.357971$ centimeters

$a := 9.5 \cdot 2.54$ Radius of the ORION body

$a = 24.13$ cylinder

$k_o := \frac{2 \cdot \pi}{\lambda_0}$ Free space wave number

$k_o = 0.377252$

$i := 1 \ldots 121$

Routine for calculating the roll plane radiation pattern

$\theta_i := \frac{\pi}{2}$

$\phi_i := (i - 1) \cdot \frac{2 \cdot \pi}{120}$

$n := 1 \ldots N$

$v_n := (n - 1) \cdot \frac{2 \cdot \pi}{N}$

$$f_{\phi_i} := \left| \frac{\sin\left[\frac{k_o \cdot W}{2} \cdot \cos[\theta_i]\right]}{\frac{k_o \cdot W}{2} \cdot \cos[\theta_i]} \cdot \sin[\theta_i] \right| \cdot \left| \sum_n \left[\left[e^{-j \cdot nu \cdot v_n} \right] \cdot \left[e^{j \cdot k_o \cdot a \cdot \sin[\theta_i] \cdot \cos[\phi_i - v_n]} + e^{j \cdot k_o \cdot a \cdot \sin[\theta_i] \cdot \cos\left[\phi_i - v_n - \frac{1}{a}\right]} \right] \right] \right|$$

$f_{\phi x_i} := \left| f_{\phi_i} \right| \cdot \cos[\phi_i]$ $\quad$ $f_{\phi y_i} := \left| f_{\phi_i} \right| \cdot \sin[\phi_i]$

$f_{\phi_i} := \text{if}\left[f_{\phi_i} \approx 0, 0.000001, f_{\phi_i} \right]$

$M_{0,0} := 121$

$M_{0,1} := 2$

$M_{i,0} := \left| f_{\phi_i} \right|$ $\quad$ $M_{i,1} := \phi_i$

WRITEPRN(RANT) := M

$i := 1 \,..121$

Routine for calculating the elevation plane radiation pattern

$\phi_i := 0$

$\theta_i := (i - 1)\cdot\frac{2\cdot\pi}{120}$

$n := 1 \,..N$

$v_n := (n - 1)\cdot\frac{2\cdot\pi}{N}$

$$f_{\theta_i} := \left[\frac{\sin\left[\frac{k_o \cdot W}{2}\cdot\cos\left[\theta_i\right]\right]}{\frac{k_o \cdot W}{2}\cdot\cos\left[\theta_i\right]}\cdot\sin\left[\theta_i\right]\right]\cdot\left[\sum_n\left[\left[e^{-j\cdot nu\cdot v_n}\right]\cdot\left[e^{j\cdot k_o\cdot a\cdot\sin\left[\theta_i\right]\cdot\cos\left[\phi_i - v_n\right]} + e^{j\cdot k_o\cdot a\cdot\sin\left[\theta_i\right]\cdot\cos\left[\phi_i - v_n - \frac{l}{a}\right]}\right]\right]\right]$$

$f_{\theta x_i} := \left|f_{\theta_i}\right|\cdot\sin\left[\theta_i\right]$ $\quad$ $f_{\theta y_i} := \left|f_{\theta_i}\right|\cdot\cos\left[\theta_i\right]$

$f_{\theta_i} := \text{if}\left[f_{\theta_i} \approx 0, 0.000001, f_{\theta_i}\right]$

$NN_{0,0} := 121$

$NN_{0,1} := 2$

$NN_{i,0} := \left|f_{\theta_i}\right|$ $\quad$ $NN_{i,1} := \theta_i$

WRITEPRN(RANT1) := NN

Uplink Omnidirectional Radiation Pattern Results

N = 9 nu = 1

Roll Plane

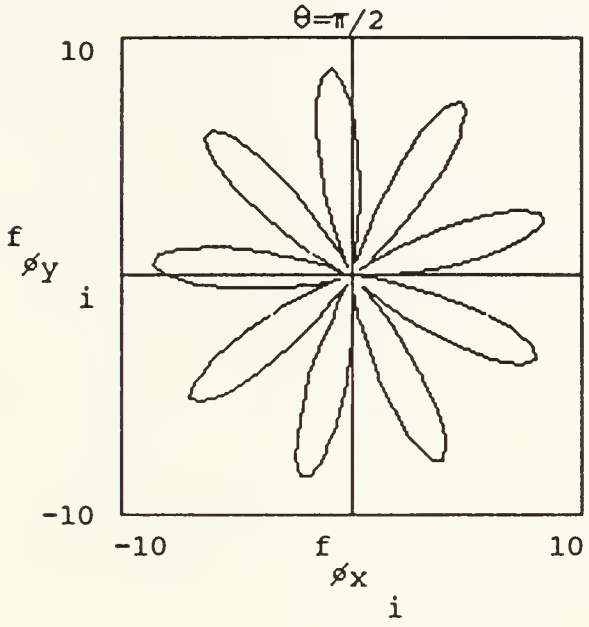

Elevation Plane

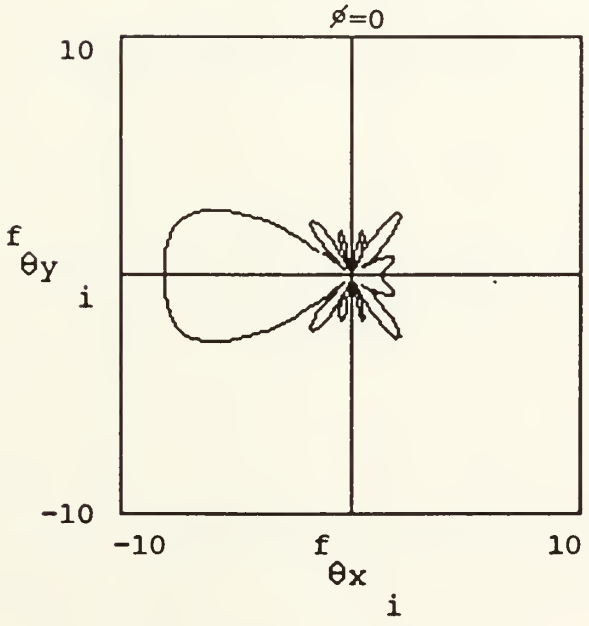

N = 9 nu = 2

Roll Plane

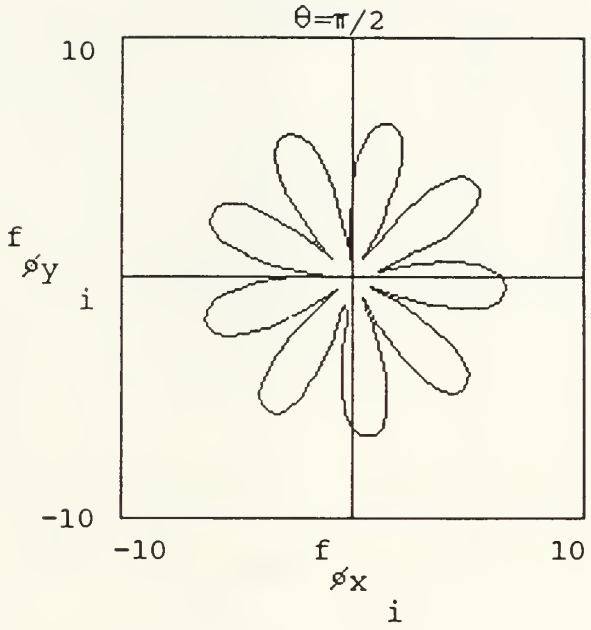

Elevation Plane

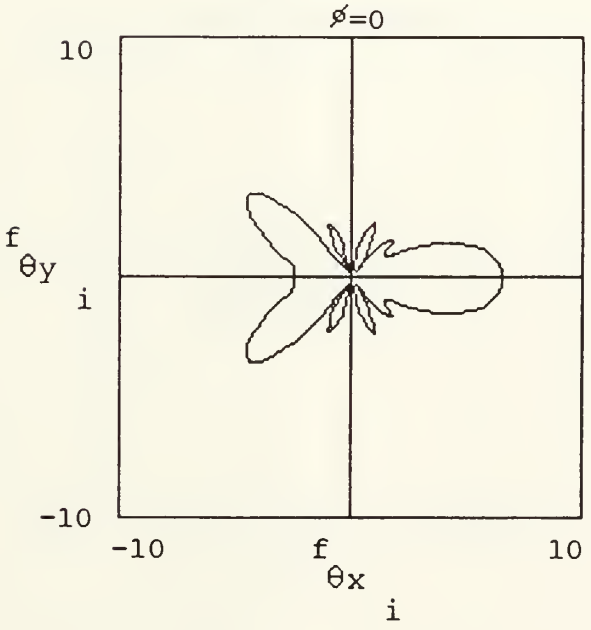

N = 9 nu = 3

Roll Plane

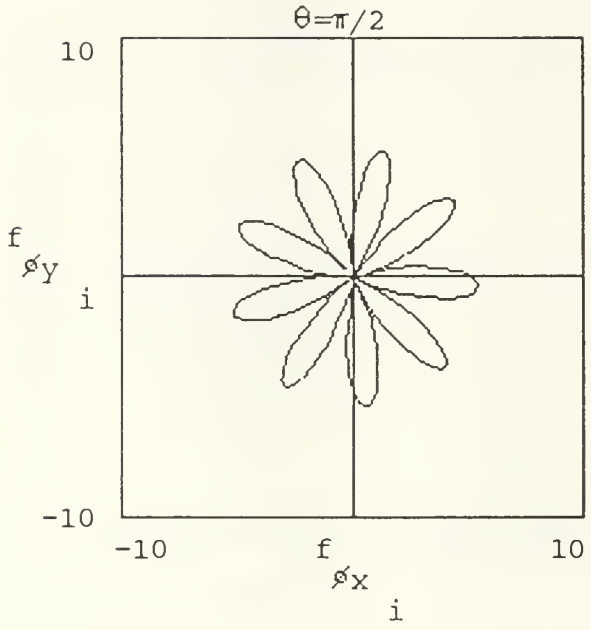

Elevation Plane

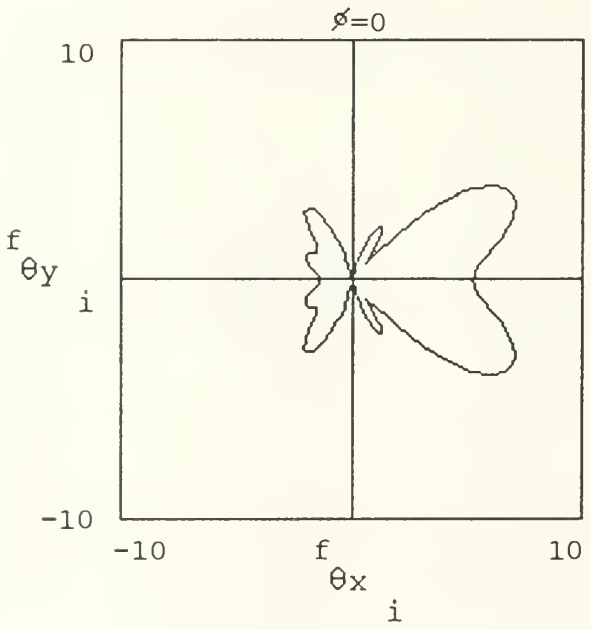

N = 10 nu = 1

Roll Plane

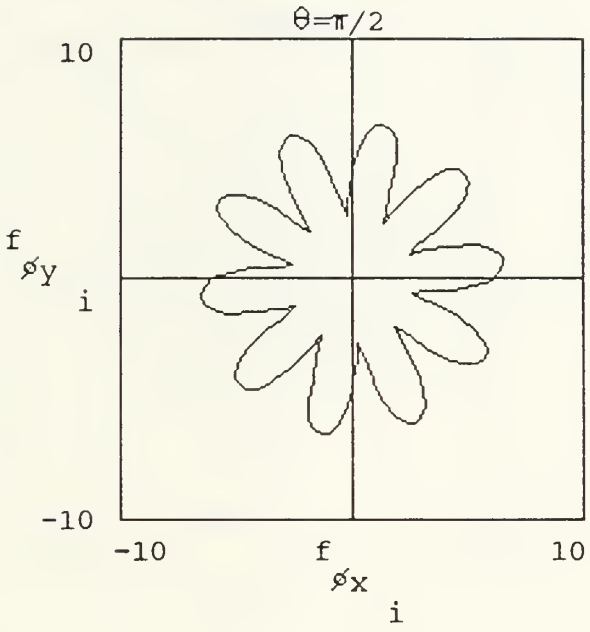

Elevation Plane

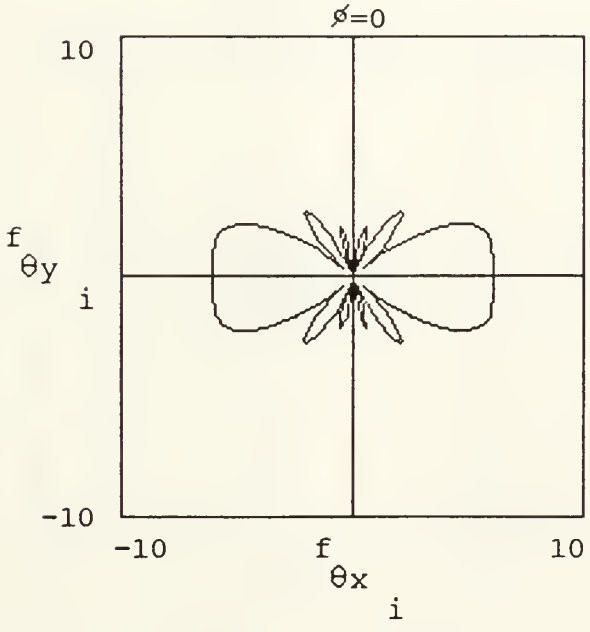

N = 10 nu = 2

Roll Plane

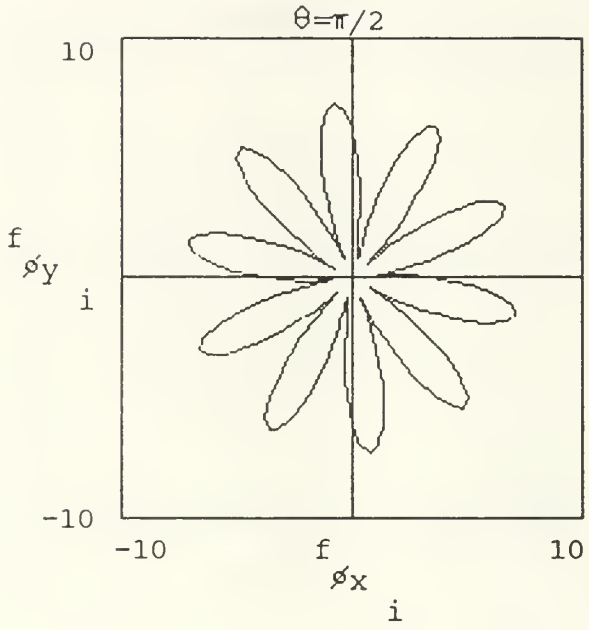

Elevation Plane

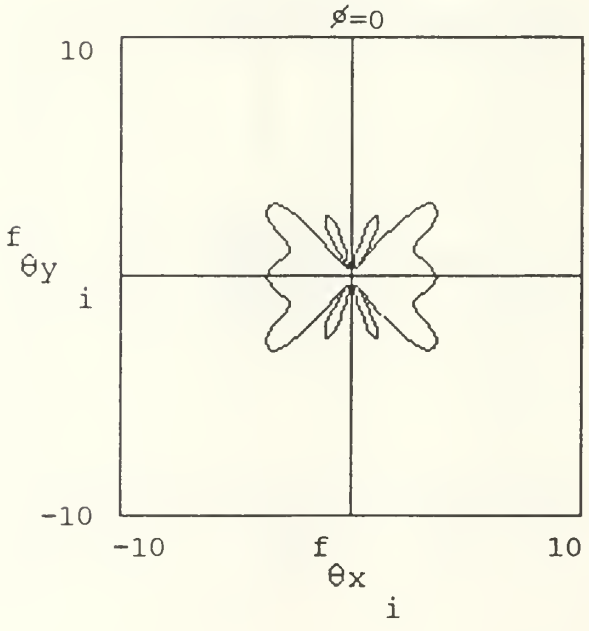

N = 10 nu = 3

Roll Plane

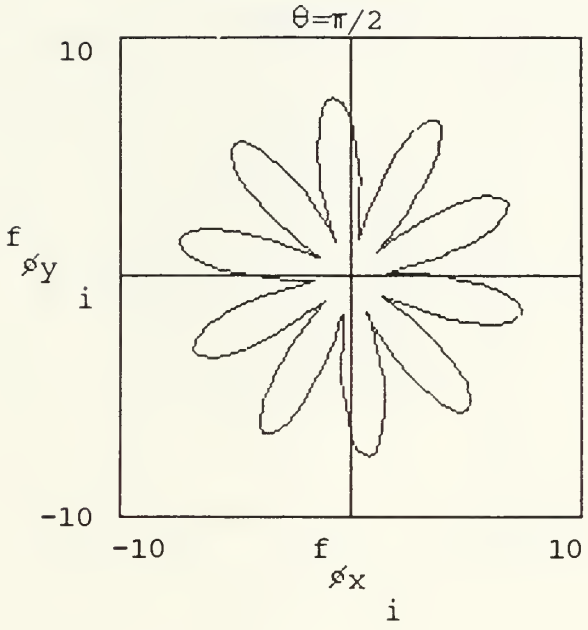

Elevation Plane

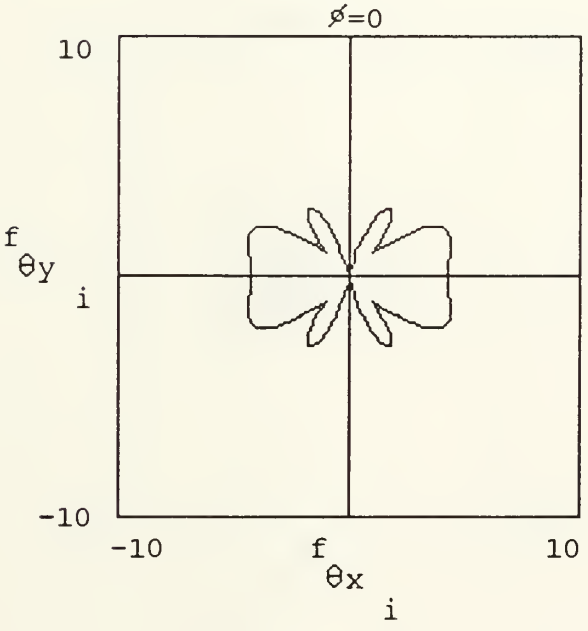

N = 11 nu = 1

Roll Plane

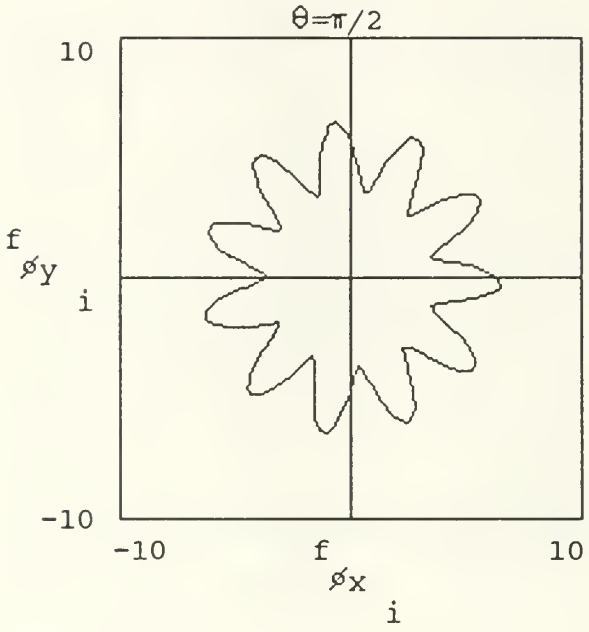

Elevation Plane

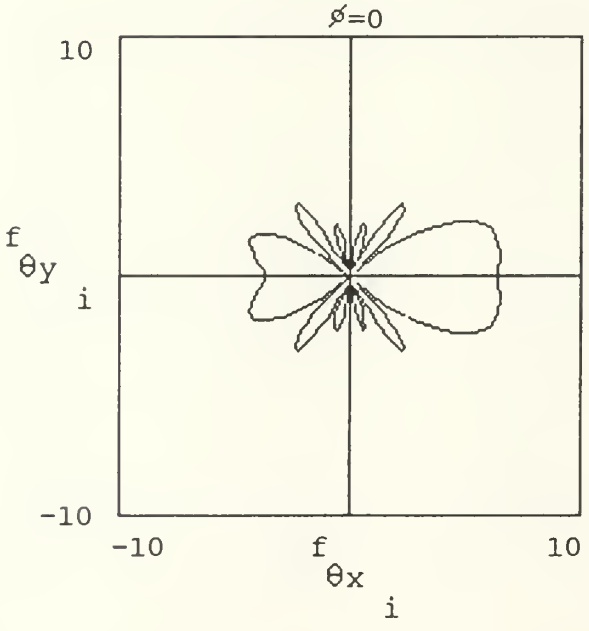

N = 11 nu = 2

Roll Plane

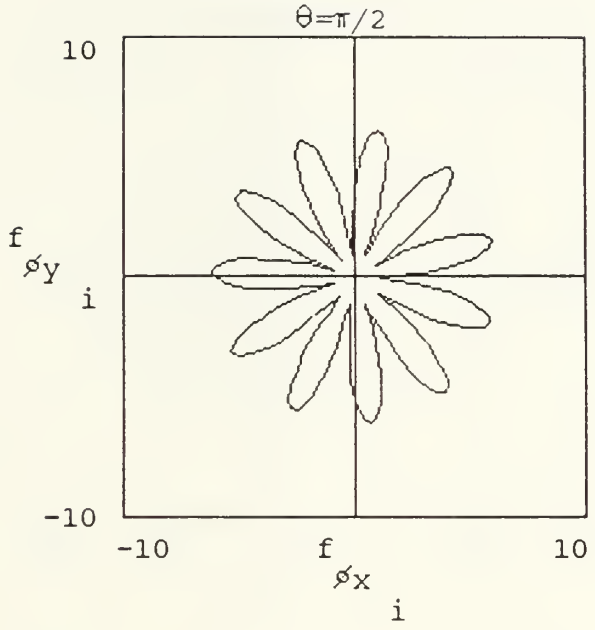

Elevation Plane

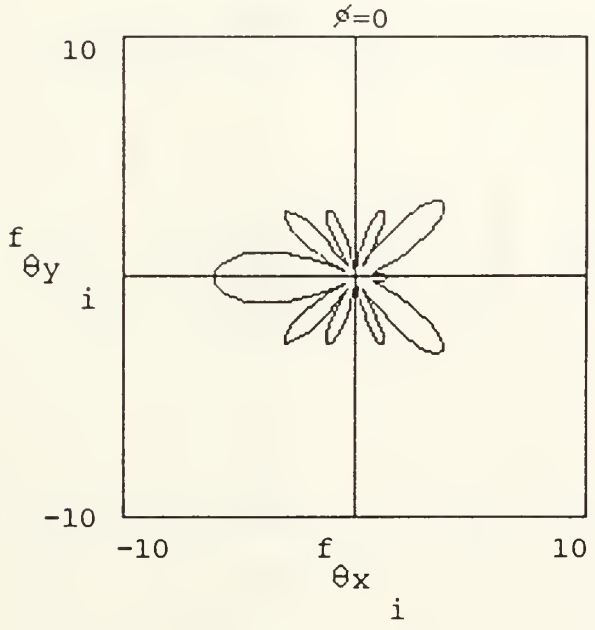

N = 11 nu = 3

Roll Plane

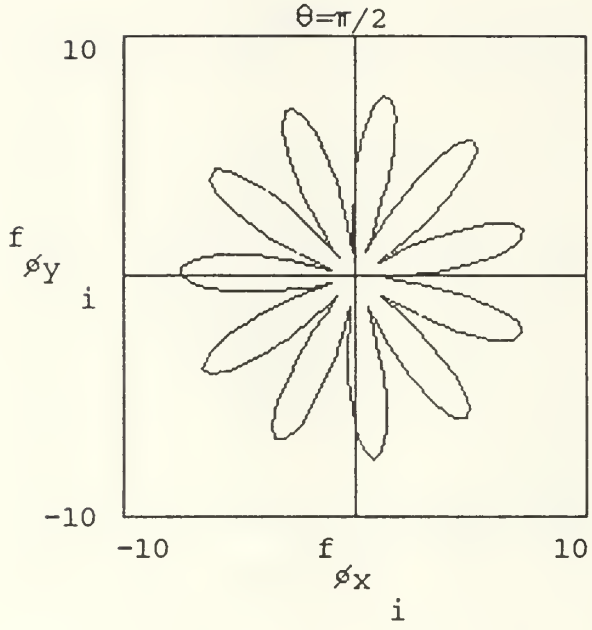

Elevation Plane

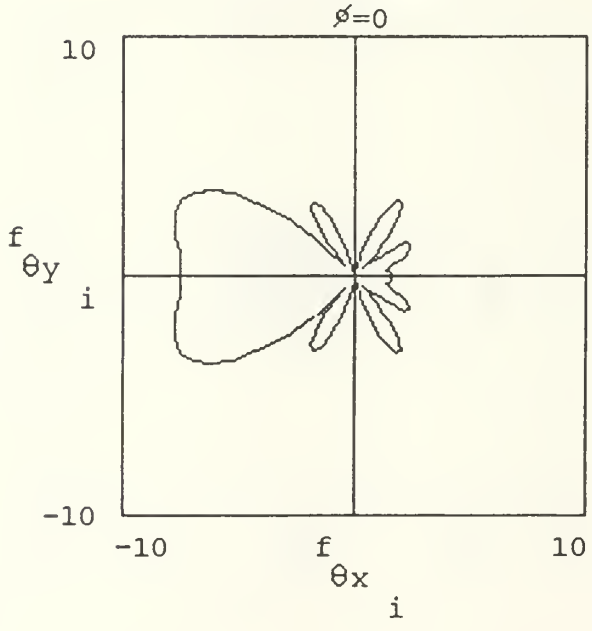

N = 12 nu = 1

Roll Plane

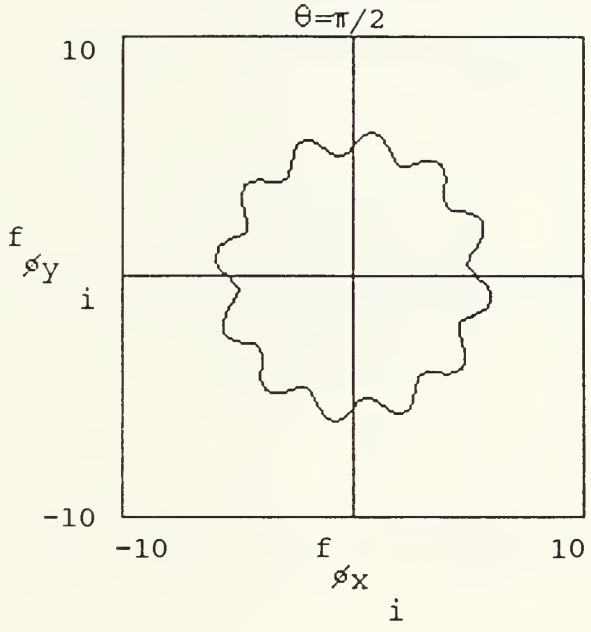

Elevation Plane

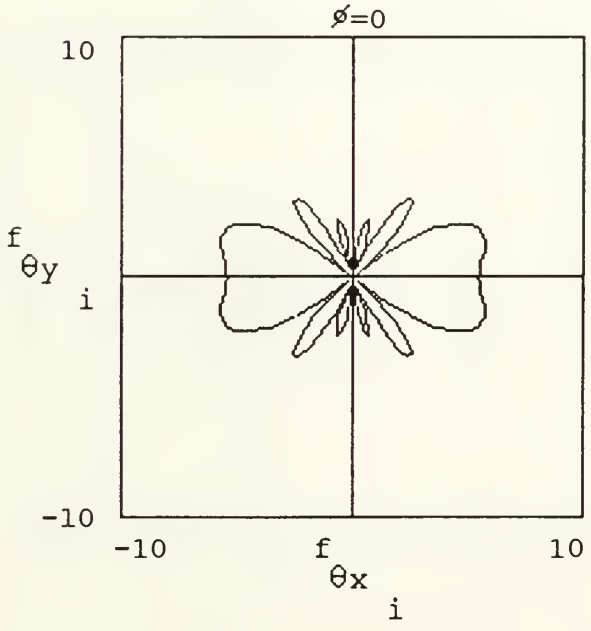

N = 12 nu = 2

Roll Plane

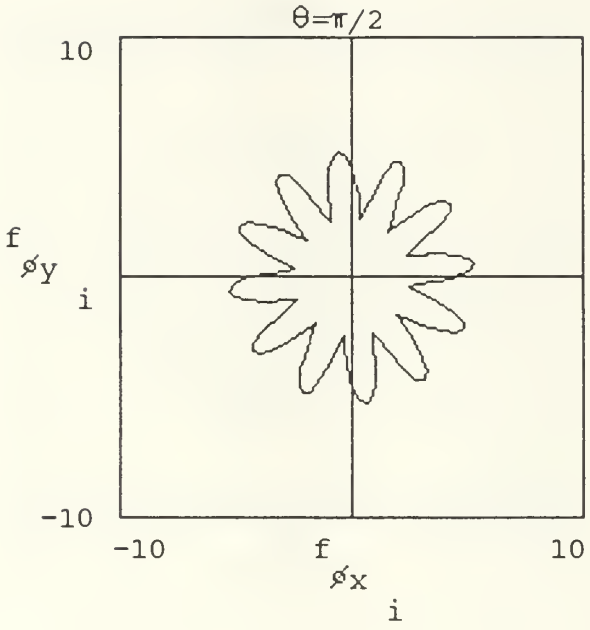

Elevation Plane

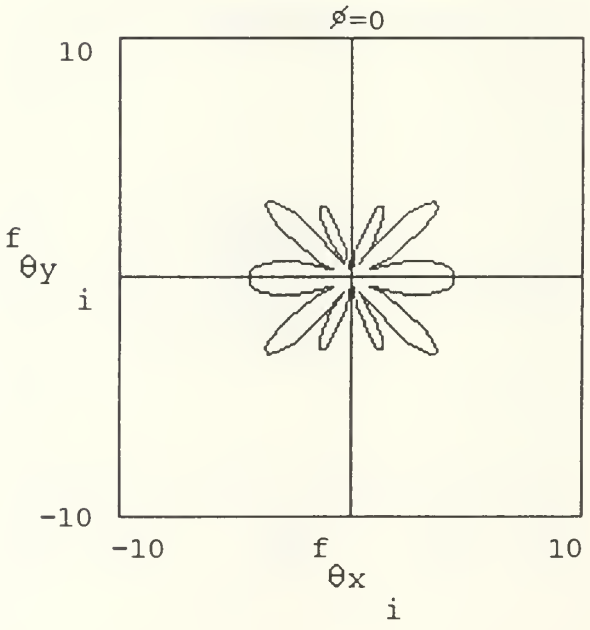

N = 12 nu = 3

Roll Plane

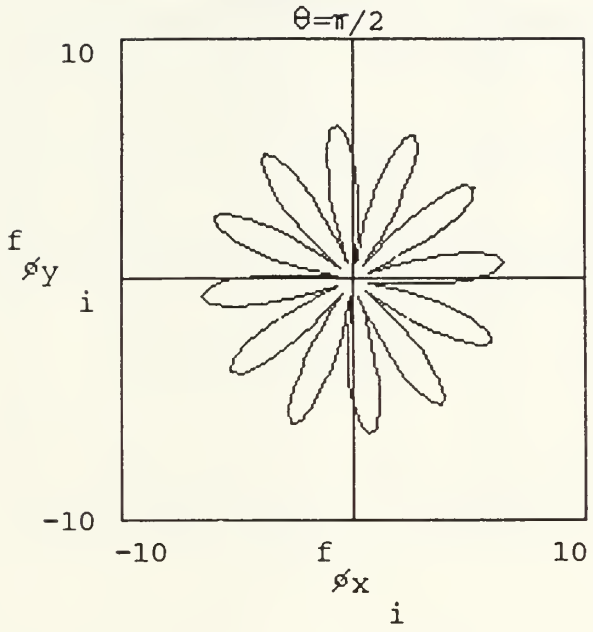

Elevation Plane

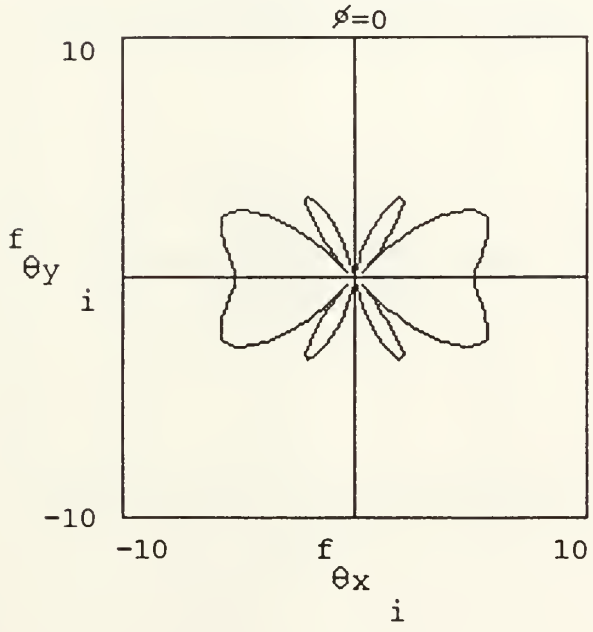

N = 13 nu = 1

Roll Plane

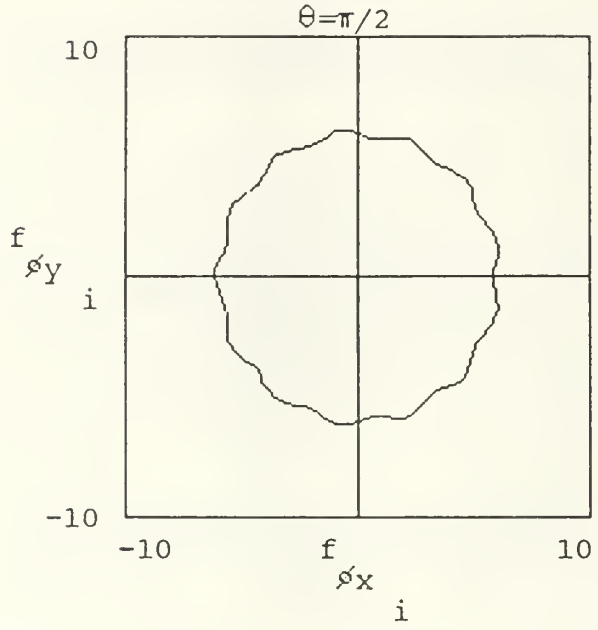

Elevation Plane

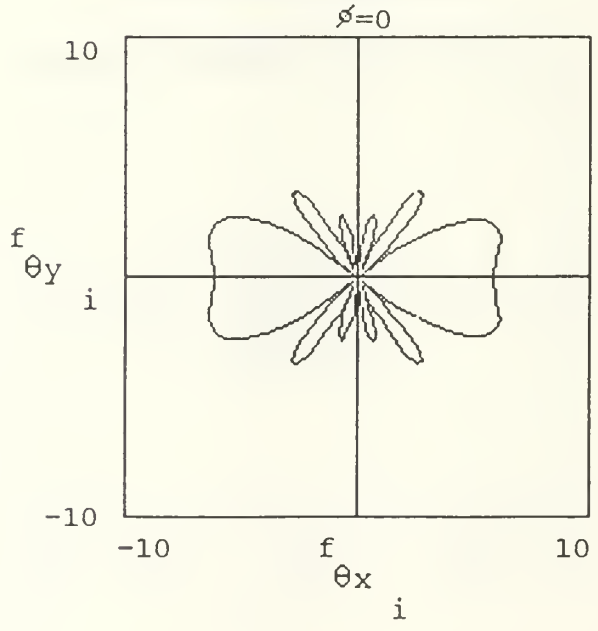

N = 13 nu = 2

Roll Plane

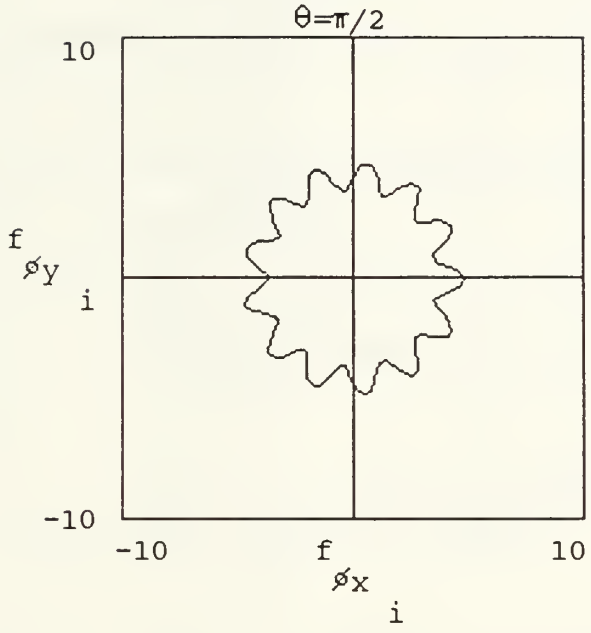

Elevation Plane

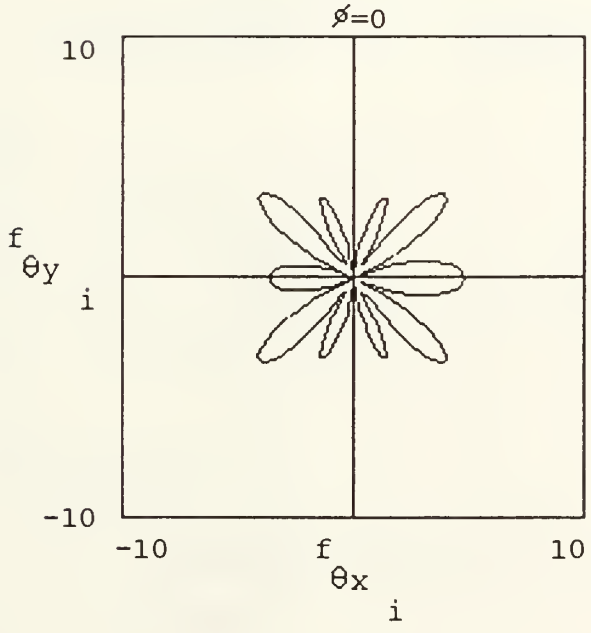

N = 13 nu = 3

Roll Plane

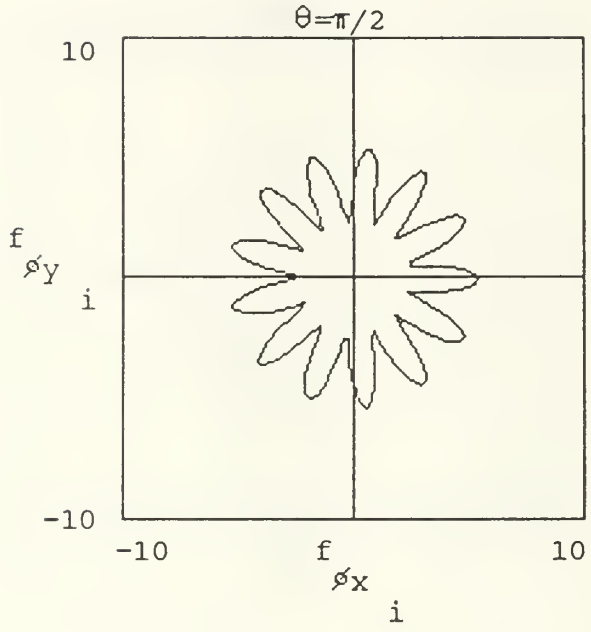

Elevation Plane

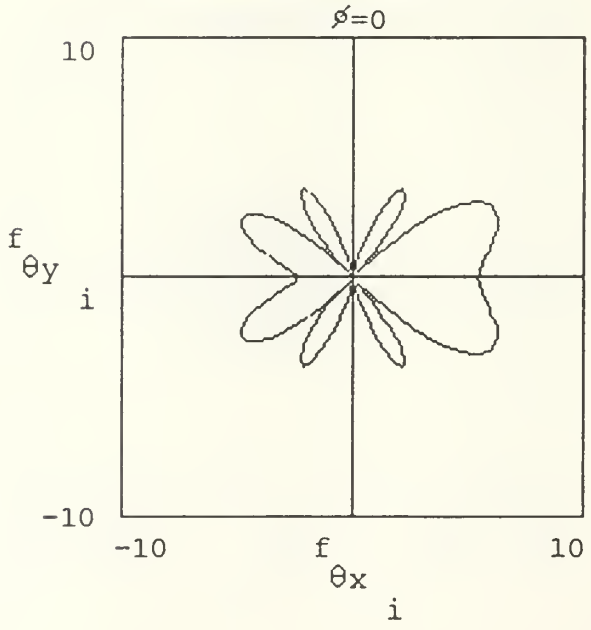

APPENDIX C. OMNIDIRECTIONAL AVERAGE RADIATION INTENSITY

Average Radiation Intensity

This program calculates the average radiation intensity for use in the directive gain equation.

$N := 12$ Number of microstrip patches

$nu := 1$ Number of multiple decrease in the phase around the array

$f := 1800 \cdot 10^{6}$ Hertz Center frequency of the operating band

$c := 2.997925 \cdot 10^{8}$ meters/second Speed of light

$BW := 100 \cdot 10^{6}$ Hertz Bandwidth

$$h := \frac{BW}{128 \cdot 10^{6}} \cdot \left[\frac{10^{9}}{f}\right]^{2} \cdot 2.54$$ Thickness of a patch in centimeters.

$h = 0.612461$ centimeters

$\epsilon_r := 2.32$ Dielectric constant of the substrate material.

$$W := \frac{c}{2 \cdot f} \cdot \left[\frac{\epsilon_r + 1}{2} \right]^{-\left[\frac{1}{2}\right]} \cdot 100$$ Width of a patch in centimeters

$W = 6.463447$ centimeters

$$\lambda_0 := \frac{c}{f} \cdot 100$$ Free space wavelength

$\lambda_0 = 16.655139$ centimeters

$$L := 0.49 \cdot \left[\frac{\lambda_0}{\sqrt{\epsilon_r}} \right]$$ Length of a patch

$L = 5.357971$ centimeters

$$k_o := \frac{2 \cdot \pi}{\lambda_0}$$ Wave number

$k_o = 0.377252$

$a := 9.5 \cdot 2.54$ Radius of the ORION cylinder

$a = 24.13$ centimeters

$n := 1 \ldots N$

$$v_n := (n - 1) \cdot \frac{2 \cdot \pi}{N}$$ Location of a leading edge slot of a patch

$$
U_{av} := \frac{1}{4\cdot\pi}\cdot\int_0^{2\cdot\pi}\int_0^{\pi}\left[\frac{\sin\left(\frac{k_o\cdot W}{2}\cdot\cos(\theta)\right)}{\frac{k_o\cdot W}{2}\cdot\cos(\theta)}\cdot\sin(\theta)\right]\cdot\left|\begin{array}{l}
\left[e^{-j\cdot nu_1\cdot v}\cdot\left[e^{j\cdot k_o\cdot a\cdot\sin(\theta)\cdot\cos\left[\phi-v_1\right]}+e^{j\cdot k_o\cdot a\cdot\sin(\theta)\cdot\cos\left[\phi-v_1-\frac{L}{a}\right]}\right]\right]\ldots\\
+\left[e^{-j\cdot nu_2\cdot v}\cdot\left[e^{j\cdot k_o\cdot a\cdot\sin(\theta)\cdot\cos\left[\phi-v_2\right]}+e^{j\cdot k_o\cdot a\cdot\sin(\theta)\cdot\cos\left[\phi-v_2-\frac{L}{a}\right]}\right]\right]\ldots\\
+\left[e^{-j\cdot nu_3\cdot v}\cdot\left[e^{j\cdot k_o\cdot a\cdot\sin(\theta)\cdot\cos\left[\phi-v_3\right]}+e^{j\cdot k_o\cdot a\cdot\sin(\theta)\cdot\cos\left[\phi-v_3-\frac{L}{a}\right]}\right]\right]\ldots\\
+\left[e^{-j\cdot nu_4\cdot v}\cdot\left[e^{j\cdot k_o\cdot a\cdot\sin(\theta)\cdot\cos\left[\phi-v_4\right]}+e^{j\cdot k_o\cdot a\cdot\sin(\theta)\cdot\cos\left[\phi-v_4-\frac{L}{a}\right]}\right]\right]\ldots\\
+\left[e^{-j\cdot nu_5\cdot v}\cdot\left[e^{j\cdot k_o\cdot a\cdot\sin(\theta)\cdot\cos\left[\phi-v_5\right]}+e^{j\cdot k_o\cdot a\cdot\sin(\theta)\cdot\cos\left[\phi-v_5-\frac{L}{a}\right]}\right]\right]\ldots\\
+\left[e^{-j\cdot nu_6\cdot v}\cdot\left[e^{j\cdot k_o\cdot a\cdot\sin(\theta)\cdot\cos\left[\phi-v_6\right]}+e^{j\cdot k_o\cdot a\cdot\sin(\theta)\cdot\cos\left[\phi-v_6-\frac{L}{a}\right]}\right]\right]\ldots\\
+\left[e^{-j\cdot nu_7\cdot v}\cdot\left[e^{j\cdot k_o\cdot a\cdot\sin(\theta)\cdot\cos\left[\phi-v_7\right]}+e^{j\cdot k_o\cdot a\cdot\sin(\theta)\cdot\cos\left[\phi-v_7-\frac{L}{a}\right]}\right]\right]\ldots\\
+\left[e^{-j\cdot nu_8\cdot v}\cdot\left[e^{j\cdot k_o\cdot a\cdot\sin(\theta)\cdot\cos\left[\phi-v_8\right]}+e^{j\cdot k_o\cdot a\cdot\sin(\theta)\cdot\cos\left[\phi-v_8-\frac{L}{a}\right]}\right]\right]\ldots\\
+\left[e^{-j\cdot nu_9\cdot v}\cdot\left[e^{j\cdot k_o\cdot a\cdot\sin(\theta)\cdot\cos\left[\phi-v_9\right]}+e^{j\cdot k_o\cdot a\cdot\sin(\theta)\cdot\cos\left[\phi-v_9-\frac{L}{a}\right]}\right]\right]\ldots\\
+\left[e^{-j\cdot nu_{10}\cdot v}\cdot\left[e^{j\cdot k_o\cdot a\cdot\sin(\theta)\cdot\cos\left[\phi-v_{10}\right]}+e^{j\cdot k_o\cdot a\cdot\sin(\theta)\cdot\cos\left[\phi-v_{10}-\frac{L}{a}\right]}\right]\right]\ldots\\
+\left[e^{-j\cdot nu_{11}\cdot v}\cdot\left[e^{j\cdot k_o\cdot a\cdot\sin(\theta)\cdot\cos\left[\phi-v_{11}\right]}+e^{j\cdot k_o\cdot a\cdot\sin(\theta)\cdot\cos\left[\phi-v_{11}-\frac{L}{a}\right]}\right]\right]\ldots\\
+\left[e^{-j\cdot nu_{12}\cdot v}\cdot\left[e^{j\cdot k_o\cdot a\cdot\sin(\theta)\cdot\cos\left[\phi-v_{12}\right]}+e^{j\cdot k_o\cdot a\cdot\sin(\theta)\cdot\cos\left[\phi-v_{12}-\frac{L}{a}\right]}\right]\right]\ldots
\end{array}\right|^2\cdot\sin(\theta)\,d\theta\,d\phi
$$

```
U     := 19.58
 av

N := 12

nu := 1
```

APPENDIX D. OMNIDIRECTIONAL DIRECTIVE GAIN PATTERN

OMNIDIRECTIONAL DIRECTIVE GAIN PATTERN

This program calculates the directive pain pattern for an omnidirectional microstrip circular array antenna.

N := 12 Number of microstrip patches

nu := 1 Number of complete phase shifts once around the array

$U_{av} := 19.64$ Average radiation intensity

$f := 1800 \cdot 10^{6}$ Hertz Middle of the frequency band

h := 0.61 centimeters Thickness of the patch

W := 6.46 centimeters Width of the patch

L := 5.36 centimeters Length of the patch

a := 24.13 centimeters Radius of the ORION satellite cylinder

$c := 2.997925 \cdot 10^{8}$ meters/second Speed of light

$\lambda_o := \frac{c}{f} \cdot 100$ Free space wavelength of the operating frequency

$\lambda_o = 16.655$ centimeters

$k_o := \frac{2 \cdot \pi}{\lambda_o}$ Wave number

$k_o = 0.377$

$i := 1 \ldots 121$ Routine for calculating the directive gain for the roll plane

$\theta_i := \frac{\pi}{2}$

$\phi_i := (i - 1) \cdot \frac{2 \cdot \pi}{120}$

$n := 1 \ldots N$

$v_n := (n - 1) \cdot \frac{2 \cdot \pi}{N}$

$$D_{\phi_i} := \frac{\left| \left| \left[\frac{\sin\left[\frac{k_o \cdot W}{2} \cdot \cos\left[\theta_i\right] \right]}{\frac{k_o \cdot W}{2} \cdot \cos\left[\theta_i\right]} \cdot \sin\left[\theta_i\right] \right] \cdot \left[\sum_n \left[\left[e^{-j \cdot nu \cdot v_n} \right] \cdot \left[e^{j \cdot k_o \cdot a \cdot \sin\left[\theta_i\right] \cdot \cos\left[\phi_i - v_n\right]} + e^{j \cdot k_o \cdot a \cdot \sin\left[\theta_i\right] \cdot \cos\left[\phi_i - v_n - \frac{L}{a}\right]} \right] \right] \right] \right|^2}{U_{av}}$$

$$D_{\phi x_i} := \left|D_{\phi_i}\right| \cdot \cos\left[\phi_i\right] \qquad D_{\phi y_i} := \left|D_{\phi_i}\right| \cdot \sin\left[\phi_i\right]$$

$$DD_{\phi_i} := 10 \cdot \log\left[\left|D_{\phi_i}\right|\right]$$

$$M_{0,0} := 121 \qquad M_{0,1} := 2$$

$$M_{i,0} := \left|D_{\phi_i}\right| \qquad M_{i,1} := \phi_i$$

WRITEPRN(ANTPAT) := M

i := 1 ..121

Routine for calculating the directive gain elevation pattern

$\phi_i := 0$

$$\theta_i := (i - 1) \cdot \frac{2 \cdot \pi}{120}$$

n := 1 ..N

$$v_n := (n - 1) \cdot \frac{2 \cdot \pi}{N}$$

$$D_{\theta_i} := \frac{\left[\left|\left[\left[\sin\left[\frac{k_o \cdot W}{2} \cdot \cos\left[\theta_i\right]\right]}{\frac{k_o \cdot W}{2} \cdot \cos\left[\theta_i\right]} \cdot \sin\left[\theta_i\right]\right] \cdot \left[\sum_n \left[\left[e^{-j \cdot nu \cdot v_n}\right] \cdot \left[e^{j \cdot k_o \cdot a \cdot \sin\left[\theta_i\right] \cdot \cos\left[\phi_i - v_n\right]} + e^{j \cdot k_o \cdot a \cdot \sin\left[\theta_i\right] \cdot \cos\left[\phi_i - v_n - \frac{L}{a}\right]}\right]\right]\right]\right|\right]^2}{U_{av}}$$

$$D_{\theta x_i} := \left| D_{\theta_i} \right| \cdot \sin\left[\theta_i\right] \qquad D_{\theta y_i} := \left| D_{\theta_i} \right| \cdot \cos\left[\theta_i\right]$$

$$D_{\theta_1} := \text{if}\left[D_{\theta_i} \approx 0, 0.000001, D_{\theta_i}\right]$$

$$DD_{\theta_i} := 10 \cdot \log\left[\left| D_{\theta_i} \right|\right]$$

$$NN_{0,0} := 121 \qquad NN_{0,1} := 2$$

$$NN_{i,0} := \left| D_{\theta_i} \right| \qquad NN_{i,1} := \theta_i$$

WRITEPRN(ANTPAT1) := NN

Directive Gain Pattern Results

N = 12 nu = 1

Uplink Results

Roll Plane

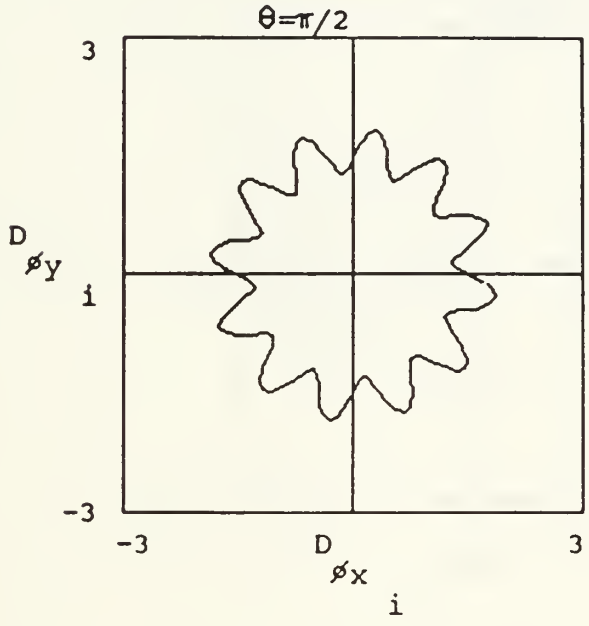

Elevation Plane

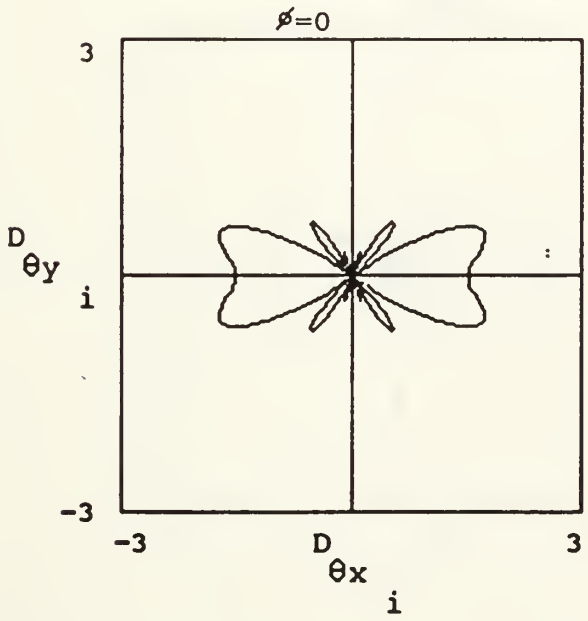

N = 13 nu = 1

Roll Plane

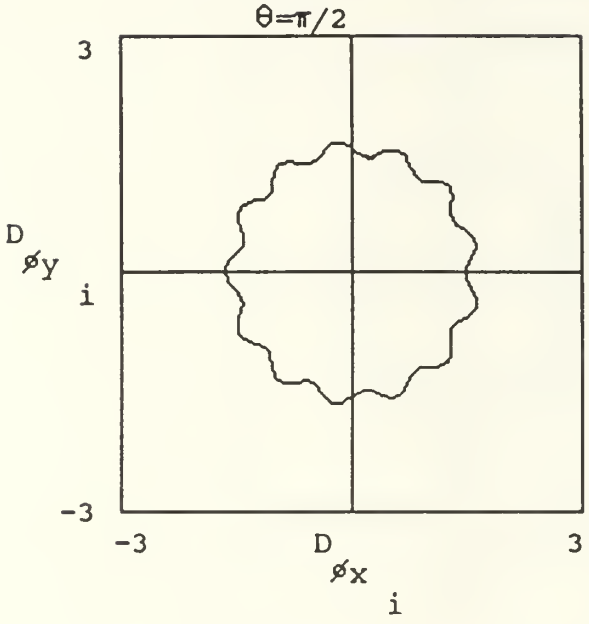

Elevation Plane

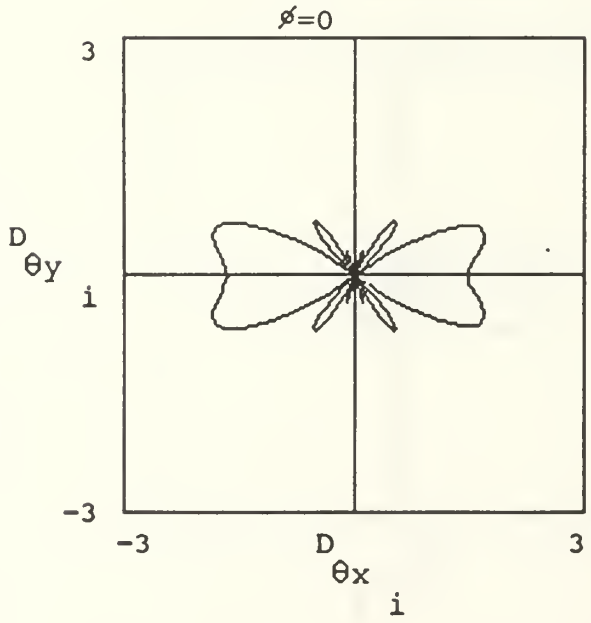

N = 12 nu = 2

Downlink Results

Roll Plane

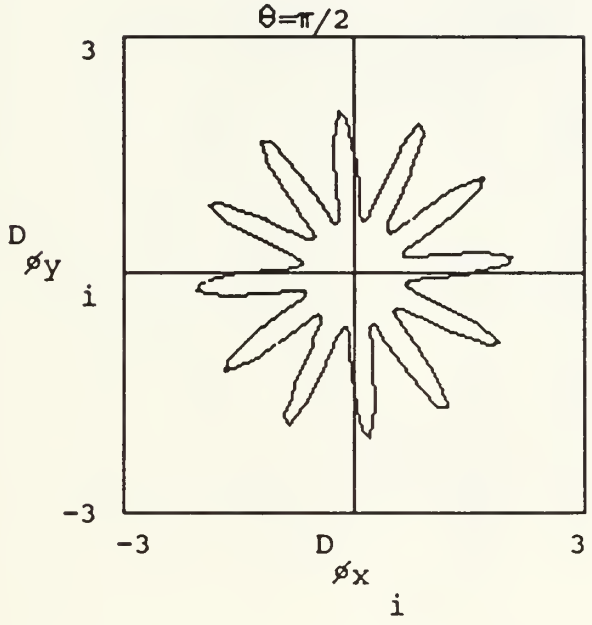

Elevation Plane

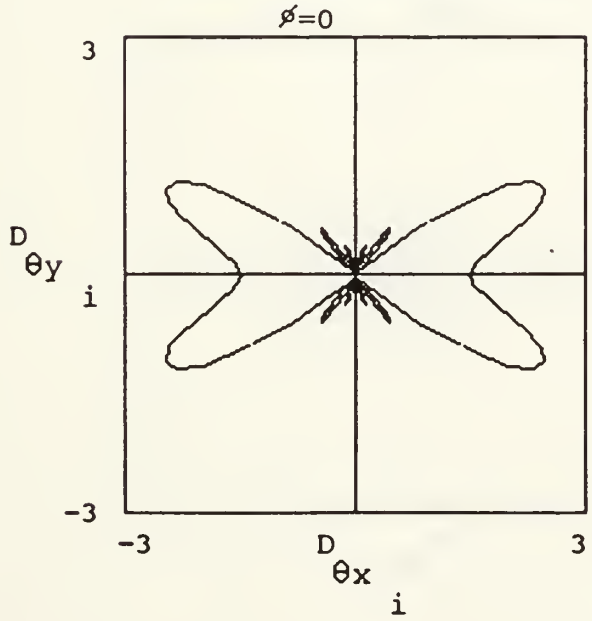

N = 15 nu = 1

Roll Plane

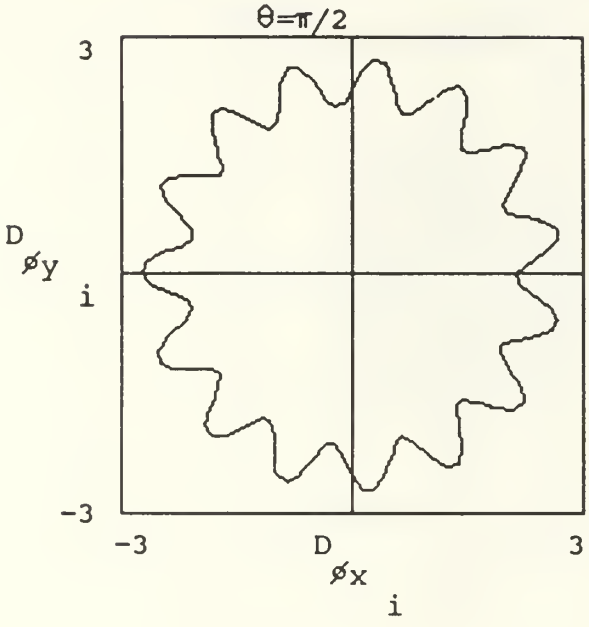

Elevation Plane

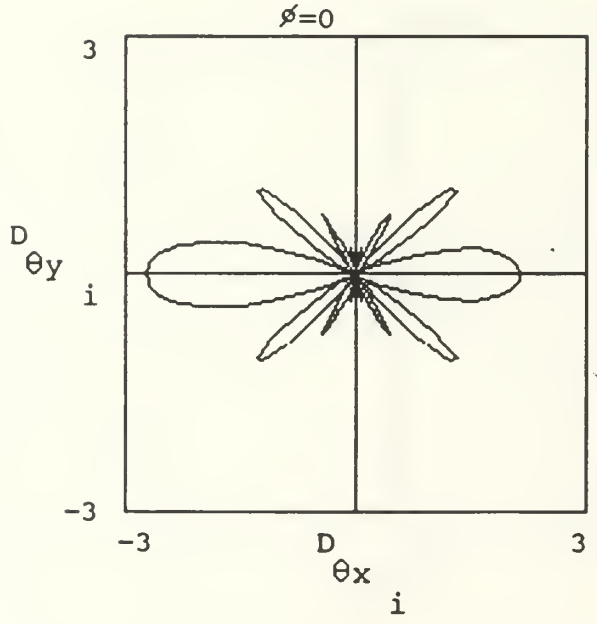

N = 16 nu = 1

Roll Plane

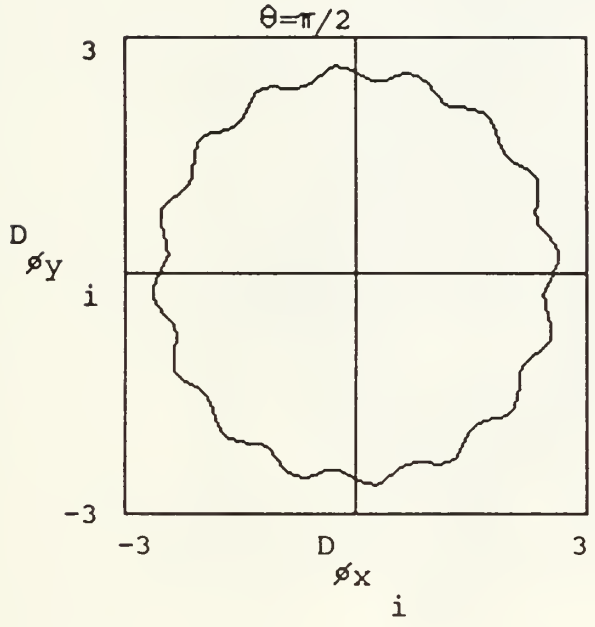

Elevation Plane

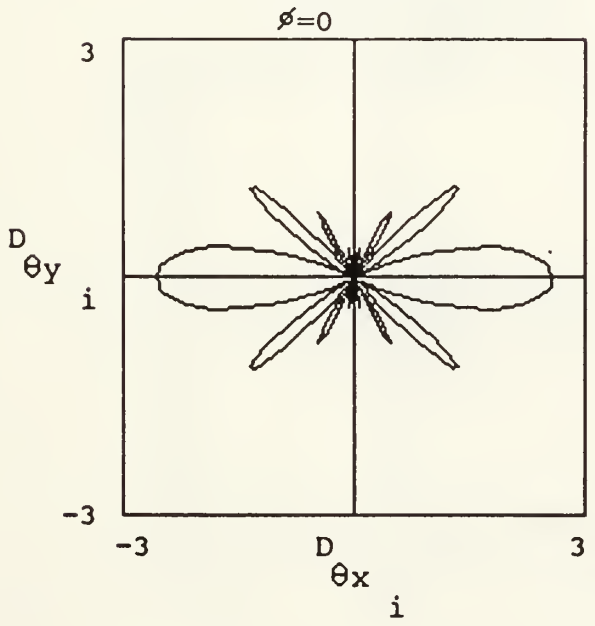

N = 16 nu = 3

Roll Plane

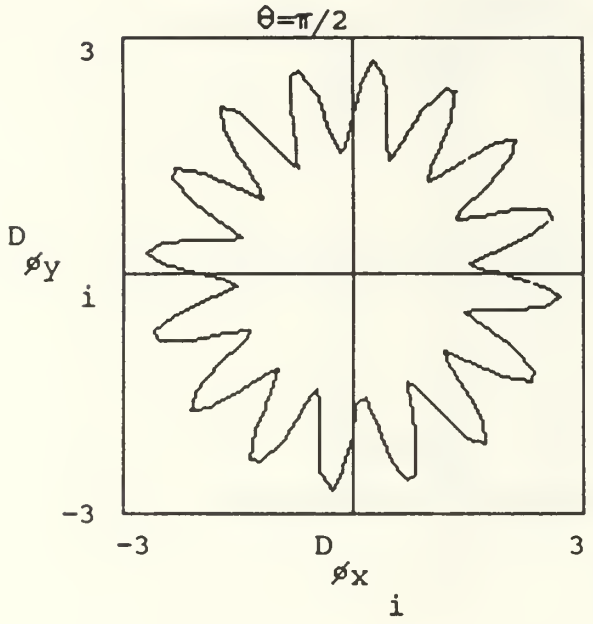

Elevation Plane

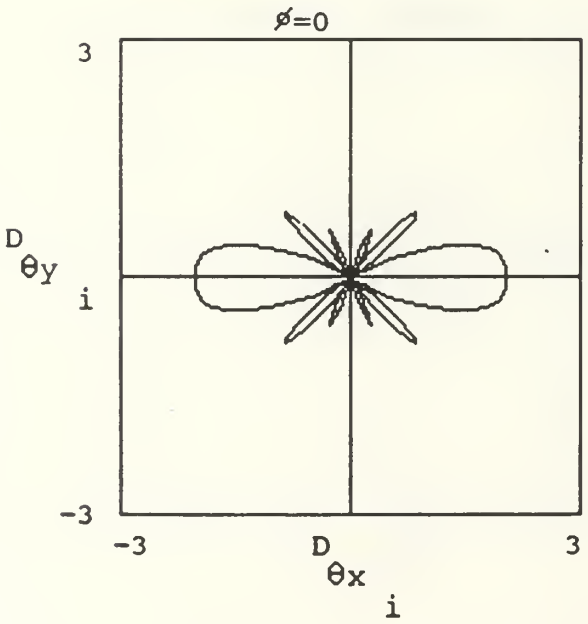

APPENDIX E. DOWNLINK OMNI RADIATION PATTERN RESULTS

N = 12 nu = 1

Roll Plane

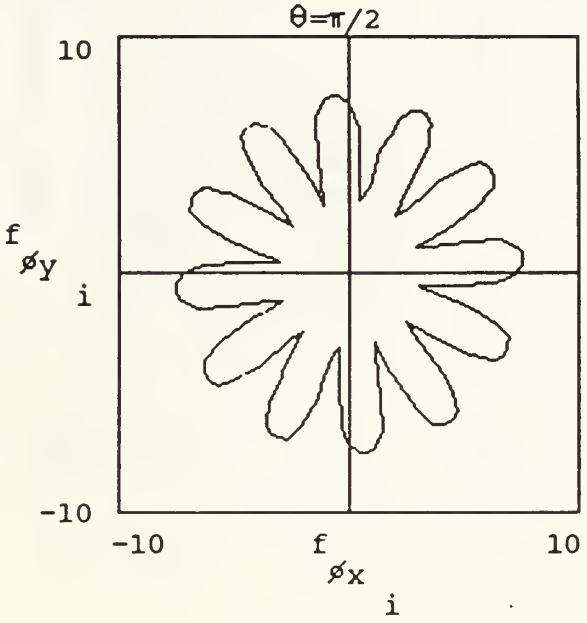

Elevation Plane

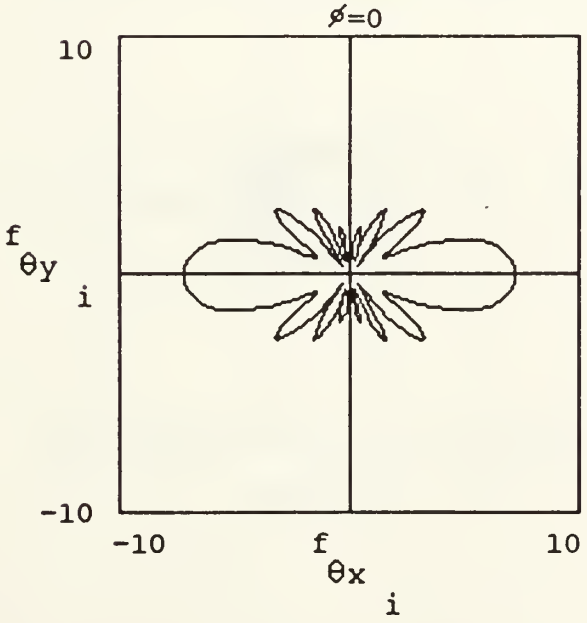

N = 12 nu = 2

Roll Plane

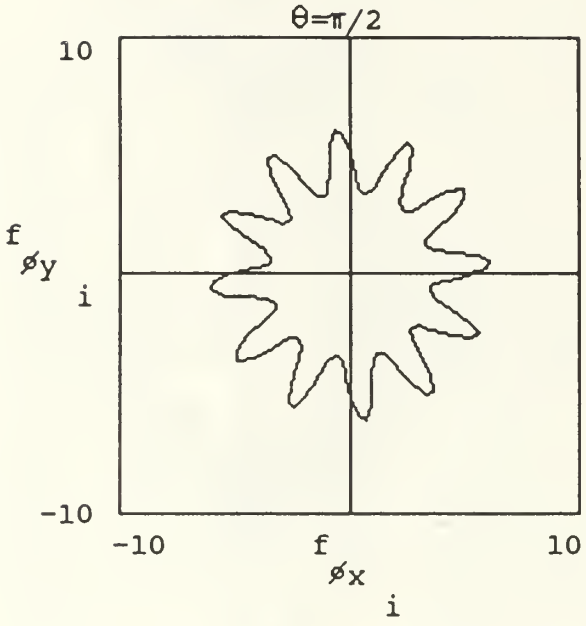

Elevation Plane

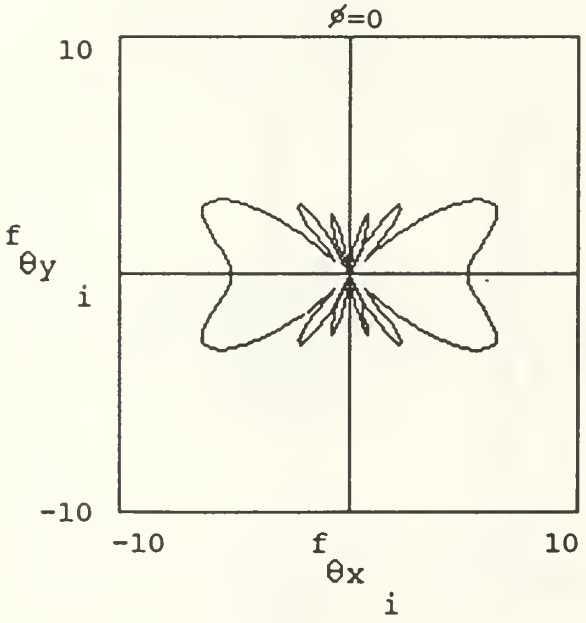

N = 12 nu = 3

Roll Plane

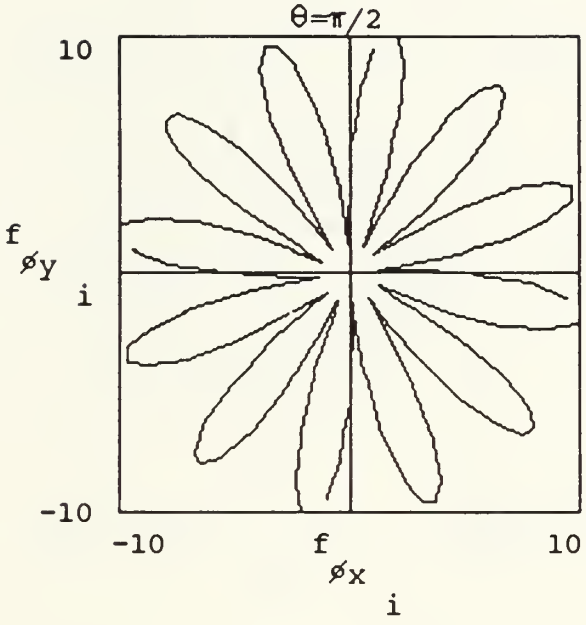

Elevation Plane

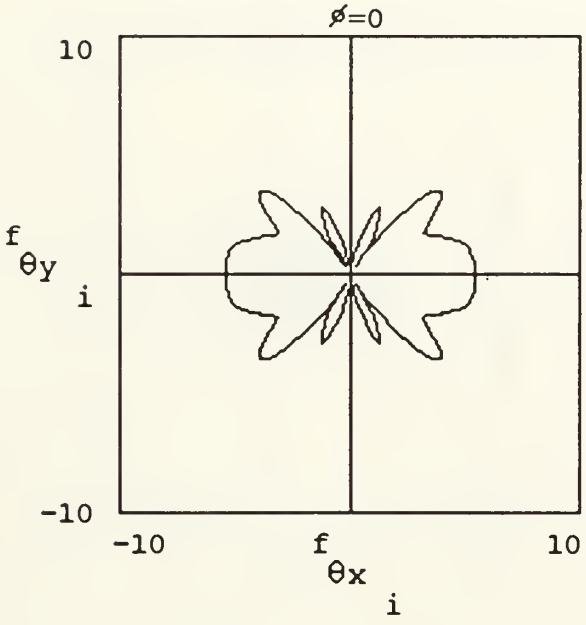

N = 13 nu = 1

Roll Plane

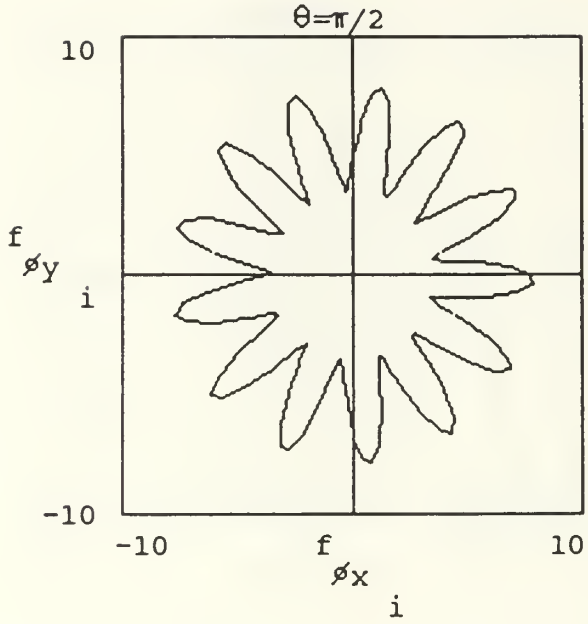

Elevation Plane

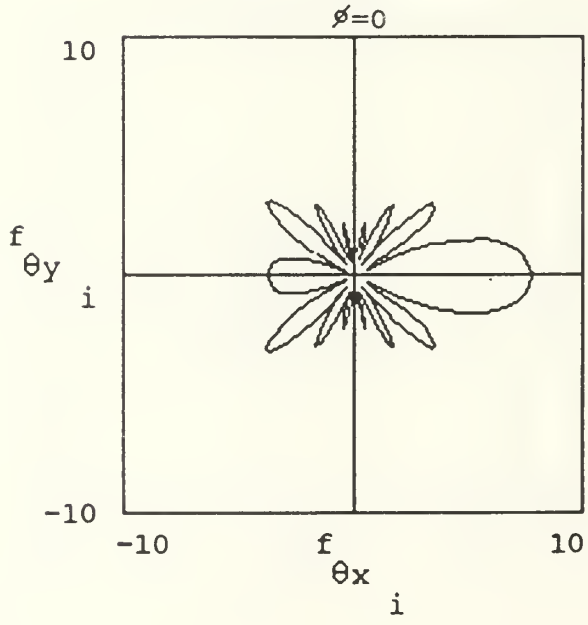

N = 13 nu = 2

Roll Plane

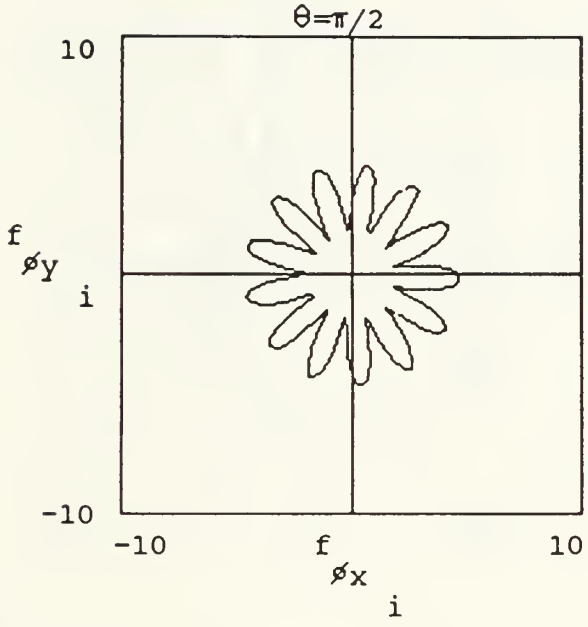

Elevation Plane

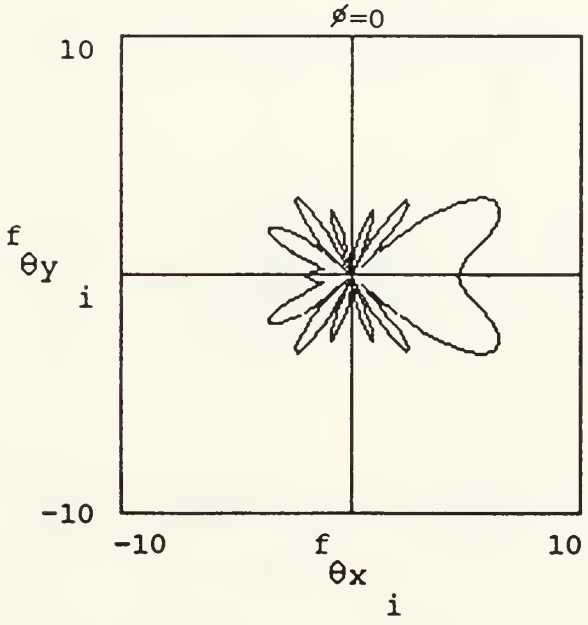

N = 13 nu = 3

Roll Plane

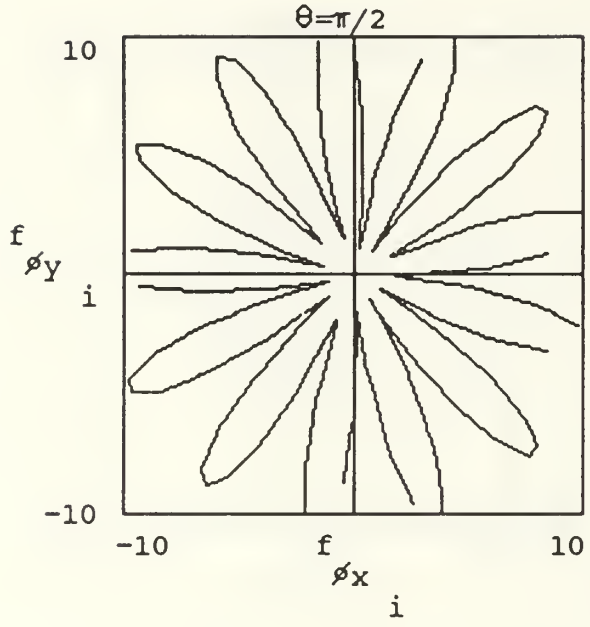

Elevation Plane

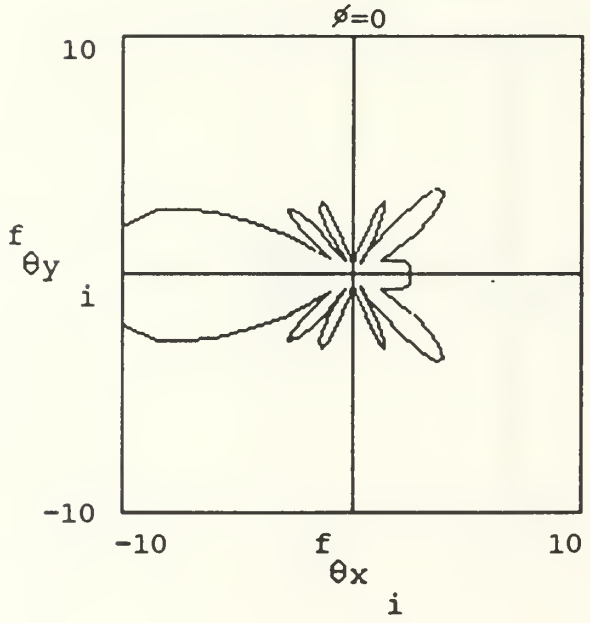

N = 14 nu = 1

Roll Plane

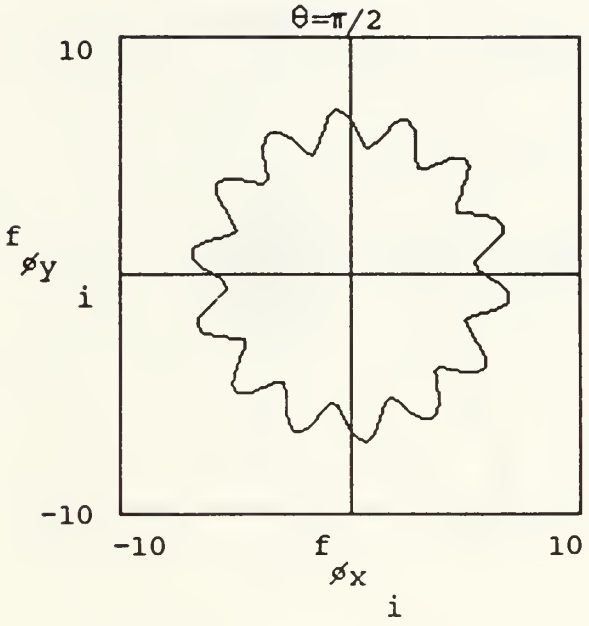

Elevation Plane

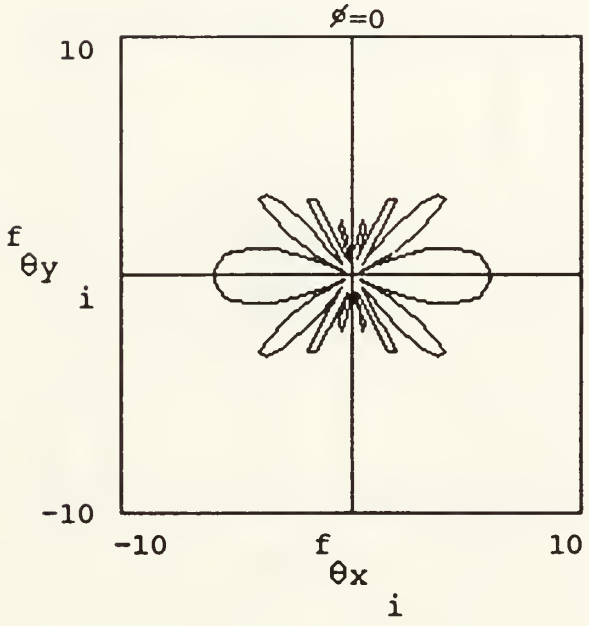

N = 14 nu = 2

Roll Plane

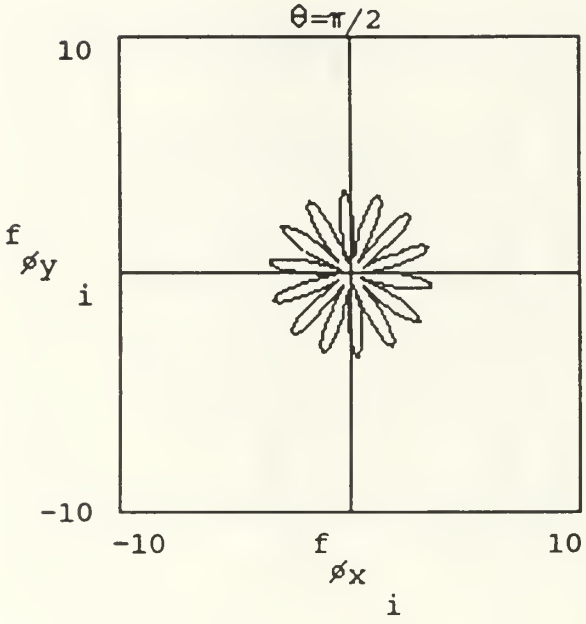

Elevation Plane

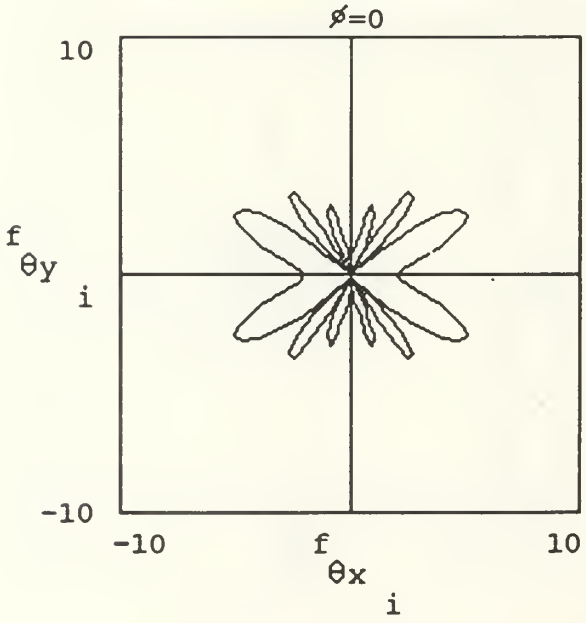

N = 14 nu = 3

Roll Plane

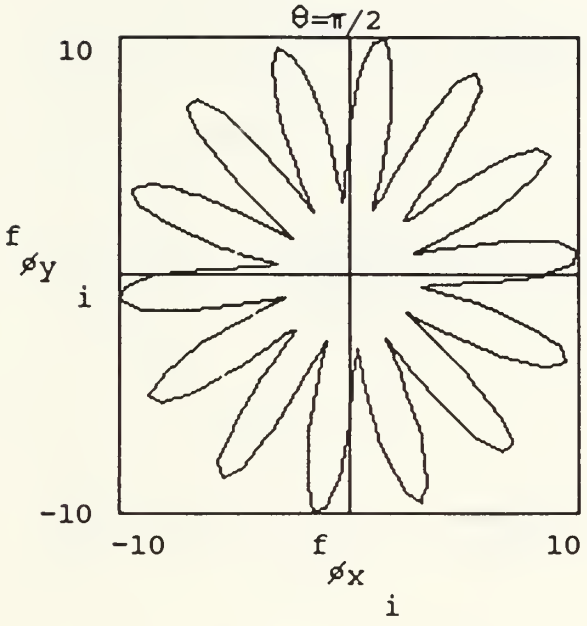

Elevation Plane

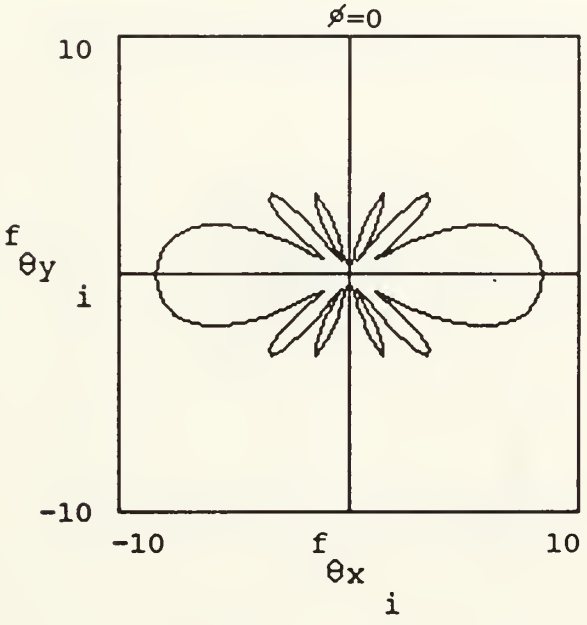

N = 15 nu = 1

Roll Plane

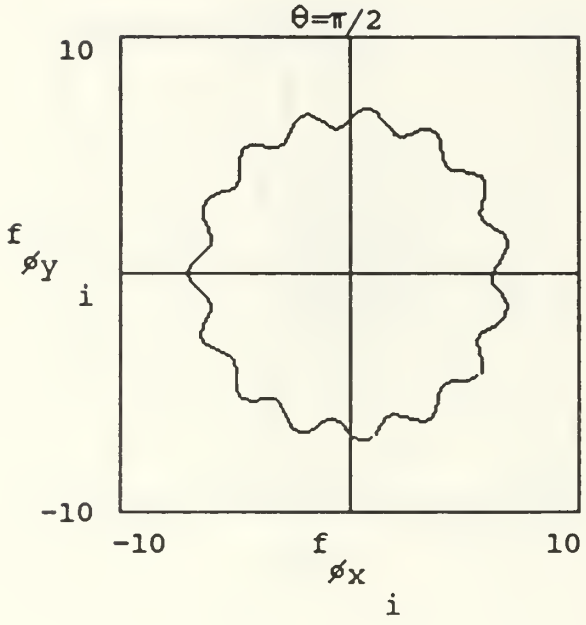

Elevation Plane

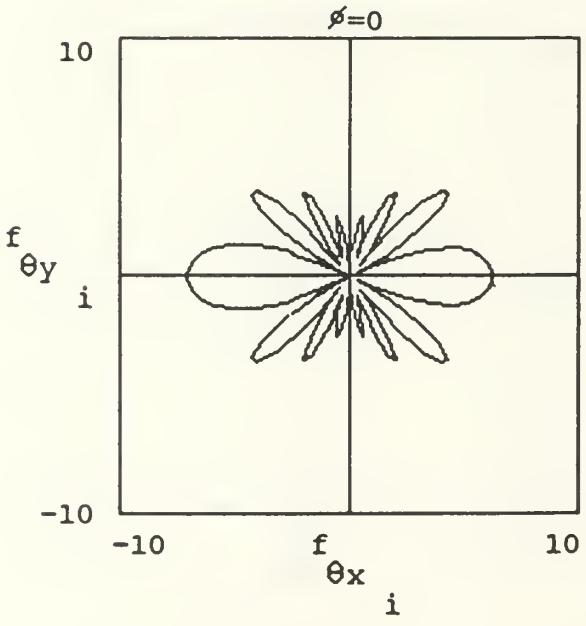

N = 15 nu = 2

Roll Plane

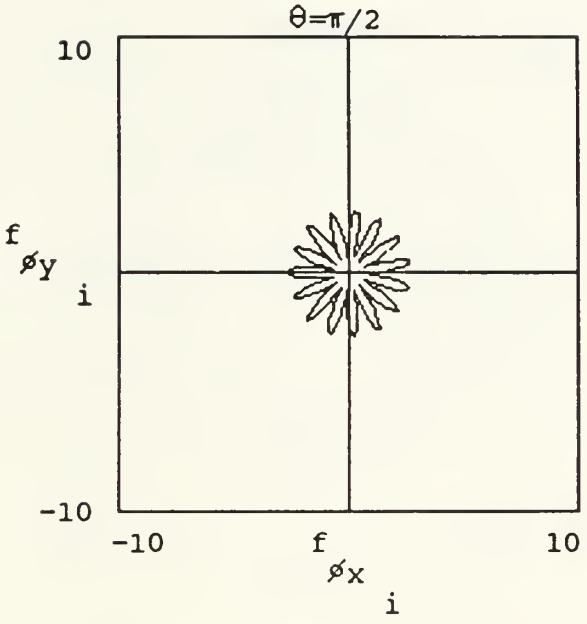

Elevation Plane

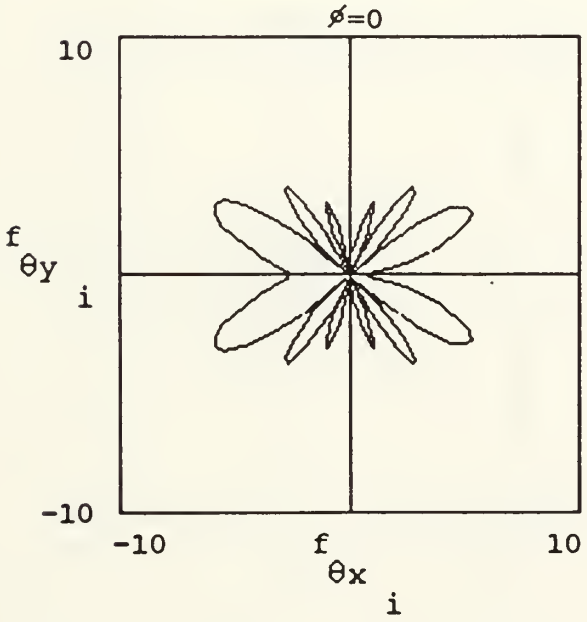

N = 15 nu = 3

Roll Plane

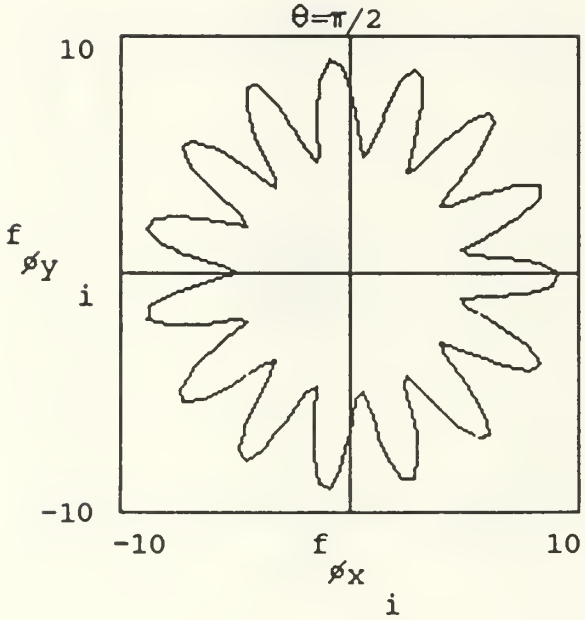

Elevation Plane

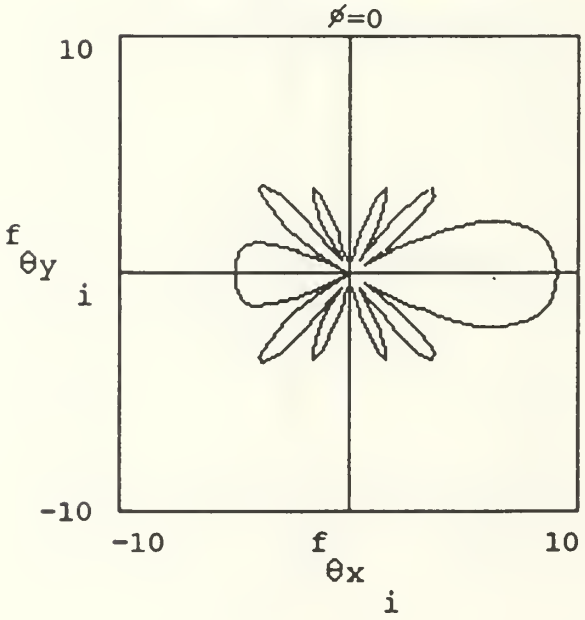

N = 16 nu = 1

Roll Plane

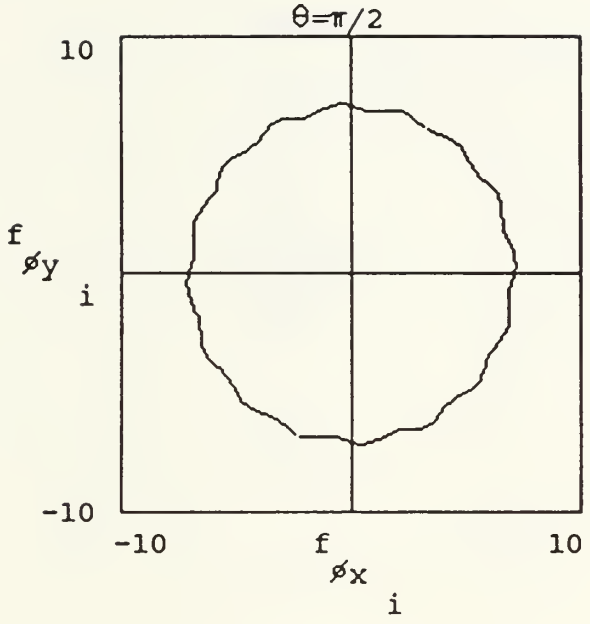

Elevation Plane

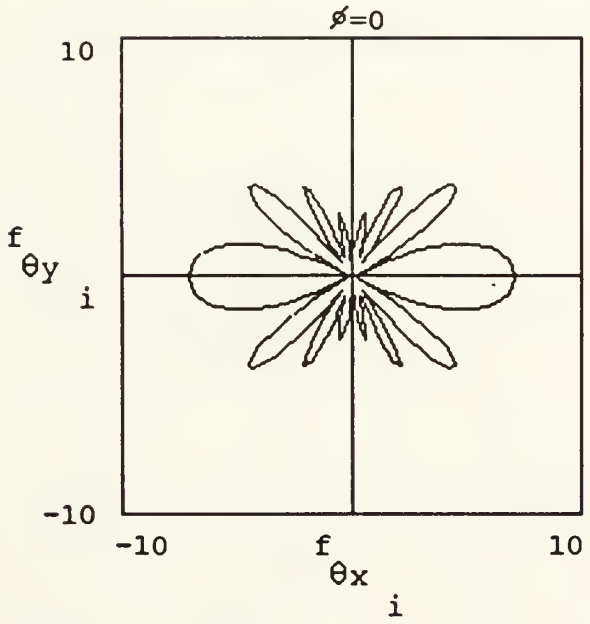

N = 16 nu = 2

Roll Plane

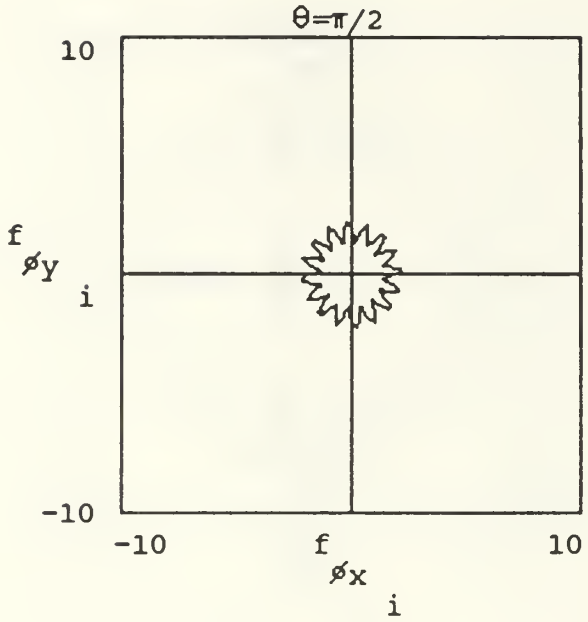

Elevation Plane

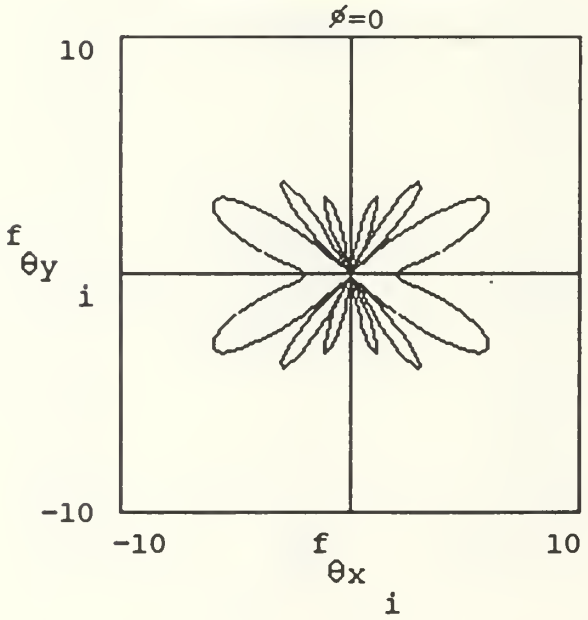

N = 16 nu = 3

Roll Plane

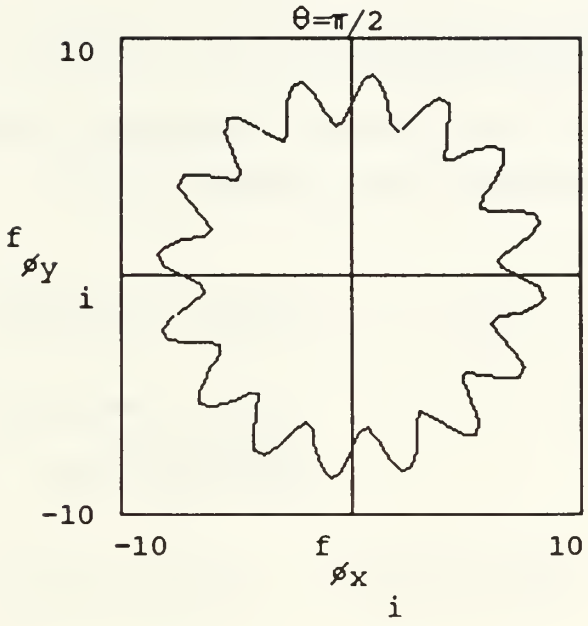

Elevation Plane

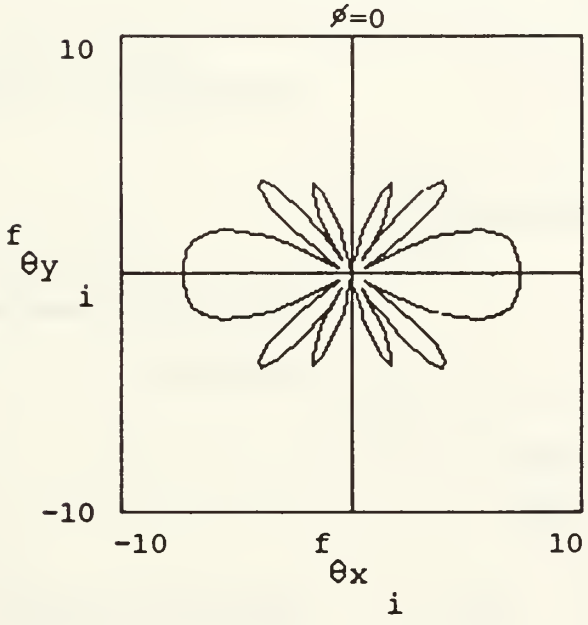

APPENDIX F. DIRECTIONAL DOWNLINK RADIATION PATTERN

Directional Radiation Pattern Program

This program generates the data and graphs the radiation pattern for a directional array antenna.

$N := 12$ — Number of patches

$f := 2250 \cdot 10^{6}$ Hertz — Center frequency of the operating band

$c := 2.997925 \cdot 10^{8}$ meters/second — Speed of light

$BW := 100 \cdot 10^{6}$ — Bandwidth

$$h := \frac{BW}{128 \cdot 10^{6}} \cdot \left[\frac{10^{9}}{f}\right]^{2} \cdot 2.54$$ — Thickness of a patch

$h = 0.391975$ centimeters

$\epsilon_r := 2.32$ — Dielectric constant of the substrate

$$W := \frac{c}{2 \cdot f} \cdot \left[\frac{\epsilon_r + 1}{2}\right]^{-\left[\frac{1}{2}\right]} \cdot 100$$ — Width of a patch

$W = 5.170758$ centimeters

$\lambda_o := \frac{c}{f} \cdot 100$ Free space wavelength

$\lambda_o = 13.324111$ centimeters

$k_o := 2 \cdot \frac{\pi}{\lambda_o}$ Wave number

$k_o = 0.471565$

$L := 0.49 \cdot \frac{\lambda_o}{\sqrt{\epsilon_r}}$ Length of a patch

$L = 4.286377$ centimeters

$a := 9.5 \cdot 2.54$ Radius of the ORION cylinder

$a = 24.13$ centimeters

$i := 1 \ldots 121$ Routine for generating the roll plane pattern

$\theta_i := \frac{\pi}{2}$

$\phi_i := (i - 1) \cdot \frac{2 \cdot \pi}{120}$

$$n := 1 \,..N$$

$$v_n := (n - 1)\cdot\frac{2\cdot\pi}{N}$$

$$\theta_0 := \frac{\pi}{2}$$

$$\phi_0 := 0$$

$$f_{\phi_i} := \left[\frac{\sin\left[\frac{k_o \cdot W}{2}\cdot\cos\left[\theta_i\right]\right]}{\frac{k_o \cdot W}{2}\cdot\cos\left[\theta_i\right]}\cdot\sin\left[\theta_i\right]\right]\cdot\left[\sum_n \begin{bmatrix} e^{-j\cdot k_o\cdot a\cdot\left[\sin\left[\theta_0\right]\cdot\cos\left[\phi_0 - v_n\right]-\sin\left[\theta_i\right]\cdot\cos\left[\phi_i - v_n\right]\right]} \\ \dots \\ + e^{-j\cdot k_o\cdot a\cdot\left[\sin\left[\theta_0\right]\cdot\cos\left[\phi_0 - v_n - \frac{L}{n\,a}\right]-\sin\left[\theta_i\right]\cdot\cos\left[\phi_i - v_n - \frac{L}{n\,a}\right]\right]} \end{bmatrix}\right]$$

$$f_{\phi x_i} := \left|f_{\phi_i}\right|\cdot\cos\left[\phi_i\right] \qquad f_{\phi y_i} := \left|f_{\phi_i}\right|\cdot\sin\left[\phi_i\right]$$

$$M_{0,0} := 121 \qquad M_{0,1} := 2$$

$$M_{i,0} := \left|f_{\phi_i}\right| \qquad M_{i,1} := \phi_i$$

WRITEPRN(RANT) := M

$$i := 1 \,..121$$

$$\phi_i := 0$$

This routine generates the elevation plane radiation pattern

$$\theta_i := (i - 1)\cdot\frac{2\cdot\pi}{120}$$

$n := 1 \,..N$

$$v_n := (n - 1)\cdot\frac{2\cdot\pi}{N}$$

$$f_{\theta_i} := \left[\frac{\sin\left[\frac{k_o\cdot W}{2}\cdot\cos\left[\theta_i\right]\right]}{\frac{k_o\cdot W}{2}\cdot\cos\left[\theta_i\right]}\cdot\sin\left[\theta_i\right]\right]\cdot\left[\sum_n\left[\begin{matrix} e^{-j\cdot k_o\cdot a\cdot\left[\sin\left[\theta_0\right]\cdot\cos\left[\phi_0 - v_n\right]-\sin\left[\theta_i\right]\cdot\cos\left[\phi_i - v_n\right]\right]} \ldots \\ + e^{-j\cdot k_o\cdot a\cdot\left[\sin\left[\theta_0\right]\cdot\cos\left[\phi_0 - v_n\right]-\sin\left[\theta_i\right]\cdot\cos\left[\phi_i - v_n\right]\right]}\end{matrix}\right]\right]$$

$$f_{\theta x_i} := \left|f_{\theta_i}\right|\cdot\sin\left[\theta_i\right] \qquad f_{\theta y_i} := \left|f_{\theta_i}\right|\cdot\cos\left[\theta_i\right]$$

$NN_{0,0} := 121$ $\qquad$ $NN_{0,1} := 2$

$NN_{i,0} := \left|f_{\theta_i}\right|$ $\qquad$ $NN_{i,1} := \theta_i$

WRITEPRN(RANT1) := NN

N = 12

Roll Plane

$$\theta := \frac{\pi}{2}$$

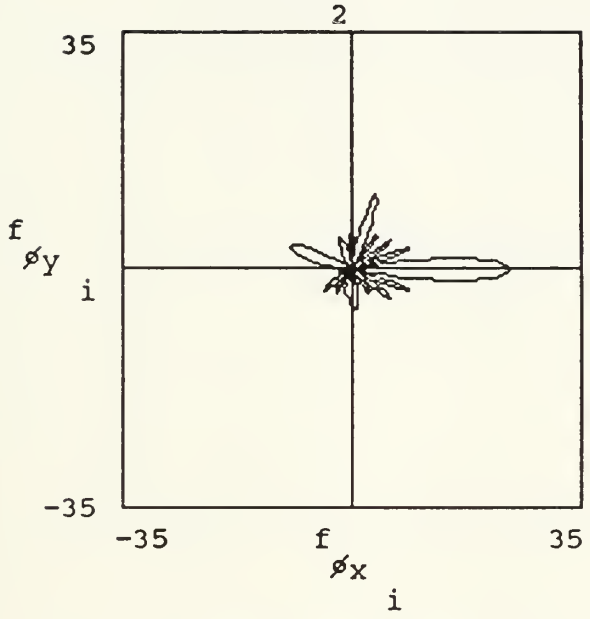

Elevation Plane

$$\phi := 0$$

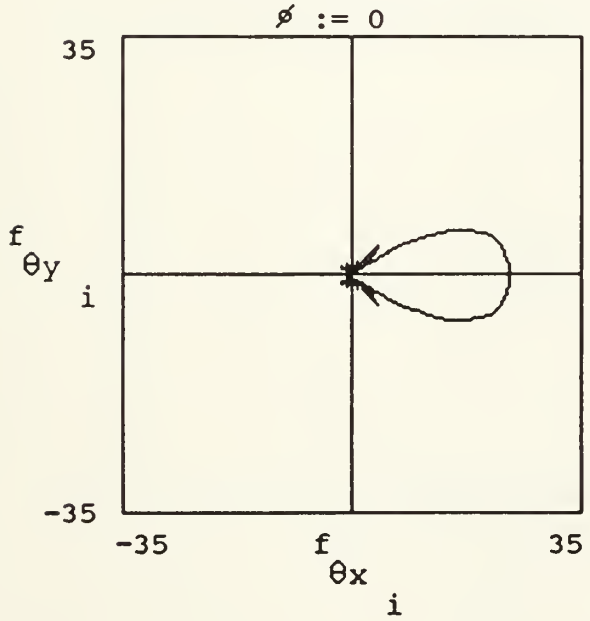

N = 15

Roll Plane

$\theta := \frac{\pi}{2}$

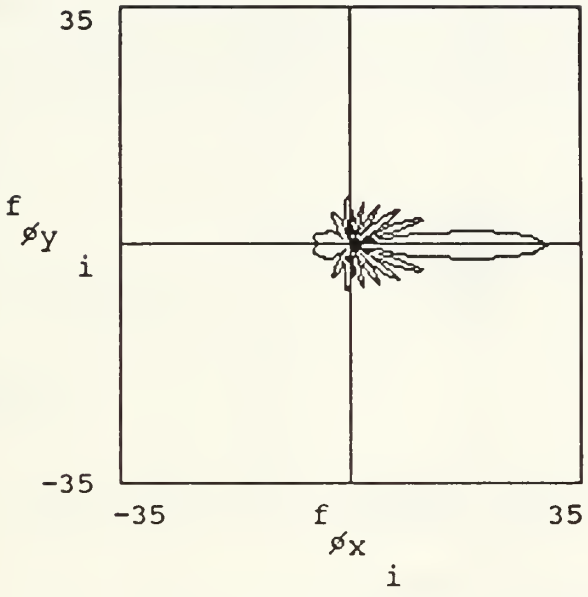

Elevation Plane

ø := 0

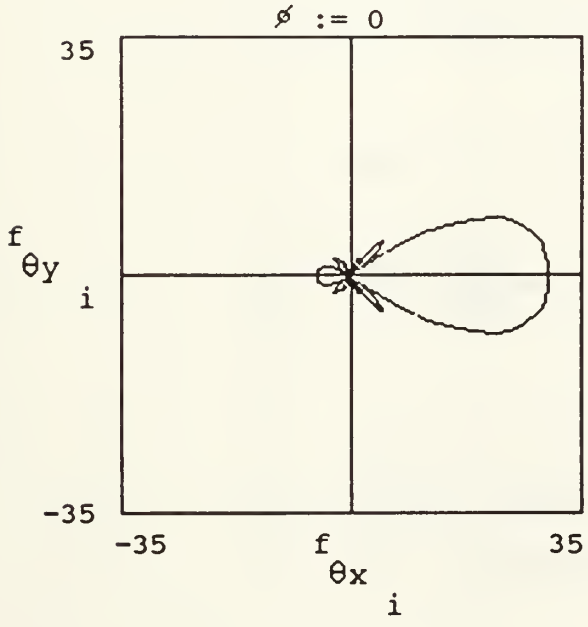

N = 16

Roll Plane

$$\theta := \frac{\pi}{2}$$

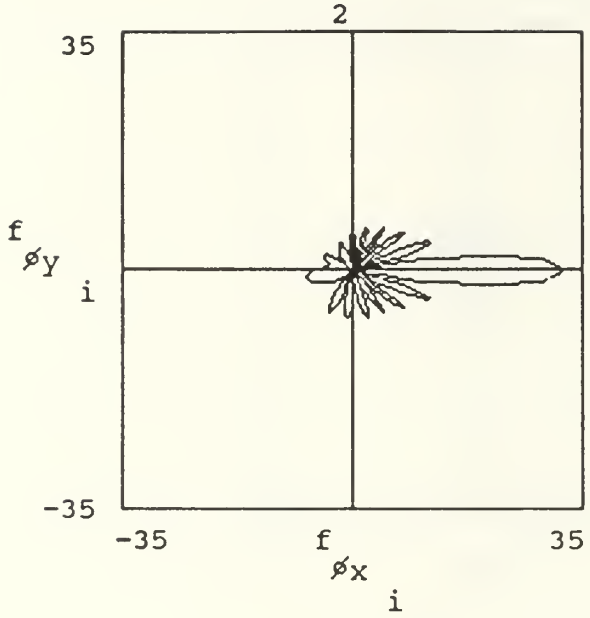

Elevation Plane

$$\phi := 0$$

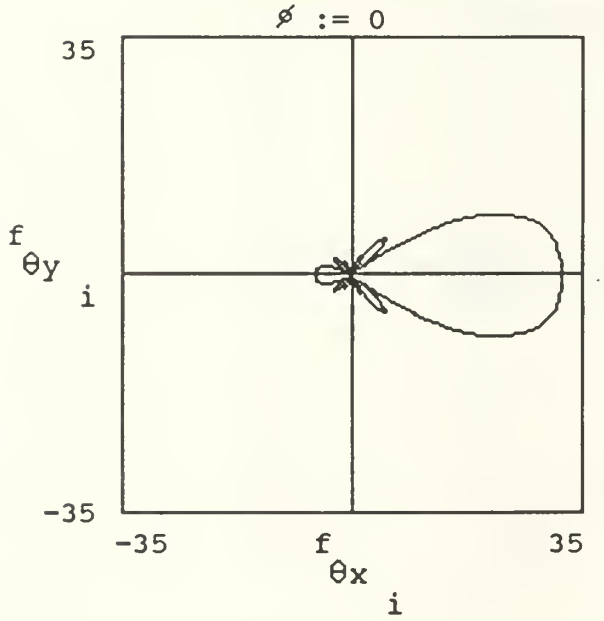

APPENDIX G. DIRECTIONAL AVERAGE RADIATION INTENSITY

DIRECTIONAL AVERAGE RADIATION INTENSITY

This program calculates the average radiation intensity for use in the directional directive gain equation.

$N := 12$ Number of patches

$W := 5.17$ centimeters Width of a patch

$k := 0.471565$

$a := 24.13$ centimeters Radius of the satellite

$\theta_o := \frac{\pi}{2}$ Desired radiation direction

$\phi_o := 0$

$L := 4.29$ Length of a patch

$\frac{L}{a} = 0.177787$ Angle between slots

$n := 1 \ldots 12$ Routine for calculating the average radiation intensity for a directional array antenna

$v_n := (n - 1) \cdot \frac{2 \cdot \pi}{N}$

```
N := 12

U    := 30.53
 av
```

APPENDIX H. DIRECTIONAL DIRECTIVE GAIN PATTERN

Directional Gain Pattern Program

This program generates the data and graphs the directive gain pattern for a directional array antenna.

$N := 12$ — Number of patches

$f := 2250 \cdot 10^{6}$ Hertz — Center frequency of the operating band

$c := 2.997925 \cdot 10^{8}$ meters/second — Speed of light

$BW := 100 \cdot 10^{6}$ — Bandwidth

$$h := \frac{BW}{128 \cdot 10^{6}} \cdot \left[\frac{10^{9}}{f}\right]^{2} \cdot 2.54$$ — Thickness of a patch

$h = 0.391975$ centimeters

$\epsilon_r := 2.32$ — Dielectric constant of the substrate

$$W := \frac{c}{2 \cdot f} \cdot \left[\frac{\epsilon_r + 1}{2}\right]^{-\left[\frac{1}{2}\right]} \cdot 100$$ — Width of a patch

$W = 5.170758$ centimeters

$\lambda_o := \frac{c}{f} \cdot 100$ Free space wavelength

$\lambda_o = 13.324111$ centimeters

$k_o := 2 \cdot \frac{\pi}{\lambda_o}$ Wave number

$k_o = 0.471565$

$L := 0.49 \cdot \frac{\lambda_o}{\sqrt{\epsilon_r}}$ Length of a patch

$L = 4.286377$ centimeters

$a := 9.5 \cdot 2.54$ Radius of the ORION cylinder

$a = 24.13$ centimeters

$U_{av} := 30.53$ Average radiation intensity

Routine for generating

the roll plane pattern

$i := 1 \,..121$

$\theta_i := \frac{\pi}{2}$

$\phi_i := (i - 1)\cdot\frac{2\cdot\pi}{120}$

$n := 1 \,..N$

$v_n := (n - 1)\cdot\frac{2\cdot\pi}{N}$

$\theta_0 := \frac{\pi}{2}$

$\phi_0 := 0$

$$D_{\phi i} := \frac{\left|\left|\left[\sin\left[\frac{k_o \cdot W}{2}\cdot\cos[\theta_i]\right]}{\frac{k_o \cdot W}{2}\cdot\cos[\theta_i]}\cdot\sin[\theta_i]\right]\cdot\left[\sum_n \begin{bmatrix} e^{-j\cdot k_o\cdot a\cdot[\sin[\theta_0]\cdot\cos[\phi_0 - v_n]-\sin[\theta_i]\cdot\cos[\phi_i - v_n]]} \\ + e^{-j\cdot k_o\cdot a\cdot\left[\sin[\theta_0]\cdot\cos\left[\phi_0 - v_n - \frac{L}{n\,a}\right]-\sin[\theta_i]\cdot\cos\left[\phi_i - v_n - \frac{L}{n\,a}\right]\right]} \end{bmatrix}\right]\right|\right|^2}{U_{av}}$$

$D_{\phi x\, i} := \left|D_{\phi i}\right|\cdot\cos[\phi_i]$ $\qquad$ $D_{\phi y\, i} := \left|D_{\phi i}\right|\cdot\sin[\phi_i]$

$M_{0,0} := 121$ $\qquad$ $M_{0,1} := 2$

$M_{i,0} := \left|D_{\phi i}\right|$ $\qquad$ $M_{i,1} := \phi_i$

WRITEPRN(RANT) := M

$i := 1 \,..121$

This routine generates the elevation plane radiation pattern

$\phi_i := 0$

$\theta_i := (i - 1)\cdot\frac{2\cdot\pi}{120}$

$n := 1 \,..N$

$v_n := (n - 1)\cdot\frac{2\cdot\pi}{N}$

$$D_{\theta i} := \left[\left|\left[\frac{\sin\left[\frac{k_o \cdot W}{2}\cdot\cos\left[\theta_i\right]\right]}{\frac{k_o \cdot W}{2}\cdot\cos\left[\theta_i\right]}\cdot\sin\left[\theta_i\right]\right]\cdot\left[\sum_n \left[e^{-j\cdot k_o\cdot a\cdot\left[\sin\left[\theta_0\right]\cdot\cos\left[\phi_0 - v_n\right]-\sin\left[\theta_i\right]\cdot\cos\left[\phi_i - v_n\right]\right]} + e^{-j\cdot k_o\cdot a\cdot\left[\sin\left[\theta_0\right]\cdot\cos\left[\phi_0 - v_n - \frac{L}{a}\right]-\sin\left[\theta_i\right]\cdot\cos\left[\phi_i - v_n - \frac{L}{a}\right]\right]} + \ldots\right]\right]\right|\right]^2}{U_{av}}$$

$D_{\theta x i} := \left|D_{\theta i}\right|\cdot\sin\left[\theta_i\right]$ $\quad D_{\theta y i} := \left|D_{\theta i}\right|\cdot\cos\left[\theta_i\right]$

$NN_{0,0} := 121$ $\quad NN_{0,1} := 2$

$NN_{i,0} := \left|D_{\theta i}\right|$ $\quad NN_{i,1} := \theta_i$

WRITEPRN(RANT1) := NN

N = 12

Roll Plane

$$\theta := \frac{\pi}{2}$$

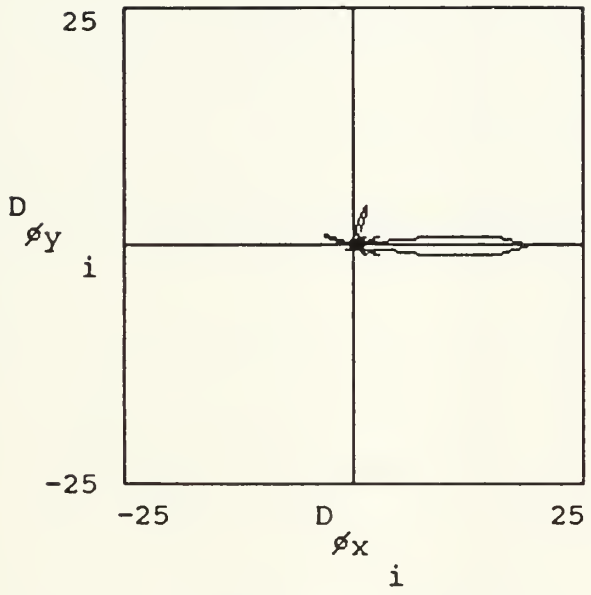

Elevation Plane

$$\phi := 0$$

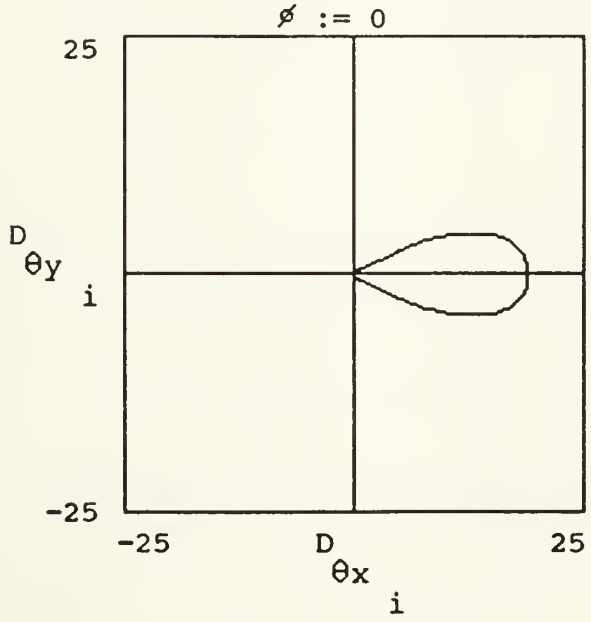

N = 15

Roll Plane

$\theta := \frac{\pi}{2}$

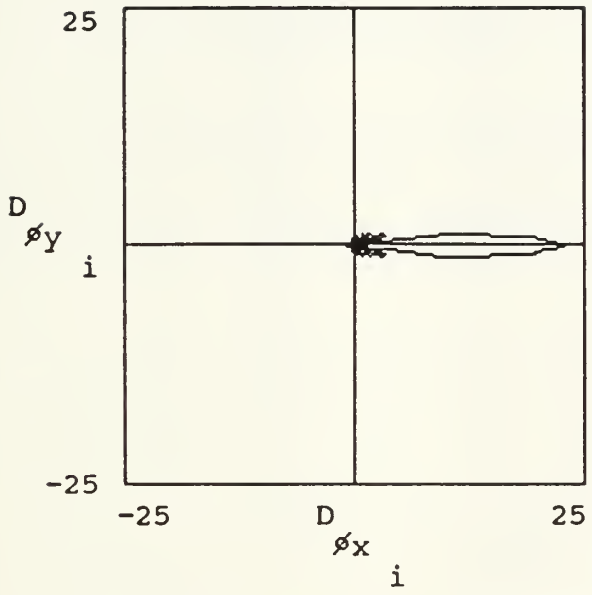

Elevation Plane

$\phi := 0$

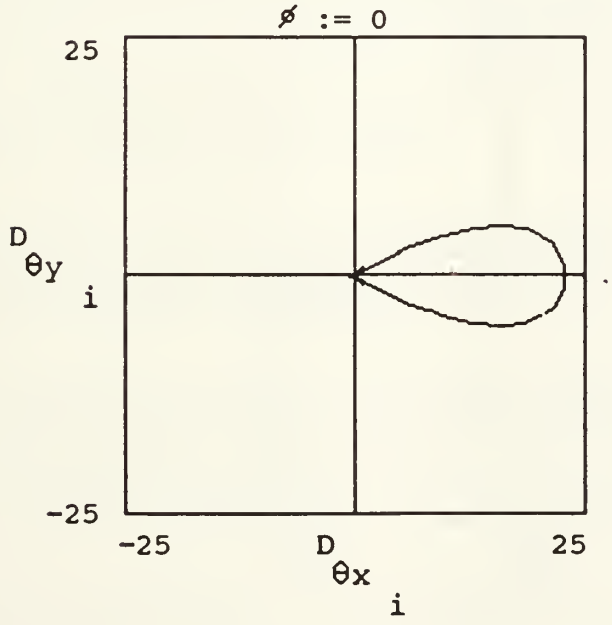

N = 16

Roll Plane

$$\theta := \frac{\pi}{2}$$

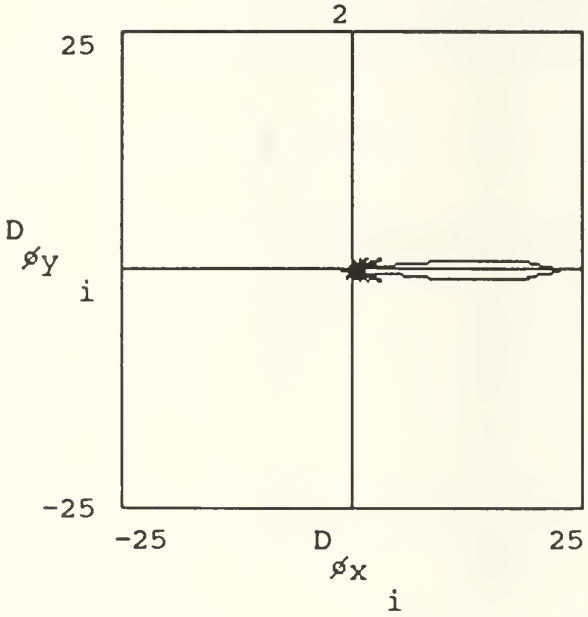

Elevation Plane

$$\phi := 0$$

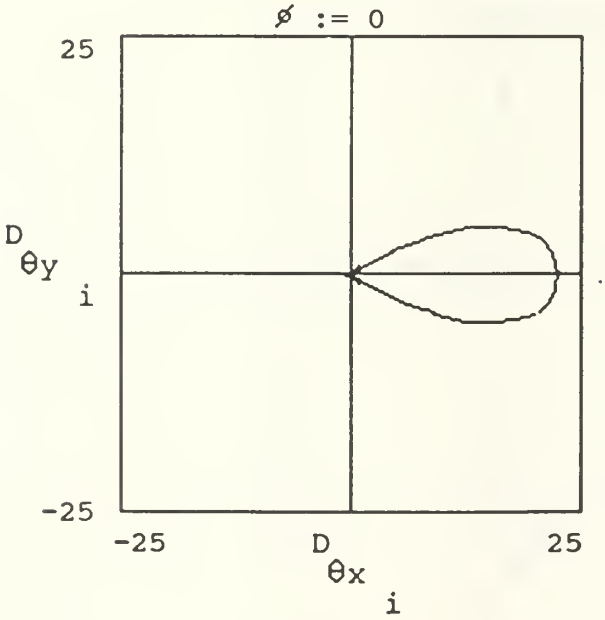

LIST OF REFERENCES

1. Mosier, M.R., *Memorandum of Agreement; Naval Postgraduate School Mini-Satellite Program (ORION) between Naval Research Laboratory, Washington D.C. and Naval Postgraduate School, Monterey, California, Draft,* Naval Postgraduate School, Monterey, California, 17 April 1987.

2. Peters, D.L., *Investigation of Design Considerations for the Telemetry, Tracking, and Command (TT&C) Antenna System on Naval Postgraduate School Orion Mini-Satellite,* M.S. Thesis, Naval Postgraduate School, Monterey, California, September 1987.

3. Bahl, I.J., and Bharta, P., *Microstrip Antennas,* Artech House, Inc., 1980.

4. *MathCAD 2.0,* Mathsoft, Inc., 1987.

5. Boyd, A.W., *Design Considerations for the ORION Satellite: Structure, Propulsion, and Attitude Control Subsystems for a Small, General Purpose Spacecraft,* M.S. Thesis, Naval Postgraduate School, Monterey, California, September 1987.

6. Fuhs, A.E., and Mosier, M.R., *"A niche for lightweight satellites",* Aerospace America , v. 26, pp. 14-16, April 1988.

7. Mosier, M.R., *A Small, General Purpose, Low Earth Orbit Satellite Bus,* informal presentation package, Summer 1987.

8. The Aerospace Corporation, Space Systems Control Division, Report TOR-0059 (6110-01)-3 Reissue G, *Air Force Satellite Control Facility Space/Ground Interface,* by H.D. Klements, June 1985.

9. Motorola Incorporated, Government Electronics Group, Specification No. 985,H32, *SGLS S-Band Transponders.*

10. Stutzman, W.L. and Thiele, G.A., *Antenna Theory and Design,* John Wiley & Sons, Inc., 1981.

11. Jasik, H. and Johnson, R.C., *Antenna Engineering Handbook,* McGraw-Hill Book Company, 1984.

12. Milligan, T.A., *Modern Antenna Design,* McGraw-Hill Book Company, 1985.

13. Collin, R.E., and Zucker, F.J., *Antenna Theory Part 1,* McGraw-Hill Book Company, 1969.

14. Ha, T.T., *Digital Satellite Communications,* Macmillan Publishing Company, 1986.

15. Gagliardi, R., *Introduction to Communications Engineering,* John Wiley & Sons, 1978.

16. Haykin, S., *Communication Systems,* John Wiley & Sons, 1983.

INITIAL DISTRIBUTION LIST

		No. Copies
1.	Defense Technical Information Center Cameron Station Alexandria, VA 22304-6145	2
2.	Library, Code 0142 Naval Postgraduate School Monterey, CA 93943-5002	2
3.	Chairman, Code 62 Department of Electrical and Computing Engineering Naval Postgraduate School Monterey, CA 93943-5004	1
4.	Chairman, Code 72 Space Systems Academic Group Naval Postgraduate School Monterey, CA 93943	1
5.	Navy Space Systems Division Chief of Naval Operations (OP-943) Washington, D C 20305-2000	1
6.	Commander Naval Space Command Attn: Code N3 Dahlgren, VA 22448	2
7.	Commander United States Space Command Attn: Technical Library Peterson AFB, CO 80914	2
8.	Naval Research Laboratory, Code 9110 4555 Overlook Avenue Southwest Washington, D C 20375	2
9.	Professor Michael A. Morgan, Code 62Mw Department of Electrical and Computer Engineering Naval Postgraduate School Monterey, CA 93943-5000	10

10. Professor Richard W. Adler, Code 62Ab — 1
Department of Electrical and
Computer Engineering
Naval Postgraduate School
Monterey, CA 93943-5000

11. Professor Rudolph Panholzer, Code 62Pz — 1
Department of Electrical and
Computer Engineering
Naval Postgraduate School
Monterey, CA 93943-5000

12. Professor Glen Myers, Code 62My — 1
Department of Electrical and
Computer Engineering
Naval Postgraduate School
Monterey, CA 94943-5000

13. LT Mark B. Smith — 2
COMCRUDESGRU ONE
FPO San Francisco, CA 96601

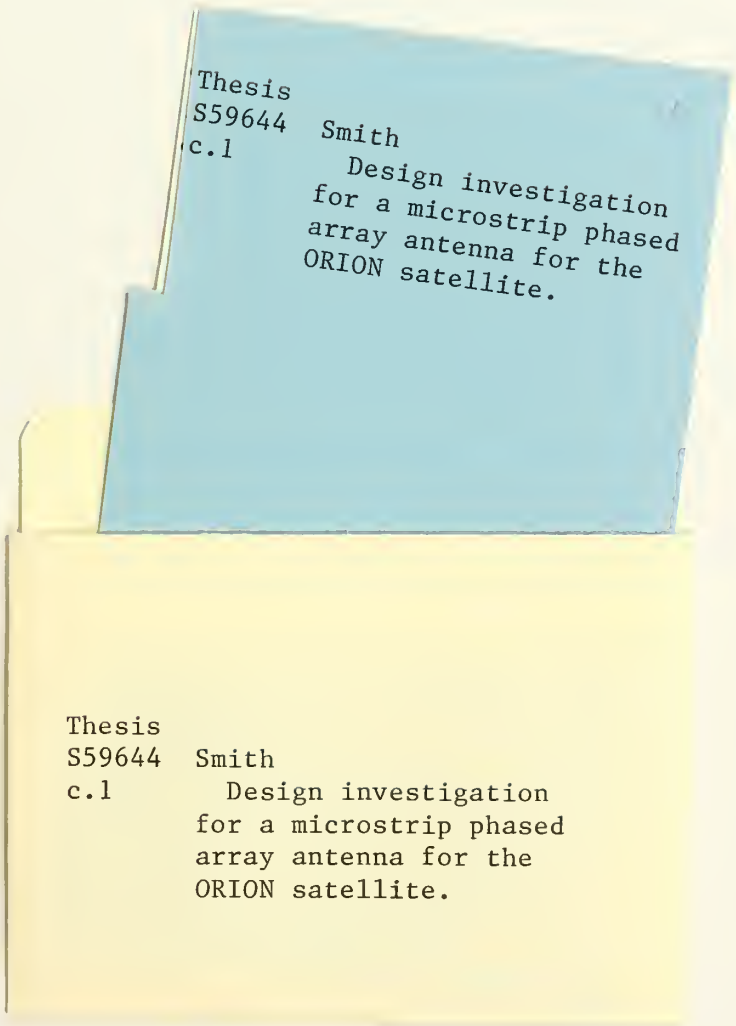

Thesis
S59644 Smith
c.1 Design investigation
for a microstrip phased
array antenna for the
ORION satellite.